



UNIVERSIDADE ESTADUAL DE CAMPINAS
FACULDADE DE ENGENHARIA QUÍMICA

ÁREA DE CONCENTRAÇÃO:
DESENVOLVIMENTO DE PROCESSOS QUÍMICOS

MODELAGEM, SIMULAÇÃO E ANÁLISE DE DESEMPENHO
DE REATORES TUBULARES DE POLIMERIZAÇÃO COM
DEFLECTORES ANGULARES INTERNOS

AUTOR: M.C. FLORENTINO LÁZARO MENDOZA MARÍN
ORIENTADOR: Prof. Dr. RUBENS MACIEL FILHO
CO-ORIENTADORA: Profª. Dra. LILIANE MARIA FERRARESO LONA

Tese de doutorado apresentada à Faculdade de Engenharia Química como parte
dos requisitos para obtenção do título de Doutor em Engenharia Química

Dezembro/2004
UNICAMP - CAMPINAS – SÃO PAULO
BRASIL

UNICAMP
BIBLIOTECA CENTRAL
SEÇÃO CIRCULANTE

UNIDADE	DC
Nº CHAMADA	TRUNICAMP
	M523m
V	EX
TOMBO BC/	62842
PROC.	6-86-05
C	<input type="checkbox"/>
D	<input checked="" type="checkbox"/>
PREÇO	11,00
DATA	31-03-05
Nº CPD	

Bifid 346666

FICHA CATALOGRÁFICA ELABORADA PELA
BIBLIOTECA DA ÁREA DE ENGENHARIA - BAE - UNICAMP

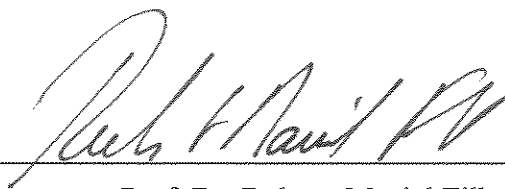
M523m Mendoza Marín, Florentino Lázaro
Modelagem, simulação e análise de desempenho de reatores tubulares de polimerização com defletores angulares internos / Florentino Lázaro Mendoza Marín.--Campinas, SP: [s.n.], 2005.

Orientadores: Rubens Maciel Filho, Liliane Maria Ferrareso Lona.

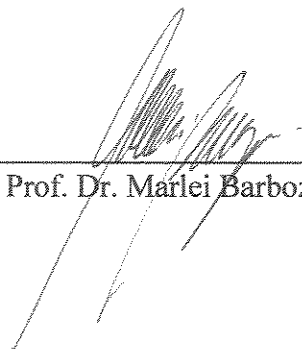
Tese (Doutorado) - Universidade Estadual de Campinas, Faculdade de Engenharia Química.

1. Modelagem. 2. Simulação (Computador digitais). 3. Reatores Químicos – Simulação (Computadores). 4. Estireno. 5. Polimerização em emulsão. 6. FORTRAN (Linguagem de programação de computador). 7. Métodos dos volumes finitos. I. Maciel Filho, Rubens. II. Lona, Liliane Maria Ferrareso. III. Universidade Estadual de Campinas. Faculdade de Engenharia Química. IV Título.

Tese de Doutorado defendida e aprovada em 17 de Dezembro do 2004 pela banca
examinadora constituída pelos professores:



Prof. Dr. Rubens Maciel Filho



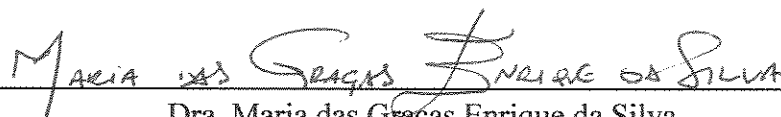
Prof. Dr. Marlei Barboza



Prof. Dr. Silvio Roberto Andrietta



Dr. Eduardo Coselli Vasco de Toledo



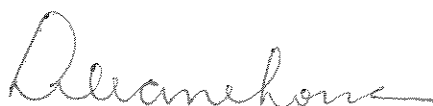
Dra. Maria das Graças Enrique da Silva

BRUNO

Esta versão corresponde à redação final da Tese de Doutorado em Engenharia Química defendida pelo Eng. Mestre Florentino Lázaro Mendoza Marín e aprovada pela Comissão Julgadora em 17/12/04.



Prof. Dr. Rubens Maciel Filho
Orientador



Profa. Dra. Liliane Maria Ferrareso Lona
Co-orientadora

DEDICATORIA

À minha querida mãe Esther por seu amor, exemplo de vida, conselhos e ajuda para concluir este trabalho e por sua presença em minha defesa de tese, obrigado por tudo. A todos meus irmãos: Aidee, Juan, Lelis, Reynaldo e Donald por seu apoio e dedicação. A Marcelina e Celia por seu apoio, a Deisi por sua alegria. Añay, gracias, thanks, Dank, obrigado.

F.L.MENDOZA MARÍN

MÁXIMAS FILOSÓFICOS

- ⇒ Projetistas fazem canais, arqueiros airam flechas, artífices modelam a madeira e o barro, o homem sábio modela-se a si mesmo (*Buda*).
- ⇒ Escolha um trabalho que você ame e não terá de trabalhar um único dia em sua vida (*Confúcio*).
- ⇒ Para ser forte, você só terá de ser como a água. Porque é suave e flexível, é a mais necessária e forte de todas as coisas (*Lao-Tsé*).
- ⇒ Nunca inicie a injustiça. Deixe que os demais gerem a injustiça em contra de você (*Kleovolos*).
- ⇒ Façam aos outros o que querem que eles façam a vocês: este é o sentido da Lei de Moisés e dos ensinamentos dos profetas (*Mateus 7.12*).
- ⇒ A humanidade tem toda a razão em colocar os proclamadores dos altos valores e padrões morais acima dos descobridores de verdades objetivas (*Albert Einstein*).
- ⇒ Há duas formas para viver sua vida. Uma é acreditar que não existe milagre. A outra é acreditar, que todas as coisas são um milagre (*Albert Einstein*).
- ⇒ Qualquer coisa que você faça, faça-a sempre cuidadosamente. (A Mãe)
- ⇒ Faça o que pode, com o que tem, onde estiver (*Roosevelt*).
- ⇒ Ainda o ultimo momento pode-se alterar uma situação ou um evento (*Solo*).
- ⇒ Não há ciência aplicada; há somente aplicações da ciência. O estudo das aplicações da ciência é muito fácil e acessível a qualquer um que domine o saber e a teoria (*Louis Pasteur*).
- ⇒ Para todo problema complexo existe uma solução clara, simples e errada (*George Bernard Shaw*).
- ⇒ As pessoas que vencem neste mundo são as que procuram as circunstancias de que precisam e, quando não as encontram, as criam (*Bernard Shaw*).
- ⇒ Incumbe a nós da ciência da computação tomarmos uma aproximação pragmática. Algum situação matematicamente modelado qual captura qualquer geração de assunto em os procedimentos com computadoras é um tema possível para ciência da computação. Isto inclui hardware, software, modelagem de dados, interface e mais (*J.Á. MAKOWSKY*).
- ⇒ Façamos o melhor que pudermos em todas as circunstâncias e deixemos o resultado para a decisão do divino (A Mãe).
- ⇒ O tempo é o recurso mais escasso e não renovável; se não se administra, nenhuma outra coisa poderá ser administrada (autor).
- ⇒ ...dominar...pratica, pratica, pratica,....., perseverança.

Añay, gracias, thanks, Dank, obrigado.

PENSAMENTOS

PERSEVERANÇA:

Manapunin imapis kawsanchu t'ikrayanapaq perceveranchista. Talentuka manan t'ikranmanchu; yachaqniyoqrunakuna thuninku. Yuyayniyoqa manan t'ikranchu; yachayniyoq mana qopuyqa yakan proverbionchishinakanku. Sapallan uywanawanrayku manan t'ikranmanchu; pachuka untarunayachayniyoq mana wasi icha lank'ay. Sapallammi, perseveranchispas, determinanchispas kashanku hatun kallpayoqhina.

No existe en absoluto ningún sustitutivo de la perseverancia. El talento no puede reemplazarla; abundan las personas talentosas que han fracasado. El genio no puede suplirla; el genio no retribuido constituye casi una expresión proverbial. La educación por sí sola tampoco puede sustituirla; el mundo esta lleno de individuos instruidos carentes de vivienda o empleo. Unicamente, la perseverancia y la determinación son omnipotentes.

No exists in absolute any substitute of the perseverance. The talent cannot replace it; talent people that have failed are plentiful. The genius cannot replace it; the genius did not reward almost constitutes a proverbial expression. The education by itself neither can substitute it; the world is full of individual well educated lacking of house or employment. Only, the perseverance and the determination are omnipotent.

Nichts kann, in einen Absolutensinn, das Durchhaltevermögen ersetzen. Der Talent kann es nicht ersetzen; vielen sind die Menschen, die gescheitert haben. Das Genie kann es auch nicht; der unbelohnte Genie ist fast ein Sprichwort. Die Ausbildung kann es ebenso weniger ersetzen; die Welt ist voll von Ausgebildeten Menschen mit wenigen Häuserbestand und ohne Arbeit. Nur das Durchhaltevermögen und die Entschlossenheit sind allmächtig.

Não existe em absoluto nenhum substitutivo da perseverança. O talento não pode substituí-la; abundam as pessoas talentosas que fracassaram. O gênio não pode supri-la; o gênio não retribuído constitui quase uma expressão proverbial. A educação por si só tampouco pode substituí-la; o mundo está cheio de indivíduos instruídos carentes de moradia ou emprego. Unicamente, a perseverança e a determinação são onipotentes.

AXIOMAS DO CIENTIFICISMO:

- O homem não é naturalmente depravado.
- A “boa” vida na terra pode ser não só definida mas também alcançada.
- A razão é o instrumento supremo do homem.
- O conhecimento libertará o homem da ignorância, da superstição e dos males sociais.
- O universo é ordenado
- Essa ordem do universo pode ser descoberta pelo homem e expressa por meio de quantidade e relações matemáticas.
- Embora haja muitas maneiras de perceber a natureza, como, por exemplo, a arte, a poesia, a música, etc., só a ciência pode chegar à verdade, que permitirá ao homem dominar a natureza.
- A observação e a experimentação são os únicos meios válidos de descobrir a ordem da natureza.
- Os fatos observados são independentes do observador.
- As qualidades secundárias não são suscetíveis de medida e, por isso, não são reais.

- Todas as coisas da Terra são para uso do homem.
- A ciência é neutra, livre de valores e independente da moralidade e da ética.

PRINCIPIOS DA CIVILIZAÇÃO TECNOLÓGICA:

Para Erich Fromm, são três os principais princípios norteadores das atuais sociedades tecnológicas:

- ❖ Tudo o que é tecnicamente possível de fazer-se, deve ser feito.
- ❖ O atual avanço científico e tecnológico deve conduzir ao ideal da eficiência absoluta.
- ❖ Quanto mais produzimos do que quer que produzimos, tanto melhor.

AS “QUASE-SOLUÇÕES” TECNOLÓGICAS:

Segundo Schwartz, proven de três fontes:

- ⊙ Natureza incompleta da solução tecnológica (ou, mais simplesmente, falta de complemento);
- ⊙ Aumento do problema original;
- ⊙ Efeitos secundários (todos os efeitos previstos e imprevisos, que resultam numa multiplicação de outros problemas que passam a reclamar solução).

SEMELHANÇAS ENTRE COMPUTADOR E CÉREBRO:

As semelhanças e dessemelhanças entre computador e cérebro segundo Michael Apter são:

- ✖ Os dois são dispositivos de USO GERAL. “poder-se-ia dizer que o cérebro e o computador de uso geral são os dois dispositivos de maior uso geral conhecidos pelo homem”.
- ✖ Ambos são dispositivos de processamento de informações.
- ✖ Ambos podem incorporar em si modelos, pois, segundo se sabe, uma das principais funções do cérebro é a de elaborar e utilizar modelos do seu ambiente.
- ✖ Ambos chegam à sua complexidade intelectual realizando um grande número de operações simples.

DESSEMELHANÇAS ENTRE COMPUTADOR E CÉREBRO:

- ◇ Deve-se observar a “equipotencialidade” que caracteriza o cérebro, não caracterizando o computador, é claro. Quer dizer: “Se certas partes do cérebro vivo forem retiradas, as partes restantes automaticamente assumem as funções das partes retiradas. Também os hábitos aprendidos não parecem estar armazenados em neurônios particulares localizados, mas espalhados de alguma maneira por amplas áreas, de tal modo que a extirpação de partes limitadas do cérebro não significa necessariamente a perda dos hábitos”. Tal não ocorre, é claro, com as partes do computador.
- ◇ Obviamente, o computador não é no sentido radical da palavra, criativo. Até onde o conhecemos hoje, ele não perderá jamais substituir o artista ou cientista de forma nem razoavelmente convincente.
- ◇ O cérebro é projetivo no lidar com formas. Isto é: se um ou outro elemento da forma falta, ele o reconstrói (o que se chama de função gestáltica). Por quanto, ao que parece, os computadores são destituídos da capacidade de complementação de configurações.
- ◇ O computador recebe as informações, diríamos, de forma passiva, enquanto que o cérebro faz perguntas, discute e crítica, como também seleciona os dados segundo o seu interesse.

Añay, gracias, thanks, Dank, obrigado.

AGRADECIMENTOS

A Deus que, em silêncio, esconde os grandes mistérios da natureza em pequenos gestos e bondade de Deus (Mateus 7.7-12).

À minha mãe Esther, a todos meus irmãos Aide, Juan, Lelis, Reynaldo e Donald, por tudo. À Deisi, Marcelina, Celia, Milton, Carmen, Monica, Reni, Rudy, Joel, Shamira, Hedi, Eloy, e demais familiares.

À minha pátria do Perú, a minha Universidade, “Universidad Nacional de San Antonio Abad del Cusco”, e Faculdade, “Ingenieria Química”.

À minha segunda pátria do Brasil, vêm me apoiando todos estos anos na UNICAMP, desde o mais simples cidadão ao mais ilustre, devoto meus mais sinceros agradecimentos.

Aos meus orientadores: Prof. Dr. Rubens Maciel Filho, pela orientação, paciência, dar me oportunidade para fazer doutorado; e à Profa. Dra. Liliane M.F. Lona B., pela orientação e conselhos.

A todos os Professores da UNICAMP e outras Universidades, pelos conselhos e tempo compartilhado na presente tese, Altemani, Bordini, M.A. Cremasco, Gustavo P.V., A.C.L. Lisboa, C. Maliska, R. Morales, S. Patankar, Petrônio P., J.C. Pinto, Rahoma S.M., M. Regina W.M, Reginaldo G., M. Silva, Reginaldo G., Vanja.

A todas as pessoas que contribuíram na minha formação profissional e humana.

A todo pessoal da DESQ, DPQ, Secretaria de Pós-Graduação da Faculdade de Engenharia Química da UNICAMP, por todos os anos de estudo. A todo pessoal do Laboratório de Otimização, Projetos e Controle Avançado (LOPCA). A todo pessoal da BAE e outras bibliotecas da UNICAMP, Ana, Antônio, Bernadete, Juliana, Márcia, Neuza, Raquel, Rosa. À Luciana e Edson da DAC. A todo pessoal do Restaurante II, muito obrigado pela atenção e serviço.

A banca examinadora pelas correções e sugestões fornecidas.

A todos meus Professores da Universidade da UNSAAC, R. Acurio, E. Alvares, A. Castillo, R. Castillo, E. Loyza, M. Masco, J.D. Molina, E. Moscoso, W. Pinarez, M. Salas, A. Trigoso, C. Vargas, E. Viscarra, M. Arapa, e M. Concha. Também J. Bejar, Concha, A.

Estrada, E. Chuquimia, Luna, Mayorga, G. Muelle, Quispe, P. Valcarcel, e A. Villena. Outros, A. Bueno, N. Caceres, F. Gamarra, M. Hurtado, E. Jara, e E. Yañes.

A todos meus professores da Universidade da UNICAMP, Ana M. Frattini F., Antonio J. G. Cobo, Elias B. Tambourgi, Elizabete Jordão(orientadora de mestrado, muito obrigado), Itacira, Maria T.M. Rodrigues, Roger J. Zemp, Rubens Maciel Filho, Salette, Telma T. Franco.

A SAE e PME por apoio e compreensão em todos estos anos, meus sinceros agradecimentos a Amarildo, Clara, M. José F.E., Regina, Z. Roberto, coordenador e demais funcionários.

A PEC/PG CAPES, sem qual não poderia ter chegado até aqui, por todo apoio e confiança recibidos. Que eu espero que continue sempre dando seu enorme apoio novas gerações de cientistas. Meus agradecimentos especiais a Cristina, obrigado por sua gentileza, também a à Conceção e Marilda.

A todos meus amigos, amigas que sempre dividiram seu tempo comigo, Abel H., Adolfo C., Amparo, Armando, Daniel E., Dante V., Janet, Juan J. L., Lecsi R., Mercedes, Nancy, Nery, Rodolfo; Alvaro, Elsa, Esmilthzinia S., Gustavo, Herman, Luis A., Luz Marina, Marivel, Mery H., Morante, Olimpia A., Patricia L., Tito, Walberto. Também à Elia C. N., Elmer, Erly A., Honorato, Jose Lujan., Hubert A., Maria P., Mario T., Monica V., Nicolas M., Pascual F., Pedro A., Victor. Ainda ao Alexandre, Andre, Aparecido, Cida, Cristina, Daniel, Diego, Edibaldo, Elba, Elenise, aos irmãos Fabio e Fernando, Gremis e esposa, Israel, Marcela, Michele, Milero, Tania, Shanti (aaooa...!), Urso, Valter D., Vera.

A todas as pessoas pelo apoio, colaboração, atenção, dedicação que de algum modo contribuíram para realização deste trabalho, muito (*añay, gracias, thanks, Dank*) obrigado.

F.L. Mendoza Marín

RESUMO

O modelo determinístico e processo homopolimerização na emulsão do estireno são aplicados em reator tubular contínuo sem e com deflectores angulares internos sob condição isotérmica e não isotérmica. Os resultados de modelagem e simulação foram realizados a estado estacionário, modelo unidimensional, coordenada cilíndrica, fluxo pistão laminar completamente desenvolvido, modelo Smith-Ewart para estimar a conversão do monômero, cinética química de Arrhenius como modelo de velocidade finita laminar para computar a geração química. O objetivo é modelar, simular e analisar o comportamento do reator de homopolimerização na emulsão do estireno com deflectores angulares inclinados internos, e comparar com reator tubular.

Os métodos experimental e matemático–dedutivo foram aplicados para obter resultados, por meio de programação computacional, usando Dinâmica de Fluido Computacional através do método de volumes finitos. As seguintes variáveis como temperatura de reação constante e variável, reator tubular sem e com deflectores, temperatura de alimentação, diâmetro de reator, processo adiabático e exotérmico, calor de reação constante e velocidade axial completamente desenvolvida foram investigados.

Os efeitos de conversão de monômero, área transversal interna, temperatura axial, concentração do polímero, radicais e iniciador, outros como densidade de polímero e monômero, perda de carga e queda de pressão foram determinados e simulados. Os produtos foram caracterizados com Número de Partículas (nucleação homogênea e heterogênea), distribuição de peso molecular, tamanho de partículas de polímero e distribuição de viscosidade. Estes resultados foram validados com resultados da literatura sob condição igual ou aproximada. Os resultados sob condições não isotérmicas foram melhores que os resultados isotérmicos em termos de caracterização do polímero. Isso mostra que o desenho alternativo proposto (com deflectores) permite obter o polímero com propriedades melhores em termos de número de partículas, distribuição de peso molecular, distribuição do tamanho de partículas e viscosidade.

Palavras chaves: modelagem, simulação, estireno, polimerização em emulsão, reator tubular, deflectores, Fortran, método dos volumes finitos.

ABSTRACT

Deterministic model and emulsion homopolymerization process of styrene are applied in continuous tubular reactor without and with internal angular baffles under isothermic and no isothermic conditions. The modeling and simulation results were approximate to steady state, one-dimensional model, cylindrical coordinate, fully developed laminar plug flow, Smith-Ewart model to estimate the monomer conversion, Arrhenius chemical kinetics as laminar finite-rate model to compute chemical source. The objective is to model, simulate and to analyze the emulsion homopolymerization reactor performance of styrene with internal-inclined angular baffles, and to compare with continuous tubular reactor.

The experimental and mathematical-deductive methods were applied to obtain results, by means of computational programming, using Computational Fluid Dynamics (program code), finite volume method. The following variables such as constant and variable reaction temperature, tubular reactor without and with baffles, feed temperature, reactor diameter, adiabatic and exothermic process, constant reaction heat and fully developed axial velocity were investigated.

The monomer conversion, internal transversal area, axial temperature, concentration of polymer, radicals and initiator, others as density of polymer and monomer, head loss and pressure drop effects were determined and simulated. The products were characterized by particles number (homogeneous and heterogeneous nucleation), molecular weight distribution, polymer particles size and polymer viscosity distribution. These results were validated with literature results under same or approximate condition. The results under no isothermic conditions were better than isothermic results in terms of polymer characterization. It is shown that the proposed alternative design (with baffles) allow to obtain the polymer with better properties in terms of number of particles, molecular weight distribution, particle size distribution and viscosity.

Keywords: modeling, simulation, styrene, emulsion polymerization, tubular reactor, baffles, Fortran, CFD, finite volume method.

SUMMARY

	Page
Resumo	vii
Abstract	viii
Summary	ix
Notation	xvi
Chapter I INTRODUCTION	02
Chapter II BIBLIOGRAPHICAL REVIEW	18
2.1 FORMULATION PRINCIPLES OF MATHEMATICAL MODEL	18
2.2 EMULSION POLYMERIZATION REACTION	20
2.2.1 Classical general theory about mechanism	21
2.2.2 Particle Nucleation	24
2.2.2.1 Micellar Nucleation	24
2.2.2.2 Homogeneous Nucleation	25
2.2.3 A Modern Theory about Mechanism	26
2.2.4 Kinetic Phenomenon of Polymerization Reaction	29
2.2.4.1 Cage Effect	29
2.2.4.2 Gel Effect	30
2.2.4.3 Glass Effect	30
2.3 EMULSION POLYMERIZATION REACTOR	30
2.3.1 Continuous Reactor	31
2.4 TRANSPORT EQUATIONS MODELING	32
2.4.1 Principle of Mass Conservation	32
2.4.2 Newton's Second Law of Momentum	33
2.4.3 Principle of Energy Conservation	33
2.4.4 Classification of Deterministic Model	34

2.5 COMPUTATIONAL-BASED KNOWLEDGE	34
2.5.1 Computational Fluid Dynamic	36
2.5.2 Computational in Chemical Reaction Engineering	38
2.6 TUBULAR REACTOR WITH INTERNAL ANGLE BAFFLES	40
Chapter III MATERIALS, PROPERTIES AND GENERAL METHODOLOGY	45
3.1 MATERIALS	45
3.1.1 Reactants	45
3.1.1.1 Monomer	47
3.1.1.2 Initiator	47
3.1.1.3 Surfactant	48
3.2 PROPERTIES	49
3.2.1 Physical Properties	49
3.2.2 Chemical Properties	50
3.2.3 Mechanical Properties	51
3.2.4 Transport Properties	51
3.2.5 Rheological Properties	51
3.2.6 Thermal Properties	52
3.2.7 Thermodynamic Properties	52
3.2.8 Geometrical Properties	52
3.2.9 Computational Parameters	53
3.3 GENERAL METHODOLOGY	54
Chapter IV MATHEMATICAL MODELING	56
4.1 PRINCIPLE OF MASS CONSERVATION	57
4.2 NEWTON'S SECOND LAW OF MOMENTUM	59
4.3 PRINCIPLE OF ENERGY CONSERVATION	60
4.4 EMULSION POLIMERIZATION REACTION MODELING	61
4.4.1 Micellar nucleation	61
4.4.2 Homogeneous nucleation	64
4.4.3 Balance of reactant	66
4.4.3.1 Initiator	66

4.4.3.2 Free Radical	66
4.4.3.3 Monomer	67
4.4.3.4 Surfactant	67
4.4.3.5 Polymer	67
4.4.4 Characterization of product	68
4.4.4.1 Particle Number	68
4.4.4.2 Molecular Weight	68
4.4.4.2.1 Active or living polymer chains	69
4.4.4.2.2 Instantaneous dead polymer	72
4.4.4.2.3 Cumulative dead polymer	74
4.4.4.3 Polymer Size	76
4.4.4.4 Viscosity of the polymer	76
4.5 EMULSION POLYMERIZATION REACTOR MODELING	77
4.5.1 Tubular Reactor without Internal Baffles	77
4.5.2 Tubular Reactor with Internal Baffles	79
4.5.2.1 Diameter of tubular reactor	79
4.5.2.1.1 Without baffles	79
4.5.2.1.2 With baffles: fixed, variable	79
4.5.2.2 Transversal area of tubular reactor	81
4.5.2.2.1 Without baffle	81
4.5.2.2.2 With baffle	81
4.5.2.3 Fluid Flow inside Tubular Reactor	84
4.5.2.3.1 Without baffle: Reynolds, velocity, head loss	84
4.5.2.3.2 With baffle: Reynolds, velocity, head loss	85
4.5.2.4 Length of baffle	86
4.5.2.5 Inclination angle of baffle	86
4.5.2.6 Lateral area of tubular reactor	87
4.5.2.7 Area of baffle	87
4.5.2.8 Internal area of tubular reactor	87
Chapter V COMPUTATIONAL TEST	89
5.1 MONOMER CONVERTION CALCULATION	90

5.2 AXIAL VELOCITY CALCULATION	90
5.3 AXIAL TEMPERATURE CALCULATION	91
5.4 CONCENTRATION OF POLYMER	92
5.5 CONCENTRATION OF RADICALS	93
5.6 CONCENTRATION OF INITIATOR	93
5.7 CONCENTRATION OF SURFACTANT	94
5.8 CONCENTRATION OF WATER	94
5.9 CHARACTERIZATION OF PRODUCT	94
5.9.1 Number of Particles	94
5.9.2 Molecular Weight	94
5.9.3 Polymer particles size	95
5.9.4 Viscosity of polymer particle	95
5.10 INTERNAL ANGLE BAFFLES EFFECT	95
5.10.1 Internal Transversal Area of Tubular Reactor	95
5.10.2 Axial Velocity of Tubular Reactor	97
Chapter VI NUMERICAL METHOD: FINITE VOLUME METHOD	100
6.1 CONSERVATION EQUATION	101
6.1.1 General formulation	101
6.1.2 Specific formulation	101
6.2 GRID GENERATION	103
6.2.1 Procedure	103
6.2.2 Boundary conditions	104
6.2.2.1 Inlet boundary	105
6.2.2.2 Outlet boundary	105
6.2.2.3 Wall boundary	106
6.2.2.4 Pressure boundary	106
6.2.2.5 Symmetry boundary	106
6.2.2.6 Periodicity boundary	106
6.3 DISCRETIZATION	106
6.3.1 Discrete approximation	106
6.3.1.1 Conservative balance	106

6.3.1.2 Linear approximation	107
6.3.1.3 Integration	112
6.3.1.4 Interpolation	115
6.3.2 Linear algebraic equations	115
6.3.2.1 Internal control volume	115
6.3.2.2 Minimum control volume	116
6.3.2.3 Maximum control volume	118
6.4 SOLUTION OF ALGEBRAIC EQUATIONS	119
6.5 CONVERGENCE	120
6.5.1 Isothermal condition	121
6.5.2 No isothermal condition	122
Chapter VII COMPUTATIONAL SIMULATION	124
7.1 PROGRAM CODE STRUCTURE	125
7.1.1 Isothermal condition	127
7.1.2 No isothermal condition	131
7.2 CONVERSION OF MONOMER	136
7.3 INTERNAL TRANSVERSAL AREA	138
7.4 AXIAL VELOCITY	139
7.5 AXIAL TEMPERATURE DISTRIBUTION	141
7.6 CONCENTRATION OF POLYMER	142
7.7 CONCENTRATION OF RADICALS	144
7.8 CONCENTRATION OF INITIATOR	147
7.9 NUMBER OF PARTICLES	149
7.10 MOLECULAR WEIGHT DISTRIBUTION	151
7.11 SIZE OF POLYMER PARTICLES	156
7.12 VISCOSITY DISTRIBUTION	159
7.13 CHARACTERISTICS OF BAFFLES	161
7.14 OTHER CALCULUS	162
7.14.1 Density of polymer and monomer	162
7.14.2 Head loss	163
7.14.3 Pressure drop	165

Chapter VIII VALIDATION	169
8.1 ANALYTIC VALIDATION	170
8.2 EXPERIMENTAL VALIDATION	173
8.3 COMPUTATIONAL VALIDATION	174
8.4 VALIDATION OF NUMBER OF PARTICLES	177
Chapter IX PERFORMANCE ANALYSIS OF THE NEW REACTOR	181
9.1 FEED TEMPERATURE	181
9.1.1 Conversion of monomer	181
9.1.2 Axial velocity	184
9.1.3 Number of particles	187
9.2 DIAMETER OF REACTOR	191
9.2.1 Conversion of monomer	191
9.2.2 Internal transversal area	195
9.2.3 Axial velocity	196
9.2.4 Number of particles	200
9.3 NUMBER OF BAFFLES INSIDE TUBULAR REACTOR	205
9.3.1 Conversion of monomer	205
9.3.2 Internal transversal area	206
9.3.3 Axial velocity	206
9.3.4 Axial temperature distribution	207
9.3.5 Concentration of polymer	207
9.3.6 Concentration of radicals	207
9.3.7 Concentration of initiator	207
9.3.8 Number of particles	208
9.3.9 Molecular weight distribution	208
9.3.10 Size of polymer particles	209
9.3.11 Density of polymer and monomer	209
9.3.12 Viscosity distribution	209
9.3.13 Head loss	210
9.3.14 Pressure drop	210

Chapter X RESULTS AND DISCUSSION	212
10.1 TUBULAR REACTOR WITHOUT BAFFLES	212
10.2 TUBULAR REACTOR WITH BAFLES	217
10.3 ISOTHERMAL AND NO ISOTHERMAL TUBULAR REACTOR	222
CONCLUSIONS	225
SUGGESTIONS	226
BIBLIOGRAPHY	227

NOTATION

<u>Symbols</u>	<u>Description</u>	<u>Unit</u>
<i>Latin</i>		
A	area	m ²
A _{ba}	area of baffle	m ²
A _{fb}	fixed area inside tubular reactor beneath or over baffles	m ²
A _{lr}	lateral area of tubular reactor	m ²
anrp	average number of radicals per particle	
A _r	area of tubular reactor	m ²
A _{t0}	total internal area of tubular reactor	m ²
A _{vb}	variable area of fluid flow inside tubular reactor beneath or over baffles	m ²
A _z	transversal area inside tubular reactor	m ²
B _b	base of baffle	m
C	molar concentration of solution	mol/L
C _{Et}	total concentration of emulsifier	mol/L
C _I	concentration of initiator (=CI)	mol/L
C _{Iin}	initial concentration of initiator	mol/L
C _j	the molar concentration of species j	mol/L
C _M	concentration of monomer: styrene (=CM)	mol/L
CMC	critical micelle concentration	mol/L
C _{Min}	initial concentration of monomer	mol/L
C _{Mw}	monomer concentration in water phase	mol/L
C _{N_p}	total particles number concentration	mol/L
C _{Npa}	concentration of particles at a point of the Series Taylor	mol/L
C _{Npin}	initial concentration of the particle numbers	mol/L

C_P	specific heat (0°C)	cal/K.g K
c_{pj}	specific heat of species j	kJ/kg K
C_{Ps}	concentration of polystyrene	mol/L
CR_w	concentration of radicals in water phase	mol/L
CR_{wa}	concentration of radicals at a point of the Series Taylor	mol/L
CR_{win}	initial concentration of radicals	mol/L
D_{AB}	mass diffusivity in a binary system	cm ² /s
D_f	fixed diameter in tubular reactor beneath or over baffles	m
D_h	hydraulic diameter	m
D_p	diffusivity of monomer radicals in polymer phase	dm ² /min
DP_n^c	cumulative number-average degree of polymerization (=DPnc)	
DP_n^i	instantaneous number-average degree of polymerization (=DPni)	
DP_w^c	cumulative weight-average degree of polymerization (=DPwc)	
DP_w^i	instantaneous weight-average degree of polymerization (=DPwi)	
D_r	diameter of tubular reactor	m
D_v	variable diameter in tubular reactor beneath or over baffles	m
D_{vb}	variable diameter of fluid flow in tubular reactor beneath or over baffles	m
D_w	diffusivity of monomer radicals in water phase	dm ² /min
E_d	activation energy of styrene decomposition	cal/mol
E_p	activation energy of styrene propagation	cal/mol
E_t	activation energy of styrene termination	cal/mol
f	laminar friction factor	
F	convective mass flux	Kg/m ² s
f_i	initiator efficiency	
\bar{g}	body force per unit mass	
g_r	acceleration due to gravity in radial direction	
$G(s)$	generating function of the dead polymer species	
g_z	acceleration due to gravity in axial direction	
g_θ	acceleration due to gravity in angle direction	
H_f	total lost of charge	m

Hff	lost of charge of form	m
Hffc	lost of charge of form by contraction	m
Hffe	lost of charge of form by expansion	m
Hfs	lost of charge of superficies	m
H _j	partial molar enthalpies	kJ/kmol
H(s)	generating function of the active polymer species	
I ⁻	primary radicals from initiator	mol/L
ID	interval of increments of diameter from the point of fixed diameter until total diameter	m
[I] _w	concentration of initiator in the water phase	mol/L
J _j	the molar flux vector for species j with respect to the mass average velocity	kmol/m ² s
K _{cm}	= $4\pi D_w r_{mic} N_A$; rate constant of aqueous phase radical capture by micelles	1/min
K _{cmd}	rate constant of desorption from micelles	1/min
K _{cmw}	rate constant of radicals diffusion in the water phase over micelle surface	L/min
K _{cp}	= $4\pi D_p r_p N_A$; rate constant of radicals captured by polymer particles	1/min
K _{cpd}	rate constant of desorption from polymer particle	1/min
K _{cpw}	rate constant of radicals diffusion in the water phase upon polymer particle	1/min
K _d	rate constant of initiator decomposition	1/min
K _{f_A}	rate constant of chain transfer to solvent	L/mol min
K _{f_{cta}}	rate constant of transfer to chain transfer agent	L/mol min
K _{fm}	rate constant of chain transfer to monomer	L/mol min
K _{fp}	rate constant of chain transfer to polymer	L/mol min
K _p	rate constant of propagation in polymer particles	L/mol min
K _p [*]	rate constant of chain transfer to terminal double bound	L/mol min
K _p ^{**}	rate constant of chain transfer to internal double bound	L/mol min
K _{pw}	rate constant of propagation in water phase	L/mol min
K _t	global rate constant for termination	L/mol min

Ktc	rate constant for termination by combination	L/mol min
Ktd	rate constant for termination by disproportionation	L/mol min
Ktw	rate constant for termination in aqueous phase	L/mol min
Kz	rate constant of chain transfer to inhibitor	L/mol min
Lb	length of baffle	m
Lbr	length of baffle separation	m
Lr	length of tubular reactor	m
\dot{m}	mass velocity	Kg/min
[MIC]	total micelle concentration	mol/L
\bar{M}_j	molecular mass of species j	g/mol
M_n^c	cumulative number-average molecular weight (=Mnc)	
M_n^i	instantaneous number-average molecular weight (=Mni)	
[M] _p	$= \frac{(1 - \phi_p) \rho_m}{MWS}$; monomer concentration in polymer particle (= [M])	mol/L
Mw	monomer concentration in the water phase(=[M] _w)	mol/L
M_w^c	cumulative weight-average molecular weight (=Mwc)	
M_w^i	instantaneous weight-average molecular weight (=Mwi)	
MW _j	molecular weight of species j, (j=i=initiator, j=s=styrene j=e= surfactant, j=w= water, j=p= polymer)	g/mol
\bar{n}	average number of radicals per particle (=anrp)	
N	number of finite volumes	
n%	molar percentage	
Na	Avogadro's number (6,02x10 ²³)	molecules/mol
Nab	Number of transversal area beneath or over baffles	
Nb	number of baffles	
nem	number of emulsifier molecules in a micelle	No.Emul/mic
n _j	mole fraction of j	
Np	total number of polymer particles concentration, Eq.(4.96)	mol/L
Np	total number of polymer particles per liter(=1/l)	#PP/L
[Npa]	concentration of number of particles in one point tangent	

	to one curve in Taylor's Series linearization	mol/L
N _{ph}	generated particles number by homogeneous nucleation	#PP/L
[N _p] _h	generated particles number concentration by homogeneous nucleation	mol/L
[N _p] _m	generated particles number concentration by micellar nucleation	mol/L
N _{pm}	number of particles generated by micellar nucleation	#PP/L
[N _p] _P	concentration of number of particles in nodal point P	mol/L
P	pressure	Pa
P _b	perimeter of the baffle base	m
P _r	polymer of chain length r, r=1, ..., n or m	
P _s	perimeter of sector circular	m
P _w	wet perimeter	m
q	probability of propagation (=p _r)	
Q	polydispersity, instantaneous (=P _{Oi}), cumulative (=P _{Oc})	
Q _{rad}	radiation heat flux	kJ/m ³
r	radial cylindrical coordinate	m
r _i	rate of reaction of the equation i	mol/ L min
R	unswollen particle radius (cnm= centimeter nm)	nm
R ₁	radical or oligomeric radical with chain length 1	mol/L
[R ₁] _w	concentration of free radicals of chain length 1 in the water phase	mol/L
Re	Reynolds number	
Re _b	Reynolds with baffle	
R _E	rate of reaction of surfactant	mol/L min
R _g	gas constant (1,987)	cal/mol K
R _{HN}	rate of particle formation by homogeneous nucleation	mol/L min
r _i	rate of reaction by volume for ith reaction	mol/L min
R _i	rate of initiation	mol/L min
[R _i] _w	concentration of free radicals of chain length i in the water phase	mol/L
R _j	total rate change of the amount of j because of reaction	mol/L min
R _M	rate of reaction of monomer styrene	mol/L min

r_m	radius of monomer	A
r_{mic}	radius of micelle	A
r_{mp}	radius of the micelle/particle	A
R_{MN}	rate of particle formation by micellar nucleation	mol/L min
R_{Np}	overall rate of formation of particles	mol/L min
r_p	radius of particle	A
R_P	rate of formation of polymer	mol/L min
R_r	radical of chain length r, $r=1, \dots, i, \dots, n$ or m	
R_{rMIC}	radical absorption by micelle	
R_{rPP}	radical absorption by polymer particle	
R_{rwMIC}	Radical of chain length r on the micelle surface	
R_{rwPP}	Radical of chain length r on the polymer particle surface	
R_{Rw}	rate of radicals formation in water phase	mol/L min
R_{rw}	radical diffusion of chain length r in the water phase	
R_s	swollen particle radius	
$[R]_w$	total free radical concentration in the water phase	mol/L
s	parameter of the generation function	
S_a	area covered by one molecule of emulsifier	$dm^2/\text{molecule}$
S_ϕ	volumetric source term of dependent variable ϕ	
t	time	min
T	temperature	K
Ta	temperature in a point of the Series Taylor	K
Tin	inlet temperature to the reactor	K
\vec{u}	the three dimensional molar-average velocity vector	m/min
V	control volume of nodal point	m^3
Vb	velocity of fluid flow inside tubular reactor beneath or over baffles	m/min
Vin	inlet velocity in tubular reactor	m/min
V_P	total volume of polymer particles	L
V_r	radial velocity	m/min
V_θ	angular velocity	m/min
V_z	axial velocity or transversal velocity	m/min

V_{z0}	initial axial velocity	m/min
w_j	mass fraction of j	
wt%	weight percentage	
X_M	conversion of monomer: styrene	
z	axial cylindrical coordinate	m
Greek		
α_h	probability for homogeneous propagation	
α_m	probability for micelle propagation	
α_r	angle of increment of fluid flow	rad
γ	inclination angle of baffle with tubular reactor wall	
Γ	diffusion coefficient	dm ² /min
ΔH	polymerization reaction heat of styrene	cal/mol
$-\Delta H_i$	heat of reaction of species i	kJ/kmol
ΔP_r	pressure drop (=DPr)	Pa
∇	nabla operator of scalar or vector function	
θ	angular cylindrical coordinate	
θ_g	angle of increment of fluid flow	grad
λ	thermal conductivity of the mixture	kJ/m s K
μ	viscosity	Kg/m.s
μ_k	moments k=0, 1, 2, ...	
π	angular constant ($\pi=PI=3,14159$)	
ρ	polymer density (=RHO)	Kg/L
ρ_0	initial density	Kg/L
ρ_p	polymer density	Kg/L
ρ_m	monomer density (styrene)	Kg/L
$\bar{\sigma}$	total stress tensor	1/min
$\bar{\tau}$	extra stress tensor	Pa/m ²
τ_{rr}	normal stress tensor in radial direction	
τ_{zz}	normal stress tensor in axial direction	
$\tau_{\theta\theta}$	normal stress tensor in angle direction	

$\tau_{\theta r}$	tangential stress tensor of the plane $\theta r=r\theta$	
$\tau_{\theta z}$	tangential stress tensor of the plane $\theta z=z\theta$	
τ_{zr}	tangential stress tensor of the plane $zr=rz$	
ϕ	the general dependent variable of the conservative form	
ϕ_m	volume fraction of monomer	
ϕ_p	volume fraction of polymer	
Ω	cross section inside the rigid boundary	m^2

Subscripts

h	homogeneous nucleation
i	chain length
j	species or elements
m	micelle nucleation
w	water phase

Superscripts

i	chain length
ncr	critical chain length at which water phase radical can be absorbed

Abbreviations

ca	colloquially also
C0	conversion of styrene without baffles in isothermic condition
CTA	chain transfer agent
eg	exempli gratia (for instance)
I ₂	initiator
ie	id est (that is)
KPS	potassium persulfate
M	monomer
MIC	micelle
PP	polymer particle or polystyrene particle
S	solvent
SDS	sodium dodecyl sulfate

V0	conversion of styrene with baffles in no isothermic condition
Z	inhibitor

Acronym

CFD	computational fluid dynamics
CSTR	continuous-flow stirred-tank reactor
EP	emulsion polymerization
EPS	emulsion polymerization of styrene
HN	homogeneous nucleation
LBR	loop fluidized bed reactor
MN	micellar nucleation
NSLM	Newton's second law of momentum
PEC	principle of energy conservation
PMC	principle of mass conservation

RESUMO DO CAPÍTULO I

MENDOZA MARÍN, F.L. *Modelagem, simulação e análise de desempenho de reatores tubulares de polimerização com deflectores angulares internos*, 241p. Tese (Doutorado em Engenharia Química – Área de Processos Químicos) – Faculdade de Engenharia Química, Universidade Estadual de Campinas - UNICAMP, 2004.

O Capítulo I apresenta uma visão global da pesquisa desenvolvido nesta tese, incluindo a motivação da pesquisa, breve históricos da reação de polimerização em emulsão e de reatores de polimerização com ênfase na obtenção do estireno e poliestireno. Discute-se ainda a importância do uso das chicanas como misturadores estáticos. Apresenta-se também a organização da tese.

CHAPTER I

INTRODUCTION

The present work makes use of knowledge related to physical-chemistry and mathematical science, applied chemistry and computational science applied to the development of deterministic models and polymerization process. In particular is considered the emulsion polymerization mechanism for the homopolymerization of styrene. Deterministic models for a tubular reactor were developed for a conventional tubular reactor as well as for a system with internal incrustated angular baffles.

Plastics are mayor industrial goods used in the building, construction, packing, transportation, electronic, appliances, etc., industries. The world plastics production was estimated at about 100 million tons. Plastic can be in general classified into thermoplastics, thermosetting resins and engineering plastics (Elias, 1993).

The two mayor tasks facing engineers and scientists in chemical industry are (1) the operation and optimization of existent process and (2) the design of new or improved ones. Bearing this in mind, in this work is proposed an alternative design for tubular reactor where a polymerization reactor takes place, by the introduction of angular baffles inside the reactor.

Motivation

The development of engineering and specialty polymers with a better balance of properties or with a particular unique property has been growing rapidly. In this regard, it has been found to be often more economic to produce a new polymer from existing commodity polymers rather than to start with a new monomer and produce polymer in the usual manner (Seppala and Reichert, 1990).

A rational approach to all problems relating to a physical or chemical change of mass must be based on elementary physical conservation laws. They have been handled systematically in Bird (1960) and Beek (1975) for example. For the treatment of chemical

engineering phenomena, the laws of conservation of mass and energy are of primary importance. Flow phenomena, governed by the principle of conservation of momentum, naturally are equally important for chemical engineering calculations. The second kind of information needed for a quantitative treatment of chemical engineering is concerned with rates. The rate at which a reaction proceeds may be determined not only by the chemical kinetics of the reaction proper, but also by physical transport phenomena (Westerterp and Wijngaarden, 1992).

The interaction between chemical kinetics and physical transport rates has received considerable attention during the past decades. Damköhler (1957), and particularly Frank-Kamenetzki (1969) have systematically developed this field. The later author distinguished between microkinetics (i.e. chemical kinetics) and macrokinetics (i.e., physical rate). Many scientists (e.g., Van Krevelen, 1958; Astarita, 1967; and Danckwerts, 1970) have stressed the importance of the scale of scrutiny, at which the phenomena in a reacting system are considered. In principle, three different scales must be taken into account: 1) The scale of a molecule, where, for example, molecular collision and the molecule mean free path (diffusion) are studied; 2) The scale of an eddy or dispersion in a heterogeneous system, where, for example, a catalyst particle or a gas bubble is taken as the basis for deriving the appropriate equations; 3) The scale of a reactor as a whole, where small-scale phenomena must be integrated over the entire reactor and macroscopic mixing becomes important (Westerterp and Wijngaarden, 1992).

This work is mainly concerned to the last scale although knowledge of the first two items are in fact incorporated in the kinetic and transfer parameters used in the simulation.

Computation

The history of calculating devices reaches well beyond the boundaries of the history of science; business and accounting have made routine use of reckoning aids, and many special purpose tools have been devised to reduced the burden of calculation within engineering disciplines. Today powerful computers have become almost universally available in both schools and industry. During the period when the analog computer was used to solve process dynamics problems (1955-1965), there existed, by necessity, a specialized at staff computer installation that performed the programming and computer operation chore for clients with problems to be solved. The analysis of the problem, that is,

its definition in mathematical terms, was performed by either the client or the computer specialist, or sometimes both in collaboration. During the middle and late 1960s, the digital computer, because of its increase in speed and size, and the accumulation of library routines, became the favored computer for chemical process simulations. The advent of digital simulation with user access to library routines that perform a wide variety of calculations has enabled sophisticated simulator tools to be developed (Franks, 1972; Hessenbruch, 2000). Among those the computational fluid dynamics (CFD) concepts are very usual ones.

CFD is the analysis of systems involving fluid flow, heat transfer and associated phenomena such as chemical reactions by means of computer-based simulations. The technique is very powerful and spans a wide range of industrial and non-industrial applications areas. Some examples are: hydrodynamics of ships, power plant: combustion in IC engines and gas turbines, chemical process engineering: mixing and separation, polymer moulding, etc. The ultimate aim of developments in the CFD field is to provide a capability comparable to other CAE (Computer-Aided Engineering) tool such as stress analysis codes. The main reason why CFD has lagged is the tremendous complexity of the underlying behavior, which preclude a description of fluid flows that is at the same time economical and sufficiently complete (Versteeg, 1998).

In these times computer science is an engineering science, an empirical science of the artificial rather than the natural world, so in category not allowed for in the standard division (Makowsky, 1994; Newel and Simon, 1976). Like other empirical engineering science, it conducts experiments and constructs theories to explain the results of them (Burkholder, 2001).

Polymers

The worldwide production of synthetic polymers, now estimated at ca. 100×10^6 t/a (Seppala and Reichert, 1990), continuous to grow in spite of criticism from environmentalists. The technical principles of polymer reaction engineering will no doubt play a significant role in the solution of some of these problems.

Polymers are macromolecules in which at least a thousand atoms are linked together by covalent bonds. They may be linear chains or three-dimensional networks. Many natural substances, especially the biological construction materials, are macromolecules. In

contrast with these complex natural macromolecules, many synthetic macromolecules have a relatively simple structure, since they consist of identical constitutional repeating units (structural units). In essence there are only two really fundamental characteristics of polymers: their chemical structure and their molecular mass distribution pattern. These fundamental characteristics determine all the properties of the polymer. In a direct way they determine the cohesive forces, the packing density (and potential crystallinity) and the molecular mobility (with phase transitions). In a more indirect way they control the morphology and the relaxation phenomena, i.e. the total behavior of the polymer (Van Krevelen, 1990).

Process parameters, such as residence-time distribution, micromixing, and segregated flow, whose influence on productivity and selectivity for small molecule reactions has been studied for many years, appear to be far more important for polymerization reactors in that they influence polymer properties dramatically (Gerrens, 1981, 1982; Ray, 1983; Sebastian and Biesenberger, 1983; Reichert and Moritz, 1989, Seppala and Reichert, 1990).

It should be emphasized that product quality is a much more complex issue in polymerization process than in conventional short chain reaction since the molecular morphological properties of a polymer product strongly influence its physical, chemical, thermal, rheological, mechanical properties as well as the polymer's end-use applications. Therefore, the development of comprehensive mathematical models to predict the "polymer quality" in terms of process operating conditions in a polymer reactor is the key to the efficient production of high quality, tailored polymers and improvement of plant operability and economics (Kiparissides, 1996).

Bearing this in mind, in this work the proposed reactor configuration is considered as a mean to be able to obtain polymers with better controlled properties.

As case study styrene is considered since the required information are available in open literature. Styrene (known as styrax) was first isolated in 1831 by Bonastre from the resin of the amber tree. In 1839 E. Simon, who also first described the polymer, gave the monomer its name. He observed that styrene was slowly converted into a viscous solution on standing. The styrene used for polymerization should have a purity greater than 99,6%

because the contaminants arising from the production process, mainly ethylbenzene, cumene, and xylenes, affect the molecular mass of the polystyrene (Maul and Hüls, 1992).

Polystyrene belongs to the group of standard thermoplastics that also includes polyethylene, polypropylene, and poly (vinyl chloride). Because of its special properties, polystyrene can be used in an extremely wide range of applications. The annual consumption worldwide in 1990 was ca. $6,7 \times 10^6$ ton; thus polystyrene is one of the most quantitatively important chemicals (Maul and Hüls, 1992; James and Castor, 1994).

The industrial polymerization of styrene to PS (polystyrene molding material) and HIPS (high-impact polystyrene) molding materials is carried out exclusively by a free radical mechanism. The chain reaction does not necessarily have to be started by the addition of radical-forming, readily decomposing initiators because styrene itself can form polymerization-initiating radicals (Hui and Hamielec, 1972, Hui et al., 1983). The propagation mechanism for the chain growth proceeds by addition of further monomer to the radical chain end. Growth of the radical chains is mainly terminated by recombination (disproportionation plays a very minor role). The grown of chain proceeds rapidly with the result that removal of the generated heat of polymerization presents one of the main problems of the industrial process. Average molecular weight between 100000 and 400000 are obtained within a short time (Maul and Hüls, 1992).

Emulsion Polymerization Process

From a contemporary perspective, the interlinked scientific and technical history of emulsion polymerization can be divided into three periods: The first period (termed *Heroic Age*) was when emulsion polymers were originally produced. The results were functional but limited. The natural rubber which is found in the form of a latex, was interpreted technically at a false logic as addition polymerization, but it seen to have really been suspension polymerization, they did not involve a true emulsion polymerization because they did not have any surfactant and/or water-soluble initiator (Blackley, 1975). The first attempts to develop a process to imitate natural rubber were made in Germany during the First World War. This led to the work of Luther and Hueck (1932) in Germany, who presented the first viable emulsion polymerization method and thereupon sold the patent rights to interested parties in the United States. Major development in emulsion polymerization took place during the second World War, when the artificial rubber project

was of Manhattan Project dimensions (and indeed some of the work from this project was only declassified in 1980). Although some papers on emulsion polymerization appeared prior to World War II, it was not until the period immediately subsequent to the war that the most widely accepted qualitative (Karkins, 1947) and quantitative (Smith and Ewart, 1948) theories of emulsion polymerization were first enunciated (Gilbert, 1995).

The second period in emulsion polymerization might be termed the *Age of Exploration*. The period of the 1950s through to the 1980s saw a rapid blossoming in the range and variety of products, and enormous research efforts to produce better quality. Industrial efforts were frequently based on empirical trial and error; extensive formulations with a range of ingredients and conditions, gradually working towards a product with the desired qualities. Mechanistic principles were used less than optimally for guidance, and some of the supposition on which this limited guidance was based were not correct. At the same time as industrial laboratories were vastly refining and extending their products, extensive pure research efforts were undertaken in many academic, government and industrial laboratories on the fundamental science of emulsion polymerization. Many of the important concepts in this second period were developed by, for example, Fitch, Gardon, Vanderhoff, Ugelstad and Hansen (Gilbert, 1995).

The third period of emulsion polymerization might be termed the *Age of Enlightenment*, and is now dawning. The scientific effort of many teams over previous decades, aided by the advent of new physical techniques for investigation, has resulted in a sound understanding of the most of the fundamental mechanism governing emulsion polymerizations. The fundamentals are now sufficiently well understood that new products can be made, and old ones re-formulated, in new ways that can lead to a quantum leap in performance and production characteristics. Intelligent, knowledge-based design is the way of the future for this important technology (Gilbert, 1995).

Emulsion polymerization is economically important: for example, in Western countries alone, current production of all polymers in excess of 10^8 tonnes per year, and approximately 30% of these polymers are made by free-radical means; emulsion methods are used for 40-50% of these free-radical polymerizations. There are thus considerable incentives for understanding emulsion polymerization processes (Gilbert, 1995).

Emulsion polymerization is one of the most important techniques for the commercial production of polymers (Basset and Hamielec, 1981; Piirma, 1982; Poehlein et al., 1983). Economics favor a continuous process over a batch system when product volumes are large enough or when product grades differ slightly. A continuous process also offers improved quality by eliminating batch to batch variations. A continuous stirred-tank reactor (CSTR) and tubular reactor are two potential candidates for such a process (Paquet and Ray, 1994).

Emulsion polymerization is a heterogeneous reaction process in which unsaturated monomers or monomer solutions are dispersed in a continuous phase with the aid of an emulsifier system and polymerized with free-radical initiators. The product, a colloidal dispersion of the polymer or polymer solution, is called latex. The chemistry involves free-radical reactions that are common to many bulk, solution, and suspension polymerization systems, but the physical degree of subdivision of the reaction mixture in the colloidal size range can have a pronounced influence on the course of the polymerization and the characteristics of the product and its performance (Basset and Hamielec, 1981; Piirma, 1982; Poehlein et al., 1983). This claims to better mixing properties reactors design, especially when tubular systems are taken into account.

The product latex, a submicron suspension of colloidally stable polymer particles in (usually) aqueous medium, has many desirable properties. The low viscosity of the latex reduces pumping and agitation equipment requirements and improves heat transfer to the reactor walls. The heterogeneous nature of the process enables the simultaneous achievement of high molecular weight polymer and high reaction rates in many cases. Latices call also have desirable properties in coating applications so that performance and experimental concerns suggest an increased use of aqueous-based products for architectural and structural coatings (Paquet and Ray, 1994).

Emulsion polymerization is a process in which most of the propagation reaction takes place in the segregated particles (50-1000 nm in diameter) dispersed in water. These innumerable particles can be stabilized by anionic surfactants which impart repulsive forces between similarly charged electric double layer to the emulsion polymer (Chern, 1995).

If emulsion polymerization is used for the production of engineering plastics or artificial rubber, the polymer is collected from the water phase. As mentioned previously

specific advantage of the emulsion polymerization process, compared to other polymerization techniques, is the low viscosity of the continuous water phase. Furthermore, the segregated nature of the polymerization process, taking place in the individual particles, allows the production of high molecular mass polymers at considerable higher polymerizations rates compared to bulk or solution polymerization (Scholtens, 2002).

A drawback of using emulsion polymerization for the production of the polymers is that some additives, e.g. emulsifier and initiator, may be difficult to remove and might affect the product properties in a negative way. Additionally, if the polymer is separated from the water phase, e.g. by precipitation, the effluent has to go through a costly wastewater treatment (Scholtens, 2002).

Reactors

The reactor provides the volume necessary for the reaction and holds the amount of reactant required for the reaction. The energy required to overcome the activation threshold of each partial reaction is also supplied in the reactor, and the proper temperature and concentration are maintained. The most important reaction-related factors for the design of a reactor are: 1) The activation principle selected, together with the states of aggregation of the reactants and the resulting number and types of phases involved; 2) The concentration and temperature dependence of the chemical reactions; 3) The heat of the reaction taking place (Henkel and Schkopau, 1992).

The (negative or positive) heat of reactions taking place in a reactor influences the extent and nature of provisions for heat transfer. Exothermic or endothermic reactions frequently require supply or removal of large quantities of heat. Thermally neutral reactions involve considerably less technical sophistication (Henkel and Schkopau, 1992).

Three major types of chemical reactor systems are used to produce emulsion polymers; batch, semicontinuous, and continuous. Continuous reactors are operated with continuous, and it is hoped, steady input flows of reagents and output flows of products. Such reactor are generally economically advantageous when high production rates of closely related products are required. Continuous systems are not used if rather long run times cannot be achieved. Thus, latexes that foul badly and cause frequent shutdowns are usually produced in batch or semicontinuous reactors. Likewise, continuous reactors are not

practical for product distributions which require frequent, significant recipe changes (Piirma, 1982).

The use of a *tubular reactor* for polymerization is an attractive concept due to simplicity of design and potential low cost. A monomer is introduced at beginning of the tube and, if all goes well, a high molecular weight polymer emerges at the other. Practical implementation of this concept is, however, fraught with difficulties because of large reaction exothermic, high viscosities and laminar flow (Chen and Nauman, 1989).

In a tube are two kinds of flow, laminar and turbulent, depending upon the velocity and viscosity of the fluid and the diameter of the tube. In laminar flow, fluid in the center of the tube flows faster than that near the walls, so that residence times in the reactor will be widely different, leading to an extremely broad distribution of conversion and other properties of the product. In turbulent flow, there is good mixing across the diameter of the tube, resulting in essentially plug flow, where very small “plug” or volume of the reaction mixture spends the same amount of time in the reactor as all others. But turbulence occurs only at high flow velocities, as measured by the Reynolds’s number. Turbulence usually occurs at Reynolds > 2000 in pipes. It is possible to overcome the limitations of laminar flow by introducing gas bubbles at regular intervals, thereby isolating plugs of the reaction mixture. This can only be done, though, on laboratory scale where the diameter is sufficiently small so that the bubbles fill the entire cross-section of the tube. In either case the plugs can be considered as minute batch reactors, and batch reactor theory should be applied (Fitch, 1997). Otherwise some mechanical design alternatives as the proposed on this work have to be investigated.

Modeling - Simulation

Mathematical model is used to formulate widely different physical and physicochemical phenomena: transfer of heat, mass, and momentum, as well as chemical reactions in homogeneous and heterogeneous systems. Mathematical modeling is thus used in the design of mass-transfer operations, calculation of heat exchangers, chemical reaction engineering, and finally process control. A wide range of methods are used to formulate models and to solve the resulting systems of equations. Mathematical models can be classified according to their physical background, the type of system of equations, and the corresponding methods of solution. Deterministic models or model elements have a

determined value or set of values for each variable or parameter for any given set of conditions (Bockhorn, 1992).

Since 1980, modeling of polymerization reactors has become more comprehensive. Interest has focussed on the prediction of polymer properties (chemical composition and molecular mass distribution, long-chain branching, cross-link density, polymer particle size distribution, and particle morphology). To develop a predictive model, account must be taken on the chemistry and physics of all relevant microscopic processes which occur in the polymerization process (Hamielec and Tobita, 1992).

Internal Baffles

Due to the complexity of the flow cross-section, mixed convection in internally finned tubes was considered only in a limited number of analytical studies. Prakash and Patankar (1981) solved numerically the case of fully-developed, laminar mixed convection in vertical tubes. This orientation simplified the analysis since the pertaining flow is purely axial and identical conditions exist in the bays formed by any two adjacent fins. Mirza and Soliman (1985) analyzed mixed convection in the horizontal orientation; however, the cross-section was simplified by considering only two identical vertical fins. In both investigation, the presence of the fins was found to retard and suppress the free convective effects compared to smooth tubes (Rustum and Soliman, 1990). The presence of internal fins alters the flow patterns, temperature distribution and Nusselt number of the configuration when buoyancy effects are not negligible (Farinas et al., 1997).

The *chemical reaction* inside reactor can be considered as simple or multiple, homogeneous or heterogeneous, catalytic or no catalytic, exothermic or endothermic, reversible or irreversible type. The chemical reaction in the present thesis is a heterogeneous, exothermic and irreversible polymerization reaction, particularly emulsion homopolymerization of styrene, a compound complex process of three phases in general such as gas, liquid and solid, and other phases as bubbles, vapor and drops, in those mentioned phases can be present the monomer drops, the micelles, monomer-polymer and ions emulsifier. The styrene and other reactants like initiator, surfactant and water mainly react to produce polystyrene. Polystyrene is a system with very low monomer and polymer solubility in water and very high monomer solubility in polymer. In a chemical reactor can happen thermal, catalytic, biochemical and polymerization process. The operations in the

chemical reactor can be discontinuous, semi-continuous or continuous (tubular with plug flow and tank with perfect agitation), a reactor or several reactors, isothermic and no isothermic, transient or stationary, catalytic (homogeneous, pseudo homogeneous and heterogeneous (fixed bed, fluidized bed, transport reactor)) or no catalytic, competitive or contraflow or crossed current refrigeration. In the present thesis will be considered tubular reactor like emulsion polymerization reactor, operating in continuous, plug flow, isothermic, no isothermic, stationary, no catalytic and without or with baffles inside tubular reactor (Min and Ray, 1974; Carberry, 1976; Kumar, 1978; Piirma, 1982; Levenspiel, 1983 a, 1983 b; Fogler, 1986; Froment and Bischoff, 1990; Van Krevelen, 1990; Gilbert, 1995; Dotson, 1996; Fitch, 1997).

The Tubular reactors have the advantage of simplicity, relatively low cost of maintenance and flexibility operation. When the reactions happen to high temperatures and pressures and with solid catalyst, they present facilities with relationship to other projects for the temperature control of the given heat or removed. Furthermore for the fact they have not had mechanical motion of their parts they are convenient for high pressures. The tubular reactors present some disadvantages for their high degree of specificity, frequently with complicated project and high cost of investment and they will sometimes be subject to high pressure drops. The use of tubular reactors at the moment it is growing and diversified by the advance of fundamental knowledge, the prediction of parameters (mass, heat, transport, momentum), data collection systems, data analysis methods, data solutions methods (numeric, differential equations), high acting computers and the reactors costs reduction (Tarmy, 1982; Shah, 1991; Henkel et al., 1992; Farkas, 1992; Toledo, 1999).

In the tubular reactors multiple applications in the chemical industry arise heat transfer no standardize difficulties, the most reaction happens in the reactor entrance, the reaction rate is variable at the reactor entrance for exothermic reactions, the exothermic adiabatic operation conditions show the axial temperature different to the wall temperature and the endothermic adiabatic operation conditions present the wall temperature different to the axial temperature. In such situations have been offered different solutions types like using multi-tubular reactors (McGreavy e Maciel Filho, 1988), to improve bed conditions, to use solvents, catalytic dilution, external refrigeration temperature and reactor internal temperature control (Domingues, 1992; Maciel Filho e Domingues, 1992).

Justification

One can notice through behavior analysis of the industrial polymerization reactors (specially through computational simulation) that the thermal transfer limitations in systems with viscous fluids (with aggravating that the viscosity varies with the operational conditions) cause significant restrictions to the generated product quality control, hindering the desired specifications obtaining. Clearly new reactor projects have been idealized and tested looking for to reach high operational performance, that can be achieved with high conversions, smaller residence times and a better thermal conditions control.

A reactor project without a detailed model is impossible to make reliable predictions because the regions localization with unstable behavior in the time and space are dependent of the entrance interferences and control actions (McGreavy e Maciel Filho, 1989).

With regard to the modeling objectives can be the project study, operation and optimization of existent processes, design of new processes or to improve some processes or processes control, e.g. the models used by Moura (1984), Maciel Filho (1985) and Domingues (1992). Moreover model type and its complexity level in the system representation depends of the use for which the model will be developed (Khanna and Seinfeld, 1987). A pragmatic guideline for a simplification according to Azevedo et al. (1990) are the model should not be more detailed than the absolutely necessary for the implicated particular purpose, the model should contain so few parameters as much as possible, the reliable correlation should exist for the selected model parameter, the required effort mathematics/computational for the model solution should be reasonable. Others the models sometimes can be reduced for different techniques, as those developed by McGreavy and Naim (1977), McGreavy (1983), Maciel Filho (1989), McGreavy and Maciel Filho (1989), Stremel et al. (1997), 1998, 1999), Toledo and Maciel Filho (1997 a, 1997 b, 1997 c).

According to the simulation objectives show in the stage of chemical reactor project, the departure and stop strategies, the control and optimization of process, the static and dynamic analysis of the system behavior. In agreement to the control objectives are the product quality, operational security, process economy, understanding of the nature and characteristics of the system, obtaining of control algorithm, variables modification, to obtain control strategies or to apply in real time. Moreover, the reactor-project objectives

are in general the obtaining of quality products, operational security and process economy (Toledo, 1992, 2000; Toledo and Maciel Filho, 1997 a, 1997 b, 1998 a, 1998 b).

In the emulsion polymerization tubular reactor, the reactive mixture and the heat transfer limitations affect the polymerization reaction and hence the product quality.

General Scope

In the present work is considered the emulsion polymerization of styrene, in an alternative tubular reactor with internal baffles. The mathematical modeling considers the axial concentration, temperature and polymer properties variations. The fluid flow axial velocity was considered fully-developed. A physical-chemistry characterization model for the polymer number by homogeneous and heterogeneous nucleation was developed, and the method of moments was applied to live and dead polymers in order to determine the molecular weight distribution. The resulting systems of equations correspond to a partial differential equations system. This equation system was discretized in linear system and solved by the finite volume method. The adopted kinetic model considers the initiation, propagation and termination by combination mechanism. The speed dependence of termination and propagation with the molecule diffusional limitation (gel and glass effect respectively) were not considered in the kinetic model. The styrene reaction is used as case study. A performance analysis of internal angular baffles inside the emulsion polymerization tubular reactor is carried out, and the results obtained by computational fluid dynamics (program code in Fortran), are compared with polymerization tubular reactors without baffles, and the literature results.

Hypothesis

The emulsion polymerization tubular reactor (EPTR) has a reactive mixture and internal and external heat transfer limitation for lack of an appropriate mixture and agitation of the reactive elements, for lack of higher contact among the reactive elements inside reactor. Placing angular baffles as static mixers inside the reactor would be possible to improve the reactive mixture and the heat transfer, in consequence the optimum process and a better quality product would be achieved. The results obtained by computational fluid dynamics (program code in Fortran) would be compared with the literature results for the model validation. As far the baffles could also vary the flow direction, to control the total flow, to change a determined region, to improve the reactive mass mixture, higher contact

among the reactive mixture, to improve the heat transfer, to uniformize radial and axial temperature, bigger increase of the superficial area of heat transfer, to improve the conversion radial and to economize the energy.

Objectives

The general objective is to model, to simulate and to analyze the emulsion homopolymerization tubular reactor performance of styrene with internal-inclined angular baffles, and to compare with continuous conventional tubular reactor. The specific objectives are:

- 1) To developed a representative model that is capable of to describe, to predict and to reproduce the essential characteristic of the system in agreement with the emulsion polymerization reactor performance of styrene. In the emulsion polymerization reactor will be considered the effects of the feed temperature, reactor diameter, internal baffles (geometry, location, distribution and number of baffles) in the reactor performance.
- 2) To predict the simulation through finite volume method, and to use deterministic mathematical model to determine the reactor performance in specific condition.
- 3) To analyze the sensibility of the system, the first effect of operation and project by means of computational fluid dynamic (program code in Fortran).

Thesis Organization

The Chapter I presents the introduction, the Chapter II describes the literature scientific foundations about modeling, simulation, emulsion homopolymerization of styrene, and internal angular baffles inside tubular reactor. Chapter III provides data that are used in the Fortran programs and simulations, mainly in Chapters VII, VIII and IX, respectively.

In Chapter IV is presented the global models of physics-chemistry principles on base the deterministic model that includes mass, momentum and energy conservative equations for emulsion polymerization reaction and reactor without and with baffles. The developed mathematical models in Chapter IV are used directly in the Chapter V and indirectly in the Chapters VI, VII, VIII and IX. Chapter V describes the mathematical models that were used according to the approximations, simplifications, suppositions, assumptions, estimation and limitations in the programs code (Visual Compaq Version

6.1), and the simulation results. The approximations, simplifications, suppositions, assumptions, estimation and limitations were deduced from Chapter IV to reproduce the investigated phenomenon with essential characteristics. These models are applied in the Chapters VII, VIII and IX. Chapter V shows the final mathematical models that were used in the programs and the simulations, respectively.

The numeric method of finite volume that was applied to solve the resulting mathematical models is described in the Chapter VI. In this chapter is showed the application of the finite volume method to the resulting mathematical models, e.g. particles number, which can be extended for monomer conversion, temperature, concentration of polymer, radicals and initiator.

Chapter VII contains the programs structure and the computational simulation results. In This Chapter is used the information of the Chapters IV and V, and shows the results of the Chapter V. Chapter VII shows simple programs code structure at isothermic and no isothermic conditions, without and with internal angle baffles inside tubular reactor in steady state; it shows all simulation results by means of deterministic models in combined balance of mass, velocity, energy, reaction and reactor-baffle.

Chapter VIII describes the verification and validation of computational results with literature results. This chapter allows to validate the approximations, simplifications, suppositions, assumptions, estimation and limitations that were made in the mathematical models and were approached to the phenomenon.

Chapter IX shows the performance of tubular reactors without and/or with baffles under other different conditions from those ones presented in Chapter VII, in order to analyze the baffles presence inside tubular reactor. This Chapter take account the same approximations, simplifications, suppositions, assumptions, estimation and limitations already applied in Chapter VII.

Chapter X represents the results discussion of the present thesis in comparative form, without and/or with baffles inside tubular reactor under isothermic and no isothermic conditions. Chapter X uses the information of the Chapters VI, VIII and IX. Chapter X allows to examine and to obtain some explanations and conclusions on the investigated phenomenon.

RESUMO DO CAPÍTULO II

MENDOZA MARÍN, F.L. *Modelagem, simulação e análise de desempenho de reatores tubulares de polimerização com deflectores angulares internos*. 241p. Tese (Doutorado em Engenharia Química – Área de Processos Químicos) – Faculdade de Engenharia Química, Universidade Estadual de Campinas - UNICAMP. 2004.

O Capítulo II apresenta uma descrição dos fundamentos científicos mais significativos, essenciais e importantes sobre os modelos matemáticos, simulação, reação de homopolimerização em emulsão do estireno e deflectores angulares dentro do reator tubular. Foram também apresentados os fundamentos científicos necessários para entender e compreender os termos aplicados na tese, interpretar os resultados de modelagem e simulações e os programas de Fortran desenvolvidos. Os objetivos do Capítulo II são: descrever os princípios básicos da formulação dos modelos matemáticos, da reação de polimerização em emulsão, do reator de polimerização em emulsão, modelagem de equações de transporte (massa, momento e energia); descrever os conhecimentos sobre computação e reator tubular em relação às deflectores e aleitas.

Conclusão do capítulo II: No Capítulo II os conhecimentos descritos formaram uma base suficiente para entender, compreender e interpretar os resultados de simulação e a proposição do mecanismo do processo de polimerização em emulsão baseado nas teoria clássica e moderna. Também foram apresentados os desenvolvimentos dos mecanismos que descrevem a nucleação das partículas homogênea e heterogênea no processo de emulsão considerados.

CHAPTER II

BIBLIOGRAPHICAL REVIEW

In this chapter it is described the relevant literature review about modeling, simulation, emulsion homopolymerization of styrene, and internal angular baffles inside tubular reactor. These knowledge are necessary to understand and to comprehend the applied terms in the present thesis, to interpret the modeling and simulation results. The contents are as follow:

- 1) Formulation principles of mathematical models.
- 2) Emulsion polymerization reaction.
- 3) Emulsion polymerization reactor.
- 4) Transport equations modeling.
- 5) Computer-based knowledge.
- 6) Tubular reactor with internal angle baffles.

2.1 FORMULATION PRINCIPLES OF MATHEMATICAL MODELS

The bases for mathematical models are the fundamental physical and chemical laws, such as the law of conservation of mass, energy, and momentum as shown in Figure 2.1. To study dynamics the general form with time derivatives is included (Luyben, 1990).

Assumptions mean probably the most vital role that the engineer plays in modeling and is in exercising his engineering judgment as to what assumptions can be validly made as shown in Figure 2.1. Obviously an extremely rigorous model that includes every phenomenon down to microscopic detail would be so complex that it would take a long time to develop and might be impossible to solve. An engineering compromise between a rigorous description and getting an answer that is good enough is always required. This has been called "optimum sloppiness". It involves making as many simplifying assumptions as

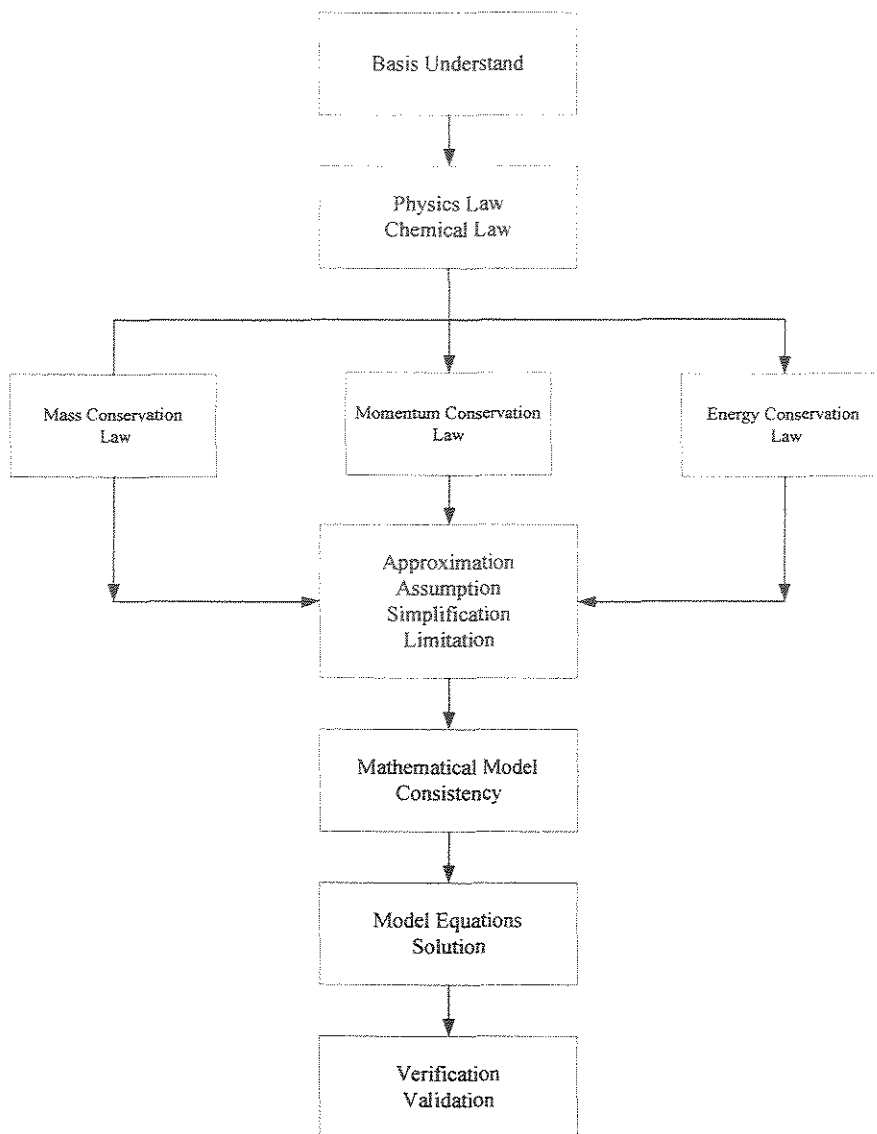


Figure 2.1 Schematic representation of the basis principles of mathematical model formulations.

are reasonable without “throwing out the baby with the bath water.” In practice, this optimum usually corresponds to a model which is as complex as the available computing facilities will permit. The assumptions that are made should be carefully considered and listed in each part where is required. They impose limitations on the model when evaluating its predicted results.

The mathematical consistency of model means to make sure that the number of variables equals the number of equations as shown in Figure 2.1. The so-called “degrees of freedom” of the system must be zero in order to obtain a solution. Checking the units of all terms in all equations is perhaps another trivial and obvious step and it is essential to be particularly careful of the time units of parameters in dynamics models (Luyben, 1990).

The verification is an important but often neglected part of developing a mathematical model and it is concerned with the fact of model describes the real-world situation as shown in Figure 2.1. At the design stage this sometimes cannot be done because the plant has not yet been built. The design of experiments to test the validity of a model can sometimes be a real challenge and should be carefully thought out.

A simple schematic representation for the model building exercise is show in Figure 2.1, when the main stages are presented in logical sequence.

2.2 EMULSION POLYMERIZATION REACTION

Recently Van Herk and German (1998) asked the question whether it will ever be possible to model emulsion co-/termopolymerization after reviewing several difficult aspects in emulsion polymerization. It has been long recognized that emulsion polymerization is a complex heterogeneous process involving transport of monomer and other species and free radicals between aqueous and organic phases. Compared to other heterogeneous polymerization, like suspension or precipitation, emulsion polymerization is likely the most complicated system. The rate of polymerization in the organic phase is not only controlled by monomer partitioning but also affected by other phenomena like particle nucleation, and radical absorption and desorption. Particle stability is affected by emulsifier type, amount of emulsifier and ionic strength of the dispersion media. All this factor make modeling of this system very difficult. Though emulsion polymerization has been commercialized for more than half a century, some important aspects like particle nucleation, coagulation, etc. are still not well understood. To simulate this complicated process, a general approach has been adopted. Information from classical modeling sources in the literature has been carefully reviewed and general mass (molar), energy, population (dead polymer molecules and radicals) and particle balances has been written and evaluated with experimental data, with the final aim to develop a model that is flexible, reliable and practical at the same time.

2.2.1 Classical General Theory about Mechanism

Advances in achieving a basic understanding of emulsion polymerization have been made by many researchers. Because of the complexity of the system, contradictory conclusions often exist since early studies. It is not the scope of this work to give a historical literature review on all aspects of emulsion polymerization. Instead, emphasis was focused on more recent developments. The basic mechanism of emulsion polymerization was first postulated by Harkins (1946) and by different authors such as, Smith and Ewart (1948), Song et al. (1988, a, b; 1989, a, b; 1990), Gilbert (1995), Dotson et al. (1996) and Gao and Penlidis (2002).

The qualitative theory of batch emulsion polymerization is due primarily to the groups of Fikentscher (1938, 1960, 1963) and Harkins (1945, 1946, 1947, 1950). It is based on a system consisting of water, a monomer with low water solubility, an emulsifier, and water soluble initiator that decomposes to produce radicals in the aqueous phase (see Figure 2.2). The emulsifier concentration is above the critical micelle concentration (CMC) and the micelles form. The hydrophobic interior of the micelles contains solubilized monomer, which is apportioned by diffusion out of the emulsified monomer drops and through the aqueous phase. Initiator decomposes in the water phase to generate primary radicals, which propagate with monomer dissolved in water to form oligomeric radicals. When an oligomeric radical enters a micelle it propagates rapidly with solubilized monomer to form polymer particle.

In a typical emulsion polymerization there are about 10^{13} monomer droplets per liter of emulsion, with size between 1-10 μm . This compares with ca. 10^{18} micelles, each consisting of ca. 60-100 emulsifier molecules with a diameter of about 5-10 nm. The total interfacial area of the micelles is about three orders-of-magnitude larger than that one of the monomer droplets. Consequently, oligomeric radicals in the aqueous phase are much more likely to diffuse into a micelle swollen with monomer than into a monomer droplet. Micelles are thus gradually transformed into polymer (latex) particles with a diameter of ca. 0,1 μm and a concentration of ca. 10^{17} particles per liter. When all the micelles are consumed and the concentration of emulsifier in the aqueous phase is just about to fall below the CMC, polymer particle nucleation (via micellar nucleation) ceases. The interval from the start of the generation of oligomeric radicals in the aqueous phase to the point

where micelles have been consumed is called Interval I or particle nucleation stage in the emulsion polymerization process (Hamielec, 1992).

As many as three phases can be simultaneously present in an emulsion polymerization system (Figure 2.2): (1) an aqueous phase (containing initiator, surfactant, micelles and a small amount of the relatively sparingly soluble monomer), (2) emulsion droplets dispersed in the aqueous phase and stabilized by surfactant, and (3) latex particles (containing polymer and some or almost all of the yet to be polymerized monomer, and also stabilized by surfactant). Consider the various possible polymerization loci: the aqueous phase (homogeneous nucleation), micelles (micellar nucleation), monomer droplets, water/particle interface and latex particles (Gilbert, 1995). The interval II is known as the polymer particle growth stage, during which the number of particles remains constant (in the absence of coagulation), as does the monomer concentration in the latex particles as a result of monomer diffusion from the reservoir of monomer droplets. Because of the extremely high interfacial areas (polymer particle/water and monomer droplet/water) and associated very rapid mass transfer of monomer, there is an equilibrium with respect to

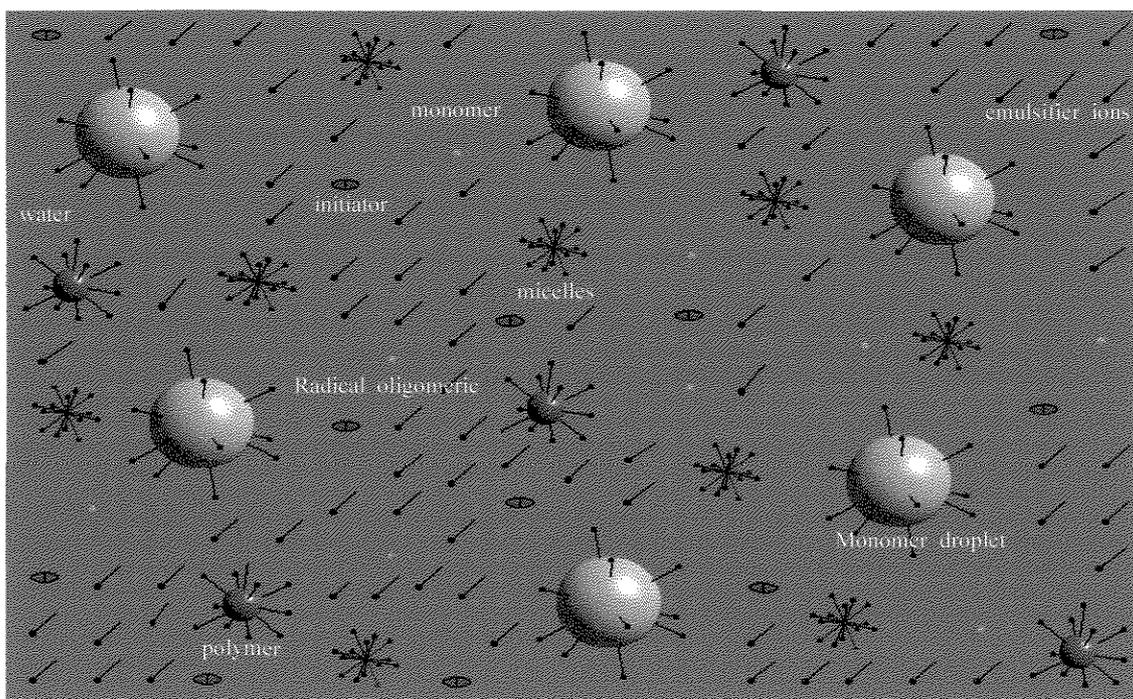


Figure 2.2 Emulsion polymerization mixture.

monomer transfer from monomer droplets to polymer particles (the chemical potential of monomer is the same in all three phases, monomer droplet/water/polymer particles) (Hamielec, 1992). The interval III, known as the depletion or monomer finishing stage, begins with the disappearance of all monomer droplets. The only reservoir of monomer for the polymerization in the latex particles is the aqueous phase. This is sufficient and in Interval III the monomer concentration $[M]_P$ falls with time and conversion. The viscosity of the latex particles increases dramatically due to increase in the number of physical chain entanglement points as the polymer concentration increases. The self-diffusion coefficients of polymeric radicals fall and the Trommsdorff-Norrish effect, which was active in both Intervals I and II, increases in intensity with monomer conversion (Gerrens, 1956, 1963). Another phenomenon which may occur is a glassy-state transition in the latex particles (Hamielec, 1992).

The model of chemical reactor of emulsion polymerization of system was constructed based on a set of assumption: Particles size is monodisperse; reactor is perfectly mixed in the cross-sectional of tubular reactor with or without baffles; the model of Smith-Ewart is applied to interval II to estimate the concentration or conversion of monomer of styrene, and other variables and parameters (Gerrens, 1969; Lynn and Huff,

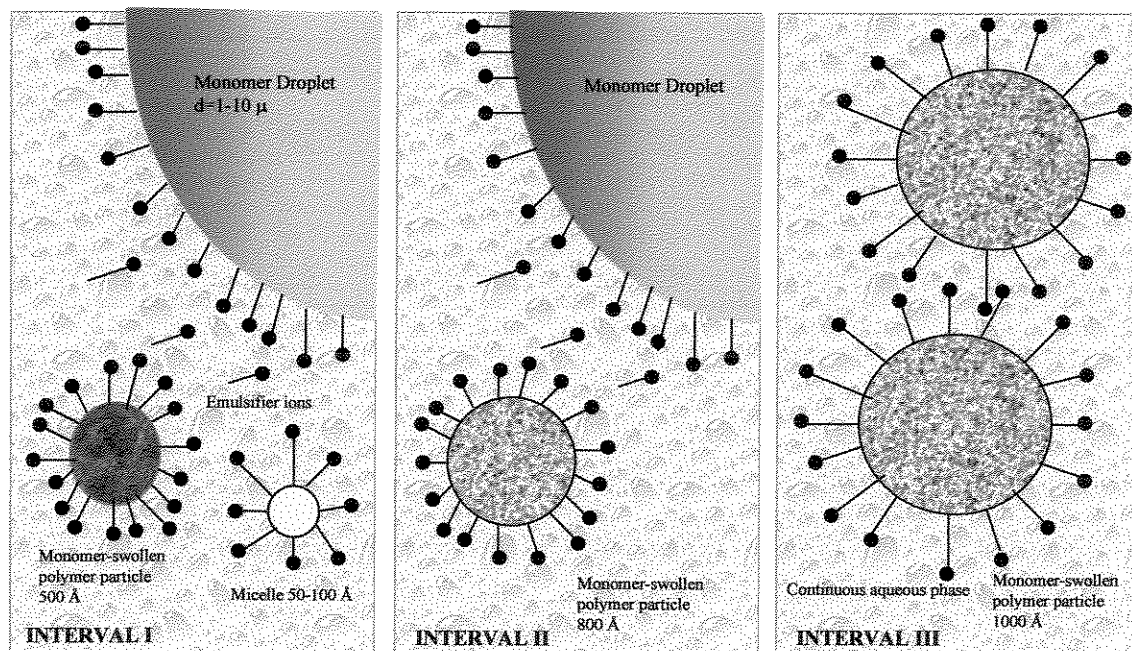


Figure 2.3 Schematic representation of an emulsion polymerization mechanism.

1971; Ray, 1972; Min and Ray, 1974; Pendilis et al. 1986; Rawlings and Ray, 1988 a, b; Chen and Nauman, 1989; Paquet et al. 1994 a,b; Chern, 1995; Gao and Penlidis, 2002). Schematic and brief are presented the mechanism of emulsion polymerization in the Figure 2.3 by intervals.

2.2.2 Particle Nucleation

Particle nucleation by far is the most important phenomenon in emulsion polymerization. This is because not only the rate of polymerization is directly related to the total number of particles but also particle size distribution is a key indicator of latex physical properties. Despite many efforts made by various groups so far, the understanding of particle generation is poor, and the prediction of particle number and size is still not very successful. There are several reason for this.

- 1.- The measurement of number and size of polymer particles which are in the region of a few hundred angstroms presents extremely difficult experimental problems.
- 2.- There are many complex microprocesses occurring simultaneously, e.g. radical absorption, precipitation, coagulation, etc. and each microprocess itself is difficult to understand and model.

2.2.2.1 Micellar Nucleation

There are basically two different theories that describe radical absorption by micelles or particles. Smith and Ewart (1948) postulated that this phenomenon is a diffusion process, however the Smith and Ewart theory in interval II actually reflects a collision process. Micellar nucleation can also described as a collision process (Gardon, 1968 a,b,c,d,e)). The expression for the rate of micellar nucleation(R_c) based on diffusion and collision theories is given in Eqs. (2.1) and (2.2), respectively.

$$R_c = 4\pi r_{mp} D_w [R]_w \quad (2.1)$$

$$R_c = 4\pi r_{mp}^2 K_{mp} [R]_w \quad (2.2)$$

where D_w in Eq.(2.1) is the diffusivity coefficient of the radicals in the water phase and K_{mp} in Eq.(2.2) is the mass transfer coefficient for water phase radical oligomers. In both equations, r_{mp} is the radius of the micelle/particle and $[R]_w$ is the concentration of water phase radical oligomers.

Both diffusion and collision theories have been used to describe particle nucleation by a number of authors. Hansen and Ugelstad (1978, 1982) and Song and Poehlein (1988a,b) used the diffusion theory to calculate the rate of radical absorption. Groups using collision theory include Fitch and Tsai (1971a,b), Min and Ray (1971) and Dickinson (1976). Generally speaking, it is difficult to distinguish which theory is more advantageous over the other. Barret (1975) pointed out that radicals are assumed to travel in a straight line in the collision approach and this underestimates the probability of collision with a particle. Fitch and Tsai (1971 a, b) were the first to use collision theory to quantify the rate of radical capture. As a matter of fact, the micellar nucleation process is neither diffusional nor a collision process, but rather a combination of both. The approach adopted in this work is based in diffusion theory simply because there is more kinetic information available in the literature.

2.2.2.2 Homogeneous Nucleation

Priest (1952) first observed that particle can still formed without the presence of micelle (in this case there is either no emulsifier or its concentration is below the CMC). When radicals in the aqueous phase propagate beyond their solubility (due to the continuous addition of monomer units), they became a primary particle, also called a particle precursor. A primary particle is stabilized either by initiator charges (segments) at the chain ends or available emulsifier in the system. Napper and Alexander (1962) later confirmed Priest's observation and described the homogeneous particle nucleation qualitatively. Fitch and Tsai (1971 a,b) was the first group that proposed a detailed mechanism for this self-nucleation process and give a quantitative calculation for the rate of homogeneous particle nucleation. They assumed that a water phase radical would travel a distance L before it becomes a primary particle. The longer the distance, the more likely it will absorbed an existing particle. If it is absorbed by an existing particle, no new particle is formed. These primary particles will subsequently undergo extensive flocculation. According to Fitch and Tsai's (1971 a,b) postulation, the rate of particle nucleation is then

$$\frac{dN_p}{dt} = R_i - R_c - R_f \quad (2.3)$$

where R_c is the rate of absorption of radicals, R_i is the rate of radical generation through initiation and R_f is the rate of flocculation. Fith and Tsai (1971 a) derived an expression for the rate of radical absorption (capture) as:

$$R_c = \pi r_p^2 L R_i N_p \quad (2.4)$$

where L is the average distance of diffusion in water phase radical travels before it has grown to a size at which precipitates as primary particle and r_p is the particle radius. Fith (1981) treated the radical absorption as a diffusion process, and the overall rate of radical absorption was expressed as:

$$R_c = 4\pi r_p D_w N_p [R]_w \quad (2.5)$$

$[R]_w$ is the radical concentration in the water phase and N_p is the total number of particles.

2.2.3 A Modern Theory about Mechanism

The mass balance for radicals in the water phase is affected by radical entering the water phase, radicals leaving the water phase and reaction involving water phase radicals. A complete list of possible reactions of radicals of the aqueous phase is the following (Gao and Penlidis, 2002).

- 1) *Radical initiation by generation.* Chemical initiation decomposition is the major source for radicals entering the water phase. As long as there is initiator present, there will be radicals generated.
- 2) *Radicals desorption from particles.* Chain transfer reactions like transfer to monomer and to CTA in a polymer particle will produce a monomer or CTA radicals. Such small radicals may desorb into the water phase, especially when monomer or CTA radicals are more water soluble.

- 3) *Radicals capture by micelles.* If a micelles capture a radicals, it then become a particle. This is the so-called micellar nucleation. Most particle are generate by this way.
- 4) *Radicals capture by particle.* Particles compete with micelles in absorbing water phase radicals. The amount of radicals entering particles is proportional to the total particle surface area.
- 5) *Radical propagate with monomers.* Primary radicals generate either by initiation or by chain transfer reaction will propagate with monomer dissolved in the aqueous phase and grow into oligomers. Oligomers produce in this step may form particles when they reach a critical size.
- 6) *Radical terminate with another radicals.* This reaction stop water phase radical growth and produce oligomeric polymer. This reaction is usually considered unimportant by many groups.
- 7) *Radicals react with impurities.* Water-soluble impurities kill active radicals and generate a dead (inert) molecule. The overall effect is the delay of the start of emulsion polymerization (induction time). This reaction usually neglected by most model in the literature.
- 8) *Reaction involves small molecules.* In general, chain transfer to small molecules has little effect on the overall particle number and size. However, chain transfer to small molecules actually produces emulsifier-like oligomers which may have some effect in emulsifier-free reactions.
- 9) *Radicals precipitate and form a particle.* This is another source of particle nucleation (homogeneous nucleation).

EMULSION POLIMERIZATION MECHANISM

Schematically and briefly are presented the mechanism of emulsion where the chain transfer, terminal double bond polymerization and internal double bond polymerization were not considered in the first approximation.

INITIATION



RADICAL ABSORPTION BY MICELLES (Micellar Nucleation)

Diffusion in the water phase

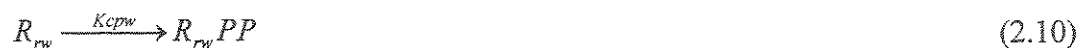


Absorption in the micelle surface



RADICAL ABSORPTION BY PARTICLES (Homogeneous nucleation)

Diffusion in the water phase



Absorption in the particle surface



PROPAGATION



TERMINATION

1.- By combination



2.- By disproportionation



CHAIN TRANSFER

1.- To monomer



2.- To solvent



3.- To polymer



4.- To chain transfer agent (CTA)



5.- Inhibitor/impurities



TERMINAL DOUBLE BOND POLYMERIZATION



INTERNAL DOUBLE BOND POLYMERIZATION



2.2.4 Kinetic Phenomenon of Polymerization Reaction

2.2.4.1 Cage Effect

The initiator efficiency f is defined as the fraction of radicals formed in the primary step of initiator decomposition, which are successful in initiating polymerization. The initiator efficiency is considered exclusive of any initiator wastage by included decomposition (Odian 1991).

The values of f for most initiator lie in the range 0,3 – 0,8. To understand why the initiator efficiency will be less than unity, consider the presence of a solvent cage, which traps the radicals for some period before they diffuse apart. The decomposed radicals are held within the solvent cage. The radicals in the solvent cage may undergo recombination, reaction with each other, reaction with monomer or diffusion out of the solvent cage. Once outside the solvent cage the radicals may react with monomer or decompose to yield a radical which undergo various reactions. Lowering of the initiator efficiency by reaction is referred to as the cage effect (Koenig and Fischer, 1973; Martin, 1973; Bamford, 1988). It is a general phenomenon observed in almost all initiation systems.

The initiator efficiency varies to differing extents depending on the identities of the monomer, solvent, and initiator. f decreases as the viscosity of the reaction medium increases. With increasing viscosity, the lifetimes of radicals in the solvent cage area increase – leading to grater extents of radical – radical reaction within the solvent cage (Odian, 1991).

2.2.4.2 Gel Effect

The terms *Trommsdorf effect* and *Norrish-Smith effect* are also used in recognition of the early workers in the field. The increase in polymerization rate with increased monomer conversion is well known and is called the autoacceleration or gel effect (Norrish and Brookman, 1939; Schulz and Harborth, 1947; Trommsdorff et al., 1948). The increase in reaction rate is due to diffusional limitations causing a decrease in the rate of chain termination reactions (Rawling and Ray, 1988a).

The gel effect is modeled in the literature as a decrease in the termination rate constant, K_t . At sufficiently high conversions, the propagation reaction rate also decreases. A review and comparison of several gel effect models is given by Smith and Ray (1981).

The gel effect is the “normal” behavior for most polymerization. The gel effect should not be confused with the autoacceleration that would be observed if a polymerization were carried out under nonisothermal conditions such that the reaction temperature increased with conversion (since ΔH is negative). The gel effect is observed under isothermal reaction conditions (Odian, 1981).

2.2.4.3 Glass Effect

At even higher monomer conversions, the polymerization system solidifies. This glass effect reduces not only the diffusion of macroradicals and the termination reactions but also the diffusion of monomer molecules and thus the chain propagation. The polymerization rate approaches zero: the monomer can no longer be polymerized completely (Elias, 1997).

2.3 EMULSION POLYMERIZATION REACTOR

Besides stoichiometry and kinetics, reactor technology includes requirements for introducing and removing reactants and products, supplying and withdrawing heat, accommodating phase changes and materials transfer, assuring efficient contacting among reactants, and providing for catalyst replenishment or regeneration. These issues are taken into account when one translates reaction kinetics and bench-scale data into effective pilot plants, scales larger sized units, and ultimately designs and operates commercial plants (Tarmy, 1982).

The requirements for contacting reactants and removing products are the paramount focus of reactor technology; the other factors usually are set by the original selection of the reacting system and intended levels of reactant conversion and product selectivity (Tarmy, 1982). All reactors have in common selected characteristics of three basic reactor types: the well-stirred batch reactor, the continuous-flow stirred-tank reactor, and the tubular reactor (Tarmy, 1982).

The thermally ideal operating states are the isothermal and adiabatic states, i.e., either very intensive heat exchange with the surroundings or no exchange at all is assumed. In practical operation, the ideal states are achieved only approximately (Henkel, 1992).

2.3.1 Continuous Reactor

The *tubular reactor* is vessel through which flow is continuous, usually at steady state, and configured so that process variables are functions of position within the reactor rather than of time as shows in Figure 2.4. In the ideal tubular reactor, the fluids flow as if they were solid plugs or piston, and reaction time is the same for all flowing material at any given tube cross section; hence, position is analogous to time in the well-stirred batch reactor. Tubular reactors also resemble batch reactors in providing initially high driving forces, which diminish as the reactions progress down the tubes.

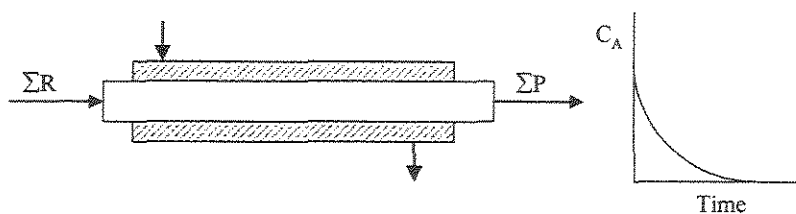


Figure 2.4 Continuous Tubular Reactor.

In actually tubular reactors, flow can be laminar and, thus, greatly deviate from plug flow or, more likely, flow can be turbulent as shown in Figure 2.5. Turbulent flow generally is preferred to laminar flow, because mixing and heat transfer when normal to flow are improved and less back-mixing is introduced in the direction of flow (Tarmy, 1982).

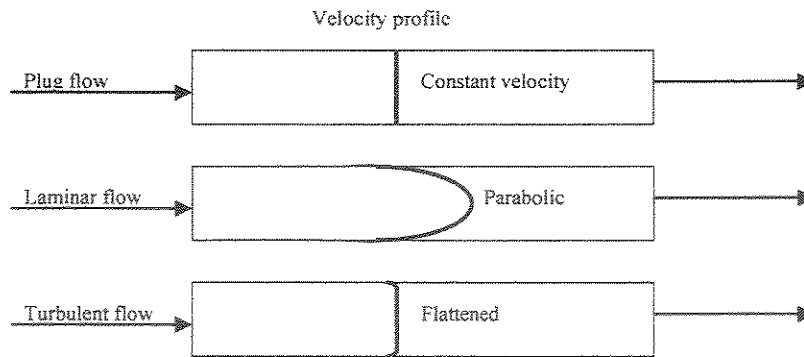


Figure 2.5 Flow characteristics for single-phase flows

Continuous tubular reactors can also be used to produce emulsion polymers. Such reactors have been in series with CSTRs (Gonzales, 1974), as flow-through reactors (Rollin et al., 1979; Ghosh and Forsyth, 1976) and in a continuous loop process (Lanthier, 1970) in which material is fed and removed from a tubular loop with a circulating flow greater than the throughput.

2.4 TRANSPORT EQUATIONS MODELING

The transport equations are continuous analogs of three fundamental laws of physics, namely, the principle of conservation of mass, Newton's second law of motion, and the principle of conservation of energy (Bird et al. 1960; Carberry, 1976; Lenk, 1978; Patankar, 1980; Nauman, 1987; Holland, 1989; Tucker, 1989; Froment, 1990; Bockhorn, 1992; Wendt, 1992; McGreavy, 1994; Versteeg, 1998;).

2.4.1 Principle of Mass Conservation

This equation is developed by writing a mass balance over stationary volume element through which the fluid is flowing. The equation of continuity describes the rate of change of density at fixed point resulting from the changes in the mass velocity vector $\rho\vec{v}$ (Bird, 1960)

$$\frac{\partial \rho}{\partial t} + (\nabla \cdot \rho\vec{v}) = 0 \quad (2.22)$$

Here $(\nabla \cdot \rho \vec{v})$ is called the “divergence” of $\rho \vec{v}$. Note that the vector $\rho \vec{v}$ is the mass flux, and its divergence has a simple significance: it is the net rate of increase of the density within a small volume element fixed in space is equal to the net rate of mass influx to the element divided by its volume (Bird, 1960).

2.4.2 Newton’s Second Law of Momentum

When applied to an arbitrary control volume, it states that the rate at which momentum inside the control volume is increasing, plus the total flux of momentum into the volume, equals the sum of all external forces exerted on the volume. These can either be contact forces or body forces. If we let the control volume become infinitesimal, the result is a differential equation that express the requirement of momentum conservation for every point in a continuum. The most general form of motion equation and in terms of $\vec{\tau}$ is (Bird, 1960; Patankar, 1980; Tucker, 1989; Wendt, 1992; Versteeg, 1998).

$$\rho \frac{D\vec{u}}{Dt} = (\nabla \cdot \vec{\sigma}) + \rho \cdot \vec{g} = -\Delta P + (\nabla \cdot \vec{\tau}) + \rho \cdot \vec{g} \quad (2.23)$$

Here \vec{g} represent the body force per unit area; ρ is the density; \vec{u} is the velocity vector; ∇ is the gradient operator; $\vec{\tau}$ is the extra stress tensor, and D/Dt is the material or substantial derivative. Where (1) is mass per unit volume times acceleration; (2) is pressure force on element per unit volume; (3) is viscous force on element per unit volume, and (4) is gravitational force on element per unit volume.

2.4.3 Principle of Energy Conservation

This principle can be applied to a control volume in a manner analogous to the mass and momentum conservation principles. The most useful versions of the energy equation in general tensorial form. It can be written in rectangular, cylindrical and spherical coordinate system (Tucker, 1989).

$$\rho C_v \frac{DT}{Dt} = -\nabla \cdot \vec{q} - T \left[\frac{\partial P}{\partial T} \right]_{\vec{v}} (\nabla \cdot \vec{u}) + \tau : \nabla \vec{u} + \dot{S} \quad (2.24)$$

Where ρ is the density, P is the pressure, C_v is the specific heat at constant volume, T is the temperature, \hat{V} is the specific volume, \dot{S} is the rate of heat generation due to chemical reaction, \bar{v} is the velocity vector, \bar{q} is the heat flux vector, ∇ is the gradient operator, τ is the extra stress tensor, and D/Dt is the material or substantial derivative (Tucker, 1989).

2.4.4 Classification of Deterministic Model

A further subdivision of models based on physicochemical principles according to the type of model equations is shown in Figure 2.6. The complexity of the method of solution decreases from right to left. The division is based on the most commonly used types of models but is not definitive. Thus, multidimensional models can be formulated in the form of algebraic relationships; models which can be described by algebraic relationships do not have to be steady-state models. Steady-state models describe processes in which the accumulation terms (the changes in the variables over time) disappear. Nonsteady-state models include changes in the variables over time. In models with constant variables, the properties and state are not functions of space so that the system is homogeneous. Description with locally distributed variables considers local changes in the dependent variables (Gould, 1969; Kafarow, 1971; Buckley, 1979; Bockhorn, 1992).

2.5 COMPUTATIONAL-BASED KNOWLEDGE

In the last few decades computational fluid dynamics has become a very powerful and versatile tool for the analysis and solution of problems that are of considerable interest to the chemical engineer, despite the fact that CFD has not yet reached its full potential. The chemical engineering discipline has developed many valuable semiempirical strategies to solve problems of practical interest (Kuipers and Van Swaaij, 1998).

In the process technology raw materials are converted into desired products via chemical and physical processes. These products are often intermediates that are subsequently converted in other production processes. This general scheme from raw material like materials, crude oil, natural gas, agricultural products, etc., via processing and purification is very common. A process engineer developing, designing, or optimizing a process has to deal with many disciplines varying from chemistry or biochemistry to economy. His or her ultimate aim is to produce valuable product in a safe way at acceptable

cost and burden to the environment. Also time is a scarce quantity because her or she has to take the changing market and competitor into account. The traditional chemical engineering sciences like transport phenomena and chemical reaction engineering play an essential role in achieving the aforementioned aims. In these sciences elements from physics (like transport theories, fluid dynamics, and thermodynamics), chemistry (kinetics, catalysis), and mathematics have been integrated to form dedicated tools to tackle extremely complicated problems that come up in studying and developing processes (Kuipers and Van Swaaij, 1998).

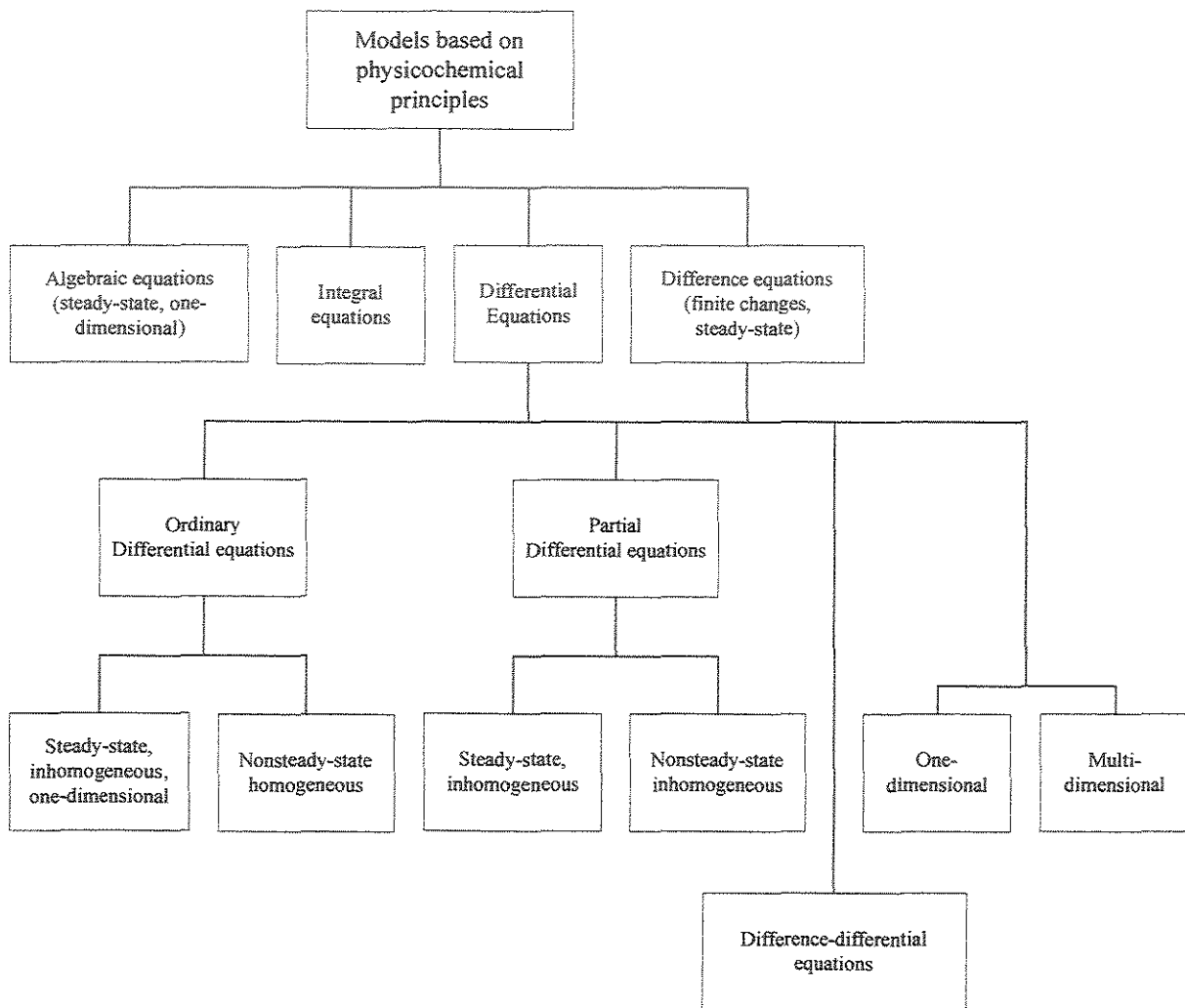


Figure 2.6 Classification of deterministic models based on physicochemical principles according to the type of resulting equations.

A new emerging tool is a combination of fluid dynamics and numerical mathematics backed up by the immense growth of computer power: computational fluid

dynamics (CFD). It is affecting the chemical engineering sciences and the art of the chemical engineer in a profound way (Kuipers and Van Swaaij, 1998).

2.5.1 Computational Fluid Dynamic

The historical development of the science of fluid mechanics, and subsequently the development and present areas of application of CFD are highlighted. The equations that form the theoretical foundation for the whole science of fluid mechanics were derived more than one century ago by Navier (1827) and Poisson (1831) on the basis of molecular hypotheses. Later the same equations were derived by de Saint Venant (1843) and Stokes (1845) without using such hypothesis. These equations are commonly referred to as the Navier-Stokes equations. Despite the fact that these equations have been known of for more than a century, no general analytical solution of Navier-Stokes equation is known. This state of the art is due to the complex mathematical (i.e., nonlinearity) nature of these equations (Kuipers and Van Swaaij, 1998).

Toward the end of the nineteenth century the science of fluid mechanics began to develop in two branches, namely theoretical hydrodynamics and hydraulics. The first branch evolved from Euler's equations of motion for a frictionless, non-viscous fluid, whereas the development of the second branch was driven by the rapid progress in technology where engineers, faced with the solution of practical problems for which the "classical" science of theoretical hydrodynamics had no answer, developed their own highly empirical science of hydraulics (Kuipers and Van Swaaij, 1998).

During the first half of this century a spectacular development in the boundary layer theory took place that was driven mainly by the needs of the aerodynamics community. Most of the initial development involved approximate analytical solution or transformation and subsequent numerical integration of the relevant fluid flow equation (Schlichting, 1975).

Although the initial development of the CFD discipline was driven by the aerodynamics community, nowadays CFD is truly interdisciplinary since it cuts across all disciplines where the analysis of fluid flow and associated phenomena is of importance. CFD has found application in the automobile industries to study both the internal in combustion engines (Griffin *et al.*, 1978) and the external flow (Shaw, 1988, Matsunaga *et al.*, 1992). Also in civil engineering CFD has found application in the study of problems

involving flow dynamics of rivers, lakes, and estuaries and external flow around buildings. In environmental engineering CFD has been used to analyze the complex flow patterns that exist in various types of furnaces (Bai and Fuchs, 1992). CFD has also been applied to calculate air current, throughout buildings in order to arrive at improved designs of (natural) ventilation systems (Alamdari *et al.*, 1991).

In industrial manufacturing applications a myriad of applications exist of which of modeling of chemical vapor deposition reactors in the semiconductor industries (Stejsiger *et al.*, 1992) and the modeling of the casting process of liquid metals (Mampaey and Xu, 1992) can be mentioned as examples. For further details on CFD applications in various industrial manufacturing processes the reader is referred to previous reviews (Colenbrander, 1991; Trambouze, 1993; Johansen and Kolbeinsen, 1996). Colenbrander has prepared a review on CFD applications in the petrochemical industries with specific emphasis on CFD applications and related experimental work carried out in the Shell Group laboratories. The application of CFD to chemical reaction engineering has been reviewed by Trambouze (1993). During the last two decades CFD has also become a powerful tool for analyzing and designing metallurgical processes. Johansen and Kolbeinsen (1996) have recently prepared a review on this subject, where CFD applications at SINTEF Materials and Technology were highlighted. Finally, Harris *et al.* (1995) have presented a review on the applications of CFD in Chemical Reaction Engineering (CRE) with emphasis on single-phase applications.

The physical aspects of any fluid flow are governed by the following three fundamental principles: 1) mass is conserved; 2) Newton's second law; and 3) energy is conserved. These fundamental principles can be expressed in terms of mathematical equations, which in their most general form are usually partial differential equations. CFD is, in part, the art of replacing the governing partial differential equations of fluid flow with numbers, and advancing these numbers in space and/or time to obtain a final numerical description of the complete flow field without advancing in time or space, and there are some applications which involving integral equations rather than partial differential equations. CFD solution generally require the repetitive manipulation of thousands, or even millions, of numbers, a task that is humanly impossible without the aid of a computer. Therefore, advances, in CFD, and its applications to problems of more details and

sophistication, are intimately related to advances in computer hardware, particularly in regard to storage and execution speed (Anderson, 1991).

CFD involves the analysis of fluid flow and related phenomena such as heat and/or mass transfer, mixing, and chemical reactions using numerical solution methods. Usually the domain of interest is divided into a large number of control volumes (or computational cells or elements) which have a relatively small size in comparison with the macroscopic volume of the domain of interest. For each control volume a discrete representation of the relevant conservation equations is made after which an iterative solution procedure is invoked to obtain the solution of the nonlinear equations. Due to the advent of high-speed digital computer and the availability of powerful numerical algorithms the CFD approach has become feasible. CFD can be seen as a hybrid branch of mechanics and mathematics (Kuipers and Van Swaaij, 1998).

2.5.2 Computational in Chemical Reaction Engineering

The role of CFD in engineering predictions has become so strong that today it can be viewed as a new 'third dimension' in fluid dynamics, the other two dimension being the classical cases of pure experiment and pure theory. From 1687, with the publication of Isaac Newton's Principia, to the mid-1960s, advancements in fluid mechanics were made with the synergistic combination of pioneering experiments and basic theoretical analyses, analyses which almost required the use of simplified models of the flow to obtain closed-form solutions of the governing equations. They frequently have the disadvantage of not including all the requisite physics of the flow. Into this picture stepped CFD in the mid-1960s. With its ability to handle the governing equations in 'exact' form, along with the inclusion of detailed physical phenomena such as finite-rate chemical reactions, supports and complements both pure experiment and pure theory (Anderson, 1991).

The applications of CFD may be divided into broad categories, namely, those involving single-phase systems and those involving multiphase systems. The motivation for this distinction is due to 1) large difference in degree of complexity of physical description and 2) large differences in numerical solutions strategies. Within single-phase systems a further distinction can be made between systems involving 1) laminar flows, 2) turbulent flows, 3) flows with complex rheology, and 4) fast chemical reactions. The multiphase systems can be encountered in industrial practice, multiphase flows are encountered and in

general it can be stated that, due to the inherent complexity of such flows, general applicable models and related CFD codes are nonexistent. The reason for this relatively unsatisfactory state of the art is due to the following causes: 1) Many types of multiphase flow exist (i.e., gas-liquid, gas-solid, liquid-liquid, gas-liquid-solid) where within one type of flow several possible flow regimes exist; 2) the detailed physical laws and correct mathematical representation of phenomena taking place in the vicinity of interfaces (coalescence, breakup, accumulation of impurities) are still largely undeveloped. Very often multiphase flow systems show inherent oscillatory behavior that necessitates the use of transient solution algorithms. Examples of such flows are encountered in bubbling gas-fluidized beds, circulating gas-fluidized beds, and bubble columns where, respectively, bubbles, clusters, or strands and bubbles plumes are present that continuously change the flow pattern. Prior to the discussion of the progress in CFD analysis of multiphase flows, first some general requirements for modeling multiphase systems are mentioned: 1) regime characterization and flow regime transition, 2) spatial distribution of the phase, 3) sensitivity of system behavior for physicochemical parameters, 4) prediction of effect of internals (Kuipers and Van Swaaij, 1998).

CFD was applied in different type of reactor such as batch reactor, CSTR, tubular reactor, biochemical reactor and polymerization reactors. Some applications for tubular reactor are the following:

Kruis *et al.* (1996) applied CFD to describe the turbulent flow field in describing the transport production and dissipation of a non-reactive tracer in a tubular jet reactor. The turbulent flow field was obtained from a CFD code Phoenics using the $k-\varepsilon$ model.

Kuochen *et al.* (1996) described the dissipation rate for a turbulent flows present in many chemical reactors with series-parallel reaction. They used the Lagrangian probability density function formulation of the spectral relaxation model for to study a series-parallel reaction in a single-jet tubular reactor.

Kolhapure *et al.* (1999) used a novel multi-environment CFD micromixing model to describe the small-scale mixing of chemical species inside tubular low-density polyethylene (LDPE) reactor under different operating conditions. They showed that the multi-environment CFD micromixing model offers a computationally highly efficient description of turbulent reacting flow inside the LDPE reactor.

Forney and Nafia (2000) presented the eddy contact model to describe the mixing rate between two miscible liquids in nearly homogeneous turbulence. They described the aqueous distribution of several pure fluid engaged in mixing sensitive parallel reactions. The model prediction was used in a scaled down plug flow reactor.

2.6 TUBULAR REACTOR WITH INTERNAL ANGLE BAFFLES

The baffles are classified in transverse type and longitudinal type with arrangement symmetric, asymmetric and mix. In the project is proposed an angular type with arrangement mix. The baffles inside of the columns are used in industry of chemical process to modify the hydrodynamic characteristics: flux of gas and/or liquid, gas resistance and others. The baffles verticals inside column of fluctuation was investigated by Moys *et al.* (1991), Finch *et al.* (1990) and Rice *et al.* (1974). The residence time distribution was studied in flat column by Mavros *et al.* (1995). The baffles can be applied in shell to deal the fluid flow through pipes to increase a rate of fluid and the heat transfer (Coulson *et al.*, 1997).

The baffles was applied in different type of chemical reactors, such as reactor batch, CSTR, tubular reactor, biochemical reactor, polymerization reactor, thermonuclear reactor, anaerobic reactor, etc.

Feldon *et al.* (1953) studied continuous emulsion polymerization in a tubular reactor where was added to the otherwise completed charge by means of a positive displacement piston-type pump at the inlet of the tube. The tubular polymerizer consisted of 40 straight sections of 5/8-inch O.D. 20-gage stainless-steel tubing, each of which was 8,83 feet in length, connected by U-shaped sections of 3/4-inch tubing, 0,75-foot in length. The total length of the tubular reactor was 382 feet, and the total volume was 4,9 gallons. The tube was immersed in a 420-gallon tank filled with hot water; the water was maintained uniformly at 122°F (50°C) by means of a pneumatic reset controller, and the contents of the tank were recirculated by a centrifugal pump. A constant pressure of 80 lb/sq.in (5,44 atm) gage was maintained in the tubular reactor by means of a single-port pressure-activated valve.

Carnavos (1979) studied the heat transfer performance for cooling air in turbulent flow with 21 tubes having integral internal spiral and longitudinal fins. The inner fin tubes have wide range of geometries. In evaluating an inner fin tube for a heat exchanger the heat

transfer performance gain at constant pumping power, the normal standard of comparison being a smooth tube of the same outer diameter and wall thickness.

Patankar et al. (1979) analyzed the fully developed turbulent flow and heat transfer characteristics for tubes and annuli with longitudinal internal fins via a mixing model. The model takes account of the proximity of both the fin surfaces and tube wall as well as of the gradients in the radial and circumferential directions. Applications was made to air flows, and a single adjustable constant in the model was fixed by comparisons with experimental data for the friction factor and circumferential-average Nusselt number for internally finned tubes. The analysis was based on the differential equations for momentum and energy conservation in the flowing fluid supplemented by a turbulence model having na adjustable constant. Their attention was focused on the case of fully developed flow and heat transfer, with thermal boundary condition being uniform heat input to the fluid per unit axial length.

Rustum and Soliman (1990) investigated steady, laminar, mixed convection in the fully developed region of horizontal internally finned tubes for the case of uniform heat input axially and uniform wall temperature circumferentially. Fins were assumed to be negligible thickness with sides oriented radially within the tube cross-section. Therefore, the geometry was completely defined by two parameters: the number of fins and the relative fin height. This analysis was applied to steady, laminar flow of incompressible, Newtonian fluids. Constant fluid properties are assumed, except for the density which was temperature to be fully developed hydrodynamically and thermally with uniform heat input axially and uniform wall temperature (tube wall and fins) circumferentially.

Chen *et al.* (1996) found that the baffles inside a loop fluidized bed reactor (LBR) divide the reactor in two mixing zones and to reduce backmixing with a certain open area ratio of cross section of the baffle. The mathematical model in this work is capable of describing the LBR reactor reasonable well. In view of the comparison of computation and pilot plant. The model can be applied in commercial type fluidized bed reactors as well, and simulation results show good agreement with realistic commercial type reactor.

Lazzarini (1996) studied the beam tube baffles to reduce the amount of phase-modulated scattered light reaching the photodetectors in the length sensing subsystems of the interferometer. They prevent the guided reflection of light from one end of the beam tube to the other, and they mask the beam tube walls from direct viewing by the LIGO

suspended test mass mirrors. The baffles must have two key properties: they must have acceptable low backscatter and they must minimize the amount of forward diffraction which can reach the far test mass mirror.

Wragg *et al.* (1996) measured of average and local mass transfer distribution were made in a parallel plate electrochemical cell using the limiting diffusion current technique. The cell was operated with and without baffles. They studied hydrodynamic phenomena, including jet entry effects, recirculation, flow development, flow reversal, wall impingement, preferential flow effects and exit disturbances, the mass transfer distribution, swirling motion.

Farinas *et al.* (1997) studied the heat transfer in a horizontal cylinder with fins on the flow pattern, temperature distribution and heat transfer between concentric horizontal cylinders. They used different fin configurations, geometric (sharp, round and divergent tip) and lengths ($l=0.25$ and 0.75). The Nusselt number is proportional to Rayleigh and the fin length. The best heat transfer results will derive with round-tip fins of length $l=0.75$.

Hamier *et al.* (1998) showed a new type of reactor designed for continuous halogen-assisted digestion: pseudo fluidized bed reactor (PFBR). The use of a baffle drastically improved the digestion efficiency by virtue of an increased solid residence time.

The proposal in the present work consists of a system of incrustated angular multi-baffles inside tubular reactor with arrangement mix (symmetric and asymmetric) to improve the reactive mixture and emulsifier agents, as well as the heat transfer conditions. The polymerization tubular reactor with internal angle baffles as shown in Figures 2.7 and 2.8 is the proposed design. This reactor shows plane angular multi deflectors or multi baffles inside tubular reactor. The multi baffles are static mixer, it will improve the chemical process of polymerization. The angle, number of baffles, length, baffle separation, thickness, reactor diameter, reactor length and geometry form are analyzed to obtain an adequate operation condition of emulsion homopolymerization of styrene.

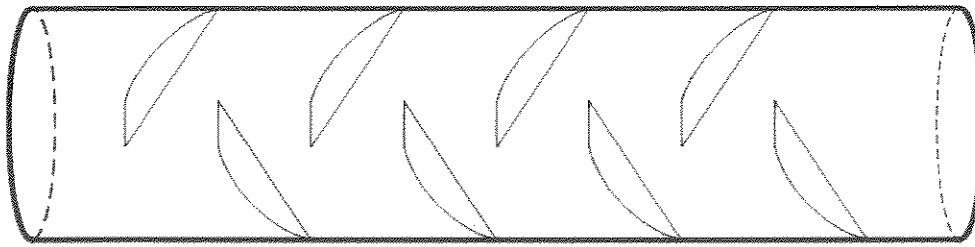


Figure 2.7 Schematic representation of polymerization tubular reactor with baffles

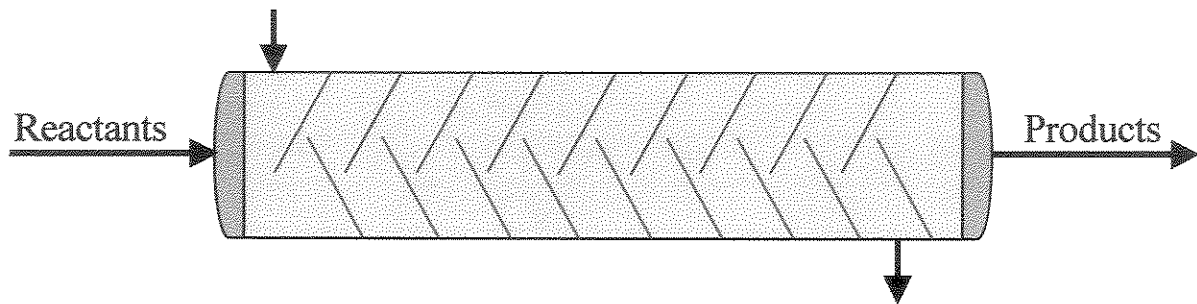


Figure 2.8 Profile of polymerization tubular reactor with internal angle baffles

RESUMO DO CAPÍTULO III

MENDOZA MARÍN, F.L. Modelagem, simulação e análise de desempenho de reatores tubulares de polimerização com deflectores angulares internos. 241p. Tese (Doutorado em Engenharia Química – Área de Processos Químicos) – Faculdade de Engenharia Química. Universidade Estadual de Campinas - UNICAMP, 2004.

O Capítulo III apresenta os dados utilizados nas simulações realizadas nos respectivos capítulos. Os dados do presente capítulo serão utilizados nos Capítulos VII, VIII e IX. O Capítulo III é importante porque apresenta as condições e as propriedades nos quais foram obtidos os resultados de simulação e as conclusões. No Capítulo III são descritos os materiais (como reagentes ou receita), o hardware e softwares utilizados; e classificação das propriedades. É mostrado a metodologia geral do desenvolvimento da tese segundo procedimento natural de causa-efeito e antecedente-conseqüente, o qual foi apresentado por meio de um esquema.

Conclusão do Capítulo III: No Capítulo III os materiais, as propriedades e a metodologia geral foram descritos apropriadamente com a finalidade de desenvolvimento dos programas em Fortran e desenvolvimento da presente pesquisa em suas diferentes capítulos. Com base nas condições e receita apresentadas da literatura foram realizados as simulações, validações e conclusões na presente tese.

CHAPTER III

MATERIALS, PROPERTIES AND GENERAL METHODOLOGY

The Chapter III provides data required for the Fortran programs and simulations. These data are used in the Chapters VII, VIII and IX and they provide the conditions in which the simulation results are valid.

The continuous development of the modern process industries has made, draw attention how increasingly important is to have information about the properties of materials, including many new chemical substances whose physical properties have never been measured experimentally. This is especially true polymer substances. The design of manufacturing and processing equipment requires considerable knowledge of the processed materials and related compounds. Also for the application and final use of these materials this knowledge is essential. In some handbook, for instance the “polymer Handbook” (Brandrup and Immergut, 1966, 1975, 1989), “Physical Constant of Linear Homopolymers” (Lewis, 1968), the “International Plastics Handbook for the Technologist, Engineer and User” (Saechtling, 1988), and similar, one finds part of the data required, but in many cases the property needed cannot be obtained from such sources (Van Krevelen, 1990).

3.1 MATERIALS

3.1.1 Reactants

BATAILLE *et al.* (1982) conducted emulsion homopolymerization of styrene at 60°C. They performed five runs and simulated all five runs using the recipes/conditions. One conditions of recipe was execute and simulated in this present thesis, and it is shown in the Table 3.1. It was reported by BATAILLE *et al.* (1982) that all reactions were conducted in a 1L glass reactor.

Table 3.1: Reaction recipes for Bataille et al. (1982)

Recipe	w_j (wt%)	w_j	n_j (n%)	C_j (mol/L)
Potassium persulfate	0,24	0,0018	0,0151	0,026
Sodium dodecyl sulfate	0,67	0,0051	0,0397	0,070
Styrene	30	0,2292	4,9333	8,390
Water	100	0,7639	95,0118	161,52
TOTAL	130,91	1,0000	100,000	170,006

The molar concentration of solution (C) was calculated by Eq. (3.4), and its results is 170,006 mol/L which is shown in Table 3.1. Before was necessary to calculate the molar concentration of j (C_j), the mole fraction of j (n_j), and the mass fraction of j (w_j) by Eq. (3.3), Eq. (3.2) and Eq. (3.1), respectively. All calculations are shown in Table 3.1. These equations can be found in Bird (1960).

Mass fraction of j

$$w_j = \frac{m_j}{m} \quad (3.1)$$

Mole fraction of j

$$n_j = \frac{\frac{w_j}{MW_j}}{\sum_{j=1}^{N_c} \left(\frac{w}{MW} \right)_j} \quad (3.2)$$

Molar concentration of j

$$C_j = \frac{\rho_j}{MW_j} \quad (3.3)$$

Molar concentration of solution

$$C = \frac{C_j}{n_j} \quad (3.4)$$

In such equations m_j is mass of j ; m is total mass; MW_j is molecular weight of j ; N_r is total number of species j ; ρ_j is density of species j .

3.1.1.1 Monomer

The monomer is styrene. The styrene, also is known as phenyl-ethylene, vinylbenzene, styrol, or cinnamene, $C_6H_5-CH=CH_2$, is an important industrial unsaturated aromatic monomer. It occurs naturally in small quantities in some plants and foods. In the nineteenth century, styrene was isolated by distillation of the natural balsam storax (Simon, 1839). It has been identified in cinnamon, coffee beans, and peanuts (Steele, 1992), and it is also found in coal tar (James and Castor, 1994).

Styrene has been long considered the most thoroughly studied monomer in emulsion polymerization because it fits into Smith-Ewart case II Kinetic scheme well. Gardon et al. (1968 a, b, c, d) in a series of papers, distinguished three intervals in styrene emulsion homopolymerization in batch. According to the Smith-Ewart case II postulation, the average number of radicals per particle remains constant at 0,5 throughout stages I and II of the reaction. Styrene has very low water solubility and negligible desorption, and the gel effects is pronounced in styrene emulsion polymerization.

Many papers have been reviewed to study the kinetic of styrene emulsion homopolymerization and collect kinetic as well as experimental data. Table 3.2 list papers that focus on styrene emulsion polymerization kinetics.

3.1.1.2 Initiator

The potassium persulfate (KPS) was used as initiator in the present work as database for simulation of emulsion polymerization of styrene (EPS) as shown in Table 3.3. According to the Table 3.3 it is possible to observe different properties of KPS. The bibliographical reference is at final column as shown in Table 3.12.

Table 3.2: Papers on styrene emulsion polymerization kinetics

Authors	Remarks
Asua et al.(1991)	Estimation of rate constant for radical absorption and desorption
Bataille et al. (1982, 1984, 1988)	Full conversion data, studies of redox system
Blackley and Sebastian (1987, 1989)	Experimental data, redox system
Canegallo et al. (1993)	On-line densitometer measurements
Campbell (1985)	Experimental data, modeling
De la Rosa et al. (1996)	Calorimetry measurements
Giannetti (1993)	Particle size distribution, modeling, kinetic parameter information
Harada et al. (1972)	Full conversion range experimental data, modeling
Hawkett et al. (1981)	Radical absorption efficiency
James and Piirma (1975)	Molecular weigh development, gel effect studies
Lichti et al (1981)	Particle size distribution
Mayer et al (1996)	Particle nucleation
Miller et al. (1997)	Molecular weights
Morton et al. (1952)	Kinetic parameters
Morbidelli et al. (1983)	Modeling, studies on gel effect and ionic strength
Nomura et al. (1971)	CSTR operation
Penboss et al.(1983)	Seeded emulsion polymerization, particle nucleation
Piirma et al. (1975)	Molecular Weight development and kinetic studies
Said (1991)	Molecular Weight
Salazar et al. (1998)	Molecular Weight control policy studies
Sudol et al. (1986 a, b)	Seeded emulsion polymerization, monodispersed particle latex

Table 3.3: Initiator (potassium persulfate) database for Simulation of EPS

Items	Value	Unit	Reference
C _{Iin}	0,026	mol/L	9
f _i	0,5	-	9
K _d	$1,524 \times 10^{18} \exp(-33320/RgT)$	1/min	5, 9, 10
M _{Wi}	271,3	g/mol	9

3.1.1.3 Surfactant

The sodium dodecyl sulfate (SDS) was used as surfactant or emulsifier in the present thesis for simulation of emulsion polymerization of styrene (EPS) in isothermic and no isothermic condition without and with baffles inside tubular reactor as shown in Table 3.4. According to the Table 3.4 one can observe different properties of SDS. The bibliographical reference is at final column for each one as shown in Table 3.12.

Table 3.4: Surfactant (sodium dodecyl sulfate) database for simulation of EPS

Items	Value	Unit	Reference
C_{Et}	0,07	mol/L	9
CMC	0,008	mol/L	9
MWe	288,38	g/mol	9
nem	60	No.Emul/mic	12, 13, 22
Sa	3×10^{-17}	dm^2	9

The styrene as monomer, the potassium persulfate as initiator, the sodium dodecyl sulfate as surfactant and water as dissolvent were principally used in the present thesis as reactant, the others reactants were not considered.

3.2 PROPERTIES

The properties were classified as physics, chemicals, mechanics, of transport, rheologys, thermals, thermodynamics, geometrical of grid, particle, reactor and baffle and computational. The classification was made to use as database for simulation of emulsion polymerization of styrene (EPS) in isothermic and no isothermic condition without and with baffles inside tubular reactor. The properties were used to calculate and to simulate the conversion of monomer, the internal transversal area, the axial velocity, the axial temperature, the concentration of polymer, the concentration of radicals, the concentration of initiator, the number of particles, on the average molecular weight, the size of polymer particle, the viscosity distribution, the density of polymer and monomer, the head loss and the pressure drop. Some bibliographical references with the property of such materials are: Gerrens (1969); Brandrup (1975); Rollin et al. (1977); Kumar (1978); Bataile (1982, 1984); Van Krevelen (1990); Odian (1991); Paquet et al. (1994); Gilbert (1995); Chern (1995); Handbook (1998); Gao et al. (2002); etc. The other bibliographical references are shown in Table 3.12.

3.2.1 Physical Properties

The physical properties are shown in Table 3.5 that were used as database for simulation of emulsion polymerization of styrene (EPS) in isothermic and no isothermic condition without and with baffles inside tubular reactor. In the Table 3.5 there are parameters and variable physical each one with its bibliographical reference as shown in Table 3.12.

Table 3.5: Physical properties as database for simulation of EPS.

Items	Value	Unit	Reference
Cp	390	Cal/Kg K	16, 24, 25
Na	$6,02 \times 10^{23}$	molecule/mol	3, 14
Rg	1,987	cal/mol K	3, 14
π	3,14159		3, 14
ρ_p	1,11 (at 60°C)	Kg/L	9, 23
ρ_p	1,25-0,0004202T	Kg/L	4
ρ_m	0,949-0,00128(T-273,15)	Kg/L	9

3.2.2 Chemical Properties

The chemical properties of styrene are shown in Table 3.6 as database for simulation of emulsion polymerization of styrene in isothermic and no isothermic condition without and with baffles inside tubular reactor. There are parameters and variables each one with its bibliographical reference at final column as shown in Table 3.12. Some values of the Table 3.6 were estimated at beginning of the calculation in the Fortran program.

Table 3.6: Chemical properties of Styrene as database for simulation of EPS.

Items	Value	Unit	Reference
anrp	0,5	-	9
CMin	8,39	mol/L	9
CMw	0,005	mol/L	9
CNpa	1×10^{-10}	mol/L	estimated
CNpin	0	mol/L	estimated
CRwa	1×10^{-5}	mol/L	estimated
CRwin	0	mol/L	estimated
Ep	9805	cal/mol	9
Et	2950,45	cal/mol	9
Icr	5	-	9
Kp	$4,703 \times 10^{11} \exp(-9805/RgT)$	L/mol min	5, 9, 10
Kt	$1,04619 \times 10^{10} \exp(-2950,45/RgT)$	L/mol min	5, 9, 10
MWs	104	g/mol	9
ncr	5	-	7, 15
ϕ_p	0,4	-	6, 12, 19, 20
ϕ_m	0,6	-	6, 12, 19, 20

3.2.3 Mechanical properties

The mechanistic properties of styrene are shown in Table 3.7. There are values that were used as database for simulation of emulsion polymerization of styrene in isothermic and no isothermic condition without and with baffles inside tubular reactor. Also values are each one with its bibliographical reference at final column as shown in Table 3.12.

Table 3.7: Mechanical properties of styrene as database for simulation of EPS.

Items	Value	Unit	Reference
Re	= 5000 (laminar)	-	8, 11, 18, 21
Re	= 13600 (turbulent)	-	8, 11, 18, 21
Vin	0,27027 (laminar)	m/min	8, 11, 18, 21
Vin	0,7351 (turbulent)	m/min	8, 11, 18, 21

3.2.4 Transport Properties

The transport properties of styrene are shown in Table 3.8 as database for simulation of emulsion polymerization of styrene in isothermic and no isothermic condition without and with baffles inside tubular reactor. There are values each one with its bibliographical reference at final column as shown in Table 3.12.

Table 3.8: Transport properties of styrene as database for simulation of EPS.

Items	Value	Unit	Reference
Dp	$1,76 \times 10^{-12}$	dm^2/min	9
Dw	$1,76 \times 10^{-9}$	dm^2/min	9

3.2.5 Rheological Properties

The rheological properties of styrene are shown in Table 3.9. There are values that were used as database for simulation of emulsion polymerization of styrene in isothermic and no isothermic condition without and with baffles inside tubular reactor. The values are each one with its bibliographical reference at final column as shown in Table 3.12.

Table 3.9: Rheological properties of styrene as database for simulation of EPS.

Items	Value	Unit	Reference
μ	0,001	Kg/m s	4, 11, 17, 18

3.2.6 Thermal Properties

The thermal properties of styrene are not used in the present thesis because the simulation of emulsion polymerization of styrene was made in adiabatic process in constant and variable reaction temperature without and with baffles inside tubular reactor.

3.2.7 Thermodynamic Properties

The thermodynamic properties of styrene are shown in Table 3.10. There are values that were used as database for simulation of emulsion polymerization of styrene in isothermic and no isothermic condition without and with baffles inside tubular reactor. Some values of the Table 3.10 were estimated at beginning of the calculus in Fortran program. The T_a was estimated as shown in Section 6.3.1.2. The values are each one with its bibliographical reference at final column as shown in Table 3.12.

Table 3.10: Thermodynamic properties as database for simulation of EPS.

Items	Value	Unit	Reference
T_a	336,15	K	estimated
T_{in}	333,15	K	9
ΔH	-16682,2	cal/mol	1, 4,9,14,19

3.2.8 Geometrical Properties

The geometrical properties were classified as grid, particle, reactor and baffle because its geometrical characteristic of tubular reactor, the inclined internal angles baffles, and the polymer particle size affect as parameter or variable in the grid design. The geometrical properties of grid, particle, reactor and baffles are shown in Table 3.11. There are values that were used as database for simulation of emulsion polymerization of styrene in isothermic and no isothermic condition without and with baffles inside tubular reactor. Some values of the Table 3.11 were estimated to calculate in Fortran program. The values are each one with its bibliographical reference at final column as shown in Table 3.12.

Table 3.11: Geometrical properties as database for simulation of EPS.

Items	Value	Unit	Reference
Grid			
N	51		estimated
Particle			
rm	27,5	Å	9, 12, 20
rp	275	Å	9, 12, 20
Reactor			
Dr	1	m	estimated
Lr	20	m	estimated
Baffle			
Lbr	1	m	estimated
Nb	6, 18		estimated

3.2.9 Computational Parameters

The computational properties of programming are defined into program code such as factor of convergence, factor of sub-relaxation, factor of division, factor of units, etc. They can help to the beginning, during the programming and other parts of a Program Unit or Program Project according to the calculus. They can defined as assumption or estimation.

The bibliographical reference are shown in Table 3.12. From Table 3.3 to Table 3.11 are mentioned at the final column the bibliographical reference of the Table 3.12.

Table 3.12: Bibliographical reference of the properties

Number	Reference
1	Agarwal and Kleinstreuer (1986)
2	Bataile (1982)
3	Brandrup (1975)
4	Chen and Nauman (1989)
5	Chern (1995)
6	Dotson et al. (1996)
7	Dougherty (1986)
8	Fox and McDonald (1992)
9	Gao and Penlidis (2002)
10	Gerrens (1969)
11	Ghosh and Forsyth (1976)
12	Gilbert (1995)
13	Hamielec (1992)
14	Handbook (1998)
15	Hansen and Ugelstad (1978)
16	Kumar (1978)
17	Lenk (1978)
18	Lynn and Huff (1971)
19	Odian (1991)
20	Paquet et al. (1994)
21	Rollin et al. (1977)
22	Song (1988b)
23	Van Krevelen (1990)
24	www.psrc.usm.edu/macrog/matdb/styrene.htm
25	www.sabic.com/ar/products/basic/aromatics_styrene.htm

3.3 GENERAL METHODOLOGY

The Figure 3.1 shows the general methodology that was applied in the present thesis. The comprehensive mathematical model is apparent capable of predicting the molecular and morphological development in a polymer reactor with inside baffles in terms of the process operating conditions should include appropriate model representation of all chemical and physical phenomena occurring at the appropriate scale. Polymer reactor with inside baffles models vary in their complexity but in general a modeling engineer should address the following issues: bibliographical review, materials, properties, mathematical model, finite volume method, computational code, computational test, simulation, and analysis of results. In the general methodology was applied principles-based algorithm of cause-effect, antecedent-consequent, and sequential to control its application.

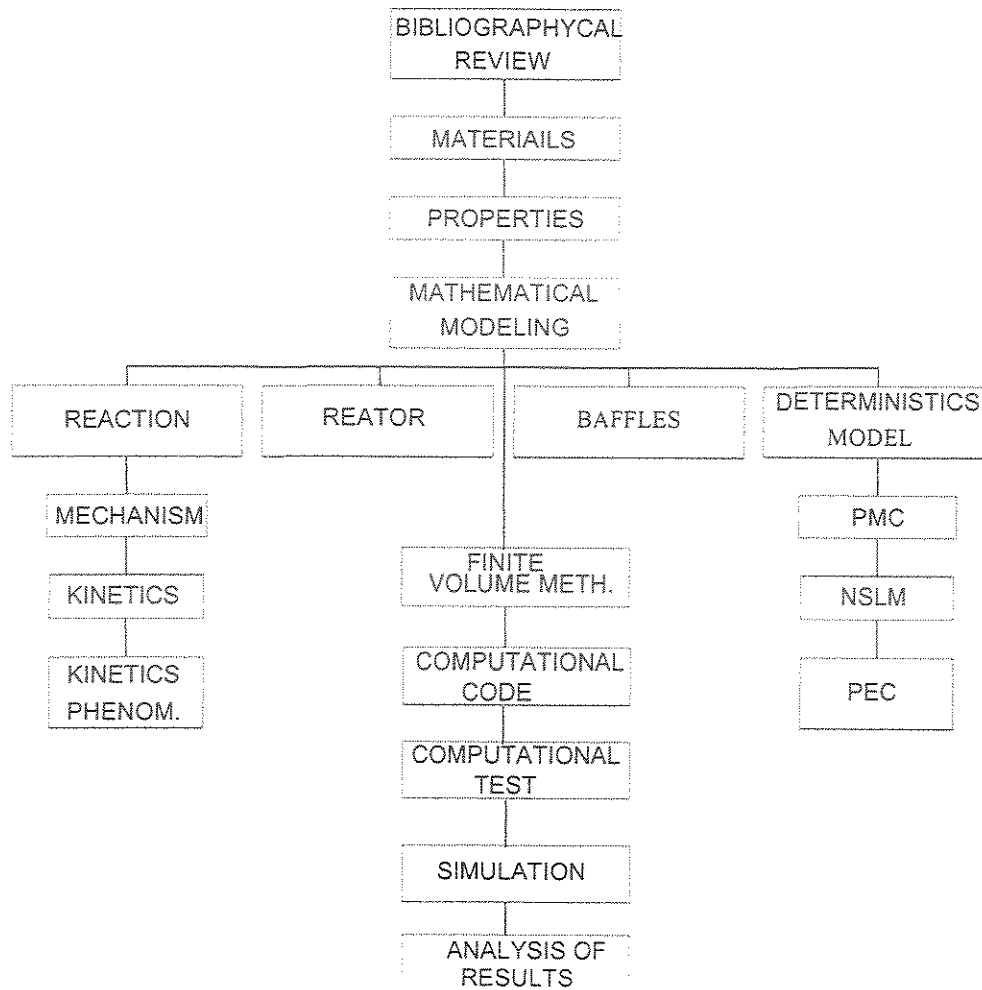


Figure 3.1 Schematic representation of the general methodology.

In Figure 3.1 PMC is Principle of Mass Conservation, NSLM is Newton's Second Law of Momentum, and PEC is Principle of Energy Conservation.

RESUMO DO CAPÍTULO IV

MENDOZA MARÍN, F.L. *Modelagem, simulação e análise de desempenho de reatores tubulares de polimerização com deflectores angulares internos*, 241p. Tese (Doutorado em Engenharia Química – Área de Processos Químicos) – Faculdade de Engenharia Química. Universidade Estadual de Campinas - UNICAMP, 2004.

O Capítulo IV apresenta o modelagem matemático global dos modelos determinísticos baseados em princípios físico-químicos das equações conservativas de massa, momento e energia; apresenta a reação de polimerização em emulsão e o reator de polimerização em emulsão. Os modelos desenvolvidos são utilizados diretamente nos Capítulos VII – IX. O Capítulo IV é importante porque apresenta as condições usadas nos modelos matemáticos, em forma de aproximações, simplificações, suposições e as limitações. Os objetivos do Capítulo IV são: descrever as equações conservativas de massa, momento e energia em coordenadas ortogonais cilíndricas baseada na literatura; descrever a reação de polimerização em emulsão; descrever a caracterização do produto por meio do número de partículas, distribuição de peso molecular, tamanho das partículas e a viscosidade das partículas como mostrado em Seção 4.4; descrever o modelagem do reator tubular de polimerização em emulsão sem e com chicanas.

Conclusão do Capítulo IV: No Capítulo IV o modelagem do reator tubular sem e com chicanas foram mostrados conforme os princípios de massa, momento, energia e reação de polimerização em sistemas de coordenadas ortogonais cilíndricas. Os produtos foram caracterizados pelo número de partículas, peso molecular, tamanho das partículas e viscosidade do polímero. Os modelos determinísticos foram desenvolvidos essencialmente com princípios conservativos de massa, momento e energia para reator tubular, reação de polimerização e as chicanas em forma geral. Como exemplo foi apresentado o modelagem do número de partículas com 18 chicanas e 51 pontos nodais, o qual pode ser estendido para outras variáveis escalares a serem transportadas conservativamente.

CHAPTER IV

MATHEMATICAL MODELING

In this chapter is presented the fairly global modeling of physics-chemistry principles-based deterministic model such as mass, momentum and energy conservative equations, also emulsion polymerization reaction and reactor. The developed mathematical models are used directly in the Chapter 5 and indirectly in the Chapters 6-9. It is important to point out in this chapter the conditions that were used in the mathematical models according to the approximations, simplifications, suppositions, assumption, estimation and limitations, respectively. Also the analytical solution was developed for Micelle and Homogeneous Nucleation in Section 4.4.

The mathematical models can be classified according to their physical background, the type of systems of equations, and the corresponding methods of solution. The models with different physical backgrounds are models based on physicochemical principles, probability density functions model, and empirical models. The models based on physicochemical principles are based on the mathematical formulation of transport phenomena. It applies the principles of the transport to chemical engineering process. Use of this principles requires that the process can be subdivided into process elements that can be described by the laws governing the transport of mass, momentum, and energy, i.e., their conservative principles (Bockhorn, 1992). Such models are subdivided into deterministic and static models. Deterministic model or model elements have a determined value or set of values of each variable or parameter for any given set of conditions (Bockhorn, 1992).

The representation of the process by the type of model consists of the formulation of the conservative equation for the total mass, the mass of the individual chemical species, components of momentum, and the enthalpy for the system or subsystem under consideration. The conservative equations can be given in the form: accumulation + change due to convective transport = change due to molecule transport + source. The require number, combination, and formulation of conservation equations and any other

physicochemical relationships necessary for closing the set of equations depend on the kind of process and the physical boundary conditions for the systems under consideration (Bockhorn, 1992).

Before discussing a numerical procedure, some fundamental characteristic of the modeling of reactor will be shown by a simplified version of the system of equations. The first simplification is the assumption of constant density, isothermal conditions, chemical reaction that not involve volume changes, and frictionless flow (Bockhorn, 1992).

The source term could not have any dimension, then when the mathematical model is in Cartesian, Cylindrical, Spherical or Generalize Coordinate, should not exist any difference for the source term. For this reason, the mathematical modeling may be developed in one dimension according with the mass action law for source term.

In this Chapter is described the mass, momentum and energy conservative equations in cylindrical orthogonal coordinate according to the literature and they were the basis for the development of the proposal models. The emulsion polymerization reaction modeling is described as product characterization by means of number of particles, molecular weight distribution, polymer particle size and viscosity distribution as shown in the Section 2.2; the emulsion polymerization reactor modeling is described without and with baffles.

4.1 PRINCIPLE OF MASS CONSERVATION

The fairly general form of the continuity equation for a chemical species j reacting in a flowing fluid with varying density, temperature, and composition is (Froment, 1990)

$$\frac{\partial C_j}{\partial t} + \nabla \cdot (C_j \bar{u}) + \nabla \cdot J_j = R_j \quad (4.1)$$

Species j occurs in liquid phase. This equation can take in single-phase or “homogeneous” or, by extension, in “pseudohomogeneous” reactors as a consequence of the flow pattern. C_j is the molar concentration of species j ; $\partial C_j / \partial t$ is the nonsteady-state term expressing accumulation or depletion; ∇ is the “nabla”, or “del”, operator. In a cylindrical coordinate system, r, θ, z , the gradient of a scalar function f is represented by ∇f and the divergence of a vector function \bar{u} by $\nabla \cdot \bar{u}$. Here, \bar{u} is the three-dimensional

mass-average velocity vector. The term $\nabla \cdot (C_j \bar{u})$ thus accounts for the transport of mass by convective flow. The J_j term is the molar flux vector for species j with respect to the mass-average velocity. The term $\nabla \cdot J_j$ results from molecular diffusion only. R_j is the total rate of change of the amount of j because of reaction (Bird, 1960; Froment, 1990).

Mathematical modeling of mixing and chemical species transport can be solved by conservation equations describing convection, diffusion, and reaction sources for each component species. Multiple simultaneous chemical reactions were modeled, with reaction occurring in the bulk phase (volumetric reactions). Modeling for reacting system can be by the generalized finite-rate model, the non-premixed systems, the premixed combustion model, the partially premixed combustion model, the mixture fraction approach and the reaction progress variable approach. The generalized Laminar finite-rate model was applied to compute the chemical source terms in the present thesis. The model is exact for laminar flames, but is generally inaccurate for turbulent flames due to highly non-linear Arrhenius chemical kinetics.

The net source of chemical species j due to reaction R_j is computed as the sum of the Arrhenius reaction sources over the N_i reactions that the species participate in:

$$R_j = \sum_{i=1}^{N_i} R_{j,i} \quad (4.2)$$

where $R_{j,i}$ is the Arrhenius molar rate of creation/destruction of species j in reaction i . The molar rate of creation/destruction of species j in reaction i is given by

$$R_{j,i} = K_{f,i} \prod_{l=1}^{N_i} [C_{l,i}]^{n_{f,l,i}} - K_{b,i} \prod_{l=1}^{N_i} [C_{l,i}]^{n_{b,l,i}} \quad (4.3)$$

where $K_{f,i}$ is the forward rate constant for reaction i , $K_{b,i}$ is the backward rate constant for reaction i , N_i is the number of chemical species in reaction i , $C_{l,i}$ is the molar concentration of each reactant and product species j in reaction i , $n_{f,l,i}$ is the forward rate exponent for each reactant and product species j in reaction i , $n_{b,l,i}$ is the backward rate exponent for each

reactant and product species j in reaction i . The non-reversible reactions was considered in the present thesis, then the backward rate constant $K_{b,i}$ is simply omitted.

4.2 NEWTON'S SECOND LAW OF MOMENTUM

Newton's second law states that the momentum change rate of a fluid particle is equal to the forces sum on the particle. Two forces types can be distinguish on fluid particle: 1) Surface forces: pressure forces and viscous forces, 2) Body forces: gravity force, centrifugal force, coriolis force, electromagnetic force and reaction forces. It is common practice to highlight the contributions due to the surface forces as separate terms in the momentum equation and to include the effects of body forces as source terms. The equation of motion states that small volume element moving with the fluid is accelerated because of the forces acting over it.

The motion equation Eq.(2.23) is represented in cylindrical coordinate, in their components r , θ , and z .

r -component

$$\rho \left[\frac{\partial v_r}{\partial t} + v_r \frac{\partial v_r}{\partial r} + \frac{v_\theta}{r} \frac{\partial v_r}{\partial \theta} - \frac{v_\theta^2}{r} + v_z \frac{\partial v_r}{\partial z} \right] = -\frac{\partial P}{\partial r} + \left[\frac{1}{r} \frac{\partial (r\tau_{rr})}{\partial r} + \frac{1}{r} \frac{\partial \tau_{\theta r}}{\partial \theta} + \frac{\partial \tau_{zr}}{\partial z} - \frac{\tau_{\theta\theta}}{r} \right] + \rho g_r \quad (4.4)$$

θ -component

$$\rho \left[\frac{\partial v_\theta}{\partial t} + v_r \frac{\partial v_\theta}{\partial r} + \frac{v_\theta}{r} \frac{\partial v_\theta}{\partial \theta} - \frac{v_r v_\theta}{r} + v_z \frac{\partial v_\theta}{\partial z} \right] = -\frac{1}{r} \frac{\partial P}{\partial \theta} + \left[\frac{1}{r^2} \frac{\partial (r^2 \tau_{r\theta})}{\partial r} + \frac{1}{r} \frac{\partial \tau_{\theta\theta}}{\partial \theta} + \frac{\partial \tau_{z\theta}}{\partial z} \right] + \rho g_\theta \quad (4.5)$$

z -component

$$\rho \left[\frac{\partial v_z}{\partial t} + v_r \frac{\partial v_z}{\partial r} + \frac{v_\theta}{r} \frac{\partial v_z}{\partial \theta} + v_z \frac{\partial v_z}{\partial z} \right] = -\frac{\partial P}{\partial z} + \left[\frac{1}{r} \frac{\partial (r\tau_{rz})}{\partial r} + \frac{1}{r} \frac{\partial \tau_{\theta z}}{\partial \theta} + \frac{\partial \tau_{zz}}{\partial z} \right] + \rho g_z \quad (4.6)$$

Components of the stress tensor for Newtonian fluids in cylindrical coordinates:

$$\tau_{rr} = -\mu \left[2 \frac{\partial v_r}{\partial r} - \frac{2}{3} (\nabla \cdot \vec{v}) \right] \quad (4.7)$$

$$\tau_{\theta\theta} = -\mu \left[2 \left(\frac{1}{r} \frac{\partial v_\theta}{\partial \theta} + \frac{v_r}{r} \right) - \frac{2}{3} (\nabla \cdot \vec{v}) \right] \quad (4.8)$$

$$\tau_{zz} = -\mu \left[2 \frac{\partial v_z}{\partial z} - \frac{2}{3} (\nabla \cdot \vec{v}) \right] \quad (4.9)$$

$$\tau_{r\theta} = \tau_{\theta r} = -\mu \left[r \frac{\partial}{\partial r} \left(\frac{v_\theta}{r} \right) + \frac{1}{r} \frac{\partial v_r}{\partial \theta} \right] \quad (4.10)$$

$$\tau_{\theta z} = \tau_{z\theta} = -\mu \left[\frac{\partial v_\theta}{\partial z} + \frac{1}{r} \frac{\partial v_z}{\partial \theta} \right] \quad (4.11)$$

$$\tau_{zr} = \tau_{rz} = -\mu \left[\frac{\partial v_z}{\partial r} + \frac{\partial v_r}{\partial z} \right] \quad (4.12)$$

$$(\nabla \cdot \vec{v}) = \frac{1}{r} \frac{\partial}{\partial r} (r v_r) + \frac{1}{r} \frac{\partial v_\theta}{\partial \theta} + \frac{\partial v_z}{\partial z} \quad (4.13)$$

4.3 PRINCIPLE OF ENERGY CONSERVATION

The following form shows the phenomenon that are of importance in reactors (Nauman, 1987; Holland, 1989; Froment, 1990; McGreavy, 1994):

$$\sum_j \bar{M}_j C_j c_{pj} \left(\frac{\partial T}{\partial t} + \vec{u} \cdot \nabla T \right) = \sum_i (-\Delta H_i) r_i + \nabla \cdot (\lambda \nabla T) - \sum_j J_j \nabla H_j + Q_{rad} \quad (4.14)$$

(1) (2) (3) (4) (5) (6)

where c_{pj} is the specific heat of species j ; λ is the thermal conductivity of the mixture; H_j are partial molar enthalpies; T is the temperature; \bar{M}_j is molecular mass of species j ; C_j is molar concentration of species j . The respective terms arise from (1) change of heat content with time, (2) convective flow, (3) heat effect of the chemical reactions, (4) heat transport by conduction, (5) energy flux by molecular diffusion, and (6) radiation heat flux.

Other energy terms encountered with particular flow conditions are work of expansion or viscous dissipation terms, primarily important in high-speed flow; external field effects, mechanical or electrical, can also occur. Since they usually are of much less importance, they will not be considered here.

Taking the General Equation presented in the Chapter II and in this Chapter IV the model equations were developed as follows.

4.4 EMULSION POLIMERIZATION REACTION MODELING

4.4.1 Micellar nucleation

In the Micellar Nucleation model it was accepted that particles are generated by micelle absorbing radicals from the water phase. Smith and Ewart (1948) stated that the rate of particle nucleation in the presence of micelle is controlled by the diffusion law. There are basically two different theories that describe radical absorption by micelle or particles. Smith-Ewart postulated that this phenomenon is a diffusion process. Micellar Nucleation can be also described as a collision process. In the present, the micellar nucleation with proper treatment of the entry kinetic was used, on based in reference of Gilbert (1995), and complementary reference: Piirma (1982), Song et al. (1988 a, b; 1989 a, b; 1990), Fitch (1997), Gao and Penlidis (2002).

The rate of particle formation by micellar nucleation (to see Section 2.2.3)

$$R_{MN} = \frac{d[Np]_m}{dt} = K_{cm}[MIC][R]_w \quad (4.15)$$

Formation rate for the 1st oligomeric radicals in the aqueous phase (to see Section 2.2.3)

$$\frac{d[R_1]_w}{dt} = R_f - K_p M_w [R_1]_w - K_{cm} [MIC] [R_1]_w - K_{tw} [R]_w [R_1]_w \quad (4.16)$$

Formation rate for the *i*th oligomeric radicals in the aqueous phase (to see Section 2.2.3)

$$\begin{aligned} \frac{d[R_i]_w}{dt} = & K_p M_w [R_{i-1}]_w - K_p M_w [R_i]_w - K_{cm} [MIC] [R_i]_w - \sum_{j=1}^{\infty} K_{cp_j} [Np_j] [R_i]_w \\ & - K_{tw} \sum_{j=1}^{ncr-1} [R_j]_w [R_i]_w \end{aligned} \quad (4.17)$$

Definition

$$\sum_{j=1}^{\infty} K_{cp_j} [Np_j] = K_{cp} [Np] \quad (4.18)$$

Formation rate of total oligomeric radicals in the aqueous phase

$$\sum_{j=1}^{ncr-1} [R_j]_w = [R]_w \quad (4.19)$$

If the steady state hypothesis is applied to all radicals in the water phase, i.e., setting left-hand side of Eq.(4.16) and Eq.(4.17) to zero, one obtain the following equations:

$$[R_1]_w = \frac{R_f}{K_p M_w + K_{cm} [MIC] + K_{tw} [R]_w} \quad (4.20)$$

$$[R_i]_w = \frac{K_p M_w [R_{i-1}]_w}{K_p M_w + K_{cm} [MIC] + K_{tw} [R]_w + K_{cp} [Np]} \quad (4.21)$$

The probability for oligomeric radical for micelle propagation

$$\alpha_m = \frac{K_p M_w}{K_p M_w + K_{cm} [MIC] + K_{tw} [R]_w + K_{cp} [Np]} \quad (4.22)$$

Equation (4.21) can then be rewritten and solve for all oligomer (Spiegel, 1963; Gradshteyn et al. 1965; Apostol, 1967; Song et al. 1988 a,b, 1989 a,b, 1990; Boyce et al. 1997):

$$[R_i]_w = \alpha_m [R_{i-1}]_w = \alpha_m \alpha_m [R_{i-2}]_w = \alpha_m \alpha_m \alpha_m [R_{i-3}]_w = \dots = \prod_{i=1}^{ncr-1} \alpha_m^i [R_1]_w \quad (4.23)$$

$$[R_i]_w = \alpha_m^{ncr-1} [R_1]_w \quad (4.24)$$

Substituting Eq.(4.20) into Eq.(4.24) gives

$$[R_i]_w = \frac{R_f}{KpMw + Kcm[MIC] + Ktw[R]_w} \alpha_m^{ncr-1} \quad (4.25)$$

The following definitions are used to simplify symbols. Total radical concentration in the aqueous phase

$$[R]_w = \sum_{i=1}^{ncr-1} [R_i]_w \quad (4.26)$$

Substituting Eq.(4.25) into Eq.(4.26) gives

$$[R]_w = \frac{R_f}{KpMw + Kcm[MIC] + Ktw[R]_w} \sum_{i=1}^{ncr-1} \alpha_m^{ncr-1} \quad (4.27)$$

The Geometric Progression is applied to the end term of Eq.(4.27) (Spiegel, 1963; Gradshteyn et al. 1965; Leithold, 1994; Perry et al. 1997; Boyce et al. 1997):

$$\sum_{i=1}^{n-1} x^{i-1} = \frac{1-x^{n-1}}{1-x} \quad (4.28)$$

Equation (4.27) can be then rewritten and gives the total radical concentration in the aqueous phase.

$$[R]_w = \frac{R_i}{KpM_w + Kcm[MIC] + Ktw[R]_w} \left(\frac{1 - \alpha_m^{ncr-1}}{1 - \alpha_m} \right) \quad (4.29)$$

The final equation of the rate of particle formation for Micelle Nucleation is then

$$R_{MN} = \frac{d[Np]_m}{dt} = \frac{Kcm[MIC]R_i}{KpM_w + Kcm[MIC] + Ktw[R]_w} \left(\frac{1 - \alpha_m^{ncr-1}}{1 - \alpha_m} \right) \quad (4.30)$$

4.4.2 Homogeneous nucleation

In the Homogeneous Particle Nucleation was accepted that the particles could be generated by precipitated water phase oligomer radicals. This nucleation mechanism was proposed by Hansen and Ugelstad (1978) and Fitch and Tsai (1971 a, b), after the original Smith-Ewart's postulation. In quantifying homogeneous nucleation, account must be taken of the competition between entry (capture) of newly formed radicals and these radicals forming precursor particles. It is therefore necessary to incorporate the kinetics of entry into the homogeneous nucleation model. The following reference was used Piirma (1982), Song et al. (1988 a,b; 1989 a,b; 1990), Gilbert (1995), Fitch (1997), Gao and Penlidis (2002).

The rate of particle formation by Homogeneous Nucleation (to see Section 2.2.3)

$$R_{HN} = \frac{d[Np]_h}{dt} = KpM_w [R_{ncr-1}]_w \quad (4.31)$$

Formation rate for 1st oligomeric radicals in the aqueous phase (to see Section 2.2.3)

$$\frac{d[R_1]_w}{dt} = R_i - KpM_w [R_1]_w - \sum_{j=1}^{\infty} Kcp_j [Np_j] [R_1]_w - Ktw \sum_{j=1}^{ncr-1} [R_j]_w [R_1]_w \quad (4.32)$$

Formation rate for *i*th oligomeric radicals in the aqueous phase (to see Section 2.2.3)

$$\frac{d[R_i]_w}{dt} = KpMw[R_{i-1}]_w - KpMw[R_i]_w - Kcp[Np][R_i]_w - Ktw[R]_w[R_i]_w \quad (4.33)$$

If the steady state is applied to all radical in the water phase, the following equation was obtained:

$$[R_1]_w = \frac{R_f}{KpMw + Kcp[Np] + Ktw[R]_w} \quad (4.34)$$

$$[R_i]_w = \frac{KpMw[R_{i-1}]_w}{KpMw + Ktw[R]_w + Kcp[Np]} \quad (4.35)$$

The probability for an oligomeric radicals for homogeneous propagation

$$\alpha_h = \frac{KpMw}{KpMw + Ktw[R]_w + Kcp[Np]} \quad (4.36)$$

Equation (4.34) and Eq.(4.35) can then be rewritten and solve for all radical oligomer (Spiegel, 1963; Gradshteyn et al. 1965; Apostol, 1967; Song et al. 1988 a,b, 1989 a,b, 1990; Boyce et al. 1997).

$$[R_1]_w = \frac{R_f}{KpMw} \alpha_h \quad (4.37)$$

$$[R_i]_w = \alpha_h [R_{i-1}]_w = \alpha_h \alpha_h [R_{i-2}]_w = \alpha_h \alpha_h \alpha_h [R_{i-3}]_w = \dots = \prod_{i=1}^{ncr-1} \alpha_h^i [R_1]_w \quad (4.38)$$

Substituting Eq.(4.37) into Eq.(4.38) gives

$$[R_i]_w = \alpha_h^{ncr-1} [R_1]_w = \frac{R_f}{KpMw} \alpha_h^{ncr} \quad (4.39)$$

Definition of radicals where chain length at the critical chain length (n_{cr}). The last propagation step involving a radical of chain length $n_{cr}-1$ and a monomer can actually be considered as the particle formation step (Gilbert, 1995; Gao and Penlidis, 2002).

$$[R_{n_{cr}-1}]_w = \frac{R_i}{K_p M_w} \alpha_h^{n_{cr}-1} \quad (4.40)$$

Substituting Eq.(4.40) into Eq.(4.31) gives the final equation of the rate of particle formation by homogeneous nucleation:

$$R_{HN} = \frac{d[N_p]_h}{dt} = R_i \alpha_h^{n_{cr}-1} \quad (4.41)$$

4.4.3 Balance of reactant

Mass balance equations for each species was considered and the polymer particle phase is the main locus of polymerization, for a complete model of the species consumption is also included the aqueous phase. It is used the Eq.(4.1) for this balance.

4.4.3.1 Initiator

$$\frac{\partial C_I}{\partial t} + \left(v_r \frac{\partial C_I}{\partial r} + v_\theta \frac{1}{r} \frac{\partial C_I}{\partial \theta} + v_z \frac{\partial C_I}{\partial z} \right) = D_{IB} \left(\frac{1}{r} \frac{\partial}{\partial r} \left(r \frac{\partial C_I}{\partial r} \right) + \frac{1}{r^2} \frac{\partial^2 C_I}{\partial \theta^2} + \frac{\partial^2 C_I}{\partial z^2} \right) + R_I \quad (4.42)$$

$$R_I = -f_i K_d [I]_w \quad (4.43)$$

4.4.3.2 Free Radical

$$\frac{\partial C_{Rw}}{\partial t} + \left(v_r \frac{\partial C_{Rw}}{\partial r} + v_\theta \frac{1}{r} \frac{\partial C_{Rw}}{\partial \theta} + v_z \frac{\partial C_{Rw}}{\partial z} \right) = D_{RB} \left(\frac{1}{r} \frac{\partial}{\partial r} \left(r \frac{\partial C_{Rw}}{\partial r} \right) + \frac{1}{r^2} \frac{\partial^2 C_{Rw}}{\partial \theta^2} + \frac{\partial^2 C_{Rw}}{\partial z^2} \right) + R_{Rw} \quad (4.44)$$

$$R_{R_w} = R_f - R_f \left[\frac{K_p M_w}{K_p M_w + K_{cp} [N_p] + K_{tw} [R]_w} \right]^{ncr-1} - K_{cp} [N_p] [R]_w - K_{cm} [MIC] [R]_w - K_{tw} [R]_w^2 \quad (4.45)$$

4.4.3.3 Monomer

$$\frac{\partial C_M}{\partial t} + \left(v_r \frac{\partial C_M}{\partial r} + v_\theta \frac{1}{r} \frac{\partial C_M}{\partial \theta} + v_z \frac{\partial C_M}{\partial z} \right) = D_{MB} \left(\frac{1}{r} \frac{\partial}{\partial r} \left(r \frac{\partial C_M}{\partial r} \right) + \frac{1}{r^2} \frac{\partial^2 C_M}{\partial \theta^2} + \frac{\partial^2 C_M}{\partial z^2} \right) + R_M \quad (4.46)$$

$$R_M = -\frac{K_p [M]_p N_p \bar{n}}{N_A V_p} - K_{pw} [M]_w [R]_w \quad (4.47)$$

4.4.3.4 Surfactant

Surfactant is an inert species in the system so that its concentration is given by:

$$\frac{\partial C_E}{\partial t} + \left(v_r \frac{\partial C_E}{\partial r} + v_\theta \frac{1}{r} \frac{\partial C_E}{\partial \theta} + v_z \frac{\partial C_E}{\partial z} \right) = D_{EB} \left(\frac{1}{r} \frac{\partial}{\partial r} \left(r \frac{\partial C_E}{\partial r} \right) + \frac{1}{r^2} \frac{\partial^2 C_E}{\partial \theta^2} + \frac{\partial^2 C_E}{\partial z^2} \right) + R_E \quad (4.48)$$

$$R_E = 0 \quad (4.49)$$

4.4.3.5 Polymer

$$\frac{\partial C_{Ps}}{\partial t} + \left(v_r \frac{\partial C_{Ps}}{\partial r} + v_\theta \frac{1}{r} \frac{\partial C_{Ps}}{\partial \theta} + v_z \frac{\partial C_{Ps}}{\partial z} \right) = D_{PB} \left(\frac{1}{r} \frac{\partial}{\partial r} \left(r \frac{\partial C_{Ps}}{\partial r} \right) + \frac{1}{r^2} \frac{\partial^2 C_{Ps}}{\partial \theta^2} + \frac{\partial^2 C_{Ps}}{\partial z^2} \right) + R_P \quad (4.50)$$

$$R_P = \frac{K_p [M]_p N_p \bar{n}}{N_A V_p} + K_{pw} [M]_w [R]_w \quad (4.51)$$

4.4.4 Characterization of product

The polymer particle was characterized by particle number by micellar and homogeneous nucleation, molecular weight distribution, particle size and viscosity of polymer particle.

4.4.4.1 Particle Number

$$\frac{\partial C_{N_p}}{\partial t} + \left(v_r \frac{\partial C_{N_p}}{\partial r} + v_\theta \frac{1}{r} \frac{\partial C_{N_p}}{\partial \theta} + v_z \frac{\partial C_{N_p}}{\partial z} \right) = D_{NB} \left(\frac{1}{r} \frac{\partial}{\partial r} \left(r \frac{\partial C_{N_p}}{\partial r} \right) + \frac{1}{r^2} \frac{\partial^2 C_{N_p}}{\partial \theta^2} + \frac{\partial^2 C_{N_p}}{\partial z^2} \right) + R_{N_p} \quad (4.52)$$

The overall rate of formation of particles by Micellar and Homogeneous Nucleation:

$$R_{N_p} = R_{MN} + R_{HN} = \frac{K_{cm}[MIC]R_f}{K_p M_w + K_{cm}[MIC] + K_{tw}[R]_w} \left(\frac{1 - \alpha_m^{ncr-1}}{1 - \alpha_m} \right) + R_f \alpha_h^{ncr-1} \quad (4.53)$$

where

$$\alpha_m = \frac{K_p M_w}{K_p M_w + K_{cm}[MIC] + K_{tw}[R]_w + K_{cp}[N_p]} \quad (4.54)$$

$$\alpha_h = \frac{K_p M_w}{K_p M_w + K_{tw}[R]_w + K_{cp}[N_p]} \quad (4.55)$$

4.4.4.2 Molecular Weight

The active chain polymer chains we have dealt with so far are present in at most micromolar concentrations. This fact clearly is not occur with our product. Our product, rather, consist of the inactive or “dead” chains that accumulate as a result of termination and transfer processes, given by P_i and its transform, $G(s)$.

For the active chains, we made no distinction with respect to the mode of termination. For disproportionation and combination, we use an overall termination constant because the rate of termination, not the mode, affects the living chain distribution.

Since, however, the dead chain distribution does depend on the mode of termination, we must now distinguish between disproportionation and combination. The two will yield different distribution of polymers. Termination by combination was used as for styrene in the present thesis.

Calculating the chain length distribution arising from the entire system of reactions or mechanisms (see Section 2.2.3) presented thus far may at first seem too difficult, so for the sake of illustration we begin with as simple scheme involving only initiation, propagation, and termination, after the results will be generalized.

The polymerization reaction can be solved by moments of molecular weight distribution and the techniques of solution of kinetic and statistical solution. The kinetic solution includes direct sequential solution, discrete transformation method and moments method. The statistical solution includes combination approach, recursive method, Markov chain theory approach, probability generating function, Poisson distribution and Gaussian distribution. Other techniques of solution of polymerization reaction consider numerical integration, z-transform and continuous variable approach (Ray, 1972; , Rudin, 1982; Nauman, 1987; Chen and Nauman, 1989; Holland and Anthony, 1989; Odian, 1991; McGreavy, 1994; Dotson et al., 1996).

4.4.4.2.1 Active or Living Polymer chains

In the active or living polymer chains was applied the discrete transformation method which consists of chemical reaction, kinetic equation, integrating, expand in power series, drop operator, and applied moments.

The chemical reaction was considered by emulsion polymerization mechanism from Eq.(2.6) to Eq.(2.21), where were not considered the chain transfer, terminal and internal double bond polymerization as one approximation.

The kinetic equation was obtained with material balance equations on the species of interest, as active or living polymer chains:

$$\frac{d[R_i]_w}{dt} = 2fiKd[I]\delta(i-1) + Kp[M][R_{i-1}]_w - Kp[M][R_i]_w - Ktc[R_i]_w \sum_{j=1}^{\infty} [R_j]_w \quad (4.56)$$

The Generating Function was applied to the kinetic equations. This infinite set of equations can be reduced to few by defining $H(s)$ as the generating function of the active polymer species.

Definition of Generation Function

$$G(s,t) = \sum_{i=1}^{\infty} s^i P_i(t) \quad (4.57)$$

$$\frac{\partial H(s)}{\partial t} = 2fkKd[I]s - Kp[M](1-s)H(s) - KtcH(s)H(1) \quad (4.58)$$

The integrating was applied with quasi-steady state approximation (QSSA) to Eq.(4.58) when $s=1$, it means that initiation and termination are balanced. If $\partial H(1)/\partial t = 0$, then

$$H(1) = \left(\frac{2fkKd[I]}{Ktc} \right)^{1/2} \quad (4.59)$$

Applying the QSSA to Eq.(4.58) when $s=s$, we can solve for $H(s)$ at any given time, and to solve the monomer balance. If $\partial H(s)/\partial t = 0$, then

$$H(s) = \frac{2fkKd[I]s}{Kp[M](1-s) + (2fkKd[I])^{1/2}} \quad (4.60)$$

The most probable distribution may be written as:

$$H(s) = H(1) \frac{(1-q)s}{1-qs} \quad (4.61)$$

where q is the probability of propagation

$$q = \frac{Kp[M]}{Kp[M] + KtcH(1)} \quad (4.62)$$

The Eq.(4.61) was expanded in power series

$$H(s) = H(1) \sum_{i=1}^{\infty} (1-q)q^{i-1} s^i \quad (4.63)$$

The operator in Eq.(4.63) was dropped, and the geometric distribution is obtained

$$[R_i] = H(1)(1-q)q^{i-1} \quad (4.64)$$

Now the moments μ_0, μ_1, μ_2 are obtained and the definition of NCLD moments is applied

$$\mu_k = \sum_{i=0}^k a_{ki} \left[\frac{\partial^i G(s)}{\partial s^i} \right]_{s=1} \quad k=0,1,2,\dots \quad (4.65)$$

Moments μ_0 in Eq.(4.61) applying the Eq.(4.65), when $s=1$

$$\mu_0 = H(1) \quad (4.66)$$

Moments μ_1 in Eq.(4.61) applying the Eq.(4.65), when $s=1$

$$\mu_1 = \frac{H(1)}{1-q} \quad (4.67)$$

Moments μ_2 in Eq.(4.61) applying the Eq.(4.65), when $s=1$

$$\mu_2 = H(1) \frac{1+q}{(1-q)^2} \quad (4.68)$$

4.4.4.2.2 Instantaneous Dead Polymer

In the instantaneous dead polymer was applied the discrete transformation method which consists of chemical reaction, kinetic equation, expand in power series, integrating, instantaneous number-average degree of polymerization, instantaneous weight-average degree of polymerization, instantaneous number-average molecular weight, instantaneous weight-average molecular weight, and polydispersity.

The chemical reaction was considered by mechanism of emulsion polymerization from Eq.(2.6) to Eq.(2.21) with the approximation of chain transfer, terminal double bond polymerization and internal double bond polymerization were not considered.

The kinetic equation was obtained with material balance equations on the species of interest, in this case the dead polymer with termination by combination:

$$\frac{d[P_i]}{dt} = \frac{Ktc}{2} \sum_{j=1}^{i-1} [R_j][R_{i-j}] \quad i \geq 2 \quad (4.68)$$

The Generating Function was applied to the kinetic equations, Eq.(4.69). This infinite set of equations can be reduced to few by defining $G(s)$ as the generating function, Eq.(4.57), for dead polymer.

$$\frac{\partial G(s)}{\partial t} = \frac{Ktc}{2} H^2(s) \quad (4.70)$$

Substituting the Eq.(4.63) in Eq. (4.70) gives

$$\frac{\partial G(s)}{\partial t} = \frac{Ktc}{2} H^2(1) \left(\frac{(1-q)s}{1-qs} \right)^2 \quad (4.71)$$

The instantaneous dead chain distribution here is obviously not geometric, for the generating function characteristic of geometric distribution has been squared. This is what one calls a self-convoluted geometric distribution, a particular example of a negative binomial distribution. The distribution can be found from expanding equation in a Taylor series in s .

The Eq.(4.71) was expanded in power series

$$\frac{d[P_i]}{dt} = \frac{Ktc}{2} H^2 (1-q)^2 (i-1) q^{i-2} \quad i \geq 2 \quad (4.72)$$

Integrating the Eq.(4.72) gives

$$P_i = [P_i] = \frac{KtcH^2(1) t}{2} (1-q)^2 (i-1) q^{i-2} \quad i \geq 2 \quad (4.73)$$

Obtaining the instantaneous number-average degree of polymerization, dividing Eq. (4.67) and Eq.(4.66) gives:

$$DP_n^i = \frac{\mu_1}{\mu_0} = \frac{2}{1-q} \quad (4.74)$$

Instantaneous weight-average degree of polymerization, dividing Eq.(4.68) and Eq.(4.67) gives:

$$DP_w^i = \frac{\mu_2}{\mu_1} = \frac{2+q}{1-q} \quad (4.75)$$

Instantaneous number-average molecular weight, multiplying MWs to Eq. (4.74) gives:

$$M_n^i = MW_s \cdot DP_n^i = \frac{2MW_s}{1-q} \quad (4.76)$$

Instantaneous weight-average molecular weight, multiplying MWs to EQ. (4.75) gives:

$$M_w^i = MW_s \cdot DP_w^i = \frac{MW_s(2+q)}{1-q} \quad (4.77)$$

The polydispersity

$$Q = \frac{DP_w^i}{DP_n^i} = 1 + \frac{q}{2} \quad (4.78)$$

4.4.4.2.3 Cumulative Dead Polymer

In addition to active or living polymer chain and instantaneous dead polymer will be calculated cumulative dead polymer with generating function, cumulative number-average degree of polymerization, cumulative weight-average degree of polymerization, cumulative number-average molecular weight, cumulative weight-average molecular weight, and the polydispersity.

The generating function of the cumulative polymer, $G(s)$, can be put into integral form for each of the cases we have studied so far. For combination only, we have

$$G(s) = \int_0^i \frac{Ktc}{2} H^2 (1) \left(\frac{(1-q)s}{1-qs} \right)^2 dt' \quad (4.79)$$

Cumulative number-average degree of polymerization

$$DP_n^c = \frac{X_M}{\int_0^{X_M} \frac{dX'_M}{DP_n^i}} \quad (4.80)$$

$$DP_n^c = \frac{2a}{a-b} \frac{X_M}{\text{Ln} \left(\frac{b - aX_M}{b} \right)} \quad (4.81)$$

Where

$$a = Kp[M] \quad (4.82)$$

$$b = a + KtcH(1) \quad (4.83)$$

Cumulative weight-average degree of polymerization

$$DP_w^c = \frac{1}{X_M} \int_0^{X_M} DP_w^i dX_M^i \quad (4.84)$$

$$DP_w^c = \frac{a+2b}{b-a} - \frac{3a}{2(b-a)} X_M \quad (4.85)$$

Cumulative number-average molecular weight

$$M_n^c = \frac{2aMWS}{a-b} \frac{X_M}{\ln\left(\frac{b-aX_M}{b}\right)} \quad (4.86)$$

Cumulative weight-average molecular weight

$$M_w^c = MWS \left(\frac{a+2b}{b-a} - \frac{3a}{2(b-a)} X_M \right) \quad (4.87)$$

The polydispersity

$$Q = \frac{DP_w^c}{DP_n^c} \quad (4.88)$$

The Eq. (4.73) represents the GCLD without normalization. The Eq. (4.62) can be transformed and used for probability propagation. The GCLD with normalization is:

$$X_{Pi} = \frac{P_i}{\sum_{i=1}^{\infty} P_i} = (i-1)(1-q)^2 q^{i-2} \quad (4.89)$$

where q is the probability of propagation given by:

$$q = \frac{Kp.M_0(1-X_M)}{Kp.M_0(1-X_M) + Ktc.H(1)} \quad (4.90)$$

The molecular weight distribution with normalization can be calculated with Eq. (4.73) as following:

$$W_{Pi} = \frac{W_i}{\sum_{i=1}^{\infty} W_i} = \frac{1}{2}(i-1)(1-q)^2 q^{i-2} \quad (4.91)$$

where W_i is given by:

$$W_i = MW_s.P_i \quad (4.92)$$

4.4.4.3 Polymer Size

The average swollen particle radius is obtained from the particle number, molecular weight of polymer and polymer concentration: (Paquet and Ray, 1994b)

Swollen particle radius

$$R_s = \left(\frac{3}{4\pi\rho_p\phi_p} \frac{MW_p C_{Ps}}{N_A C_{Np}} \right)^{1/3} \quad (4.93)$$

Unswollen particle radius

$$R = R_s \left(\frac{\rho_m}{\rho_m + [M]_p MW_m} \right)^{-1/3} \quad (4.94)$$

4.4.4.4 Viscosity of the polymer

The viscosity function was used for the polystyrene system which included the effects of concentration, temperature, and molecular weight. This viscosity correlation was obtained from Harkness (1982).

$$\ln(\mu) = -13,04 + \frac{2013}{T} + MW_P^{0,18} \left[3,915X_M - 5,437X_M^2 + \left(0,623 + \frac{1387}{T} \right) X_M^3 \right] \quad (4.95)$$

4.5 EMULSION POLYMERIZATION REACTOR MODELING

4.5.1 Tubular Reactor without Internal Baffles

The tubular reactor was studied with the following conditions: average properties of materials, experimental values, some estimate values, phase of system pseudo-homogeneous (liquid), continuous flux in hydrodynamic condition, no frictionless, no change the volume concentration, ideal tubular reactor with plug flow, isothermal and no isothermal process, the concentration of the fluid varies from point to point along the flow path. In models with constant variables, the properties and state are not functions of space so that the system is homogeneous (Carberry, 1976; Nauman, 1987; Holland, 1989; Froment, 1990; Bockhorn, 1992; McGravy, 1994).

A technique is the use of one-dimensional situations to construct the basic algorithm, which is the quickly generalized to multidimensional cases. The one-dimensional problem serves to keep the algebraic complication to a minimum and to focus attention on the significant issues. The space as a one-way coordinate is more interesting that even a space coordinate can very nearly become one-way under action of fluid flow. If there is a strong unidirectional flow in the coordinate direction, then significant influences travel only from upstream to downstream. The conditions at a point are then affected largely by the upstream conditions, and very little by the downstream ones. The one-way nature of a space coordinate is an approximation. It is true that convection is a one-way process, but diffusion (which is always present) has two-way influences. However, when the flow rate is large, convection overpowers diffusion and thus makes the space coordinate nearly one-way (Patankar, 1980).

The model simplification objective, in mathematical terms, is to reduce one or more of the following: number of equations, number of terms in the equations, the degree of nonlinearity and degree of coupling between the equations. Generally, model simplification may be achieved from the consideration of the engineering and physics of the process (including the material behavior), the geometry, and mathematical operations (Tucker, 1989).

Mass balance in cylindrical coordinate for number of particles in tubular reactor

$$\frac{\partial N_p}{\partial t} + \left(v_r \frac{\partial N_p}{\partial r} + v_\theta \frac{1}{r} \frac{\partial N_p}{\partial \theta} + v_z \frac{\partial N_p}{\partial z} \right) = D_{AB} \left(\frac{1}{r} \frac{\partial}{\partial r} \left(r \frac{\partial N_p}{\partial r} \right) + \frac{1}{r^2} \frac{\partial^2 N_p}{\partial \theta^2} + \frac{\partial^2 N_p}{\partial z^2} \right) + R_{N_p}$$

(1) (2) (3) (4)

(4.96)

Simplified forms of the general continuity equations, the form of the fundamental continuity equations is usually too complex to be conveniently solved for practical application to reactor design. It is very common in reactors to have flow predominantly in one direction, say, z (e.g. think of tubular reactor). The major gradients then occur in that direction, under isothermal conditions at least. For many cases, then, the cross-sectional average values of dependent variable ϕ , such as concentration (or conversion) and temperature might be used in the equations instead of radial point values. A so called “one-dimensional model” is now obtained. If the convective transport is completely dominant over any diffusive transport, in particular, that in the flow direction—that is, the fluid moves like a “plug”- term (3) may be neglected. Assuming steady-state conditions. Term (1) also drops out, so that the simplified Eq.(4.96) becomes Eq.(4.97) (Froment, 1990).

Simplified Model for number of particles: One-dimensional model, Steady state, Convection radial and angular negligible, and Diffusion radial, angular and axial negligible

$$v_z \frac{\partial N_p}{\partial z} = R_{N_p} \quad (4.97)$$

The overall rate of formation of particles (R_{N_p}), then is the sum of the contributions from entry into micelles (R_{MN}), Eq.(4.30) and homogeneous nucleation (R_{HN}), Eq.(4.41):

$$R_{N_p} = R_{MN} + R_{HN} \quad (4.98)$$

4.5.2 Tubular Reactor with Internal Baffles

4.5.2.1 Diameter of tubular reactor

4.5.2.1.1 Without baffles

Fixed Diameter in tubular reactor beneath or over baffles (Figure 4.1)

$$D_f = 0,6 * D_r \quad (4.99)$$

The fixed diameter (D_f) correspond to the transversal area between tubular reactor wall and over or beneath of baffles where there is not emulsion polymerization fluid flow (Figure 4.1). The variable diameter (D_v) is the transversal area where there is fluid flow of EP beneath or over baffles (Figure 4.1). The initial value of D_v can be changed to other values. We consider $D_v=0,4$ m as initial value.

4.5.2.1.2 With baffles: fixed, variable

Number of transversal area beneath or over baffles

$$N_{ab} = 2 \frac{Lbr}{\Delta z} \quad (4.100)$$

Length of each increments of diameter for each transversal area beneath or over baffles

$$\Delta D_{vb} = \frac{D_f}{N_{ab}} \quad (4.101)$$

Variable diameter in tubular reactor beneath or over baffles (Figure 4.4 (b))

$$D_{vb}(1) = 0,4 * D_r \quad (4.102)$$

$$D_{vb}(I) = D_{vb}(I - 1) + \Delta D_{vb} \quad (4.103)$$

Area of circumference

$$Ar = \frac{\pi}{4} Dr^2$$

$$Dr = Df + Dv$$

$$Df = 0,6Dr$$

$$Dv = 0,4Dr$$

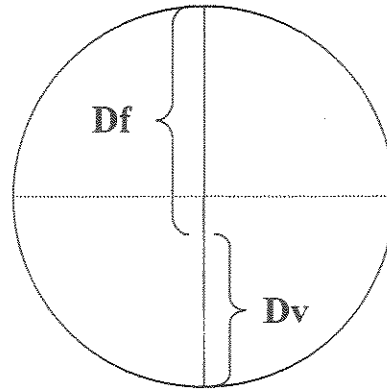


Figure 4.1 Fixed diameter (Df) and Variable diameter (Dv) inside tubular reactor

Area of circular sector

$$A = \frac{1}{2} r^2 \theta \quad (\theta \text{ in radian})$$

Length of arch

$$S = r \cdot \theta$$

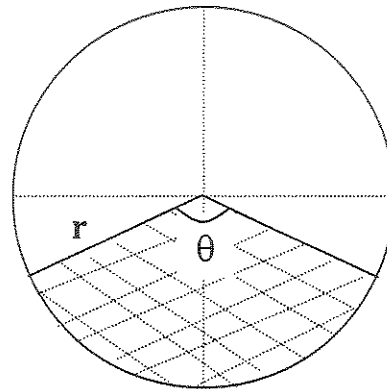


Figure 4.2 Circular sector of radius r

Area of circular segment

$$A = \frac{1}{2} r^2 (\theta - \text{sen } \theta)$$

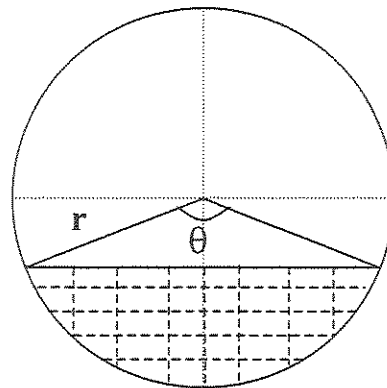


Figure 4.3 Circular segment of radius r

Diameter increment intervals from the fixed diameter point until total diameter

$$ID(1) = 0,5 * Dr - Dvb(1) \quad (4.104)$$

$$ID(I) = Dvb(I) - 0,5 * Dr \quad (4.105)$$

4.5.2.2 Transversal area of tubular reactor

4.5.2.2.1 Without baffle

Area of tubular reactor without baffles was calculated with Figure 4.1 or 4.4(a)

$$Ar = \frac{\pi}{4} D_r^2 \quad (4.106)$$

4.5.2.2.2 With baffle

The increment of the angle in Figure 4.4 (b, c, d, e, f), from the tubular reactor center point until total diameter leads to:

$$\alpha r(1) = \text{arcSen} \left(2 \frac{ID(1)}{Dr} \right) \quad (4.107)$$

The angle incrementation in Figure 4.4 (b, c, d, e, f) to calculate the circular segment area (Figure 4.3) or emulsion polymerization fluid flow area beneath or over the baffles, may be written as:

$$\theta g(1) = 180 * \left(1 - 2 \frac{\alpha r(1)}{\pi} \right) \quad [\text{grad}] \quad (4.108)$$

$$\theta r(1) = \frac{\pi}{180} \theta g(1) \quad [\text{rad}] \quad (4.109)$$

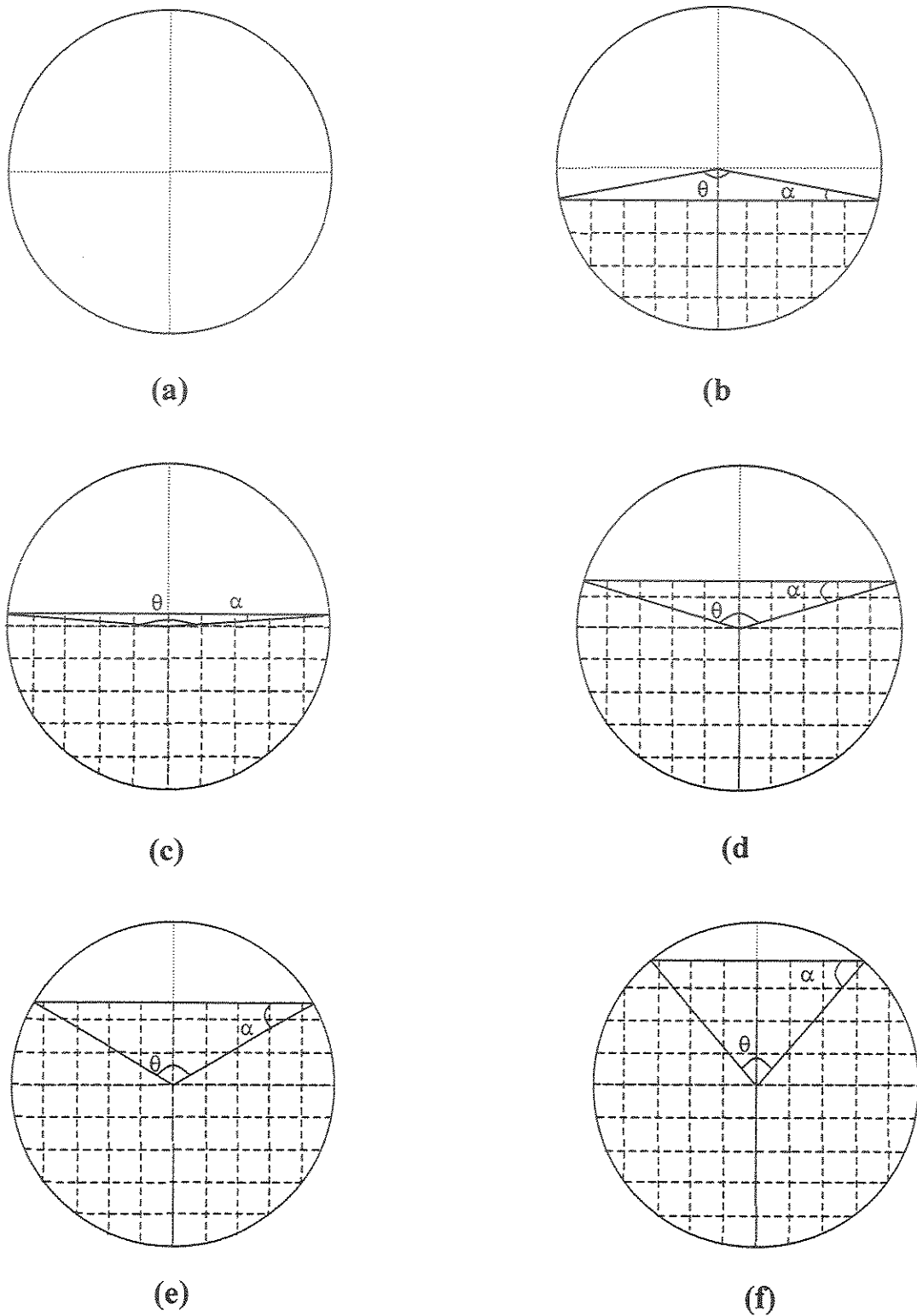


Figure 4.4 Variation of transversal area of fluid flow of emulsion polymerization inside of tubular reactor beneath or over baffles

The fluid flow variable area inside tubular reactor beneath or over baffles (Figure 4.4(b)) is given by:

$$A_{vb}(1) = \frac{Dr^2}{8} (\theta_r(1) - \text{Sen} \theta_r(1)) \quad (4.110)$$

The fixed area inside tubular reactor over or beneath baffles (Figure 4.4(b)) is

$$A_{fb}(1) = Ar - A_{vb}(1) \quad (4.111)$$

The calculation of A_{vb} with Figure 4.4 (c, d, e, f) from $I=2$ to N_{ab} is given as:

$$D_{vb}(I) = D_{vb}(I-1) + \Delta D_{vb} \quad (4.112)$$

$$ID(I) = D_{vb}(I) - 0,5 * Dr \quad (4.113)$$

$$\alpha_r(I) = \text{arcSen} \left(2 \frac{ID(I)}{Dr} \right) \quad (4.114)$$

$$\theta_g(I) = 180 * \left(1 - 2 \frac{\alpha_r(I)}{\pi} \right) \quad (4.115)$$

$$\theta_r(I) = \frac{\pi}{180} \theta_g(I) \quad (4.116)$$

$$A_{fb}(I) = \frac{Dr^2}{8} (\theta_r(I) - \text{Sen} \theta_r(I)) \quad (4.117)$$

$$A_{vb}(I) = Ar - A_{fb}(I) \quad (4.118)$$

4.5.2.3 Fluid flow inside tubular reactor

4.5.2.3.1 Without baffle: Reynolds, velocity, head loss

Reynolds

$$\text{Re} = \frac{\rho D_r V_z}{\mu} \quad (4.119)$$

The inlet velocity inside tubular reactor without baffle in Figure 4.1 or 4.4(a):

$$V_{in} = \frac{\mu \text{Re}}{\rho D_r} \quad (4.120)$$

The total head loss (H_f) is written as :

$$H_f = H_{fs} + H_{ff} \quad (4.121)$$

Pressure Drop

$$\Delta P_r = \rho H_f \quad (4.122)$$

Major head loss or head loss of superficies (H_{fs})

$$H_{fs} = f \frac{L_r V_z^2}{D_r 2} \quad (4.123)$$

Laminar friction factor

$$f = \frac{64}{\text{Re}} \quad (4.124)$$

4.5.2.3.2 With baffle: Reynolds, velocity, head loss

Reynolds

$$Re_b = \frac{\rho Dh}{\mu} V_b \quad (4.125)$$

$$Re_b = \frac{Dh}{Dr} \frac{Ar}{Avb} Re \quad (4.126)$$

Hydraulic diameter

$$Dh = \frac{4Avb}{P} \quad (4.127)$$

Wet perimeter

$$P = P_s + P_b \quad (4.128)$$

Perimeter of circular sector

$$P_s = \frac{Dr}{2} \theta \quad (4.129)$$

Perimeter of baffle base

$$P_b = \frac{Dr}{2} \frac{\text{Sen} \theta}{\text{Sen} \alpha} \quad (4.130)$$

Velocities inside tubular reactor in Figure 4.4 (b, c, d, e, f) beneath or over baffles were calculated from $I=1$ to Nab

$$Vb(I) = \frac{\mu}{\rho} \frac{Ar}{Dr} \frac{Re}{Avb(I)} \quad (4.131)$$

Minor head loss or head loss of form (H_{ff}) is written as:

$$H_{ff} = H_{ffc} + H_{ffe} \quad (4.132)$$

Contraction

$$H_{ffc} = Kc \frac{V_2^2}{2} \quad (4.133)$$

$$Kc=0,3$$

Expansion

$$H_{ffe} = Ke \frac{V_1^2}{2} \quad (4.134)$$

$$Ke=0,4$$

4.5.2.4 Length of baffle

$$Lb = \left(\frac{\Delta z^2}{4} + Df^2 \right)^{1/2} \quad (4.135)$$

Length of each control volume

$$\Delta z = \frac{Lr}{N-1} \quad (4.136)$$

4.5.2.5 Inclination angle of baffle

The baffle inclination angle inside tubular reactor wall was calculated by

$$\gamma = \text{arcTang}\left(\frac{Df}{Lbr}\right) \quad (4.137)$$

4.5.2.6 Lateral Area of tubular reactor

The lateral tubular reactor area was estimated assuming negligible thickness of the baffle:

$$Al_r = \pi D_r L_r \quad (4.138)$$

4.5.2.7 Area of baffle

This area was estimated as parable segment in reference to the Figure 4.5

$$Aba = \frac{2}{3} L_b B_b \quad (4.139)$$

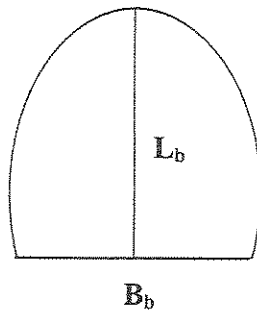


Figure 4.5 Area of parable segment

4.5.2.8 Internal area of tubular reactor

The total internal tubular reactor area was calculated with Eq.(4.138) and Eq.(4.139):

$$At_o = Al_r + Aba \quad (4.140)$$

RESUMO DO CAPÍTULO V

MENDOZA MARÍN, F.L. *Modelagem, simulação e análise de desempenho de reatores tubulares de polimerização com deflectores angulares internos*, 241p. Tese (Doutorado em Engenharia Química – Área de Processos Químicos) – Faculdade de Engenharia Química, Universidade Estadual de Campinas - UNICAMP, 2004.

O Capítulo V descreve os modelos matemáticos que foram desenvolvidos com aproximações, simplificações, suposições, estimativas e limitações com a finalidade de previsão dos efeitos essenciais, geração de dados com programas em Fortran e início de um algoritmo básico. O Capítulo V é importante porque reproduz as características essenciais do fenômeno investigado com as aproximações, simplificações, suposições e limitações consideradas desde os Capítulos IV e outros capítulos. Também é importante porque mostra os modelos matemáticos que foram desenvolvidos e utilizados nos programas com Fortran e as simulações dos Capítulos VII e IX. Os objetivos do Capítulo V são: calcular os efeitos como a conversão do monômero, velocidade axial, temperatura axial, concentração de polímero, radicais e iniciador, caracterizar o produto com número de partículas, peso molecular, tamanho das partículas e viscosidade; descrever a distribuição e os efeitos das chicanas, por exemplo para 50 volumes finitos e 18 chicanas dentro do reator tubular.

Conclusão do Capítulo V: No Capítulo V foram apresentados os modelos matemáticos determinísticos e o fenômeno de polimerização em emulsão. Os modelos deram origem a programas em Fortran. Com a aplicação de um algoritmo e o método numérico de volumes finitos, foram simulados e validados as características essenciais do fenômeno de polimerização em emulsão de estireno com diferentes cálculos do efeito dentro do reator tubular. As aproximações foram introduzidas para diminuir a complexidade da modelagem, projeto e simulação do comportamento do reator tubular sem e com chicanas em condições isotérmicas e não isotérmicas.

CHAPTER V

COMPUTATIONAL TEST

This Chapter describes the mathematical models that were developed according to the approximations, simplifications, suppositions, assumptions, estimations and limitations considered suitable with such models and appropriated numerical solution techniques program codes in Fortran (Visual Compaq Version 6.1) were written. It is important to point out that the approximations, simplifications, suppositions, assumptions, estimations and limitations were deduced from Chapter IV and applied in the Chapters VII-IX. The Chapter importance is to show the final mathematical models that were used in the programs as well as in the simulations.

As processes become more complex, incorporating ever-increasing degrees of automation, there will be a greater need for the analytical approach to problems associated with their design and operation. Modern analysis of process problem usually involves some form of mathematical modeling, and, in one sense, this should appeal to chemical engineers because modeling of processes, either on a bench or pilot scale, has long been a favored preliminary to a commercial plant. There are various mathematical modeling for the same system, each one suited to solve a particular problem associated with the system. The broad classifications constitute steady-state and dynamic models, and in either type the degree of detail required depends on the problem to be solved as well as the amount of basic data available. A very precise description of a chemical process system will often lead to a large set of unwieldy equations. Although they can be solved, it is advisable for complex set that for all practical purposes will yield an engineering solution within the accuracy of the basic data provided (Frank, 1972).

In this Chapter is calculated the impact of reactor design and operational conditions on process variables as monomer conversion, axial velocity, axial temperature, concentration of polymer, radicals and initiator. Also, to characterize the product through particles number, molecular weight distribution, polymer particle size and viscosity

distribution. In order to evaluate the impact of the internal baffles as example is presented the number of particles without and/or with baffles inside the tubular reactor.

5.1 MONOMER CONVERSION CALCULATION

The monomer conversion of styrene was calculated by Eqs.(4.46) and (4.47). The Eq.(4.46) was simplified as “one-dimensional model”, steady state, negligible radial and angular convection, negligible radial, angular and axial diffusion. The Eq.(4.47) was supposed considering that the polymer particle phase is the main locus of polymerization, Smith-Ewart model to estimate the rate of polymerization, Arrhenius chemical kinetics as laminar finite-rate model to compute kinetic coefficient.

$$v_z \frac{\partial C_M}{\partial z} = R_M \quad (5.1)$$

$$R_M = - \frac{K_p [M]_p N_p \bar{n}}{N_A V_p} \quad (5.2)$$

Boundary condition is:

$$C_M = C_{Min}, \text{ when } z=0$$

$$\left(\frac{\partial C_M}{\partial z} \right)_N = 0, \text{ when } z=Lr$$

5.2 AXIAL VELOCITY CALCULATION

The axial velocity inside the tubular reactor was calculated by Eq.(2.23). This equation was simplified in steady state and fully developed flux. It was written in cylindrical one dimensional model in z-component, viscous force on element per volume unit, and gravitational force on element per volume unit are neglected for tubular reactor with plug flow in liquid phase.

The axial velocity without baffles inside tubular reactor in isothermal condition is given by Eq.(4.120) with Re=5000.

$$v_{in} = \frac{\mu.R_c}{\rho.D_r} \quad (5.3)$$

The axial velocity with baffles inside tubular reactor in isothermal condition comes from Eq.(4.131)

$$v_b = \frac{\mu.A_r.R_c}{\rho.A_{vb}.D_r} \quad (5.4)$$

The axial velocity without and with baffles inside tubular reactor in no isothermal condition is given by Eq. (5.5) developed from Eq. (2.22)

$$v_z = \frac{v_{zo}\rho_o}{\rho} \quad (5.5)$$

5.3 AXIAL TEMPERATURE CALCULATION

The axial temperature distribution was calculated through Eq.(4.14). In this equation heat radiation in the reactor is often neglected, except in the case of fixed bed catalytic reactors operating at high temperature, the energy flux by molecular diffusion is neglected. In deriving the one-dimensional model by averaging over the cross section, a boundary condition for heat transfer at the reactor wall has to be introduced for this reason. This boundary condition was approximate as an adiabatic reactor. For the tubular reactor considered here, the heat conduction in the z direction is usually much smaller than the heat transfer by convection. Other simplifications are steady state, reactor with plug flow, the reaction heat is constant, and styrene as chemical specie and reaction.

$$\text{If } \dot{m} = \bar{M}_j C_j v_z \Omega \quad (5.6)$$

$$\rho = \sum_j \bar{M}_j C_j \quad (5.7)$$

$$\sum_i (-\Delta H_i) r_i = (-\Delta H) r \quad (5.8)$$

then

$$\rho C_p v_z \frac{\partial T}{\partial z} = (-\Delta H) r \quad (5.9)$$

$$r = R_M = -K_p o \exp\left(-\frac{E_p}{RgT}\right) \frac{[M]_p N_p \bar{n}}{N_A V_p} \quad (5.10)$$

Boundary condition is:

$$T = T_{in}, \text{ when } z=0$$

$$\left(\frac{\partial T}{\partial z}\right)_N = 0, \text{ when } z=Lr$$

5.4 CONCENTRATION OF POLYMER

The polymer concentration was calculated through Eqs.(4.51) and (4.52). These equations were simplified with the same supposition presented in the monomer concentration calculation.

$$v_z \frac{\partial C_p}{\partial z} = R_p \quad (5.11)$$

$$R_p = \frac{K_p [M]_p N_p \bar{n}}{N_A V_p} \quad (5.12)$$

Boundary condition is:

$$C_p = 0, \text{ when } z=0$$

$$\left(\frac{\partial C_P}{\partial z} \right)_N = 0, \text{ when } z=Lr$$

5.5 CONCENTRATION OF RADICALS

The radicals concentration was calculated with the Eqs.(4.44) and (4.45). The Eq.(4.44) was simplified as “one-dimensional model”, steady state, negligible radial and angular convection, negligible radial, angular and axial diffusion. The concentration rate of all water phase radicals of various chain lengths can be expressed by Eq.(5.14)

$$v_z \frac{\partial C_{Rw}}{\partial z} = R_{Rw} \quad (5.13)$$

$$R_{Rw} = R_I - R_I \left[\frac{KpM_w}{KpM_w + Kcp[N_p] + Ktw[R]_w} \right]^{ncr-1} - Kcp[N_p][R]_w - Kcm[MIC][R]_w - Ktw[R]_w^2 \quad (5.14)$$

Boundary condition is:

$$C_{Rw} = 0, \text{ when } z=0$$

$$\left(\frac{\partial C_{Rw}}{\partial z} \right)_N = 0, \text{ when } z=Lr$$

5.6 CONCENTRATION OF INITIATOR

The initiator concentration was calculated with the Eqs.(4.42) and (4.43). The Eq.(4.42) was simplified as “one-dimensional model”, steady state, negligible radial and angular convection, negligible radial, angular and axial diffusion.

$$v_z \frac{\partial C_I}{\partial z} = R_I \quad (5.15)$$

$$R_I = -fKd[I]_w \quad (5.16)$$

Boundary condition is:

$$C_I = C_{Iin}, \text{ when } z=0$$

$$\left(\frac{\partial C_I}{\partial z} \right)_N = 0, \text{ when } z=Lr$$

5.7 CONCENTRATION OF SURFACTANT

The concentration of surfactant was calculated with the Eq.(4.48) and Eq.(4.49). The Eq.(4.48) was simplified as “one-dimensional model”, steady state, negligible radial and axial convection, negligible radial, angular and axial diffusion. Surfactant is an inert species in the system so that its rate of chemical reaction is negligible.

$$v_z \frac{\partial C_E}{\partial z} = R_E \quad (5.17)$$

$$R_E = 0 \quad (5.18)$$

5.8 CONCENTRATION OF WATER

The water concentration can be calculated in the same way that the concentration of surfactant.

5.9 CHARACTERIZATION OF PRODUCT

5.9.1 Number of Particles

The particles number was calculated with the Eq.(4.97) and (4.98).

5.9.2 Molecular Weight

The instantaneous number and weight average molecular weight were calculated with the Eq.(4.76) and Eq.(4.77), respectively. The cumulative number and weight average molecular weight were calculated with the Eq.(4.86) and (4.87), respectively.

5.9.3 Polymer Particles Size

The polymer particles size was calculated with Eq.(4.93) as swollen particle radius and Eq.(4.94) as unswollen particle radius.

5.9.4 Viscosity of the Polymer Particles

The viscosity of the polymer particles were calculated by Eq.(4.95).

5.10 INTERNAL ANGLE BAFFLES EFFECT

5.10.1 Internal Transversal Area of Tubular Reactor

The calculation of the transversal area A_z as an example with Figure 5.1 for $N=51$ and $N_b=18$ is made as follow. The transversal area (A_z) in this case is the transversal area of emulsion polymerization fluid flow which bounds the control volume over the entire bounding surface. The baffles can be analyzed by the following ways: the viscosity and the fluid flow area of emulsion polymerization. Feldon (1995), Carnavos (1979), Patankar (1979), and Rustum et al. (1990) studied the viscosity for condition laminar or turbulent. Issa et al. (2003) studied a approximated mechanism for the hydrodynamic slug initiation prediction, growth and subsequent development into continuous slug flow in pipeline is presented; the approach is based on the numerical solution of the one-dimensional two-fluid model equations; the pipe cross-section was studied in source term and coefficients after discretisation. Patankar (1979) studied as mixing length at the point is taken to be resultant of two contributions, first, considering a pipe flow without fins, and second, the inter-fins space.

The baffles effect were studied like the fluid flow net-area for emulsion polymerization of styrene in source term and coefficients of the discretized equations, which is known as A_z for each face at the control volume (Figure 5.1).

Area at the tubular reactor inlet

$$A_z(1)=A_r \quad (5.19)$$

$$A_z(2)=A_r \quad (5.20)$$

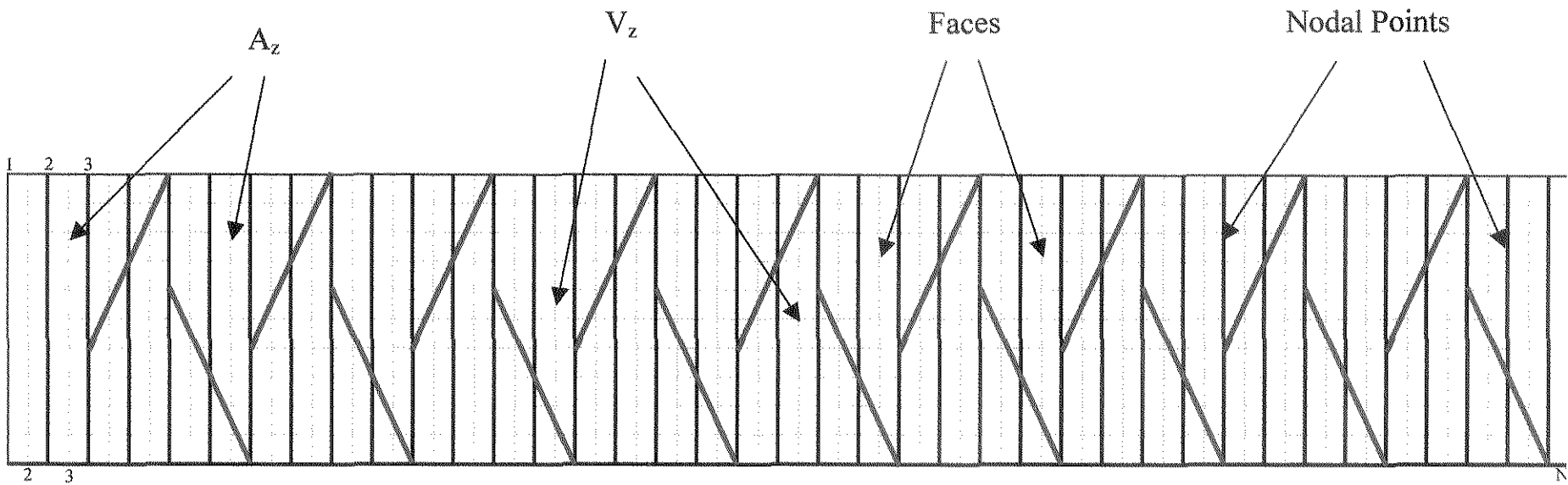


Figure 5.1 Distribution of internal angular multi-deflectors inside tubular reactor: Number of baffles, $N_b=18$ and Number of nodal point, $N=51$.

$$Az(3)=Ar \quad (5.21)$$

From I=4 to N-3, with step of 5

$$Az(I)= Avb(1) \quad (5.22)$$

$$Az(I+1)= Avb(3) \quad (5.23)$$

$$Az(I+2)= Avb(5) \quad (5.24)$$

$$Az(I+3)= Avb(2) \quad (5.25)$$

$$Az(I+4)= Avb(4) \quad (5.26)$$

From I=N-2 to N

$$Az(N-2)=Ar \quad (5.27)$$

$$Az(N-1)=Ar \quad (5.28)$$

$$Az(N)=Ar \quad (5.29)$$

5.10.2 Axial Velocity of Tubular Reactor

The velocity V_z was calculated for each face of the nodal point or control volume inside tubular reactor (Figure 5.1). The velocity V_z was discretised on a staggered grid using a finite volume method. On a staggered grid the velocities are stored at midway location between pressure nodes to avoid the decoupling of velocity and pressure (Issa et al. 2003)

Velocities at the tubular reactor inlet

$$V_z(1)= V_{in} \quad (5.30)$$

$$V_z(2) = V_{in} \quad (5.31)$$

$$V_z(3) = V_{in} \quad (5.32)$$

Velocities from $I=4$ to $N-3$, with step of 5

$$V_z(I) = V_b(1) \quad (5.33)$$

$$V_z(I+1) = V_b(3) \quad (5.34)$$

$$V_z(I+2) = V_b(5) \quad (5.35)$$

$$V_z(I+3) = V_b(2) \quad (5.36)$$

$$V_z(I+4) = V_b(4) \quad (5.37)$$

Velocities at the tubular reactor outlet from $I=N-2$ to N

$$V_z(N-2) = V_{in} \quad (5.38)$$

$$V_z(N-1) = V_{in} \quad (5.39)$$

$$V_z(N) = V_{in} \quad (5.40)$$

RESUMO DO CAPÍTULO VI

MENDOZA MARÍN, F.L. *Modelagem, simulação e análise de desempenho de reatores tubulares de polimerização com deflectores angulares internos*, 241p. Tese (Doutorado em Engenharia Química – Área de Processos Químicos) – Faculdade de Engenharia Química, Universidade Estadual de Campinas - UNICAMP, 2004.

O Capítulo VI analisa o método numérico de volumes finitos que foi aplicado para solucionar os modelos matemáticos desenvolvidos. O Capítulo VI está vinculado com o Capítulo IV em relação ao número de partículas, que foi considerado como exemplo para desenvolver o método de volumes finitos. O Capítulo VI é importante pela aplicação do método numérico de volumes finitos às modelos matemáticos resultantes, por exemplo o número de partículas. Este exemplo de aplicação foi estendido para outras variáveis escalares. Os objetivos do Capítulo VI são: descrever a formulação da equação de transporte conservativo geral e específico para diferentes casos de aplicação; descrever a geração de malha; descrever a discretização das equações conservativas de variáveis escalares; descrever as soluções das equações algébricas simples resultantes; analisar a convergência da solução das equações algébricas resultantes.

Conclusão do capítulo VI: No Capítulo VI foram apresentados as equações conservativas de transporte em forma geral e específica, e o método numérico de volumes finitos. O método numérico de volumes finitos foi analisado com relação a geração de malha, a discretização e a solução das equações algébricas resultantes considerando, por exemplo o número de partículas para 18 chicanas e 50 volumes finitos. O método foi estendido para outras variáveis escalares transportáveis conservativamente como concentração de monômero, polímero, radicais e iniciador e temperatura. Os resultados obtidos nas simulações foram satisfatórios conforme as validações realizadas. O método de volumes finitos mostrou ser um método robusto conservativo, de contorno e de transporte de fluxo de fluidos de polimerização em emulsão.

CHAPTER VI

NUMERICAL METHOD: FINITE VOLUME METHOD

This Chapter describes the numeric approach based on method of finite volume that was applied to solve the resulting mathematical models. This Chapter is linked with the Chapter IV in relation to the application case like particles number that was considered as application example of finite volume method. This Chapter is important because it shows the finite volume method application to the resulting mathematical models, e.g. particles number, which can be extended for monomer conversion, temperature, concentration of polymer, radicals and initiator.

The most usual numerical method are finite difference method (FDM), finite elements method (FEM), orthogonal collocation method (OCM), boundary elements method (BEM), which can solve ordinary or partial equations by means of approximations according to practical, computational or engineering finality, applying series Taylor, Fourier, Polynomial de Jacobi, Hermite, Legendre, Laguerre, Bessel Functions, Gamma, Delta, Fourier Transformations, Laplace, Algebraic Equations of Runge Kutta, Newton, Euler, etc. by means of operation of deriving, expanding, integrating, coupling, transforming, function composition or simplifications. Finite volume method are equations conservative balance in a finite control volume, also variables and parameter distributions in agreement with Gauss' divergence theorem, using as a finite volume condition at the domain and sub-domain like boundary conditions. Moreover it can be used to estimate the variable profiles and materials properties by means of computationally algebraic solutions (Spiegel, 1963; Gradshteyn et al. 1965; Apostol, 1967; Frank, 1972; Davis, 1984; Song et al. 1988 a, b, 1989 a, b, 1990; Luyben, 1990; Mathews, 1992; Leithold, 1994; Boyce et al. 1997; Perry et al. 1997; Versteeg, 1998).

This Chapter describes the much general formulation of conservative transport equation, and deduces the different cases of its applications. It is described the applied grid generation. As well as the discretization that was applied to particles number, leading to a

simple algebraic equations. It was analyzed the convergence solution of the numerical method that was applied at the programs code.

6.1 CONSERVATION EQUATION

6.1.1 General formulation

The general transport equations can be written in the differential form, where the variable ϕ is the general variable of the conservative form of all fluid flow equation, including equations for scalar quantities such concentration, velocity, temperature, particles number, etc. (Bird, 1960; Patankar, 1980; Tucker, 1989; Wendt, 1992; Maliska, 1995; Versteeg, 1998).

Differential forms

$$\frac{\partial(\rho\phi)}{\partial t} + \text{div}(\rho\vec{u}\phi) = \text{div}(\Gamma \text{grad}\phi) + S_\phi \quad (6.1)$$

This Equation is called transport equations for property ϕ :

$$\begin{aligned} & \text{(Rate of increase of } \phi \text{ of fluid element)} + \text{(Net rate of flow of } \phi \text{ out of fluid element)} \\ & = \text{(Rate of increase of } \phi \text{ due to diffusion)} + \text{(Rate of increase of } \phi \text{ due to sources)} \end{aligned}$$

In an abbreviation form:

$$(A) + (C) = (D) + (S) \quad (6.2)$$

6.1.2 Specific formulation

The general transport equation can be studied in steady and transient state. For example, the steady state can be applied to a open and closed system of tubular reactor, with or without chemical reaction.

The transport equation in steady state, open system with chemical reaction without diffusion was used for modeling and simulation of the number of particles in tubular reactor with or without baffles inside the reactor, Eq. (6.11).

6.1.2.1 Transient state**1.- Open system**

With chemical reaction

$$(A) + (C) = (D) + (S) \quad (6.3)$$

$$(A) + (C) = (S) \quad (6.4)$$

Without chemical reaction

$$(A) + (C) = (D) \quad (6.5)$$

$$(A) + (C) = 0 \quad (6.6)$$

2.- Close system

With chemical reaction

$$(A) = (D) + (S) \quad (6.7)$$

$$(A) = (S) \quad (6.8)$$

Without chemical reaction

$$(A) = (D) \quad (6.9)$$

6.1.2.2 Steady state**1.- Open system**

With chemical reaction

$$(C) = (D) + (S) \quad (6.10)$$

$$(C) = (S) \quad (6.11)$$

Without chemical reaction

$$(C) = (D) \quad (6.12)$$

2.- Close system

With chemical reaction

$$0 = (D) + (S) \quad (6.13)$$

Without reaction

$$0 = (D) \quad (6.14)$$

6.2 GRID GENERATION

6.2.1 Procedure

Consider the steady state particles number calculus in one-dimensional domain defined in Figure 6.1 and extend for other scalar variables such as concentration, temperature, etc. (Patankar, 1980; Wendt, 1992; Maliska, 1995; Versteeg, 1998).

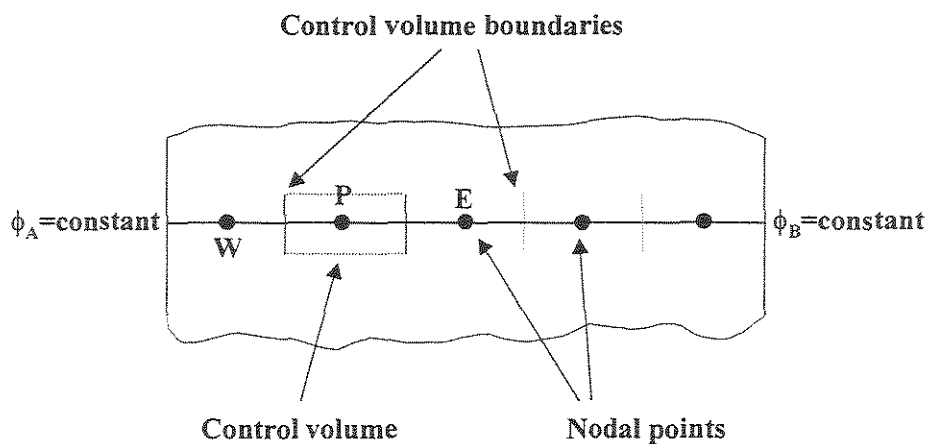


Figure 6.1 The steady state of property ϕ in one-dimensional domain.

For grid generation was used the following procedure: 1) Divide the domain into discrete control volumes; 2) Determine a number of nodal point in the space between inlet and outlet; 3) The boundaries (or faces) of control volumes are positioned mid-way between adjacent nodes. Thus each node is surrounded by a control volume or cell; 4) Establish a system of notation that can be used in future development, Figure 6.2. A general nodal point is identified by P and its neighbours in an one-dimensional geometry, the nodes to the west and east, are identified by W and E respectively. The west side face of the control volume is referred to by 'w' and the east side control volume face by 'e'. The distance between nodes W and P, and between nodes P and E, are identified by δx_{WP} and δx_{PE} , respectively. Similarly, the distance between face w and point P and between P and face e are denoted by δx_{wP} and δx_{Pe} , respectively. Figure 6.2 shows that the control volume width is $\Delta x = \delta x_{we}$; 5) The faces have the velocity, transversal area of tubular reactor with or without baffles, the properties of materials such as density, viscosity, diffusivity, etc. The main grid has scalar variables such as concentration, temperature, number of particles, particle size, etc.

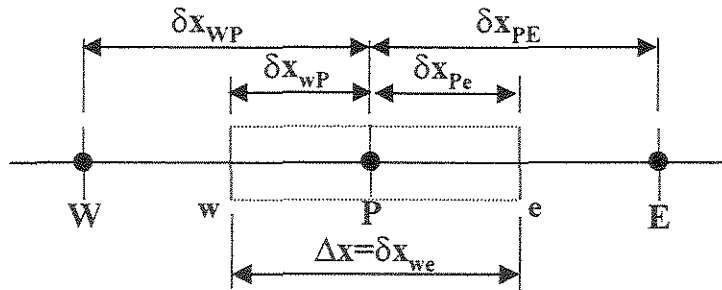


Figure 6.2 Grid-point cluster for the one-dimensional problem.

6.2.2 Boundary conditions

All CFD problems are defined in terms of initial and boundary conditions. Nevertheless, it is necessary to define the following boundary conditions such as inlet, outlet, wall, pressure, symmetry and periodicity. The staggered grid arrangement was used for calculate the particle number and others scalar variables (Patankar, 1980; Wendt, 1992; Maliska, 1995; Versteeg, 1998).

6.2.2.1 Inlet Boundary

The inlet boundary conditions or the minimum control volume. The nodes along the line $I=1$ (or $i=2$ for velocity and transversal area) are used to store the inlet values of flow variables. The Figure 6.3 shows the minimum control volume for calculate the number of particles and others scalar variables (Versteeg, 1998):

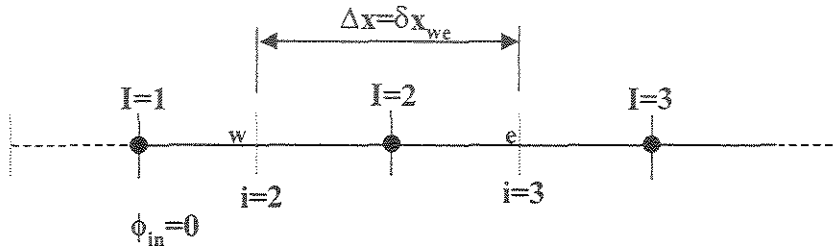


Figure 6.3 The minimum control volume for the one-dimensional problem.

6.2.2 2 Outlet Boundary

The outlet boundary condition or the maximum control volume may be used in conjunction with the inlet boundary conditions. If the location of the outlet is selected far away from geometrical disturbances the flow often reaches a fully developed state where no change occurs in the flow direction. In such region it can placed an outlet surface and states that the gradients of all variables (except pressure) are zero in the flow direction. N ($=M$) is the total number of nodes in the z -direction and the equations are solved for cells up to I (or i) = $N-1$. The Figure 6.4 shows the maximum control volume for calculate the number of particles and others scalar variables (Versteeg, 1998):

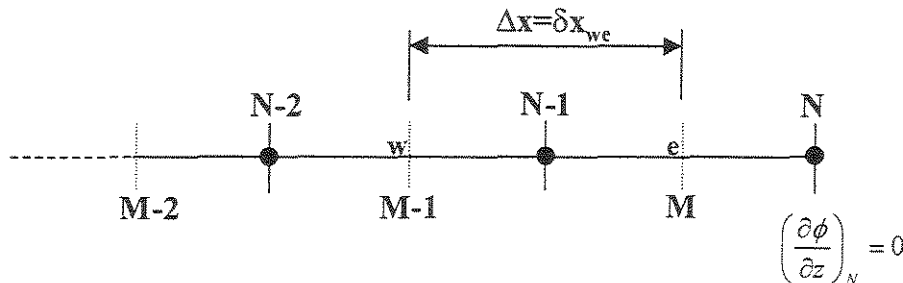


Figure 6.4 The maximum control volume for one-dimensional problem

6.2.2.3 Wall Boundary

The wall is the most common boundary encountered in tubular reactor with fluid flow of emulsion polymerization. The no-slip condition ($v_z=v_r=0$) is the appropriate condition for the velocity component at solid walls. In general for variables special sources are constructed, the precise form of which depends on whether the flow is laminar or turbulent. In the present thesis the wall condition was not considered (Versteeg, 1998).

6.2.2.4 Pressure Boundary

The constant pressure condition is used in situation where exact details of the flow distribution are unknown but the boundary values of pressure are known. Typical problems where this boundary condition is appropriate include external flows around objects, free surface flows, buoyancy-driven flows such as natural ventilation and fires, and also internal flows with multiple outlets (Versteeg, 1998).

6.2.2.5 Symmetry Boundary

The conditions of symmetry are: (1) no flows across the boundary and (2) no scalar flux across the boundary. In the implementation, normal velocities are set to zero at a symmetry boundary and the values of all other properties just outside the solution domain are equated to their values at the nearest node just inside the domain (Versteeg, 1998).

6.2.2.6 Periodicity Boundary

Periodic or cyclic boundary conditions arise from a different type of symmetry in a problem (Versteeg, 1998).

6.3 DISCRETIZATION

The discretisation will be calculated with a number of particles as example. These procedure of calculus was applied in all calculus of scalar variables in the present thesis.

6.3.1 Discrete approximation

6.3.1.1 Conservative balance

Mass balance for number of particles (see Section 4.5)

$$v_z \frac{\partial N_p}{\partial z} = R_{Np} \quad (6.15)$$

The overall rate of formation of particles by Micelle and Homogeneous Nucleation (see Section 4.4.4.1):

$$R_{Np} = R_{MN} + R_{HN} = \frac{Kcm[MIC]R_l}{KpMw + Kcm[MIC] + Ktw[R]_w} \left(\frac{1 - \alpha_m^{ncr-1}}{1 - \alpha_m} \right) + R_l \alpha_h^{ncr-1} \quad (6.16)$$

6.3.1.2 Linear approximation

When the source S_ϕ depends on ϕ , it is convenient to express the dependence in a linear form given by Eq.(6.17). This is done because (1) nominally linear framework would allow only a formally linear dependence, and (2) the incorporation of linear dependence is better than treating S_ϕ as a constant (Patankar, 1980)

When S_ϕ is a nonlinear function of ϕ , it should be linearize, i.e., it is necessary to specify the values of SUT and SPT, which may themselves depend on ϕ . Further, the basic rule about nonpositive SPT must be obeyed. The Taylor's Series method of linearization was used to linearize S_ϕ . The linearized source term S_ϕ ($=[Np]_P$) is assumed to prevail throughout the control volume (Patankar, 1980; Wendt, 1992; Maliska, 1995; Versteeg, 1998)

The overall equation of source-term linearization

$$S_{Np} = R_{Np} = S_{Npm} + S_{Nph} = SUT - SPT[Np]_P \quad (6.17)$$

Source-term linearization of Micellar Nucleation

$$S_{Npm} = SUM - SPM[Np]_P \quad (6.18)$$

Eq. (4.30) can then be rewritten as given in Eq. (6.19) and the notation of nodal point P will be omitted

$$S_{N_{pm}} = R_{MN} = \left(\frac{Kcm[MIC]R_i}{KpMw + Kcm[MIC] + Ktw[R]_w} \right) \left(\frac{KpMw + Kcm[MIC] + Ktw[R]_w + Kcp[Np]}{Kcm[MIC] + Ktw[R]_w + Kcp[Np]} \right) \left(1 - \left(\frac{KpMw}{KpMw + Kcm[MIC] + Ktw[R]_w + Kcp[Np]} \right)^{ncr-1} \right) \quad (6.19)$$

The following definitions are used to simplify the Eq.(6.19)

$$m1 = KpMw \quad (6.20)$$

$$m2 = Kcm[MIC] + Ktw[R]_w \quad (6.21)$$

$$m3 = m1 + m2 \quad (6.22)$$

$$m4 = \frac{Kcm[MIC]R_i}{m3} \quad (6.23)$$

Equation (6.19) can then be rewritten as

$$S_{N_{pm}} = m4 \left(\frac{m3 + Kcp[Np]}{m2 + Kcp[Np]} \right) \left(1 - \left(\frac{m1}{m3 + Kcp[Np]} \right)^{ncr-1} \right) \quad (6.24)$$

Taylor's Series for one variable was applied to linearizar the source-term of the Eq. (6.24), which is polynomial approximation of degree n=1. The linearization represents the tangent to the $S_{N_{pm}}-[Np]_P$ curve at $[Npa]$ (Frank, 1972; Davis, 1984; Luyben, 1990; Mathews, 1992; Boyce et al. 1997).

$$S_{N_{pm}}([Np]) = S_{N_{pm}}([Npa]) + S'_{N_{pm}}([Npa])([Np] - [Npa]) \quad (6.25)$$

The coefficients $S_{N_{pm}}([Npa])$ of the Taylor polynomial (Eq.(6.25)) was calculated as

$$S_{Npm}([Npa]) = m4 \left(\frac{m3 + Kcp[Npa]}{m2 + Kcp[Npa]} \right) \left(1 - \left(\frac{m1}{m3 + Kcp[Npa]} \right)^{ncr-1} \right) \quad (6.26)$$

The slope of the curve $S_{Npm}=f([Np])$ (Eq.(6.24) at the point $([Npa], f([Npa]))$ was calculated as

$$S'_{Npm}([Npa]) = \left(\frac{(ncr-1)m4Kcp}{m2 + Kcp[Npa]} \right) \left(\frac{m1}{m3 + Kcp[Npa]} \right)^{ncr-1} - \left(\frac{m1m4Kcp}{(m2 + Kcp[Npa])^2} \right) \left(1 - \left(\frac{m1}{m3 + Kcp[Npa]} \right)^{ncr-1} \right) \quad (6.27)$$

$[Npa]$ is one point of the line tangent (Eq.(6.18)) to the curve $S_{Npm}=f([Np])$ (Eq.6.24)). This point can be estimated by the following ways:

- 1) The average value of the intersection points in the coordinate axis of the line tangent (Eq.(6.18)) to the curve (Eq.(6.24)). The intersection points must be maximum values in each interception. Whether a curve is concave up or concave down, then the value of $[Npa]$ must be adjusted with care.
- 2) The average value of the variable $\phi = [Np]$ of the experimental conditions at tubular reactor inlet and outlet.

Substituting Eq.(6.26) and Eq.(6.27) into Eq.(6.25), and the following definitions used to simplify the coefficient SUM of Eq.(6.18) can be written:

$$SUM = SUM1 + SUM2 - SUM3 \quad (6.28)$$

$$SUM1 = m4 \left(\frac{m3 + Kcp[Npa]}{m2 + Kcp[Npa]} \right) \left(1 - \left(\frac{m1}{m3 + Kcp[Npa]} \right)^{ncr-1} \right) \quad (6.29)$$

$$SUM2 = \left(\frac{m1m4Kcp[Npa]}{(m2 + Kcp[Npa])^2} \right) \left(1 - \left(\frac{m1}{m3 + Kcp[Npa]} \right)^{ncr-1} \right) \quad (6.30)$$

$$SUM3 = \left(\frac{(ncr - 1)m4Kcp[Npa]}{m2 + Kcp[Npa]} \right) \left(\frac{m1}{m3 + Kcp[Npa]} \right)^{ncr-1} \quad (6.31)$$

The following definitions are used to simplify the coefficient SPM of Eq.(6.18)

$$SPM = SPM1 - SPM2 \quad (6.32)$$

$$SPM1 = \left(\frac{m1m4Kcp}{(m2 + Kcp[Npa])^2} \right) \left(1 - \left(\frac{m1}{m3 + Kcp[Npa]} \right)^{ncr-1} \right) \quad (6.33)$$

$$SPM2 = \left(\frac{(ncr - 1)m4Kcp}{m2 + Kcp[Npa]} \right) \left(\frac{m1}{m3 + Kcp[Npa]} \right)^{ncr-1} \quad (6.34)$$

Source-term linearization of Homogeneous Nucleation

$$S_{Nph} = SUH - SPH[Np]_P \quad (6.35)$$

Equation (4.41) can then be written as given by Eq. (6.36) and the notation of nodal point P will be omitted.

$$S_{Nph} = R_{HN} = R_I \left(\frac{KpMw}{KpMw + Ktw[R]_w + Kcp[Np]} \right)^{ncr-1} \quad (6.36)$$

The following definitions are used to simplify the Eq.(6.36)

$$h1 = KpMw \quad (6.37)$$

$$h2 = h1 + Ktw[R]_w \quad (6.38)$$

Equation (6.36) can then be rewritten as

$$S_{Nph} = R_I \left(\frac{h1}{h2 + Kcp[Np]} \right)^{ncr-1} \quad (6.39)$$

Taylor's Series for one variable was applied to linearize the source-term of the Eq.(6.39), which is polynomial approximation of degree $n=1$. The linearization represents the tangent of the $S_{Nph}-[Np]_P$ curve at $[Npa]$ (Frank, 1972; Davis, 1984; Luyben, 1990; Mathews, 1992; Boyce et al. 1997).

$$S_{Nph}([Np]) = S_{Nph}([Npa]) + S'_{Nph}([Npa])([Np] - [Npa]) \quad (6.40)$$

The coefficients $S_{Nph}([Npa])$ of the Taylor polynomial (Eq.(6.40)) was calculated as

$$S_{Nph}([Npa]) = R_I \left(\frac{h1}{h2 + Kcp[Npa]} \right)^{ncr-1} \quad (6.41)$$

The slope of the curve $S_{Nph}=f([Np])$ (Eq.(6.39) at the point $([Npa], f([Npa]))$ was calculated as

$$S'_{Nph} = - \frac{(ncr - 1)KcpR_I h1^{ncr-1}}{(h2 + Kcp[Npa])^{ncr}} \quad (6.42)$$

$[Npa]$ is one point of the line tangent (Eq.(6.35)) to the curve $S_{Npm}=f([Np])$ (Eq.(6.39)). This point can be estimated by the following ways:

- 1) The average value of the intersection points in the coordinate axis of the line tangent (Eq.(6.35)) to the curve (Eq.(6.39)). The intersection points must be maximum values in each interception. Whether a curve is concave up or concave down, then the value of $[Npa]$ must be adjusted with care.
- 2) The average value of the variable $\phi = [Np]$ of the experimental conditions at tubular reactor inlet and outlet.

The value $[Npa]$ estimated by homogeneous nucleation was used for source-term linearization by micellar nucleation.

Substituting Eq.(6.41) and Eq.(6.42) into Eq.(6.40), this can be re-arranged all their terms. Now, the following definitions are used to simplify the coefficient SUH of the Eq.(6.35)

$$SUH = SUH1 + SUH2 \quad (6.43)$$

$$SUH1 = R_i \left(\frac{h1}{h2 + Kcp[Npa]} \right)^{ncr-1} \quad (6.44)$$

$$SUH2 = \frac{(ncr - 1)KcpR_i [Npa]}{h1} \left(\frac{h1}{h2 + Kcp[Npa]} \right)^{ncr} \quad (6.45)$$

The following definition is used to simplify the coefficient SPH of the Eq.(6.35)

$$SPH = \frac{(ncr - 1)KcpR_i}{h1} \left(\frac{h1}{h2 + Kcp[Npa]} \right)^{ncr} \quad (6.46)$$

Now we sum the Eq.(6.28) and Eq.(6.43) to obtain the coefficient SUT of the Eq.(6.17)

$$SUT = SUM + SUH \quad (6.47)$$

The sum the of Eq.(6.32) and Eq.(6.46) lead to obtain the coefficient SPT of the Eq.(6.17)

$$SPT = SPM + SPH \quad (6.48)$$

6.3.1.3 Integration

The integral forms of the general transport equations represent the key step of the finite volume method. In this case is the integration of Eq.(6.1) over a three-dimensional control volume cv yielding (Patankar, 1980; Wendt, 1992; Maliska, 1995; Versteeg, 1998):

$$\int_{cv} \frac{\partial(\rho\phi)}{\partial t} dV + \int_{cv} \text{div}(\rho\phi\vec{u}) dV = \int_{cv} \text{div}(\Gamma \text{grad}\phi) dV + \int_{cv} S_\phi dV \quad (6.49)$$

The volume integrals in the second term on the left hand side, the convective term, and first term on the right hand side, the diffusive term, are re-written as integrals over the entire bounding surface of the control volume by using Gauss' divergence theorem. For a vector \vec{a} this theorem states (Boyce et al. 1997; Marcia et al. 1998; Versteeg, 1998), leading to Eq. (6.50).

$$\int_{cv} \text{div}\vec{a} dV = \int_A \vec{n} \cdot \vec{a} dA \quad (6.50)$$

The physical interpretation of $\vec{n} \cdot \vec{a}$ is the component of vector \vec{a} in the direction of the vector \vec{n} normal to the surface element dA . Thus the integral of the divergence of a vector \vec{a} over a volume is equal to the component of \vec{a} in the direction normal to the surface which bounds the volume summed (integrated) over the entire bounding surface A . Applying Gauss' divergence theorem, equation (6.49) can be written as follows:

$$\frac{\partial}{\partial t} \left(\int_{cv} \rho\phi dV \right) + \int_A \vec{n} \cdot (\rho\phi\vec{u}) dA = \int_A \vec{n} \cdot (\Gamma \text{grad}\phi) dA + \int_{cv} S_\phi dV \quad (6.51)$$

The order of integration and differentiation has been changed in the first term on the left hand side of Eq.(6.51) to illustrate its physical meaning. This term signifies the rate of change of the total amount of fluid property $\phi(=Np)$ in the control volume. The product $\vec{n} \cdot (\rho\phi\vec{u})$ express the flux component of property $\phi(=Np)$ due to fluid flow along the outward normal vector \vec{n} , so the second term on the left hand side of Eq.(6.51), the convective term, is therefore the net of decrease of fluid property $\phi(=Np)$ of the fluid element due to convection (Versteeg, 1998).

A diffusive flux is positive in the direction of a negative gradient of the fluid property $\phi(=Np)$, i.e. along direction $-\text{grad}\phi$. For instance, heat is conducted in the

direction of negative temperature gradients. Thus, the product $\bar{n} \cdot (-\Gamma \text{grad}\phi)$ is the component of diffusion flux along the outward normal vector, and so out of the fluid element. Similarly, the product $\bar{n} \cdot (\Gamma \text{grad}\phi)$, which is also equal to $\Gamma(-\bar{n} \cdot (-\text{grad}\phi))$, can be interpreted as a positive diffusion flux in the direction of the inward normal vector $-\bar{n}$, i.e. into the fluid element. The first term on the right hand side of the Eq.(6.51), the diffusive term, is thus associated with a flux into the element and represents the net rate of increase of fluid property ϕ of the fluid element due to diffusion. The final term on the right hand side of this equation gives the rate of increase of property ϕ as result of sources inside the fluid element (Versteeg, 1998)

In words, the equation (6.51) for the fluid in the control volume can be expressed as follows:

(Rate of increase of ϕ) + (Net rate of decrease of ϕ due to convection across the boundaries) = (Rate of increase of ϕ due to diffusion across the boundaries) + (Net rate of creation of ϕ)

This discussion clarifies that integration of the partial differential equation generates a statement of the conservation of the fluid property for a finite size (macroscopic) control volume (Versteeg, 1998).

In steady state problems, the rate of change term of the Eq.(6.51) is equal to zero, and applying simplified model for tubular reactor. This leads to the integrated form of the steady state transport equation for particle number without diffusion as follows:

$$\int_{cv} \frac{\partial(v_z Np)}{\partial z} Adz = \int_{cv} S_{Np} Adz = \int_{cv} (SUT - SPT \cdot Np_p) Adz \quad (6.52)$$

$$(AvNp)_e - (AvNp)_w = (S_{Np} Az)_e - (S_{Np} Az)_w = (SUT - SPT \cdot Np_p) A_p \Delta z \quad (6.53)$$

Continuity Equation in steady state and simplified model for tubular reactor (see Eq. (2.22)

$$\frac{\partial(\rho v_z)}{\partial z} = 0 \quad (6.54)$$

$$(Av\rho)_e = (Av\rho)_w \quad (6.55)$$

6.3.1.4 Interpolation

The upwind differencing scheme was applied to calculate the number of particles, but exist other method of interpolation such as: central differencing, the exact solution, the exponential scheme, the hybrid scheme, the power-law scheme, etc. (Patankar, 1980; Wendt, 1992; Maliska, 1995; Versteeg, 1998)

$$F_w\phi_w = \phi_w \|F_w,0\| - \phi_P \| -F_w,0\| \quad (6.56)$$

$$F_e\phi_e = \phi_P \|F_e,0\| - \phi_E \| -F_e,0\| \quad (6.57)$$

Where

$$F = \rho V \quad (6.58)$$

Mass Balance or continuity equation

$$A_w \| -F_w,0\| = A_w \|F_w,0\| - A_w F_w \quad (6.59)$$

$$A_e \|F_e,0\| = A_e \| -F_e,0\| + A_e F_e \quad (6.60)$$

6.3.2 Linear algebraic equations

6.3.2.1 Internal control volume (internal nodes) I=3 to I=N-2

Substituting Eq.(6.56) and Eq.(6.57) into Eq.(6.53) and dropping out clasp of $[Np]_P$ leads to Eq. (6.61).

$$A_e (Np_P \|F_e,0\| - Np_E \| -F_e,0\|) - A_w (Np_W \|F_w,0\| - Np_P \| -F_w,0\|) = (SUT - SPT.Np_P) A_P \Delta z \quad (6.61)$$

Equation (6.61) can be re-arranged as

$$(A_e \|F_e, 0\| + A_w \|-F_w, 0\| + SPT.A_p \Delta z) Np_p = A_w \|F_w, 0\| Np_w + A_e \|-F_e, 0\| Np_e + SUT.A_p \Delta z \quad (6.62)$$

The following definitions are used to find out the coefficients of discretised equation

$$a_w = A_w \|F_w, 0\| \quad (6.63)$$

$$a_e = A_e \|-F_e, 0\| \quad (6.64)$$

$$S_p = SPT.A_p \Delta z + (A_e F_e - A_w F_w) \quad (6.65)$$

$$S_U = SUT.A_p \Delta z \quad (6.66)$$

$$a_p = A_e \|F_e, 0\| + A_w \|-F_w, 0\| + SPT.A_p \Delta z \quad (6.67)$$

Substituting Eq.(6.59) and Eq.(6.60) into Eq.(6.67) gives

$$a_p = a_w + a_e + S_p \quad (6.68)$$

Now it is written the discretised equation for internal control volume Eq. (6.69) is obtained.

$$a_p Np_p = a_w Np_w + a_e Np_e + S_U \quad (6.69)$$

6.3.2.2 Minimum control volume : I=2

Boundary condition

$$N_{pin}=0, \text{ when } z=0 \quad (6.70)$$

Substituting Eq.(6.56), Eq.(6.57) and Eq.(6.70) into Eq.(6.53) and dropping clasp of $[Np]_p$ leads to:

$$A_e(N_{p_p}\|F_e,0\| - N_{p_E}\|-F_e,0\|) - A_w(N_{pin}\|F_w,0\| - N_{p_p}\|-F_w,0\|) = (SUT - SPT.N_{p_p})A_p\Delta z \quad (6.71)$$

Equation (6.71) can be re-arranged as

$$(A_e\|F_e,0\| + A_w\|-F_w,0\| + SPT.A_p\Delta z)N_{p_p} = A_w\|F_w,0\|N_{pin} + A_e\|-F_e,0\|N_{p_E} + SUT.A_p\Delta z \quad (6.72)$$

The following definitions are used to find the coefficients of discretised equation

$$a_w = 0 \quad (6.73)$$

$$a_{in} = A_w\|F_w,0\| \quad (6.74)$$

$$a_E = A_e\|-F_e,0\| \quad (6.75)$$

$$S_p = SPT.A_p\Delta z + a_{in} + (A_eF_e - A_wF_w) \quad (6.76)$$

$$S_U = SUT.A_p\Delta z + a_{in}N_{pin} \quad (6.77)$$

$$a_p = A_e\|F_e,0\| + A_w\|-F_w,0\| + SPT.A_p\Delta z \quad (6.78)$$

Substituting Eq.(6.59) and Eq.(6.60) into Eq.(6.78) gives

$$a_p = a_E + S_p \quad (6.79)$$

Now the discretised equation for internal control volume can be written as:

$$a_p Np_p = a_E Np_E + S_U \quad (6.80)$$

6.3.2.3 Maximum control volume : I=N-1

Boundary condition

$$\left(\frac{\partial Np}{\partial z} \right)_N = 0, \text{ when } z=Lr \quad (6.81)$$

Substituting Eq.(6.56), Eq.(6.57) and Eq.(6.81) into Eq.(6.53) and dropping clasp of $[Np]_p$ leads to Eq. (6.82).

$$A_e F_e Np_p - A_w (Np_w \|F_w, 0\| - Np_p \| -F_w, 0\|) = (SUT - SPT.Np_p) A_p \Delta z \quad (6.82)$$

Equation (6.82) can be re-arranged as

$$(A_e F_e + A_w \| -F_w, 0\| + SPT.A_p \Delta z) Np_p = A_w \|F_w, 0\| Np_w + SUT.A_p \Delta z \quad (6.83)$$

The following definitions are used to find the coefficients of discretised equation

$$a_w = A_w \|F_w, 0\| \quad (6.84)$$

$$a_E = 0 \quad (6.85)$$

$$S_p = SPT.A_p \Delta z + (A_e F_e - A_w F_w) \quad (6.86)$$

$$S_U = SUT.A_p \Delta z \quad (6.87)$$

$$a_p = A_e F_e + A_w \left| -F_w, 0 \right| + SPT.A_p \Delta z \quad (6.88)$$

Substituting Eq.(6.59) and Eq.(6.60) into Eq.(6.88) gives

$$a_p = a_w + S_p \quad (6.89)$$

Now the discretised equation for maximum control volume is as follow:

$$a_p Np_p = a_E Np_E + S_U \quad (6.90)$$

6.4 SOLUTION OF ALGEBRAIC EQUATIONS

The governing equations of flow and number of particles result in a system of linear algebraic equations which need to be solved. The complexity and size of the set of equations depends on the dimensionality of the problem, the number of grid nodes and the discretisation practice. There are two families of solution technique for linear algebraic equations: direct method and indirect method or iterative methods (Patankar, 1980; Versteeg, 1998)

The one-dimensional problem for the calculation of the number of particles, lead to a tri-diagonal system, a system with only three non-zero coefficients per equation. Thomas (1949) developed a technique for rapidly solving tri-diagonal systems that is now called the Thomas algorithm or the tri-diagonal matrix algorithm (TDMA). The TDMA is actually a direct method for one-dimensional situations problems and is widely used in CFD programs. It is computationally inexpensive and has the advantage that it requires a minimum amount of storage (Patankar, 1980; Wendt, 1992; Maliska, 1995; Versteeg, 1998)

Consider a system of discretisation equations that has a tri-diagonal form:

$$-A_i \phi_{i-1} + B_i \phi_i - C_i \phi_{i+1} = D_i \quad (6.91)$$

Forward elimination, for $i=1$

$$A_1=0 \quad (6.92)$$

$$p_1 = \frac{C_1}{B_1} \quad (6.93)$$

$$q_1 = \frac{D_1}{B_1} \quad (6.94)$$

Forward elimination, for $i=2,3,\dots,N-1$

$$p_i = \frac{C_i}{B_i - A_i p_{i-1}} \quad (6.95)$$

$$q_i = \frac{D_i + A_i q_{i-1}}{B_i - A_i p_{i-1}} \quad (6.96)$$

Forward elimination, for $i=N$

$$C_N = 0 \quad (6.97)$$

$$p_N = 0 \quad (6.98)$$

$$q_i = \frac{D_i + A_i q_{i-1}}{B_i - A_i p_{i-1}} \quad (6.99)$$

Back Substitution

$$\phi_N = q_N \quad (6.100)$$

$$\phi_i = q_i + p_i \phi_{i+1} \quad (6.101)$$

6.5 CONVERGENCE

A good understanding of the numerical solution algorithm is also crucial. Three mathematical concepts are useful in determining the success or otherwise the fail of such

algorithms: convergence, consistency and stability. Convergence is the property of a numerical method to produce a solution, which approaches the exact solution as the grid spacing; control volume size or element size is reduced to zero. Consistent numerical schemes produce systems of algebraic equations which can be demonstrated to be equivalent to the original governing equation as the grid spacing tends to zero. Stability is associated with damping of errors as the numerical method proceeds. If a technique is not stable even round-off errors in the initial data can cause wild oscillations or divergence (Patankar, 1980; Versteeg, 1998).

Iterative procedures used in digital computers for solving systems of algebraic equations are sometimes needed to solve the equation. In the literature there are many numerical solution of algebraic equations such as bisection, false position, modify false position, Newton-Raphson, extended Newton Raphson, and the direct substitution was used in isothermal and no isothermal condition (Frank, 1972; Davis, 1984; Luyben, 1990; Mathews, 1992).

Convergence is usually very difficult to establish theoretically and in practice could use the Lax's equivalence theorem which states that for linear problems a necessary and sufficient condition for convergence is that the method is both consistent and stable. In CFD methods this theorem is of limited use since that the governing equations are non-linear. In such problems consistency and stability are necessary condition for convergence, but not sufficient. It is difficult to prove conclusively that a numerical solution scheme is convergent is perhaps somewhat unsatisfying from a theoretical standpoint, but the mesh spacing very close to zero is not feasible on computing machines with a finite representation of numbers. Round-off errors would swamp the solution long before a grid spacing of zero is actually reached. CFD codes need to produce physically realistic results with good accuracy in simulation with finite(sometimes quite coarse) grids. Patankar (1980) has formulated rules which yield robust finite volume calculations schemes: conservativeness, boundedness and transportiveness (Versteeg, 1998).

6.5.1 Isothermal condition

The discretization equation, for example Eq.(6.69), Eq.(6.80) and Eq.(6.90) are a linear algebraic equations, and the set of such equations need to be solved by the methods

for linear algebraic equations. The problem is iterative and the objective is to find the value of the number of particle. The procedure is as follow with or without baffle:

- 1.- Guess a Number of particle, aN_p .
- 2.- Calculate the initiator and radicals distribution.
- 3.- Calculate the number of particle, N_p
- 4.- Compare the calculate N_p with the actual number of particle, aN_p .
- 5.- If absolute value of $|N_p - aN_p|$ is greater than a factor of convergence (10^{-3}), the calculated N_p is set $aN_p = N_p$ (return to the step 1).

6.5.2 No isothermal condition

In no isothermal condition, the discretization equation of initiator, radicals, number of particle, monomer and temperature are a linear algebraic equation. The solution for the discretization equations for the one-dimensional situation can be obtained by the Thomas algorithm or the TDMA (Tri Diagonal-Matrix Algorithm). The set of linear algebraic equations is on iterative problem until to obtain convergence. The convergence problem is to find out a number of particle and temperature. This process involves the following steps with or without baffles:

- 1.- Guess or assumption the values of aN_p and aT at all grid points.
- 2.- From these guessed aN_p 's and aT 's, calculate tentative values of the coefficients in the discretization equations of initiator, radicals, number of particle and temperature.
- 3.- Solve the nominally linear set of algebraic equations to get new values of N_p .
- 4.- With these N_p 's as better guesses, return to step 2 and repeat the process until absolute value of $|N_p - aN_p|$ is lower than a factor of convergence (10^{-3}).
- 5.- Calculate the temperature T with number of particle N_p of step 4.
- 6.- With these T 's as better guesses, return to step 2 and repeat the process until absolute value of $|T - aT|$ is lower than a factor of convergence (10^{-2}).

RESUMO DO CAPÍTULO VII

MENDOZA MARÍN, F.L. *Modelagem, simulação e análise de desempenho de reatores tubulares de polimerização com deflectores angulares internos*, 241p. Tese (Doutorado em Engenharia Química – Área de Processos Químicos) – Faculdade de Engenharia Química, Universidade Estadual de Campinas - UNICAMP, 2004.

O Capítulo VII apresenta a estrutura dos programas e os resultados de simulação computacional conforme a formulação dos Capítulos IV e V. O Capítulo VII é importante porque explica a estrutura dos códigos dos programas em Fortran que foram realizados em condições isotérmicas e não isotérmicas, sem e com chicanas angulares dentro do reator tubular em estado estacionário. Neste capítulo são apresentados todos os resultados simulados por meio dos modelos determinísticos em balanços combinados de massa, velocidade, energia, reação e chicana-reator. Os objetivos do Capítulo VII são: descrever e explicar a estrutura dos programas; descrever as simulações de conversão do monômero, apresentar o cálculo da área transversal interna, temperatura axial, concentração de polímero, radicais e iniciador, número de partículas, peso molecular, tamanho das partículas, viscosidade, densidade de polímero e monômero, perda de carga e queda de pressão; descrever a caracterização das chicanas.

Conclusão do Capítulo VII: No Capítulo VII foram apresentados a estrutura dos programas em Fortran, os algoritmos que descrevem a solução dos resultados das simulações de cálculo para os reatores. Também foram descritas as características e condições das chicanas. Os algoritmos sem e com chicanas em condições de temperatura de reação constante ou variável apresenta convergência, consistência e estabilidade na obtenção dos resultados de simulação. Nas simulações computacionais foram descritos os dados mais significativos e um breve comentário comparativo do aspecto comum ou representativo das trajetórias das variáveis.

CHAPTER VII

COMPUTATIONAL SIMULATION

This Chapter contains the programs structure and the computational simulation results. It shows programs code structure at isothermic and no isothermic conditions, without and/or with internal angle baffles inside tubular reactor in steady state. Simulation results are for 60°C feed temperature and at 1 m reactor diameter.

Specification of the domain geometry and grid design are important requirements. The two aspects that characterise such results are convergence of the iterative process and grid independence. The solution algorithm is iterative in nature and in a converged solution the so-called residuals - measures of the overall conservation of the flow properties – are very small. Progress towards a converged solution can be greatly assisted by careful selection of the settings of various relaxation factors and acceleration devices. There are no straightforward guidelines for making these choices since they are problem dependent. Optimization of the solution speed requires considerable experience with the code itself, which can only be required by extensive use. There is no formal way to estimate the errors introduced by inadequate grid design for a general flow. Good initial grid design relies largely on an insight into the expected properties of the flow. A background in the fluid dynamics of the particular problem certainly helps and experience with gridding of similar problems is also invaluable. The only way to eliminate errors due to the coarseness of a grid is to perform a grid dependence study, which is a procedure of successive refinement of an initially coarse grid until certain key results do not change. Then the simulation is grid independence. A systematic search for grid-independence results forms an essential part of all high quality CFD studies (Versteeg, 1998).

In this Chapter is described and explained the programs code structure. It is described the simulations of monomer conversion, internal transversal area (ITA), axial temperature (AT), concentration of polymer, radicals and initiator, particles number,

MWD, PPS, viscosity distribution (VD), density of polymer and monomer, head loss, and pressure drop. It is also described internal angle baffles characterization.

7.1 PROGRAM CODE STRUCTURE

One important aspect of mathematical modeling is the arrangement of the equations. It has been found by experience that if the equations are arranged in a logical or caused-and-effect sequence the computer model is stable. This sequence is termed the “natural” order, for it invariably closely parallels the cause-and-effect sequence found in nature. It will soon be realized that the key to understanding the internal mechanism lies in being able to define this natural cause-and-effect sequence (Franks, 1972).

FORTRAN is designed to provide better facilities for the solution of scientific and technological problems and to provide a firm base for further developments to meet the needs of last year of the 20th century and of the early 21st. FORTRAN will have importance for the future development of scientific, technological and numerical computation. The most important aspect of programming is undoubtedly its design, while the next most important is the thorough testing of the program (Ellis et al. 1994).

Writing a computer program for solve a problem is a multi-step process consisting in general of at least the five major elements shown in Figure 7.1, which are program concept, problem, algorithm development, program coding and program store. Note that only one portion of this process (program coding) focuses on the use of a specific programming language. The other four steps relate to the development of a problem-solving approach. The first stage is learnt on programming concept, in this case Fortran. The second step in the program development process consist to define the problem carefully and clearly. The third step is the generation of the algorithm, analyse the problem and break it down into its fundamental elements. An algorithm is a map or an outline to a problem solution. This outline shows the precise order in which the program will execute individual functions to arrive at the solution. The fourth step in the program development process is the program coding or conversion of the algorithm into the desired programming language. It is necessary to convert the algorithm into a more structured device, the source code or Program Unit. The program unit has main program and subprogram. The program unit is need to debugging, testing and optimization until the program works correctly in all

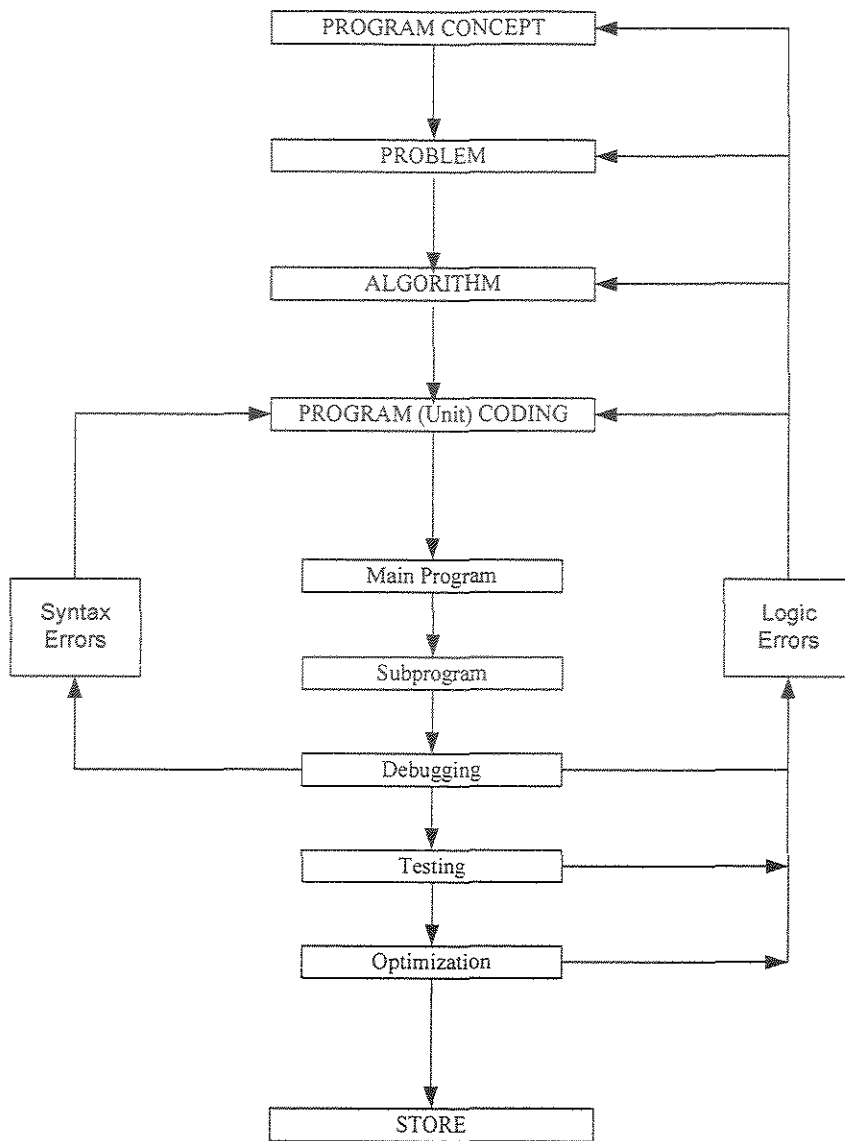


Figure 7.1 Stages of the development programs codes.

situation that can envisage. The five step is program store for use in the program development process until final Program Unit. These stages in program development were applied in isothermal and no isothermal conditions with or without baffles for emulsion homopolymerization tubular reactor of styrene.

7.1.1 Isothermal condition

The **purpose** is to write a program for calculate concentration and velocity of reactants and products without and with baffles inside emulsion homopolymerization tubular reactor of styrene, in isothermal conditions. Also particles number, molecular weight distribution, particle size and viscosity distribution are calculated and estimated and other calculus.

The **analysis** of the problem consists in break it down into its fundamental elements. The major step required is the initiation, calculate section, discretised equations solve and products characterization.

The **method** describes the computational algorithm and presents a general logic diagram of isothermal condition, without and with baffles, where are represented by the flow diagram in the Figure 7.2 and Figure 7.3, respectively.

The **program description** consist in to explain the main program, the required subroutines, description of parameters (arrays and variables), dimensions, input date, output date, and summary of user requirements. The calculation of particle number includes an iteration process (see Section 6.5.1), and program has a Main Program and a subroutine TDMA (see Section 6.4). The parameters description are the same to the notation used in formulas and equations presented so far. The input dates are at beginning of the Program Unit. The output dates are printed in two files. One file prints the total results of concentration, velocity, temperature and other baffles characteristics, reactor and product. Other file prints molecular weight distribution, total results and for each iteration the geometric and molecular distribution.

The **program code** was made according to the computational algorithm. Taking Figure 7.2, in the algorithm flow chart requires the INITIAL CONDITION of particles number. TRANSVERSAL AREA provides internal transversal area of tubular reactor without baffle (Section 4.6.2.1). INLET VELOCITY calculates the inlet velocity at the tubular reactor (Section 5.2). HEAD LOSS calculates the head loss laminar or turbulent flow (Section 4.6.3.1). PRESSION DROP calculates the preSSION drop inside tubular reactor for laminar or turbulent flow (Section 4.6.3.1). GRID GENERATION generates the

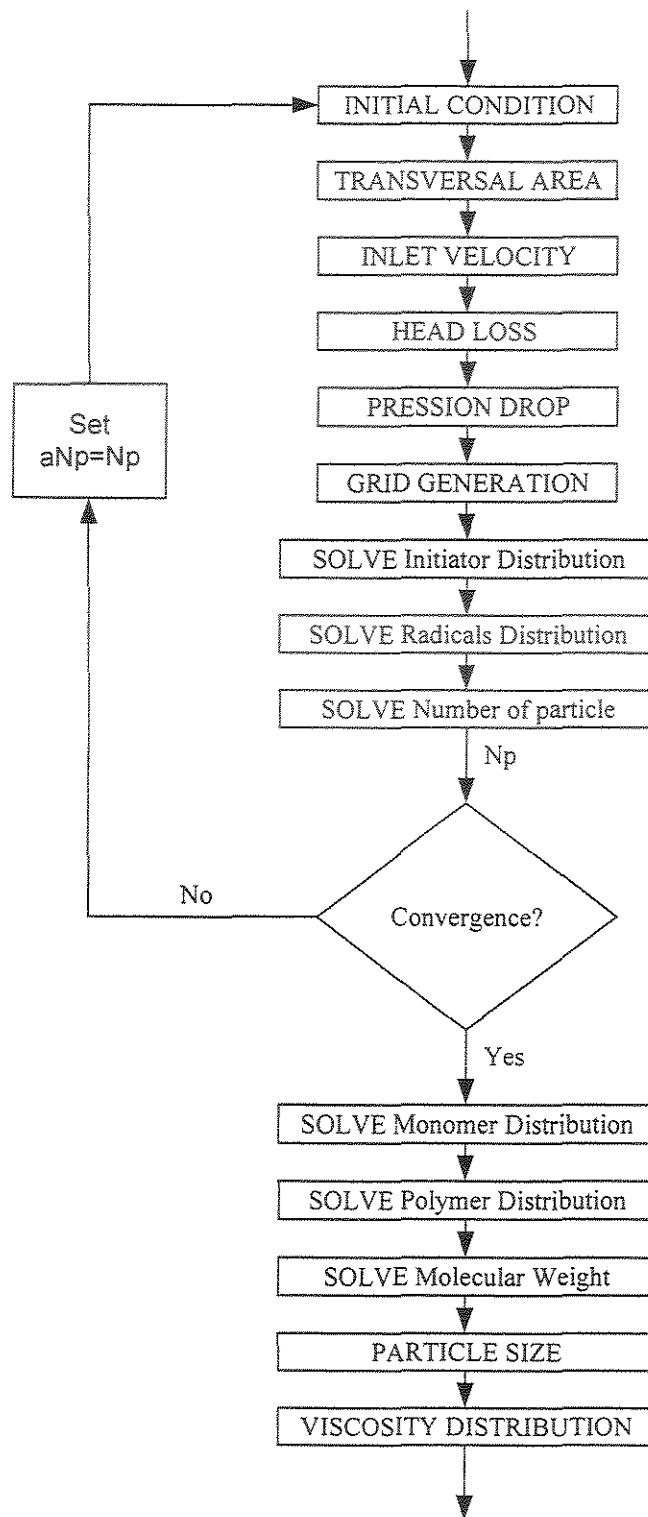


Figure 7.2 Isothermal condition logic flow diagram

grid-point in one-dimensional, in axial direction. SOLVE INITIATOR DISTRIBUTION calculates the initiator concentration distribution inside tubular reactor (Sections 5.6, 6.3 and 6.4). SOLVE RADICALS DISTRIBUTION calculates the radicals concentration distribution in axial direction inside tubular reactor (Sections 5.5, 6.3 and 6.4). SOLVE NUMBER OF PARTICLE calculates the particles number in axial direction inside tubular reactor (Sections 5.9.1, 6.3 and 6.4). The particles number is submitted to an iteration process according to Section 6.5.1. SOLVE MONOMER DISTRIBUTION calculates the monomer (styrene) concentration distribution inside tubular reactor (Sections 5.1, 6.3, and 6.4). SOLVE POLYMER DISTRIBUTION calculates the polystyrene concentration distribution inside tubular reactor as given in Sections 5.4, 6.3 and 6.4. SOLVE MOLECULAR WEIGHT calculate the molecular weight distribution instantaneous and in a cumulative fashion in axial direction inside tubular reactor (Sections 4.4.4.2 and 5.9.2). PARTICLE SIZE calculates the average polymer particle size distribution of polymer swollen and unswollen inside tubular reactor according to Sections 4.4.4.3 and 5.9.3. VISCOSITY DISTRIBUTION calculates the polymer viscosity distribution inside tubular reactor (Sections 4.4.4.4 and 5.9.4).

The flow diagram given in Figure 7.3 consists on INITIAL CONDITION of particles number to begin the calculation. TRANSV AREA BAFFLE calculates the internal transversal area of the baffles inside tubular reactor (Section 4.6.2.2). GRID GENERATION generates the grid-point in one-dimensional, in axial direction. TRANSV AREA REACTOR calculates the internal transversal area distribution inside, the tubular reactor (Section 5.10.1). TRANSV VELOCITY calculates the axial velocity distribution inside tubular reactor (Section 5.10.2). REYNOLDS NUMBER calculates the Reynolds number inside tubular reactor (Section 4.6.3.2). HEAD LOSS calculates the head loss laminar or turbulent flow (Section 4.6.3.1). PRESSION DROP calculates the pressure drop inside the tubular reactor for laminar or turbulent flow (Section 4.6.3.1). AREA OF TUBULAR REACTOR calculates the total internal area inside tubular reactor as given in Section 4.6.8. SOLVE INITIATOR DISTRIBUTION calculates the initiator concentration distribution inside the tubular reactor (Sections 5.6, 6.3 and 6.4). SOLVE

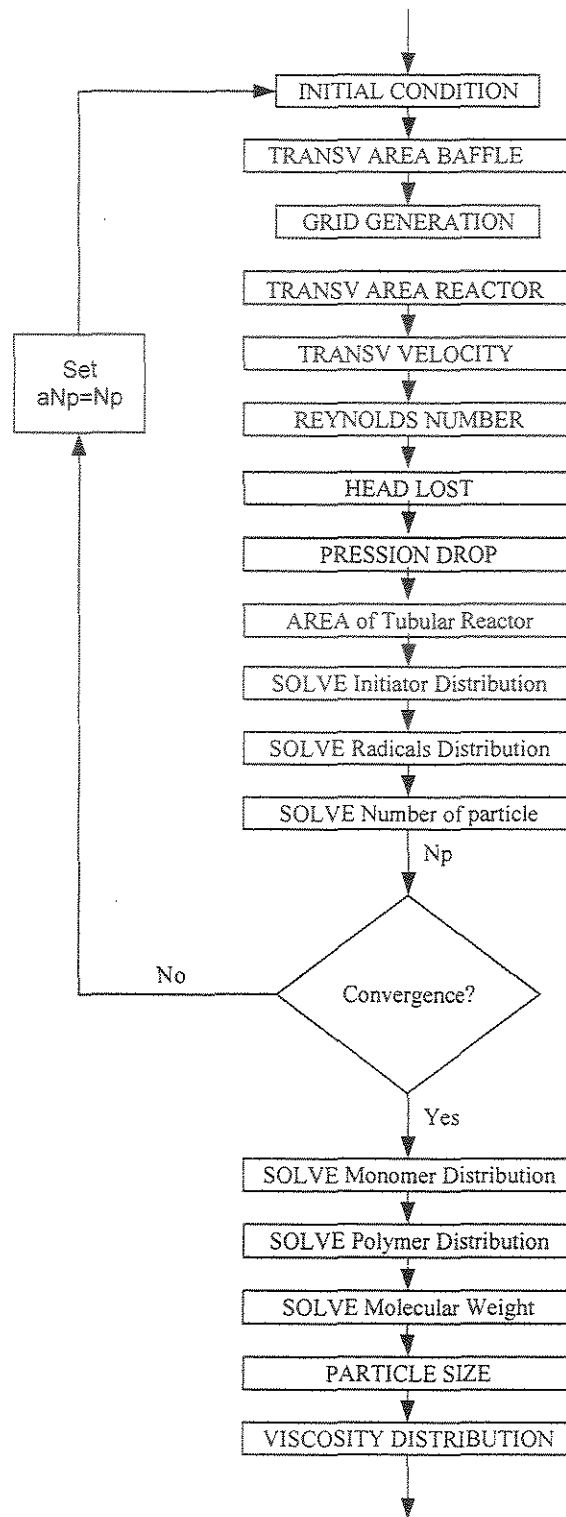


Figure 7.3 Isothermal condition logic flow diagram with baffle.

RADICALS DISTRIBUTION calculates the radicals concentration distribution, in axial direction, inside the tubular reactor as pointed out in Sections 5.5, 6.3 and 6.4. SOLVE NUMBER OF PARTICLE calculates particles number in axial direction inside the tubular reactor (Sections 5.9.1, 6.3 and 6.4). The particles number is submitted to an iteration process according to Section 6.5.1. SOLVE MONOMER DISTRIBUTION calculates the monomer concentration distribution inside tubular reactor (Sections 5.1, 6.3, and 6.4). SOLVE POLYMER DISTRIBUTION calculates the polystyrene concentration inside tubular reactor (Sections 5.4, 6.3 and 6.4). SOLVE MOLECULAR WEIGHT calculates the molecular weight distribution instantaneous and cumulative in axial direction inside the tubular reactor (Sections 4.4.4.2 and 5.9.2). PARTICLE SIZE calculates polymer particles size of polymer swollen and unswollen inside tubular reactor (Sections 4.4.4.3 and 5.9.3). VISCOSITY DISTRIBUTION calculates the polymer viscosity distribution inside tubular reactor as given in Sections 4.4.4.4 and 5.9.4.

7.1.2 No isothermal condition

The **purpose** is to write a program to calculate concentration, velocity and temperature distribution of reactants and product without and with baffles inside emulsion polymerization tubular reactor of styrene. Also to find the particles number, molecular weight distribution, particle size and viscosity distribution.

The **analysis** of the problem consists in break it down into its fundamental elements. The major step required is the initiation, calculate section, discretised equations solve and products characterization.

The **method** describes the computational algorithm and presents a general logic diagram in no isothermal condition without and with baffles which represented by the flow diagram in the Figures 7.4 and 7.5, respectively.

The **program description** consist in to explain the main program, the required subroutines, parameters description (arrays and variables), dimensions, input dates, output dates, and user requirements summary. The particle number calculation includes an iteration process (see Section 6.5.1), and the program has a Main Program and a subroutine TDMA (see Section 6.4). The parameters description are the same to the notation used in formulas and equations presented so far. The parameters data are in beginning in the Program Unit. The output data are printed in two files. One file prints the total results of

concentration, velocity, temperature and other baffles characteristics, reactor and products. Other file prints molecular weight distribution, total results and for each iteration the geometric and molecular distribution.

The **program code** was made according to the computational algorithm. Taking Figure 7.4, in the algorithm flow chart requires the INITIAL CONDITION of particle number. TRANSVERSAL AREA provides the internal transversal area inside tubular reactor without baffles (Section 4.6.2.1). GRID GENERATION generates the grid-point in one-dimensional, in axial direction. DENSITY DISTRIBUTION calculates the density distribution of polymer and monomer inside tubular reactor according to the Table 3.5. AXIAL VELOCITY calculates the axial velocity with equation of continuity according to Eq.(5.5), it calculates variable density in no isothermal condition inside tubular reactor as shown in Section 5.2. HEAD LOSS calculates the head loss laminar or turbulent flow (Section 4.6.3.1). PRESSION DROP calculates the pression drop inside tubular reactor laminar or turbulent flow (Section 4.6.3.1). SOLVE INITIATOR DISTRIBUTION calculates the initiator concentration distribution inside of tubular reactor (Sections 5.6, 6.3 and 6.4). SOLVE RADICALS DISTRIBUTION calculates the radicals concentration distribution in axial direction inside tubular reactor (Sections 5.5, 6.3 and 6.4). SOLVE NUMBER OF PARTICLE calculates the particles number in axial direction inside tubular reactor (Sections 5.9.1, 6.3 and 6.4). The particles number is submitted to an iteration process according to Section 6.5.2. SOLVE TEMPERATURE DISTRIBUTION calculates the axial temperature distribution inside tubular reactor according to Sections 5.3, 6.3 and 6.4. An iteration process was applied to the axial temperature distribution until convergence (Section 6.5.2). SOLVE MONOMER DISTRIBUTION calculates the monomer concentration distribution inside tubular reactor (Sections 5.1, 6.3, and 6.4). SOLVE POLYMER DISTRIBUTION calculates the polystyrene concentration inside tubular reactor as given in Sections 5.4, 6.3 and 6.4. SOLVE MOLECULAR WEIGHT calculates the molecular weight distribution instantaneous and in a cumulative fashion in axial direction inside tubular reactor (Sections 4.4.4.2 and 5.9.2). PARTICLE SIZE calculates the polymer particle size of polymer swollen and unswollen inside tubular reactor according to Section 4.4.4.3 and 5.9.3. VISCOSITY DISTRIBUTION calculates the polymer viscosity distribution inside tubular reactor (Sections 4.4.4.4 and 5.9.4).

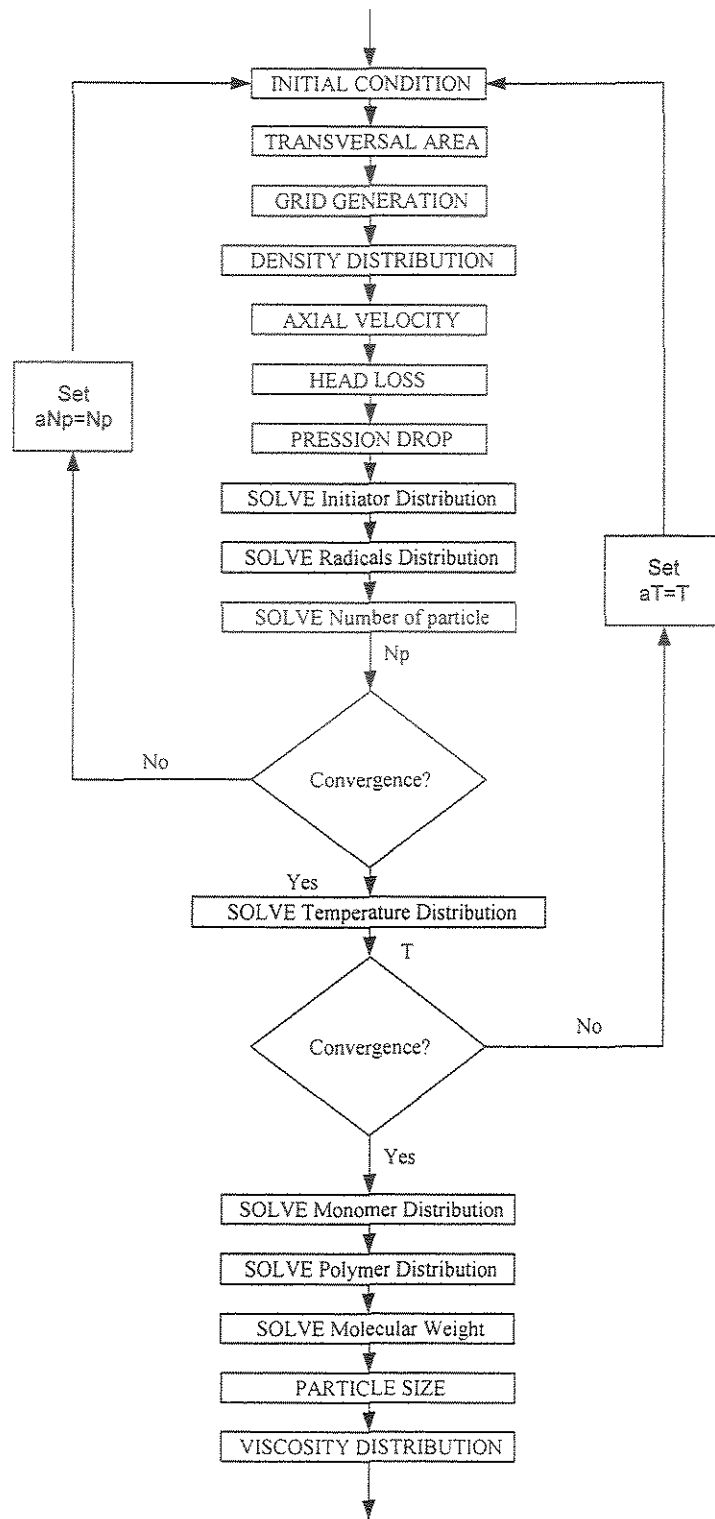


Figure 7.4 No isothermal condition logic flow diagram.

The flow diagram given in Figure 7.5 consists on INITIAL CONDITION of particles number to begin the calculation. TRANSV AREA BAFFLE calculates the baffles transversal area inside tubular reactor (Section 4.6.2.2). GRID GENERATION generates the grid-point in one-dimensional, in axial direction. TRANSV AREA REACTOR calculates the internal transversal area distribution inside tubular reactor (Section 5.10.1). DENSITY DISTRIBUTION calculates the density distribution of polymer and monomer inside tubular reactor as shown in Table 3.5. AXIAL VELOCITY calculates the axial velocity with continuity equation according to Eq.(5.5), it calculates with variable density in no isothermal condition inside tubular reactor (Section 5.2). BAFFLE DISTRIBUTION calculates the baffle length and inclined angle baffles according to Sections 4.6.4 and 4.6.5. REYNOLDS NUMBER calculates the Reynolds number inside tubular reactor as given in Section 4.6.3.2. HEAD LOSS calculates the head loss laminar or turbulent flow (Section 4.6.3.1). PRESSION DROP calculates the pression drop inside the tubular reactor laminar or turbulent flow (Section 4.6.3.1). AREA OF TUBULAR REACTOR calculates the internal total area inside tubular reactor (Section 4.6.8). SOLVE INITIATOR DISTRIBUTION calculates the initiator concentration distribution inside the tubular reactor (Sections 5.6, 6.3 and 6.4). SOLVE RADICALS DISTRIBUTION calculates the radicals concentration distribution, in axial direction, inside the tubular reactor as pointed out in Sections 5.5, 6.3 and 6.4. SOLVE NUMBER OF PARTICLE calculates the particles number in axial direction inside the tubular reactor according to Sections 5.9.1, 6.3 and 6.4. The particle number is submitted to an iteration process as given in Section 6.5.2. SOLVE TEMPERATURE DISTRIBUTION calculates the axial temperature distribution inside tubular reactor (Sections 5.3, 6.3 and 6.4). An iteration process was applied to the axial temperature distribution until convergence as shown in Section 6.5.2. SOLVE MONOMER DISTRIBUTION calculates monomer concentration distribution inside tubular reactor (Section 5.1, 6.3, and 6.4). SOLVE POLYMER DISTRIBUTION calculates polystyrene concentration inside tubular reactor (Sections 5.4, 6.3 and 6.4). SOLVE MOLECULAR WEIGHT calculates the molecular weight distribution instantaneous and cumulative in axial direction inside the tubular reactor (Sections 4.4.4.2 and 5.9.2). PARTICLE SIZE calculates the polystyrene particle size of polymer swollen and unswollen inside tubular reactor (Sections 4.4.4.3 and 5.9.3). VISCOSITY DISTRIBUTION calculates the polystyrene viscosity distribution inside tubular reactor as given in Sections 4.4.4.4 and 5.9.4.

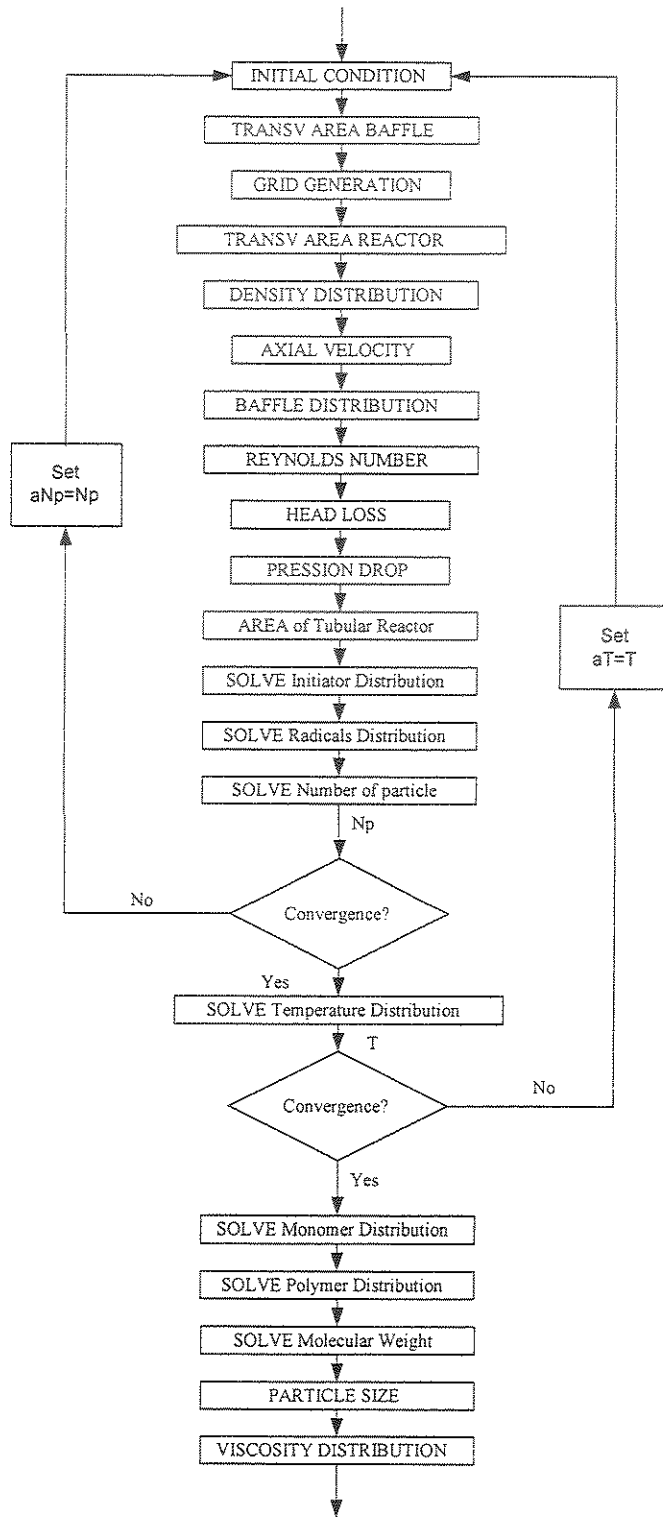


Figure 7.5 No isothermal condition logic flow diagram with baffle.

7.2 CONVERSION OF MONOMER

The simulation results of conversion (X_j) versus length of the reactor (Z) for styrene without baffle ($N_b=0$) and with baffles ($N_b=6, 18$) in isothermal condition (C) at 60°C and with no isothermal condition (V) are displayed in Figure 7.6. In no isothermal condition the temperature varies without or with baffles inside tubular reactor in exothermic and adiabatic process.

The Figure 7.6 (a) exhibits the comparative results in isothermal (C) and no isothermal (V) condition without baffles into tubular reactor. The conversion in variable temperature (V0) is higher than the conversion in constant temperature (C0) between 0-3 m from input of the reactor.

The Figure 7.6 (b) depicts the comparative results in isothermal (C) and no isothermal (V) condition with baffles, $N_b=6$. The conversion in no isothermal condition (V0) is higher than the conversion in constant temperature (C0) between 0-2 m from input of the reactor.

The Figure 7.6 (c) depicts the results in isothermal (C) condition with $N_b=18$ baffles. The conversion in isothermal condition (C) shows normal behavior.

The Figure 7.6 (d) states the comparative results in isothermal condition without baffles (C0) and with baffles (C6, C18). The conversion without baffles shows higher conversion than the ones with $N_b=6$ and 18 baffles, respectively. When increment the baffles number, the conversion exhibit a little decrease.

The Figure 7.6 (e) presents the comparative results in no isothermal condition without baffles (V0) and with $N_b=6$ baffles. The conversion with $N_b=6$ baffles shows better results than the conversion without (V0) baffles. When increment the baffles number in no isothermal condition increases the conversion.

Finally, the Figure 7.6 (f) contains all results in isothermal and no isothermal condition for $N_b=0, 6,$ and 18 baffles. In general, the no isothermal condition without baffles (V0) and with baffles (V6) shows higher conversion than the isothermal results without (C0) and with baffles (C6, C18).

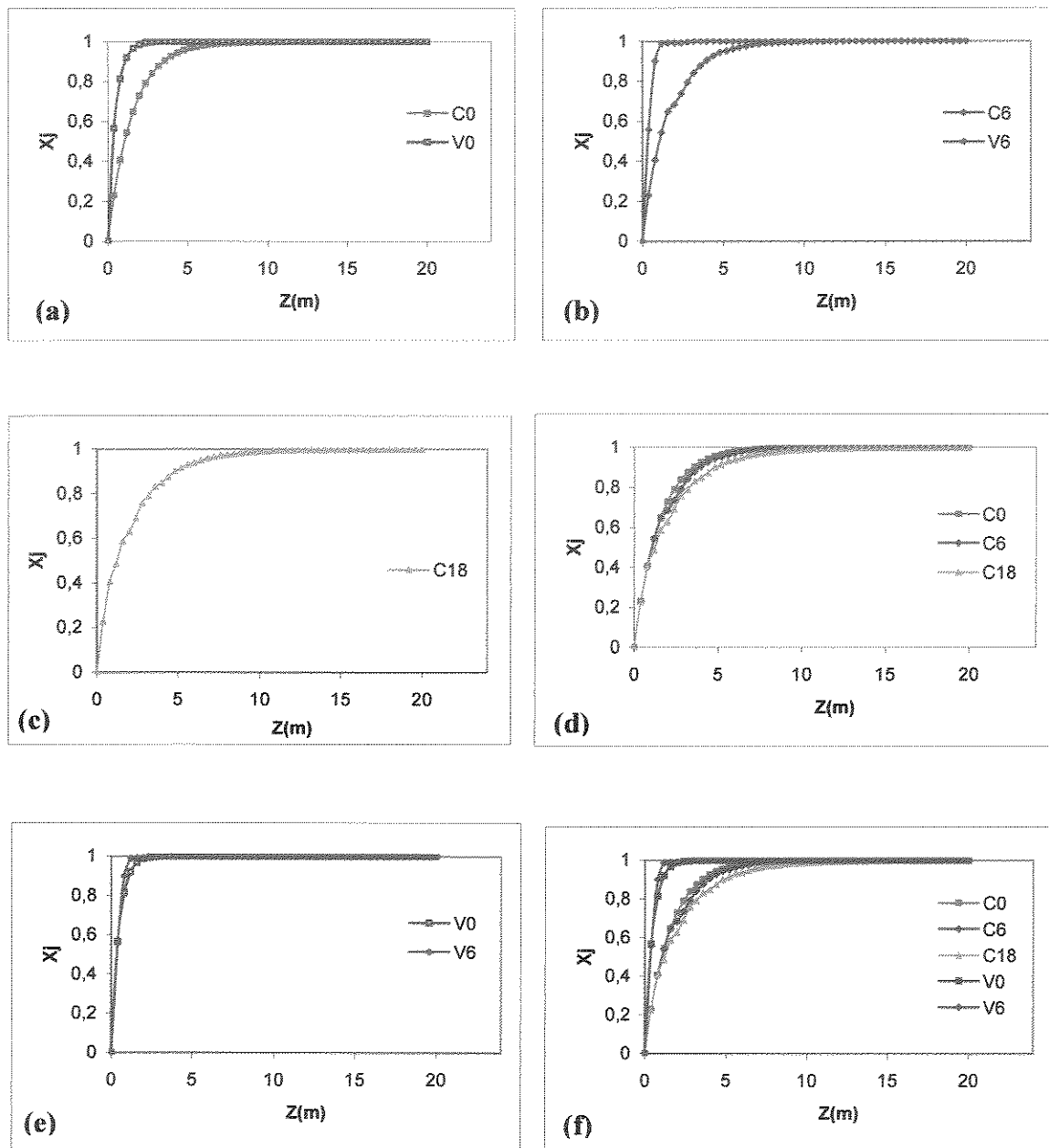


Figure 7.6 Conversion of monomer without ($N_b=0$) and with ($N_b=6, 18$) baffles in isothermal ($C_{Nb}=60^\circ\text{C}$) and no isothermal ($V_{Nb}=T$) conditions.

The type o curve in isothermal and no isothermal conversion are similar, but the conversion in no isothermal condition (V0, V6) is greater than the conversion in isothermal condition (C0, C6, C18).

7.3 INTERNAL TRANSVERSAL AREA

The simulation results of internal transversal area (A_z) inside tubular reactor versus length of the reactor (Z) without baffle, $N_b=0$, and with baffles, $N_b=6, 18$ are shown in Figure 7.7. These curves are valid for isothermal condition (C) at 60°C and for the no isothermal condition (V), both in exothermic and adiabatic process.

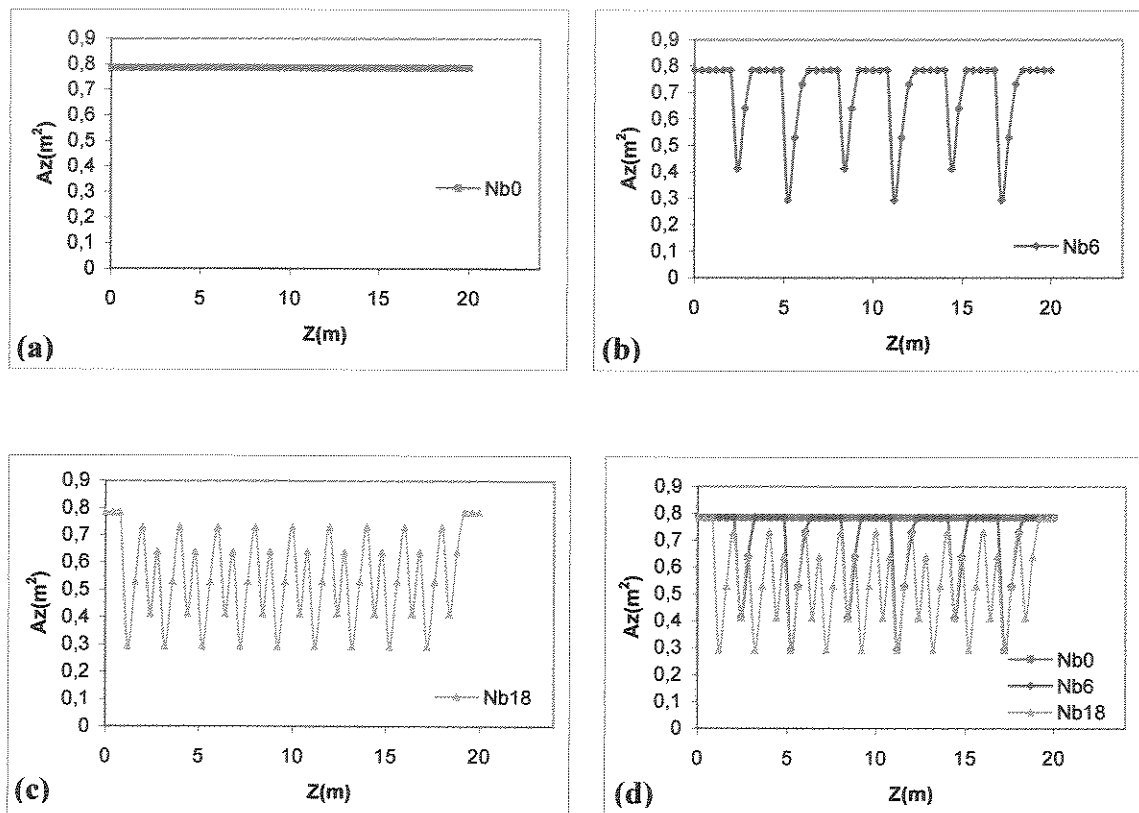


Figure 7.7 Internal transversal area without ($N_b=0$) and with ($N_b=6, 18$) baffles inside tubular reactor.

The Figure 7.7 (a) depicts the transversal area inside of the tubular reactor without baffles. The transversal area is constant inside tubular reactor without baffles. In Figure 7.7 (b) is seen the transversal area inside tubular reactor with $Nb=6$ baffles. The magnitude of the transversal area changes in polynomial model.

The Figure 7.7 (c) depicts the transversal area inside tubular reactor with $Nb=18$ baffles. This figure displays the variation of transversal area in polynomial model. The curve with $Nb=18$ baffles has more picks than the curve with $Nb=6$ baffles.

The Figure 7.7 (d) exhibits the comparative results of transversal area with $Nb=0, 6, 18$ baffles, respectively. The three curves could give different geometrical effects in the emulsion polymerization process.

7.4 AXIAL VELOCITY

The simulation results of axial velocity (V_z) versus length of the reactor (Z) without baffle, $Nb=0$, and with baffles, $Nb=6, 18$ in isothermal condition (C) at 60°C and the no isothermal condition (V), both in exothermic and adiabatic process are presented in Figure 7.8. In no isothermal condition the temperature varies, along the tubular reactor, without and with baffles.

The Figure 7.8 (a) displays the comparative results in isothermal (C) and no isothermal (V) condition without baffles ($Nb=0$) within tubular reactor. The axial velocity with variable reaction temperature (V_0) increases its velocity into tubular reactor in relation to the isothermal condition from $0,2703$ m/min to $0,2739$ m/min. The axial velocity in isothermal condition developed laminar flow from the tubular reactor inlet.

The Figure 7.8 (b) exposes the comparative results in isothermal (C) and no isothermal (V) condition with baffles, $Nb=6$. The axial velocity in isothermal and no isothermal condition have small variation in its magnitudes, both exhibit the same performance.

The Figure 7.8 (c) depicts the results in isothermal (C) condition with $Nb=18$ baffles.

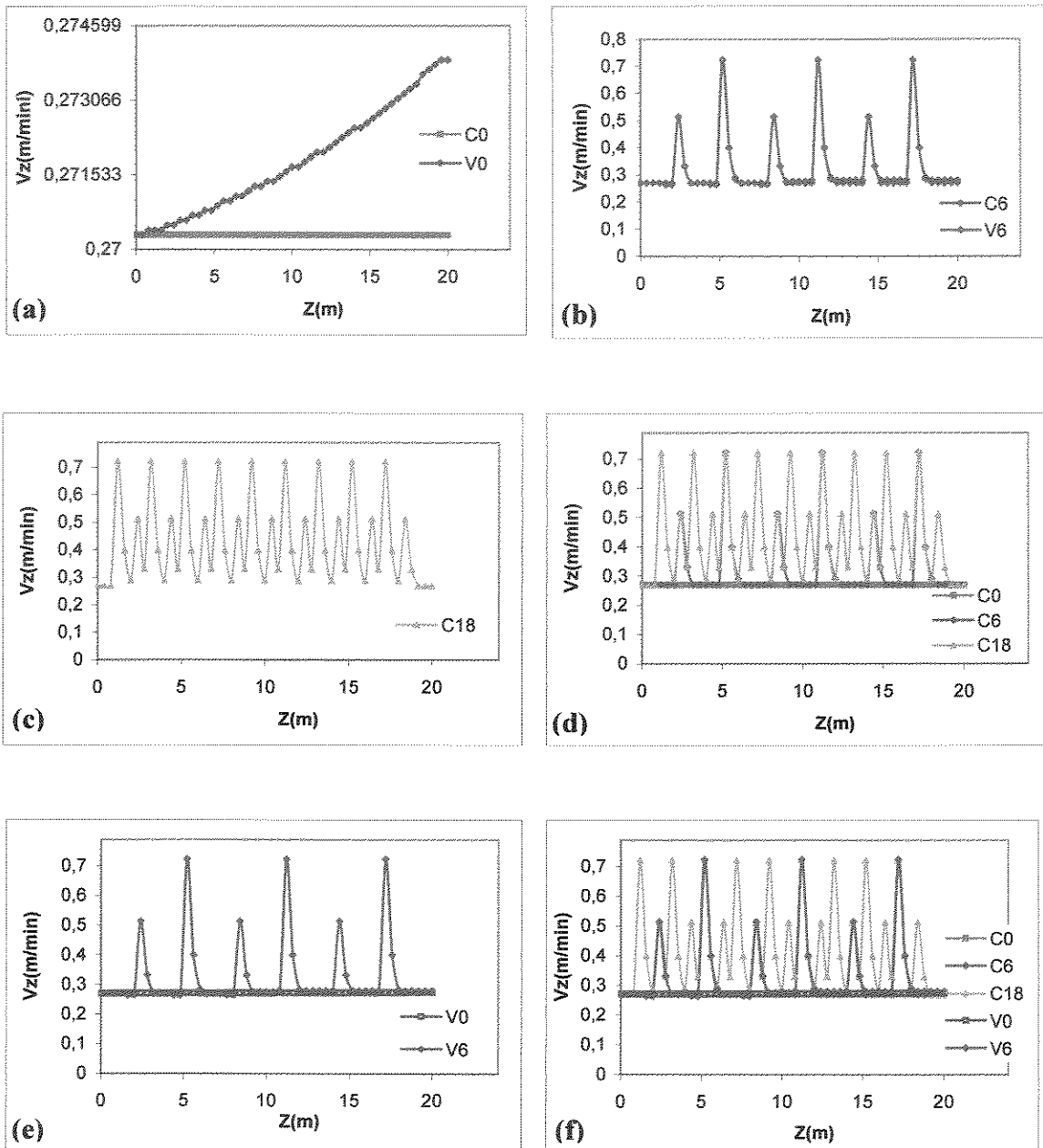


Figure 7.8 Axial velocity distribution without ($N_b=0$) and with ($N_b=6, 18$) baffles into tubular reactor in isothermal ($C_{Nb}=60^\circ C$) and no isothermal ($V_{Nb}=T$) conditions.

The Figure 7.8 (d) presents the results for isothermal condition without baffles (C0) and with baffles (C6, C18). The curve of Nb=6 and Nb=18 baffles posses analogy behavior, but the curve without baffles is a straight line.

The Figure 7.8 (e) states the results in no isothermal condition without baffles (V0) and with Nb=6 baffles. The curve V6 has picks according the number of baffles. The curve without baffle (V0) appears as straight line, but its real behavior is in Figure 7.8 (a).

The Figure 7.8 (f) contains all results in isothermal and no isothermal condition for Nb=0, Nb=6 and Nb=18 baffles. In this figure the curves C0 and V0 appear as straight line in comparison with other curves. The curves C6, C18 and V6 show same behavior according to the location and number of baffles in tubular reactor.

In general all curves with baffles show the analogy behavior, it takes in consideration the location and number of baffles inside tubular reactor. Also the axial velocity with variable temperature have more magnitudes that the axial velocity under constant temperature.

7.5 AXIAL TEMPERATURE DISTRIBUTION

The simulation results for axial temperature (T) versus length of the reactor (Z) without baffle (V0), and with baffles (V6) in no isothermal condition and isothermic condition (C) at 60°C, both in constant reaction heat, exothermic and adiabatic process are displayed in Figure 7.9.

The Figure 7.9 (a) exhibits the variation of the temperature without baffles into tubular reactor. The temperature varies from feed temperature, 333,15 K to 368,32 K with supposition of adiabatic condition to emulsion polymerization reactor of styrene.

The Figure 7.9 (b) shows the variation of the temperature with Nb=6 baffles within tubular reactor. The curve V6 presents augment and diminution in its path, the final temperature is 423,15 K.

The comparative results of isothermal condition (C) and no isothermal condition without baffles (V0) and with Nb=6 baffles as given in Figure 7.9 (c). The curves of V0 and V6 have higher values of temperature than the inlet temperature (C). The two curves such as V0 and V6 show some different performance and path.

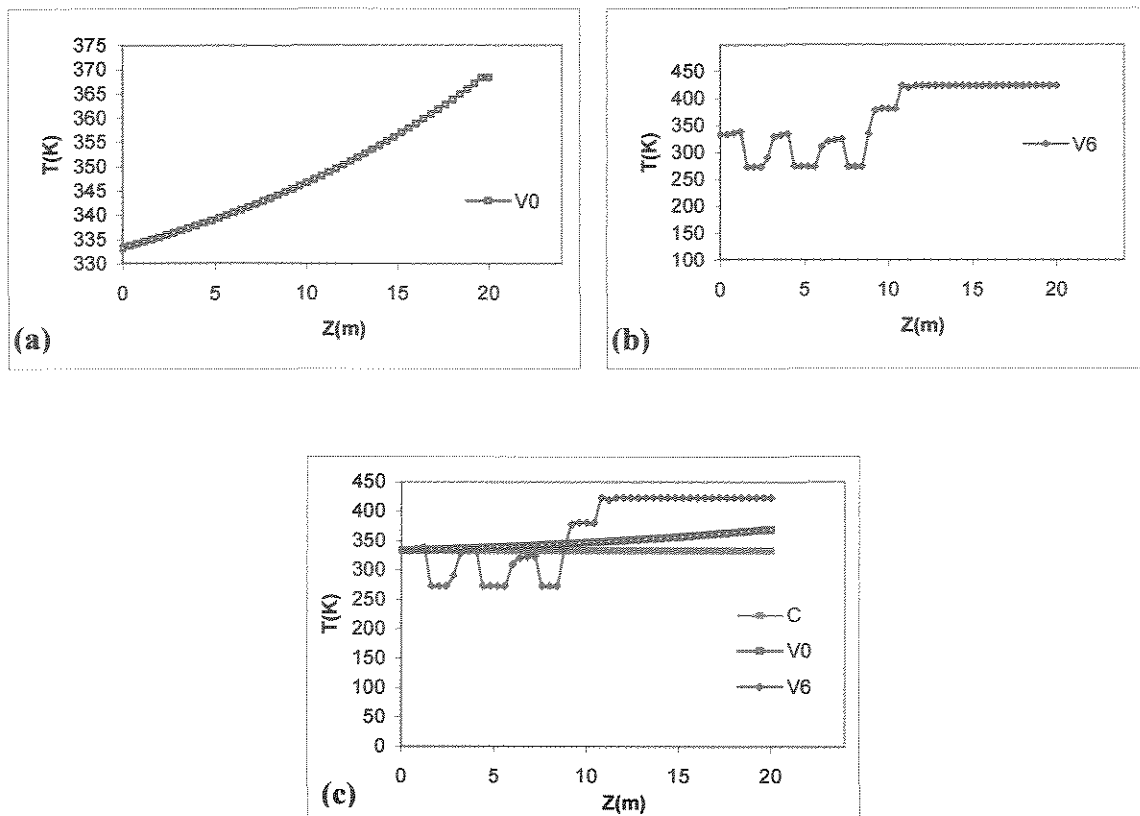


Figure 7.9 Temperature distribution without (Nb=0) and with (Nb=6) baffles inside tubular reactor. C=isothermic and adiabatic, V=no isothermic and adiabatic with 0 and 6 baffles.

7.6 CONCENTRATION OF POLYMER

The simulation results of the polystyrene concentration (CPs) versus length of the reactor (Z) without baffle, Nb=0, and with baffles, Nb=6, 18 in isothermal condition (C) at 60°C and the no isothermal condition (V), both in exothermic and adiabatic nature are exhibited in Figure 7.10.

The Figure 7.10 (a) displays a comparative results of isothermal (C) and no isothermal (V) condition without baffles, Nb=0, into tubular reactor. The polystyrene concentration with variable temperature (V0) is higher than the concentration of polystyrene in constant temperature (C0) between 0-3 m of the reactor length.

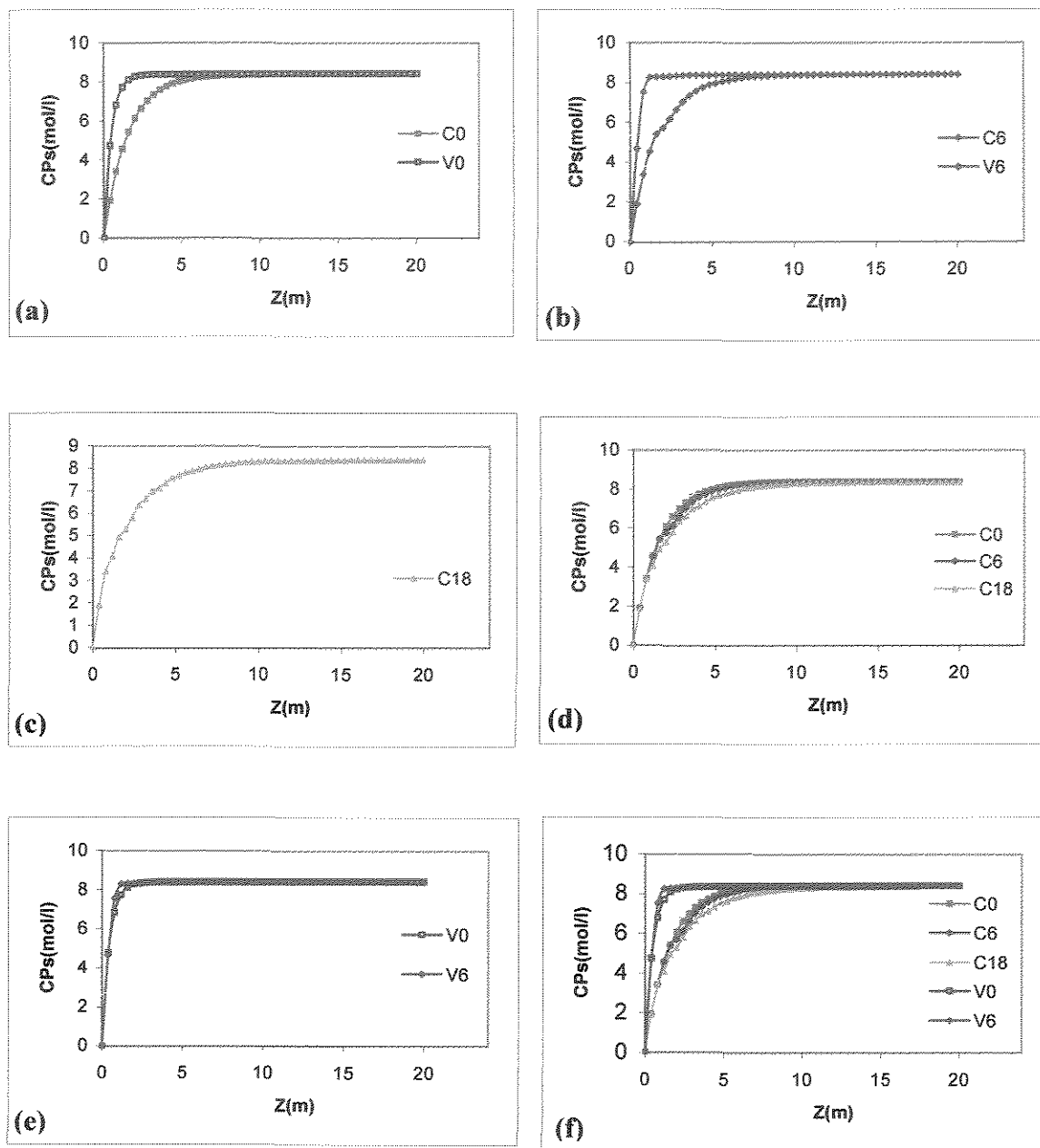


Figure 7.10 Concentration of polystyrene without (Nb=0) and with (Nb=6, 18) baffles into tubular reactor in isothermal (CNb=60°C) and no isothermal (VNb=T) conditions.

The Figure 7.10 (b) has the comparative results in isothermal (C) and no isothermal (V) condition with baffles, $N_b=6$. The concentration of polystyrene in no isothermal condition (V0) is higher than the polystyrene concentration in constant temperature (C0) between 0-2 m of length of the reactor.

The Figure 7.10 (c) depicts the results in isothermal (C) condition with $N_b=18$ baffles.

The Figure 7.10 (d) depicts the comparative results in isothermal condition without baffles (C0) and with baffles (C6, C18). The concentration of polystyrene without baffles show better results than the conversion with baffles of $N_b=6$ and 18, respectively. When increment the number of baffles, the conversion shows a little decrease.

The Figure 7.10 (e) presents the results in no isothermal condition without baffles (V0) and with $N_b=6$ baffles (V6). The concentration of polystyrene with $N_b=6$ baffles presents better results than the concentration of polymer without baffles (V6).

Now, the Figure 7.10 (f) exhibits all results in isothermal condition and in general, the no isothermal condition without baffles (V0) and with baffles (V6) has better results than the isothermal condition without, C0 and with C6 and C18 baffles. This situation would be by the simulation in exothermic and adiabatic condition, number of baffles, and variable density of polymer and monomer.

The types of curves in isothermal and no isothermal concentration of polymer are similar, but the curves of no isothermal condition is greater than the curves in isothermal condition.

7.7 CONCENTRATION OF RADICALS

The results of simulation of the concentration of radicals (CRw) in water phase versus length of the reactor (Z) without baffle, $N_b=0$, and with baffles, $N_b=6$, 18 in isothermal condition (C) at 60°C and to no isothermal condition (V), both in exothermic and adiabatic process are exposed in Figure 7.11.

The Figure 7.11 (a) exhibits the comparative results of isothermal (C) and no isothermal (V) condition without $N_b=0$ baffles, into tubular reactor. The radicals

concentration with variable temperature (V0) is the highest than the concentration of radicals in constant temperature (C0). The Figure 7.11 (d) presents the curve for the radicals concentration in constant temperature (C0), but in the Figure 7.11 (a) appears as straight line.

The Figure 7.11 (b) exposes the comparative results in isothermal (C) and no isothermal (V) condition with Nb=6 baffles. The concentration of radicals at no isothermal condition (V6) is higher than the radicals concentration at constant temperature (C6), but the curve of the concentration of radicals in variable temperature (V6) presents a strange behavior. This curve has a polynomial behavior. The Figure 7.11 (d) presents the curve of concentration of radicals in constant temperature (C6), but in the Figure 7.11 (b) appears as straight line.

The Figure 7.11 (c) shows the results in isothermal (C) condition with Nb=18 baffles.

The Figure 7.11 (d) depicts the comparative results in isothermal condition without baffles (C0) and with baffles (C6, C18). The three curves are similar.

The Figure 7.11 (e) presents the comparative results in no isothermal condition without baffles (V0) and with Nb=6 baffles (V6). The concentration of radicals with Nb=6 baffles shows the highest concentration than the without baffles.

The Figure 7.11 (f) presents all results in isothermal with Nb=0, 6 and 18 baffles and no isothermal condition with Nb=0 and 6 baffles. In general, the no isothermal condition without baffles (V0) and with Nb=6 baffles have greater radical concentration than the isothermal results without, C0 and with C6 and C18 baffles.

The type o curve for isothermal conditions are similar, but the type of curve for no isothermal conditions are different. In general the curve in isothermal and no isothermal condition increase its concentration without and with baffles into the reactor. The increase of the concentration for the no isothermal condition is higher than the concentration in isothermal condition.

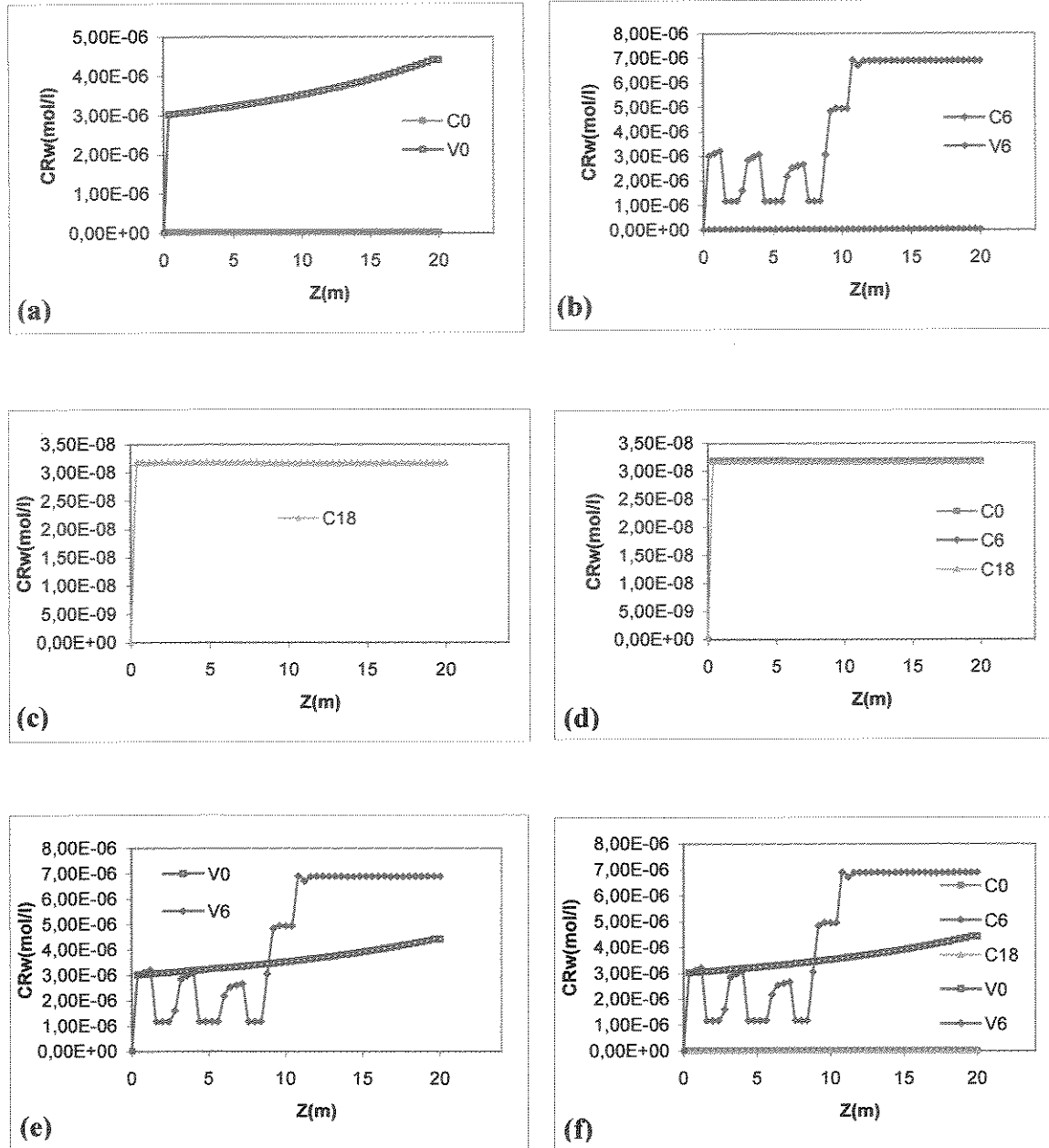


Figure 7.11 Concentration of radicals without (Nb=0) and with (Nb=6, 18) baffles into tubular reactor in isothermal (CNb=60°C) and no isothermal (VNb=T) conditions.

7.8 CONCENTRATION OF INITIATOR

The simulation results of the concentration of initiator (CI) in water phase versus length of the reactor (Z) without baffles, $N_b=0$, and with baffles, $N_b=6, 18$ in isothermal condition (C) at 60°C and no isothermal condition (V), both in exothermic and adiabatic nature are expounded in Figure 7.12.

The Figure 7.12 (a) presents the comparative results in isothermal (C) and no isothermal (V) condition without baffles, $N_b=0$, inside tubular reactor. The initiator concentration with variable temperature (V0) decreases its concentration from 0,026 mol/L to 0,0188 mol/L. The concentration of initiator in constant temperature (C0) is showed in the Figure 7.12 (d), it decreases an small values, but it is not straight line as shown in Figure 7.12(a) due to scale.

The Figure 7.12 (b) shows the comparative results in isothermal (C) and no isothermal (V) condition with $N_b=6$ baffles. The concentration of initiator in variable temperature (V0) decreases very much from initial concentration of initiator to zero concentration in approximation of four decimal. The diminution of the concentration of initiator in variable temperature is faster than the concentration of initiator in constant temperature. The Figure 7.12 (d) contains the curve the initiator concentration in constant temperature (C6), but in the Figure 7.12 (b) appears as straight line.

The Figure 7.12 (c) shows the results of isothermal (C) condition with $N_b=18$ baffles.

The Figure 7.12 (d) exhibits the comparative results of isothermal condition without baffles (C0) and with baffles (C6, C18). The three curves are similar in behavior, but they have some difference in their concentration.

The Figure 7.12 (e) displays the comparative results of no isothermal condition without baffles (V0) and with $N_b=6$ baffles (V6). The concentration of initiator with $N_b=18$ baffles decreases less than the initiator concentration of $N_b=0$ and $N_b=6$ baffles. The concentration of initiator with $N_b=6$ baffles decrease very much that the concentration of initiator without baffles (V0) baffles.

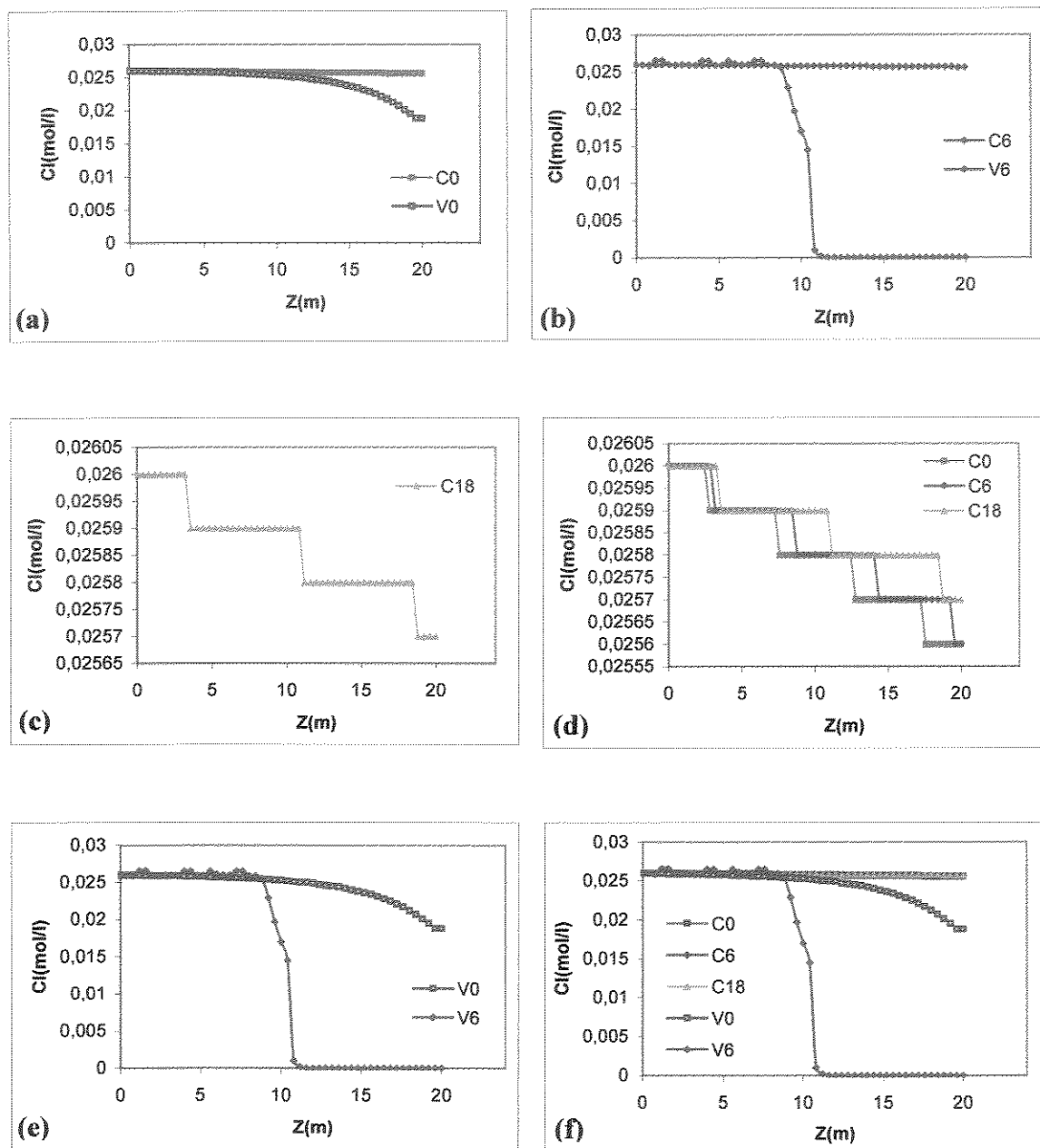


Figure 7.12 Concentration of initiator without ($Nb=0$) and with ($Nb=6, 18$) baffles into tubular reactor in isothermal ($C_{Nb}=60^\circ\text{C}$) and no isothermal ($V_{Nb}=T$) conditions.

The Figure 7.12 (f) presents all results in isothermal condition with $N_b=0$, 6 and 18 baffles and no isothermal condition with $N_b=0$ and $N_b=6$ baffles. In general, the no isothermal condition without baffles (V0) and with $N_b=6$ baffles decrease the concentration of initiator very quickly compared to the constant temperature without and baffles. Moreover in this figure, the concentration of initiator in isothermal condition appears as straight line around the initial concentration of initiator, but its real behavior is shown in Figure 7.12 (d).

The type of curve in isothermal conditions are similar, but the type of curve of no isothermal conditions are different. In general the curve in isothermal and no isothermal conditions decrease its concentration into tubular reactor.

7.9 NUMBER OF PARTICLES

The simulation results of the particles number (N_p) by micellar and homogeneous nucleation mechanism versus length of the reactor (Z) without baffle, $N_b=0$, and with baffles, $N_b=6$, 18 in isothermal condition (C) at 60°C and the no isothermal condition (V), both in exothermic and adiabatic process are exhibited in Figure 7.13.

The Figure 7.13 (a) exposes the comparative results in isothermal (C) and no isothermal (V) condition without baffles, $N_b=0$, into tubular reactor. The number of particles with variable temperature (V0) is higher than the number of particles in constant temperature (C0). The Figure 7.13 (d) presents the curve of the number of particles in constant temperature (C0) in real form, but in the Figure 7.13 (a) appears as straight line.

The Figure 7.13 (b) depicts the comparative results of isothermal (C) and no isothermal (V) condition with baffles, $N_b=6$. The number of particles in no isothermal condition (V6) is higher than the number of particles in constant temperature (C6), but the curve of radicals concentration in variable temperature (V6) presents a strange behavior. The end value of the curve V6 reaches the number of particles of $2,21 \times 10^{21}$ 1/L. The Figure 7.13 (d) presents the curve of the number particles in constant temperature (C6), but in the Figure 7.13 (b) appears as straight line.

The Figure 7.13 (c) shows the results in isothermal (C) condition with baffles, $N_b=18$.

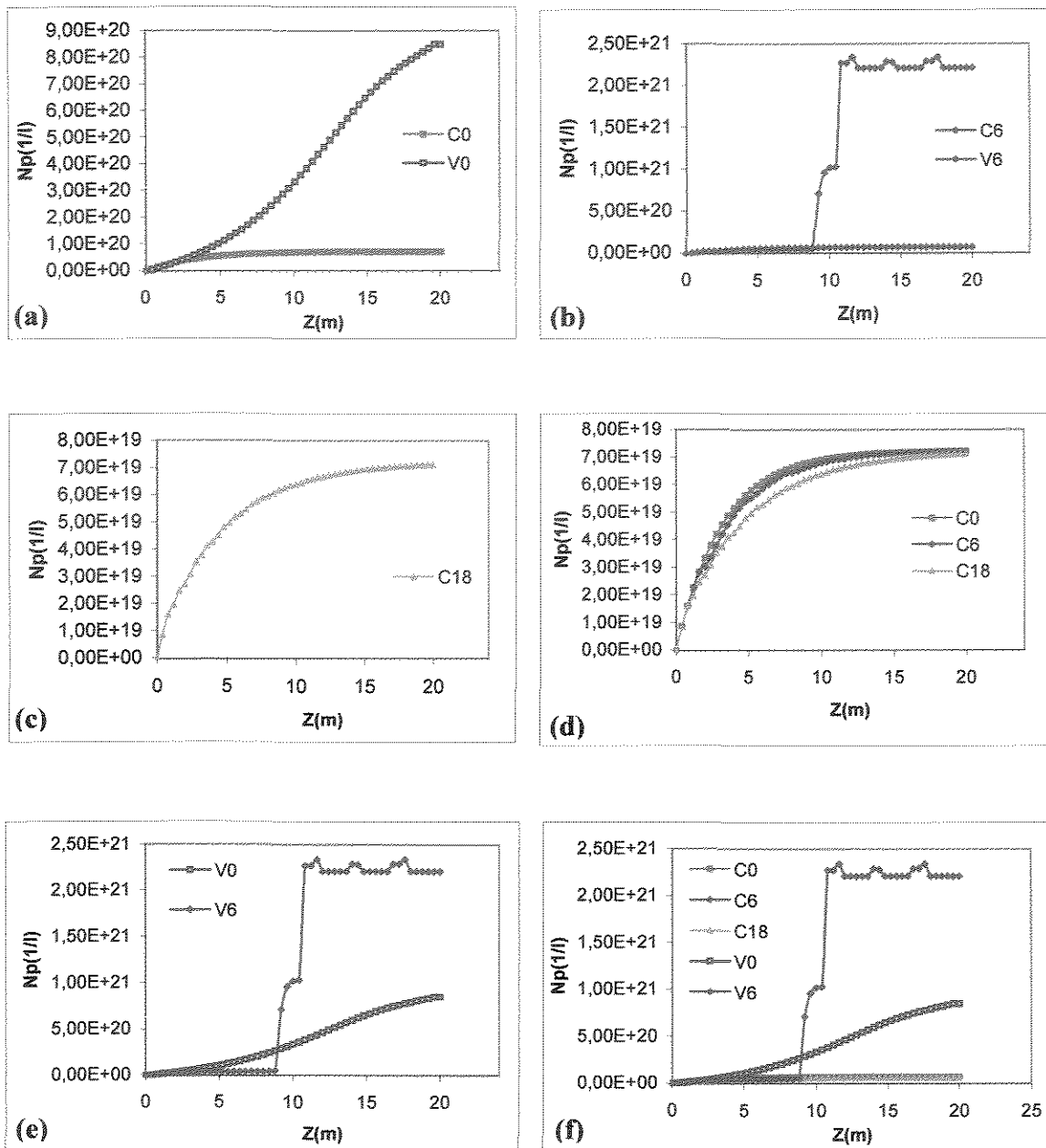


Figure 7.13 Number of particles without ($Nb=0$) and with ($Nb=6, 18$) baffles into tubular reactor in isothermal ($CN_b=60^\circ C$) and no isothermal ($VN_b=T$) conditions.

The Figure 7.13 (d) contains the comparative results in isothermal condition without baffles (C0) and with baffles (C6, C18). The three curves are similar. This figure proves in isothermal condition that when augments the number of baffles, the number of particles decrease.

The Figure 7.13 (e) presents the comparative results in no isothermal condition without baffles (V0) and with Nb=6 baffles (V6). The number of particles with curve V6 is higher than the number of particles of the curve V0. The two curves such as V0 and V6 show augment when temperature varies within tubular reactor.

The Figure 7.13 (f) presents all results in isothermal and no isothermal condition for Nb=0, 6, and 18 baffles. In general, the no isothermal condition without baffles (V0) and with Nb=6 baffles present more particles than the isothermal condition without, C0 and with C6 and C18 baffles. In this figure, the number of particles in isothermal condition appears as straight line upon the coordinate of the length, but it is not truth because its real form is at Figure 7.13 (d).

The type of curve in isothermal condition are similar, but the type of curve of no isothermal condition are different. In general the curve in isothermal and no isothermal condition increase its values inside tubular reactor. The increment of the number of particles in no isothermal condition is higher than the number of particles in isothermal condition.

7.10 MOLECULAR WEIGHT DISTRIBUTION

The results of simulation of the cumulative molecular weight distribution without normalization and polydispersity (Q) versus conversion of monomer (X_j), geometric chain length distribution with normalization (mole fraction) (X_{pi}) and molecular weight distribution with normalization (weight fraction) (W_{pi}) versus chain length of the molecules of polystyrene (i) are shown in Figures 7.14, 7.15 and 7.16. They are shown without baffle, Nb=0 in isothermal and no isothermal condition, with Nb=6 baffles in isothermal and no isothermal condition, and with Nb=18 baffles in isothermal condition, respectively. The isothermal condition is at 60°C. The isothermal and no isothermal condition success in isothermic and adiabatic process.

The Figures 7.14 (a)-(b) expose the comparative results of isothermal (C) and no isothermal (V) condition, respectively without baffles, $N_b=0$, into tubular reactor. The number (M_n) and weight (M_w) molecular are different under constant and variable temperature.

The Figures 7.14 (c)-(d) show the curves of polydispersity in constant and variable temperature, both have same behavior without or with the temperature effect.

The Figures 7.14 (e)-(f) expound the geometric chain length distribution in constant and variable temperature. The Figure 7.14 (e) shows the distribution of mole fraction in 65% of conversion of monomer. The Figure 7.14 (f) exhibits the distribution of mole fraction in 57% de conversion of monomer. Both before figures are different. The mole fraction of the Figure 7.14 (f) is higher than the mole fraction as shown in Figure 7.14 (e). The mole fraction in variable temperature presents a distribution more uniform that in constant temperature.

The Figures 7.14 (g)-(h) contain the molecular weight distribution in constant and variable temperature. The Figure 7.14 (g) shows the distribution of weight fraction of 65% of conversion of monomer. The Figure 7.14 (h) presents the distribution of weight fraction of 57% of conversion of monomer. Both before figures are different. The Figure 7.14 (h) presents the distribution more uniform than the Figure 7.14 (g).

The Figures 7.15 (a)-(b) exhibit the comparative results in isothermal (C) and no isothermal (V) condition, respectively with $N_b=6$ baffles within tubular reactor. The number (M_n) and weight (M_w) molecular are different under constant and variable temperature.

The Figures 7.15 (c)-(d) present the curves of polydispersity in constant and variable temperature. Both has same performance without or with the temperature effect.

The Figures 7.15 (e)-(f) display the geometric chain length distribution in constant and variable temperature. The Figure 7.15 (e) shows mole fraction distribution at 65% of conversion of monomer. The Figure 7.15 (f) exhibits mole fraction distribution in 56% of monomer conversion. Both before figures are different. The mole fraction

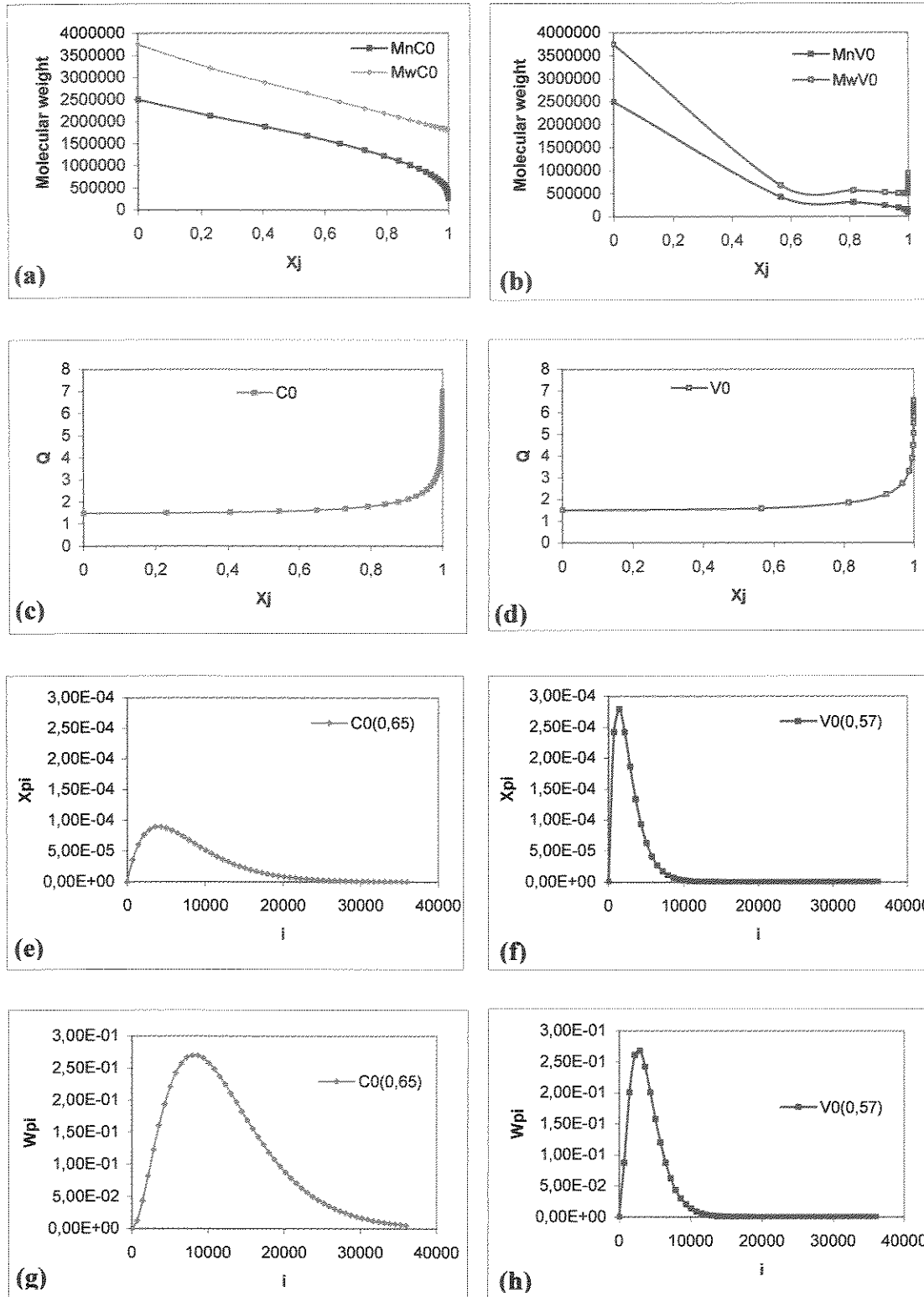


Figure 7.14 Molecular weight distribution without ($N_b=0$) baffles into tubular reactor in isothermal ($C_{N_b}=60^\circ\text{C}$) and no isothermal ($V_{N_b}=T$) conditions.

of the Figure 7.15 (f) is higher than the mole fraction of the Figure 7.15 (e). The mole fraction in variable temperature presents more uniform distribution than in constant temperature.

The Figures 7.15 (g)-(h) contain the molecular weight distribution in constant and variable temperature. The Figure 7.15 (g) shows the distribution of weight fraction at 65% of conversion of monomer. The Figure 7.15 (h) presents the distribution of weight fraction at 56% of conversion of monomer. Both figures are different. The Figure 7.15 (h) presents the more uniform distribution than the Figure 7.15 (g).

The Figure 7.16 (a) displays the comparative results in isothermal (C) condition of molecular weight distribution with $N_b=18$ baffles inside tubular reactor.

The Figure 7.16 (b) exhibits the curves of polydispersity in constant temperature. This curve shows uniform distribution along the path.

The Figure 7.16 (c) presents the geometric chain length distribution in constant temperature. The Figure 7.16 (c) shows mole fraction distribution at 62% of monomer conversion. This curve shows uniform distribution along the path.

The Figure 7.16 (d) contains the molecular weight distribution in constant temperature. The Figure 7.16 (d) shows molecular weight fraction distribution at 62% of monomer conversion. This curve shows uniform distribution of weight fraction along the path.

The number (M_n) and weight (M_w) molecular distribution in variable reaction temperature without and with baffles present uniform distribution than the number (M_n) and Weight (M_w) molecular distribution in constant reaction temperature. The polydispersity without and with baffles in variable reaction temperature presents higher polydispersity than in constant reaction temperature without and with baffles. The mole fraction in variable reaction temperature without and with

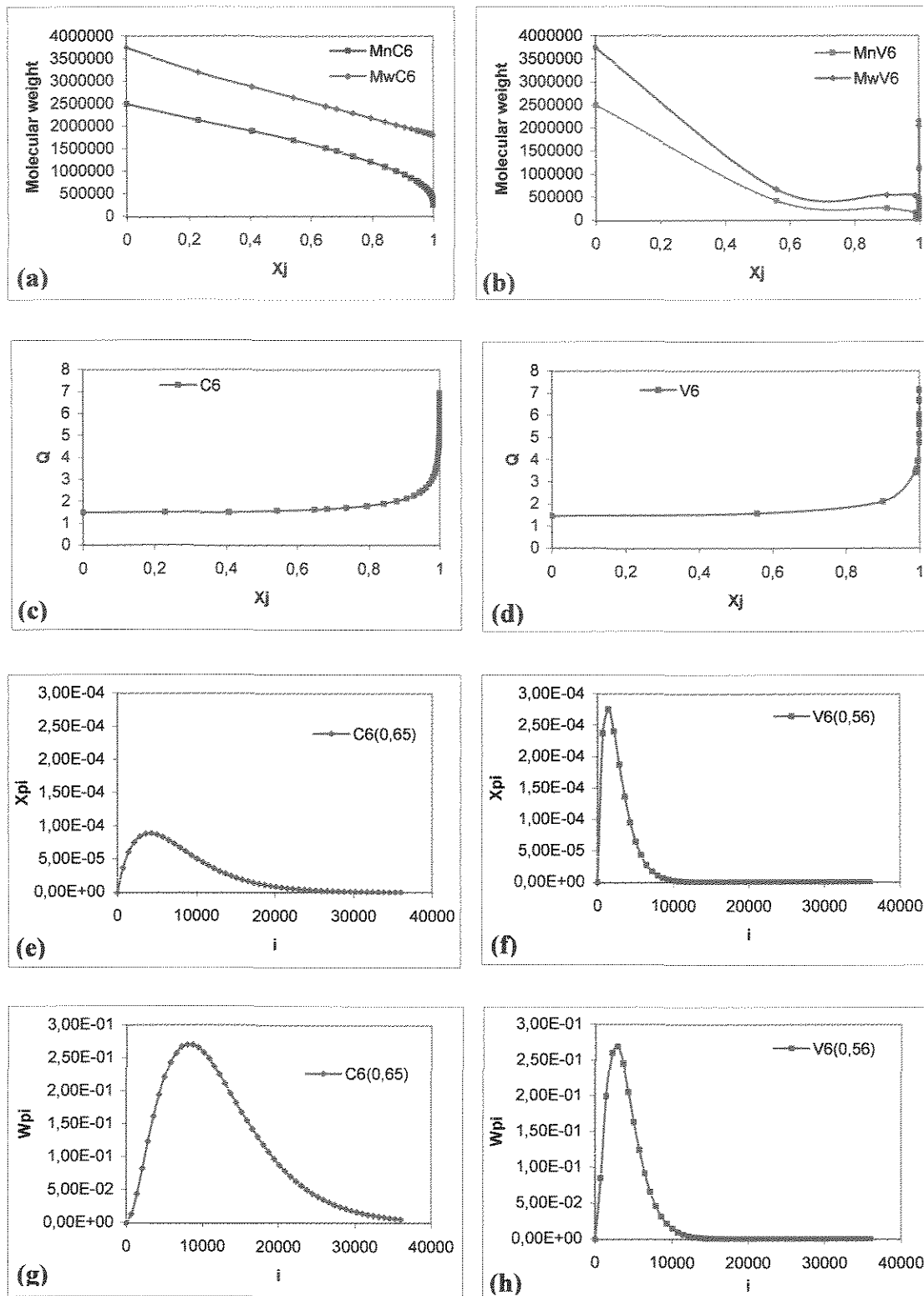


Figure 7.15 Molecular weight distribution without ($N_b=6$) baffles into tubular reactor in isothermal ($C_{Nb}=60^\circ\text{C}$) and no isothermal ($V_{Nb}=T$) conditions.

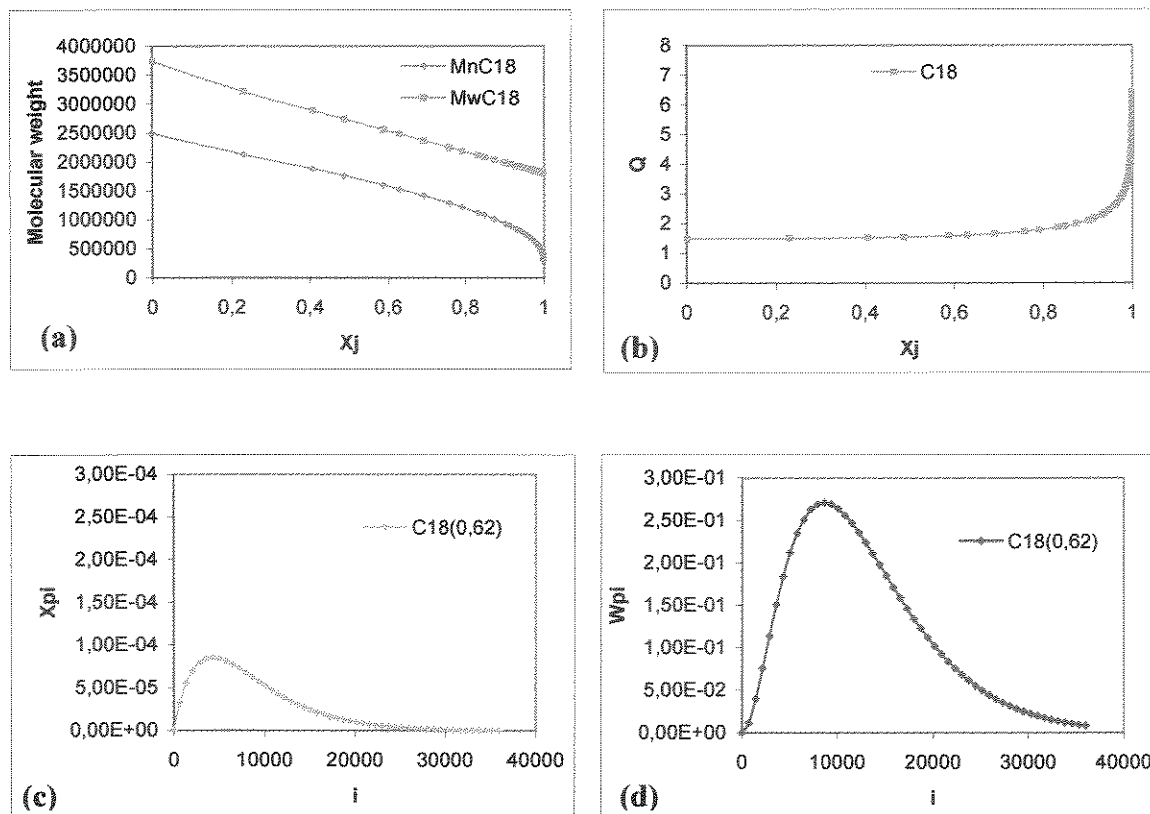


Figure 7.16 Molecular weight distribution with ($N_b=18$) baffles into tubular reactor in isothermal ($C_{Nb}=60^\circ\text{C}$) condition.

baffles show uniform behavior that the mole fraction in constant reaction temperature without and with baffles. The weight fraction in variable reaction temperature without and with baffles present uniform distribution than the weight fraction in constant reaction temperature without and with baffles. The variable temperature affects in mole and weight fraction, they have better distribution that at constant temperature.

7.11 SIZE OF POLYMER PARTICLES

The results of simulation of characterization of the particles size of polystyrene swollen (R_s) and unswollen (R) versus length of the reactor (Z) without baffle, $N_b=0$, and with baffles, $N_b=6, 18$ in isothermal condition (C) at 60°C and the no isothermal condition (V), both in exothermic and adiabatic process are shown in Figure 7.17.

The Figure 7.17 (a) exhibits the comparative results of swollen particle size (R_{sC0}) and unswollen particle size (R_{C0}) in isothermal condition (C) without $N_b=0$ baffles, into tubular reactor. The swollen particle size is higher than the unswollen particle size. The Figure 7.17 (b) shows the comparative results of swollen particle size (R_{sV0}) and unswollen particle size (R_{V0}) in no isothermal condition (V) without baffles, $N_b=0$, within tubular reactor. The swollen particle size is higher than the unswollen particle size, both swollen and unswollen particle size increase continually in tubular reactor in variable temperature, while in constant temperature remains constant from 5 m toward output of reactor.

The Figure 7.17 (c) exposes the comparative results of unswollen particle size (R) in isothermal (C) and no isothermal (V) condition without baffles, $N_b=0$. The particle size in isothermal condition (C0) is higher than the particle size in variable temperature (V0).

The Figure 7.17 (d) states the comparative results of unswollen particle size (R) isothermal (C) and no isothermal (V) condition with $N_b=6$ baffles. The particle size in isothermal condition (C6) is higher than the particle size in variable temperature (V6).

The Figure 7.17 (e) presents the results of unswollen particle size of isothermal (C) condition with $N_b=18$ baffles.

The Figure 7.17 (f) depicts the comparative results of isothermal condition without baffles (C0) and with baffles (C6, C18). The three curves are similar.

The Figure 7.17 (g) presents the comparative results of no isothermal condition without baffles (V0) and with $N_b=6$ baffles (V6). Both the curve V0 and curve V6 have similar behavior.

The Figure 7.17 (h) contains all results in isothermal and no isothermal condition for $N_b=0, 6,$ and 18 baffles. In general, the isothermal condition without baffles (C0) and with $N_b=6$ and 18 baffles presents bigger diameter than the no isothermal condition without, V0 and with V6 and V18 baffles.

The type of curve in isothermal condition are similar, but the type of curve in no isothermal condition are different. In general the curve in isothermal and no isothermal condition increase its particle size within tubular reactor. The increment of particle size in isothermal condition is higher than the particle size in no isothermal condition.

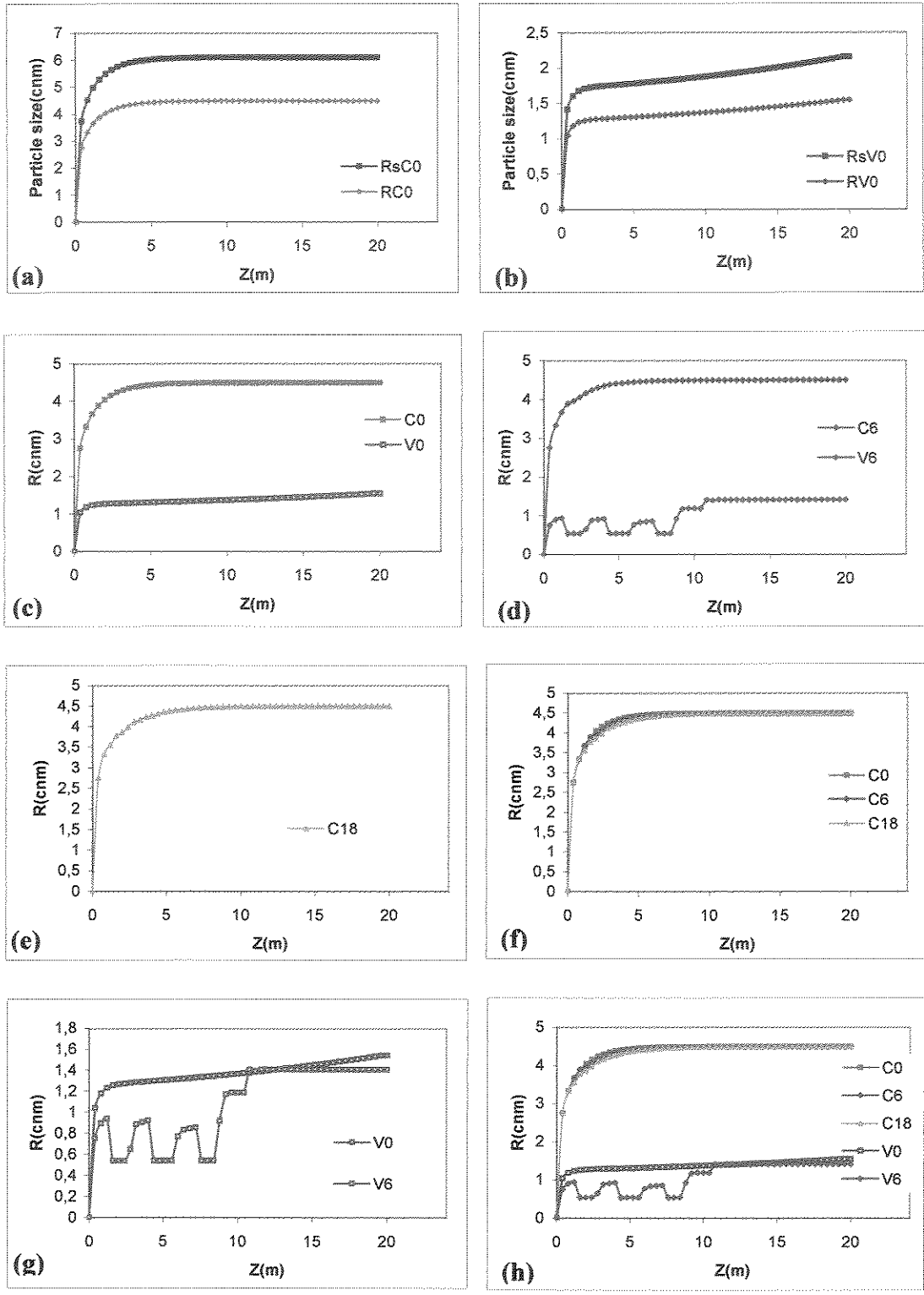


Figure 7.17 Average particle size distribution without (Nb=0) and with (Nb=6, 18) baffles into tubular reactor in isothermal (CNb=60°C) and no isothermal (VNb=T) conditions.

7.12 VISCOSITY DISTRIBUTION

The simulation results of polymer viscosity distribution ($\text{Ln}(\mu)$) inside tubular reactor versus conversion of monomer styrene (X_j) without baffle, $N_b=0$, and with baffles, $N_b=6, 18$ in isothermal condition (C) at 60°C and the no isothermal condition (V), both in isothermic and adiabatic process are presented in Figure 7.18. Each figure uses its own conversion obtained in constant or variable temperature.

The Figure 7.18 (a)-(c) expose the results of viscosity distribution in isothermal condition within tubular reactor without baffles, $N_b=0$ and with $N_b=6$ and 18 baffles. The three curves such as C0, C6 and C18 have similar behavior, and the points on path shows uniform distribution. The three curves reach approximately the same viscosity of $\text{Ln}(\mu)=42,5$ at outlet of the reactor.

The Figure 7.18 (d) and (e) present the results of viscosity distribution in no isothermal condition inside tubular reactor without baffles, $N_b=0$ and with $N_b=6$ baffles. The three curves such as V0 and V6 exhibit different behavior. The curve V0 exhibits constant viscosity around $\text{Ln}(\mu)=30$ and 100 % of conversion after 3 m into tubular reactor. The curve V6 shows constant viscosity approximately at $\text{Ln}(\mu)=30$ and 100% of conversion after 2 m inside tubular reactor.

The data of the Figure 7.18 were shown in $\text{Ln}(\mu)$ versus X_j for reasons of scale of values, e.g. if the value of $\text{Ln}(\mu)=42,5$ then its magnitude is $\mu=2,86 \times 10^{18}$ Kg/m.s and of $\text{Ln}(\mu)=-5$ is $\mu=6,738 \times 10^{-3}$ Kg/m.s.

The viscosity distribution in isothermal condition with $N_b=0, 6$, and 18 baffles have uniform distribution in tubular reactor. The viscosity distribution in no isothermal condition without baffles (V0) and with $N_b=6$ baffles (V6) have different behavior inside tubular reactor. In general the viscosity distribution in no isothermal condition shows constant viscosity after of $\frac{1}{4}$ of length of the reactor.

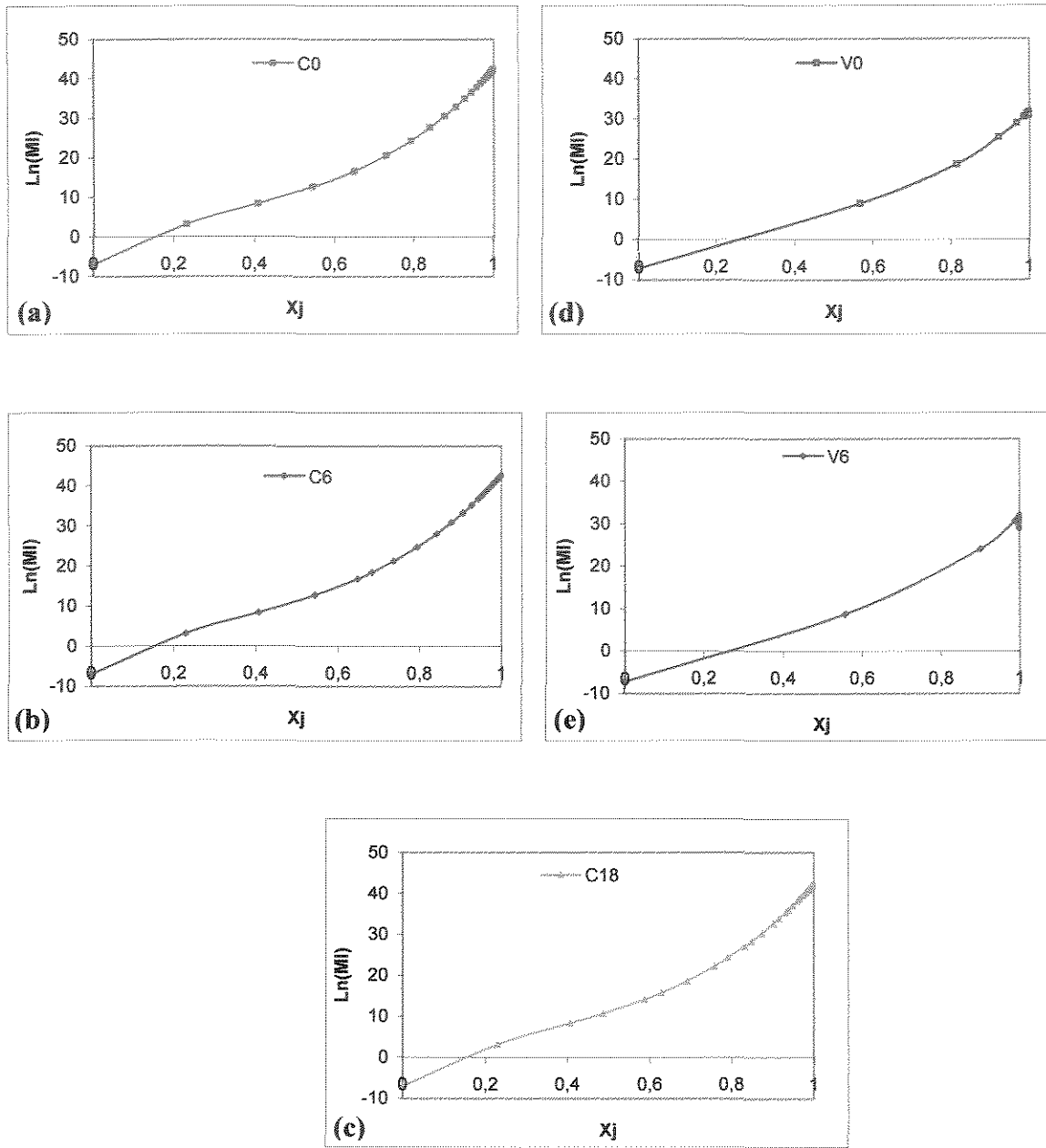


Figure 7.18 Viscosity distribution without ($N_b=0$) and with ($N_b=6, 18$) baffles into tubular reactor in isothermal ($C_{N_b}=60^\circ\text{C}$) and no isothermal ($V_{N_b}=T$) conditions.

7.13 CHARACTERISTICS OF BAFFLES

The characterizations of baffles will be described in this part with baffle length, baffle base, inclined angle baffle, separation between baffles, internal total area with baffles inside tubular reactor, Nb=6 or Nb=18 baffles it can be seen in Table 7.1. The values that were used in computational test and simulation are shown in Table 7.1. These values will be maintained constants at constant or variable reaction temperature of emulsion polymerization process of styrene at diameter and length of tubular reactor of $D_r=1$ m, $L_r=20$ m, respectively. The following values will be constant in the present thesis when the number of baffles increase inside tubular reactor such as the baffle length, baffle base, and inclined angle baffles. The Table 7.1 is valid principally for diameter of reactor $D_r=1$ m.

Table 7.1 Characteristic of baffles with $D_r=1$ m, $L_r=20$ m

BAFFLE	Symbols	Nb=6	Nb=18
Length of baffle	Lb (m)	1,1662	1,1662
Base of baffle	Bb (m)	0,9798	0,9798
Inclination angle	γ (grados)	30°57'45,5''	30°57'45,5''
Separation of baffles	Lbs (m)	3	1
Lateral area of reactor	Alr (m ²)	62,8319	62,8319
area of baffle	Aab (m ²)	9,141	27,4232
internal area of reactor	At ₀ (m ²)	71,9729	90,2551

The Table 7.2 shows the head loss results and pressure drop inside tubular reactor at feed temperature at 60°C, they suffer the baffles effects. In isothermic condition without baffles inside tubular reactor the head loss is 0,00093 m, and the pressure drop is 10,3783 Pa. In the Table 7.2 when the temperature of reaction is not constant, one can observe that the head loss and pressure drop diminish slightly when the number of baffles increase from Nb=6 to Nb=18, these situation could be by the temperature effect on the polymer and monomer density.

Table 7.2 Head loss and pressure drop with feed temperature of 60°C

REACTOR	Symbols	Nb=6		Nb=18	
		T=C=60°C	T=V	T=C=60°C	T=V
head loss	Hf (m)	1,2491	1,2456	3,7287	3,4899
pressure drop	ΔPr (Pa)	1386,556	1382,594	4138,911	3873,871

7.14 OTHER CALCULUS

7.14.1 Density of polymer and monomer

The simulation results of the density of polystyrene (P) and monomer (M) versus axial temperature without baffle, Nb=0, and with baffles, Nb=6, 18 in isothermal condition (C) at 60°C and the no isothermal condition (V), both in exothermic and adiabatic process are displayed in Figure 7.19. The temperature varies without and with baffles inside tubular reactor. Each figure uses its own variable temperature within tubular reactor.

The Figure 7.19 (a) exhibits the variation of the density of polystyrene (PC) and monomer (MC) in isothermal condition without and with baffles inside tubular reactor. The density of polystyrene and monomer was kept constant at inlet temperature.

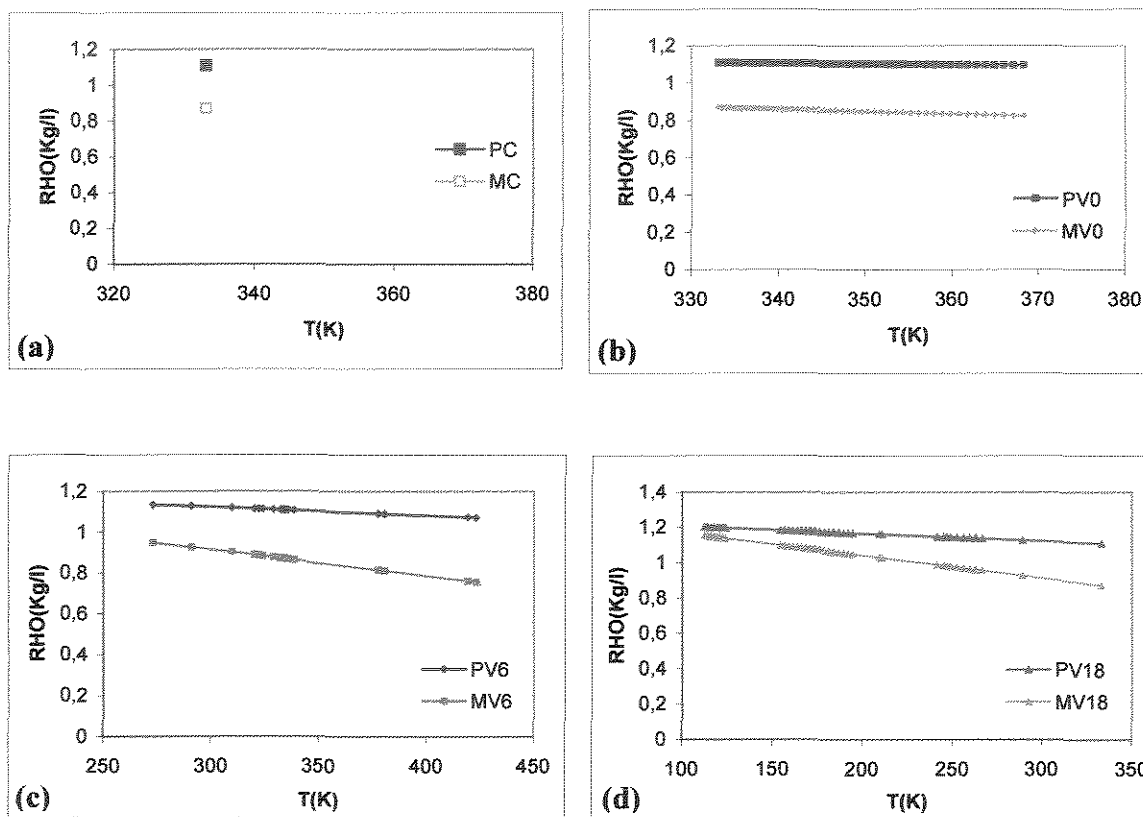


Figure 7.19 Density distribution of polystyrene (P) and monomer (M) without (Nb=0) and with (Nb=6, 18) baffles into tubular reactor in isothermal (CNb=60°C) and no isothermal (VNb=T) conditions.

The Figure 7.19 (b) shows the comparative variation of the density of polystyrene (PV0) and monomer (MV0) in variable temperature without baffles inside tubular reactor. Both densities diminish when the temperature varies into tubular reactor.

The Figure 7.19 (c) depicts the variation of the density of polystyrene (PV6) and monomer (MV6) in variable temperature with Nb=6 baffles inside tubular reactor. Both densities present abnormal distribution of points upon path, but it keep a straight line and it diminish its density when temperature augments within tubular reactor.

The Figure 7.19 (d) presents the variation comparative of the density of polystyrene (PV18) and monomer (MV18) in variable reaction temperature with Nb=18 baffles inside tubular reactor. Both densities show irregular distribution of points upon path. Both densities at the reactor inlet exhibit near points. The two densities have the points distribution in straight line when the temperature increase inside tubular reactor.

The density of polystyrene and monomer decrease in agreement with the increment of the temperature in tubular reactor.

7.14.2 Head Loss

The simulation results of the head loss (H_f) in laminar flow versus length of the reactor (Z) without baffle, Nb=0, and with baffles, Nb=6, 18 in isothermal condition (C) at 60°C and the no isothermal condition (V), both in exothermic and adiabatic process are presented in Figure 7.20.

The Figure 7.20 (a) exhibits the comparative results in isothermal (C) and no isothermal (V) condition without Nb=0 baffles, inside tubular reactor. The head loss with variable temperature (V0) is higher than the head loss in constant temperature (C0). The head loss in constant temperature persists constant.

The Figure 7.20 (b) depicts the comparative results in isothermal (C) and no isothermal (V) condition with Nb=6 baffles. The curve C6 and V6 have similar behavior, both vary in agreement to the variation of the location of baffles and the length of reactor.

The Figure 7.20 (c) contains the results in isothermal (C) condition with Nb=18 baffles.

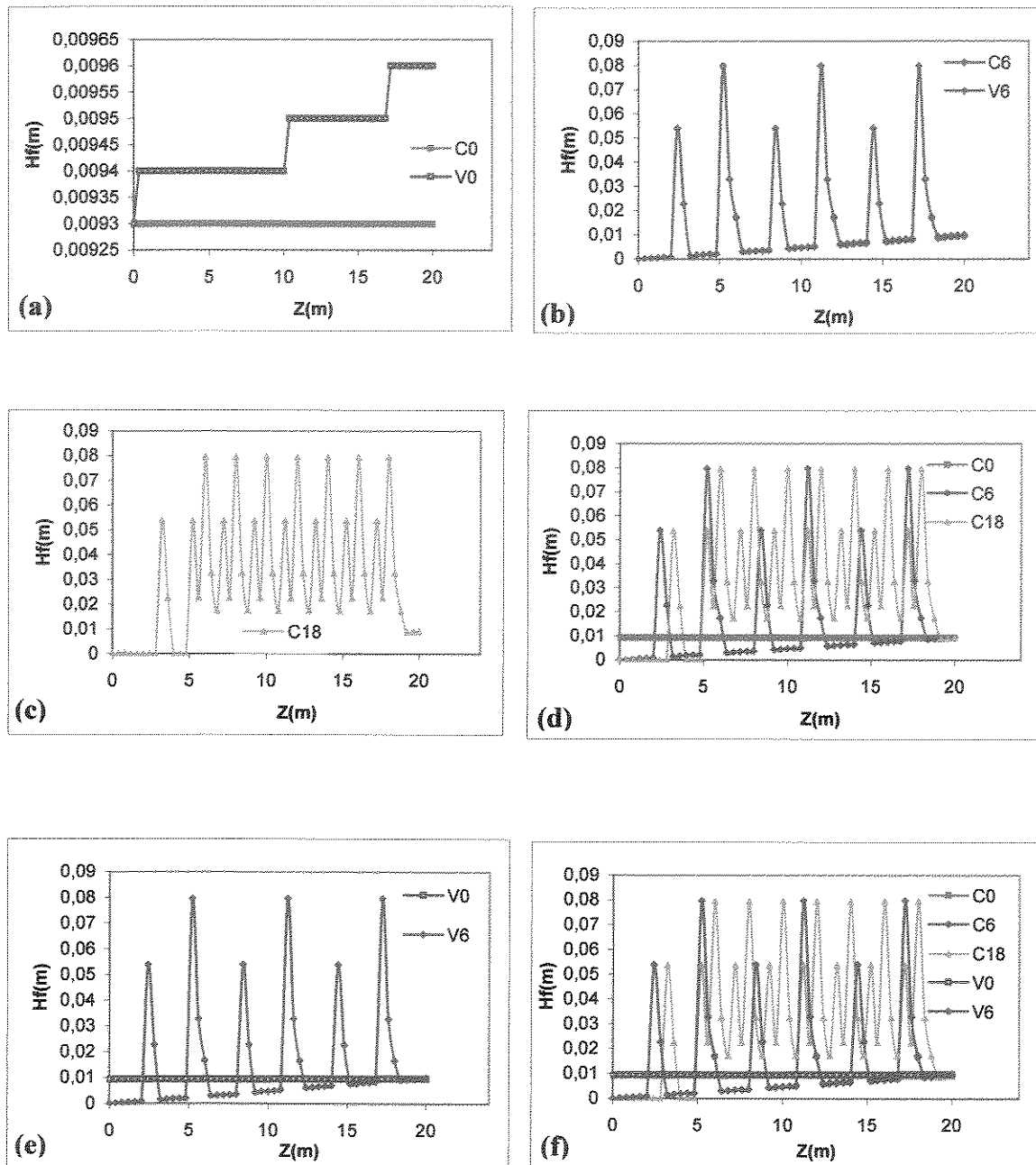


Figure 7.20 Head loss without ($N_b=0$) and with ($N_b=6, 18$) baffles into tubular reactor in isothermal ($CN_b=60^\circ C$) and no isothermal ($VN_b=T$) conditions.

The Figure 7.20 (d) exposes the comparative results of isothermal condition without baffles (C0) and with baffles (C6, C18). The three curves have different path. The curve C6 and C18 have polynomial behavior, but the curve C0 has straight line form. The path reflects the location of baffles inside tubular reactor in the curves C6 and C18.

The Figure 7.20 (e) shows the comparative results in no isothermal condition without baffles (V0) and with Nb=6 baffles (V6). The two curves have different trajectory. The curve V6 has polynomial behavior, but the curve V0 has straight line form. The polynomial behavior shows the performance of the reactor with baffles.

The Figure 7.20 (f) contains all results in isothermal and no isothermal condition for Nb=0, 6, and 18 baffles. In general, the tubular reactor with baffles in constant or variable temperature have polynomial behavior. The tubular reactor without baffles in constant or variable temperature have straight line behavior. The curve V0 appears as straight line, but it is not true, because the Figure 7.20 (a) shows its real path.

The curves in no isothermal condition shows different trajectory in relation to isothermal condition. The polynomial behavior of the curves with baffles reflects the location and number of baffles into tubular reactor.

7.14.3 Pressure Drop

The simulation results of pressure drop (ΔPr) in laminar flow versus length of the reactor (Z) without baffle, Nb=0, and with baffles, Nb=6, 18 in isothermal condition (C) at 60°C and the no isothermal condition (V), both in exothermic and adiabatic process are exhibited in Figure 7.21.

The Figure 7.21 (a) shows the comparative results in isothermal (C) and no isothermal (V) condition without Nb=0 baffles, into tubular reactor. The pressure drop with variable temperature (V0) is higher than the pressure drop in constant temperature (C0). The pressure drop in constant temperature remains constant.

The Figure 7.21 (b) states the comparative results in isothermal (C) and no isothermal (V) condition with Nb=6 baffles. The curve C6 and V6 have similar behavior, both vary in agreement with the variation of the location of baffles and length of reactor.

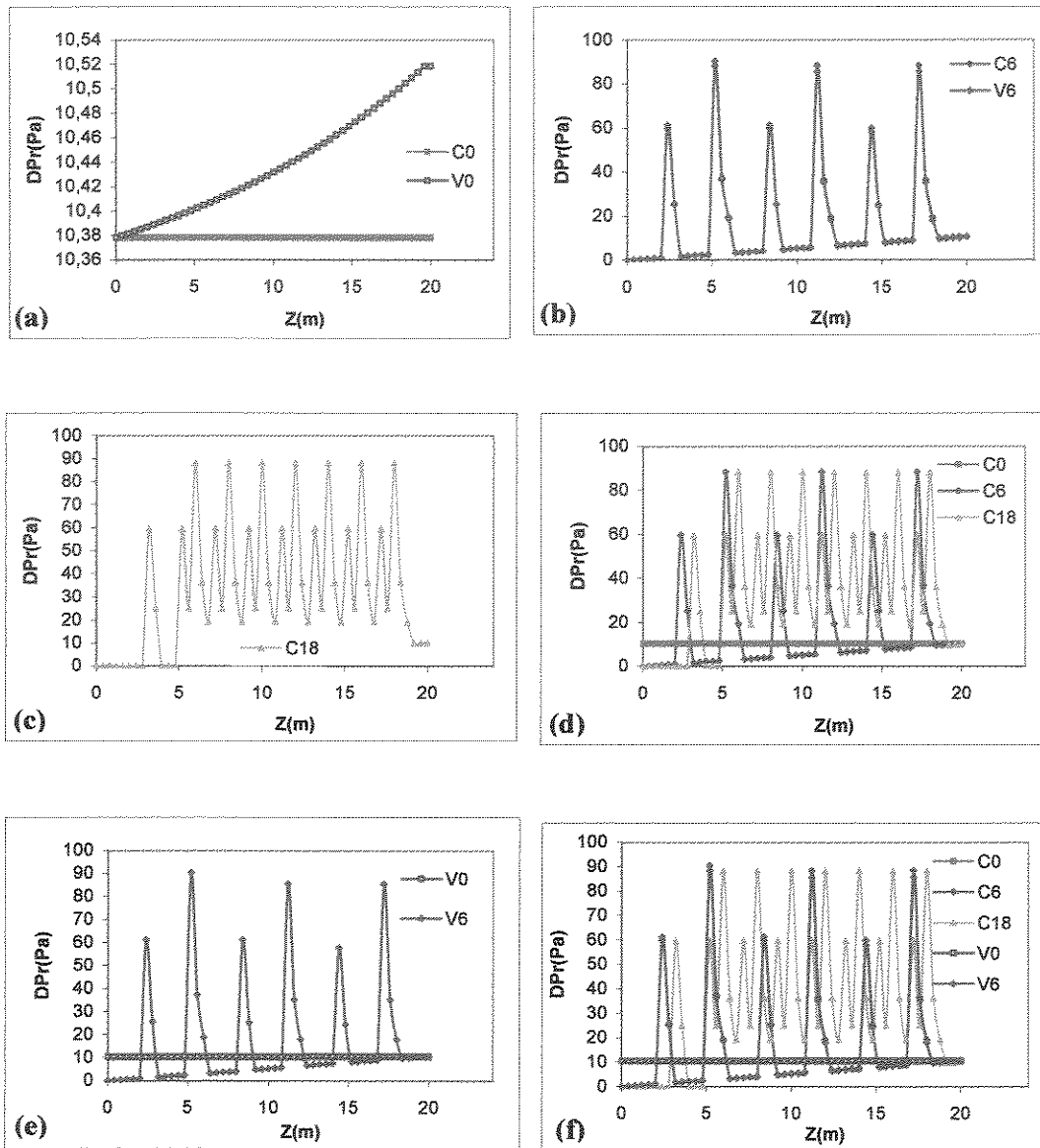


Figure 7.21 Pressure drop without ($Nb=0$) and with ($Nb=6, 18$) baffles into tubular reactor in isothermal ($CN_b=60^\circ C$) and no isothermal ($VN_b=T$) conditions.

The Figure 7.21 (c) presents the comparative results in isothermal (C) condition with $N_b=18$ baffles.

The Figure 7.21 (d) depicts the comparative results in isothermal condition without baffles (C0) and with baffles (C6, C18). The three curves have different path. The curve C6 and C18 have polynomial behavior, but the curve C0 has straight line form. The path reflects the location of baffles inside tubular reactor at the curves C6 and C18.

The Figure 7.21 (e) shows the comparative results of no isothermal condition without baffles (V0) and with $N_b=6$ baffles (V6). The two curves have different trajectory. The curve V6 has polynomial behavior, but the curve V0 has straight line form. The polynomial behavior shows the behavior of the reactor with baffles.

The Figure 7.21 (f) contains all results in isothermal and no isothermal condition for $N_b=0, 6,$ and 18 baffles. In general, the tubular reactor with baffles in constant or variable temperature have polynomial behavior. The tubular reactor without baffles in constant or variable temperature have straight line behavior. The curve V0 appears as straight line, but it is not true, because the Figure 7.20 (a) shows its real path.

The curves in no isothermal condition show different trajectory in relation to isothermal condition. The polynomial behavior of the curves with baffles reflect the location and number of baffles in tubular reactor and determine the performance of the emulsion polymerization reactor.

It is necessary to observe that the Figure 7.20 and 7.21 have same behavior, except the Figure 7.20 (a) and the Figure 7.21(a) are different.

RESUMO DO CAPÍTULO VIII

MENDOZA MARÍN, F.L. *Modelagem, simulação e análise de desempenho de reatores tubulares de polimerização com deflectores angulares internos*, 241p. Tese (Doutorado em Engenharia Química – Área de Processos Químicos) – Faculdade de Engenharia Química, Universidade Estadual de Campinas - UNICAMP, 2004.

O Capítulo VIII mostra a validação dos resultados computacionais da presente tese com os resultados da literatura. O Capítulo VIII é importante porque permite validar as aproximações, simplificações, suposições, assunções, estimações e limitações aplicados nos modelos matemáticos, do fenômeno da pesquisa. A validação foi realizado principalmente para o caso isotérmico de 60°C, velocidade constante à entrada e sem chicanas no reator tubular. Os objetivos do Capítulo VIII são: analisar os resultados computacionais e as analíticas com 50 volumes finitos; analisar a validação computacional com os resultados da literatura; analisar a validação do método numérico aplicado; analisar a validação do numero de partículas em forma aproximada com os resultados da literatura.

Conclusão do Capítulo VIII: No Capítulo VIII foram realizados as validações dos resultados das simulações, os quais foram concordantes com os dados da literatura em iguais ou parecidas condições. A validação foi apresentado por meio do analítico, experimental, computacional e numero de partículas. Os resultados de validação permitem concluir que as aproximações, simplificações, suposições, assunções, estimações e limitações aplicados às modelos matemáticos, à reator, à reação de polimerização em emulsão e às chicanas foram concordantes, conformes e correspondentes às características essenciais do comportamento do reator tubular nas condições comparadas como mostrados nos Capítulos VII, VIII e IX.

CHAPTER VIII

VALIDATION

The present deals with the validation of the computational results through the computation with the literature data. It is important to point out that this chapter allows to validate the approximations, simplifications and suppositions that were made in the mathematical models as well as of the solution procedure. The validation was realized mainly in isothermic condition at 60°, constant velocity at reactor inlet, for a tubular reactor without baffles.

Every numerical algorithm has its own characteristic error patterns. Well-known CFD euphemisms for the word error are terms such as numerical diffusion, false diffusion or even numerical flow. The likely error patterns can only be guessed on the basis of a thorough knowledge of the algorithms. At the end of a simulation the user must make a judgement whether the results are “good enough”. It is impossible to assess the validity of the models of physics and chemistry embedded in a program as complex as a CFD code or the accuracy of its final results by any means other than comparison with experimental test work. Anyone wishing to use CFD in a serious way must realize that it is no substitute for experimentation, but a very powerful additional problem-solving tool. Validation of a CFD code requires highly detailed information concerning the boundary conditions of a problem and generates a large volume of results. To validate these in a meaningful way it is necessary to produce experimental data of similar scope (Versteeg, 1998).

Sometimes the facilities to perform experimental work may not (yet) exist in which case the CFD user must rely on (1) previous experience, (2) comparisons with analytical solutions of similar but simpler flows and (3) comparisons with high quality data from closely related problems reported in the literature (Versteeg, 1998).

The computational results and analytic ones with 50 finite volumes are used, to analyze the computational validation with the literature results as well as to verify the validation of the products characterization such as particles number.

8.1 ANALYTIC VALIDATION

The analytic validation results of the monomer conversion of styrene in a tubular reactor without baffles in isothermal condition (C) at 60°C and in no isothermal condition (V) is displayed in Figure 8.1. This figure shows the analytic conversion simulation (Xa) and numerical method (or computational) conversion (Xc) versus length of the reactor (Z). In no isothermal condition the temperature varies inside tubular reactor in exothermic and adiabatic process.

The analytic solution is according to the equation simplified, Eq.(5.1) and Smith-Ewart model for interval II, Eq.(5.2) to estimate monomer conversion with supposition that the polymer particle phase is the main locus of polymerization, and Arrhenius chemical kinetics model to compute kinetics coefficients (e.g. Kp). The analytic solution is shown in Eq. (8.5).

Mass balance equations for monomer, Eq.(5.1)

$$v_z \frac{dC_M}{dz} = R_M \quad (8.1)$$

Polymer particle phase is the main locus of polymerization as :

$$C_M = C_{M0} (1 - X_M) \quad (8.2)$$

Deriving the Eq. (8.2) and substituting in Eq. (8.1) gives

$$v_z \frac{dX_M}{dz} = -\frac{R_M}{C_{M0}} \quad (8.3)$$

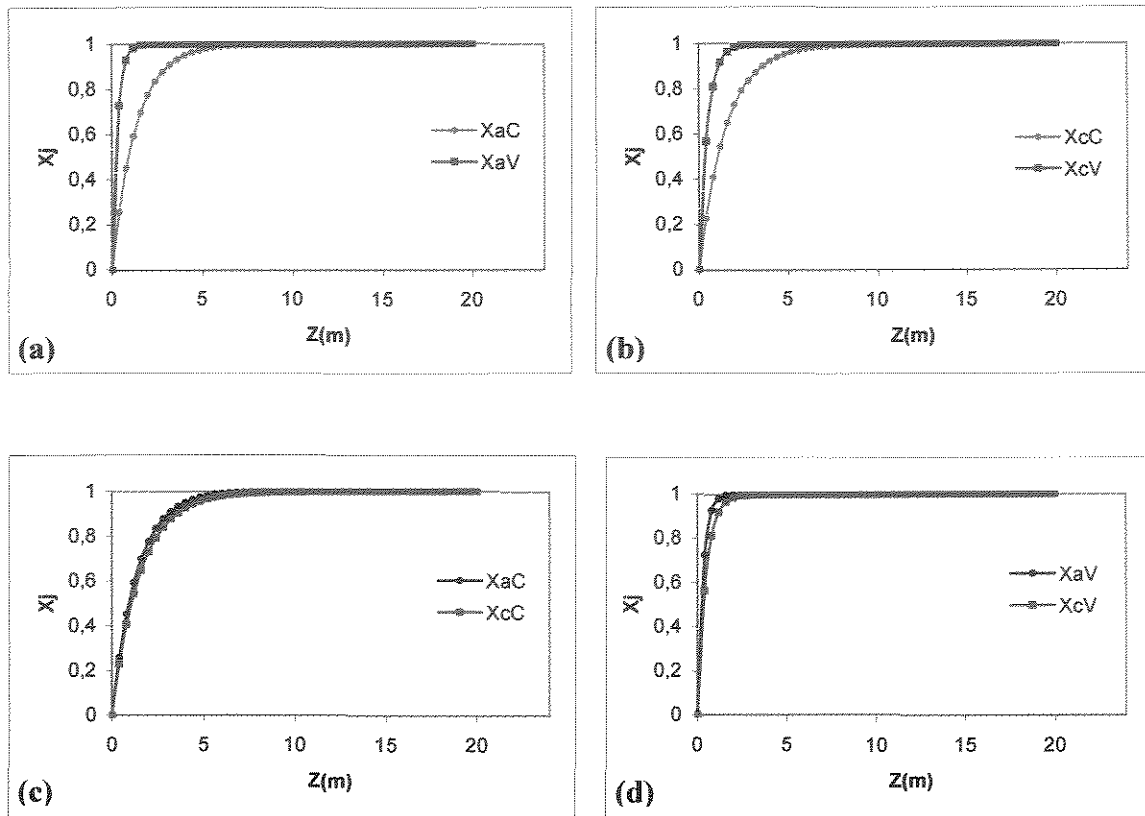


Figure 8.1 Analytic validation of monomer conversion in isothermal (C) and non isothermal (V) condition.

Smith-Ewart model for interval II to estimate monomer conversion as:

$$R_M = -K_p[M]_p \frac{N_p \bar{n}}{N_A V_p} \quad (8.4)$$

Integrating the Eq. (8.3) gives the analytic solution to estimate monomer conversion of styrene:

$$X_M = 1 - e^{-c \cdot z} \quad (8.5)$$

where:

$$c = \frac{KpN_p\bar{n}}{N_A V_P v_z} \quad (8.6)$$

$$Kp = Kp_0 \exp(-E_p / R_g T) \quad (8.7)$$

The Figure 8.1 (a) exhibits the comparative results in isothermal analytic conversion (XaC) and no isothermal analytic conversion (XaV). Both curves have the same behavior. The no isothermal analytic conversion is higher than isothermal analytic conversion. This difference has a average of 9,95% of relative error, it assumes as true value the isothermal analytic conversion. This difference could be by the variable temperature effect onto emulsion polymerization process.

The Figure 8.1 (b) exposes the comparative results for isothermal computational conversion (XcC) and no isothermal computational conversion (XcV). Both curves have same behavior. The no isothermal computational conversion is higher than the isothermal computational conversion. The difference has an average of 10,02% of relative error. This difference could be by the variable temperature effect upon the emulsion polymerization process of styrene.

The Figure 8.1 (c) expounds the comparative results in isothermal analytic conversion (XaC) and isothermal computational conversion (XcC). The average relative error is 1,4% between the curves XaC and XcC. This result proves that the numerical method of finite volume method with 50 finite volumes finite has a good performance.

The Figure 8.1 (d) states the comparative results for the no isothermal analytic conversion (XaV) and no isothermal computational conversion (XcV). Both curves are almost overlapped. The average relative error is 0,93% between the curves XaV and XcV. Again it may be said that the numerical method of finite volume method with 50 volumes finites is good enough to solve the problem.

8.2 EXPERIMENTAL VALIDATION

The comparative results in isothermal condition at 60°C of analytic conversion (X_a), experimental conversion (literature results) (X_e), computational conversion (X_c), and simulation conversion (literature results) (X_s) versus residence time(t) inside tubular reactor are shown in Figure 8.2. The experimental conversion has equal isothermal temperature and properties as the conversion calculated computationally. The simulation conversion has different mathematical model, but equal properties and isothermal temperature as computational conversion. The experimental data and simulation conversion were obtained from Bataile et al. (1982).

The Figure 8.2 (a) exposes the comparative results of isothermal analytic conversion (X_{aC}) with experimental (literature) (X_e) and simulation (literature) (X_s) conversion. The behavior of the curves X_{aC} , X_e and X_s are same, they describe the same paths and the average relative error between curve X_{aC} and X_s is 10%. These results show the validation of the finite volume numerical method with experimental and simulation results that were used by Bataile *et al.* (1982).

The Figure 8.2 (b) presents the comparative results in isothermal condition at 60°C of computational conversion (model developed in this work) (X_{cC}) with experimental (literature) (X_e) and simulation (literature) (X_s) conversion. The proposed model has a similar behavior compared to the literature data and model it has to be emphasized that quantitative difference can be handed out through parameter estimation but this was not the objective of this thesis. Besides the model the pattern of behavior of the prediction is a good indication of the proposed solution procedure.

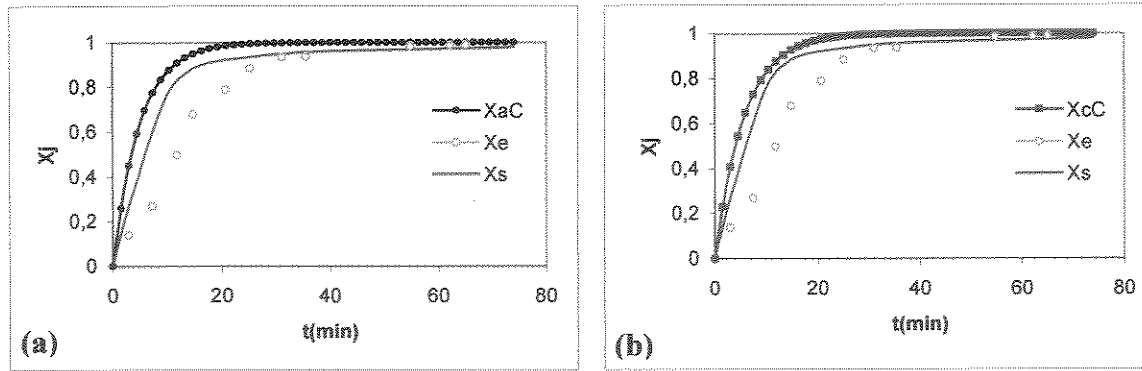


Figure 8.2 Experimental validation in isothermal (C) and no isothermal condition.

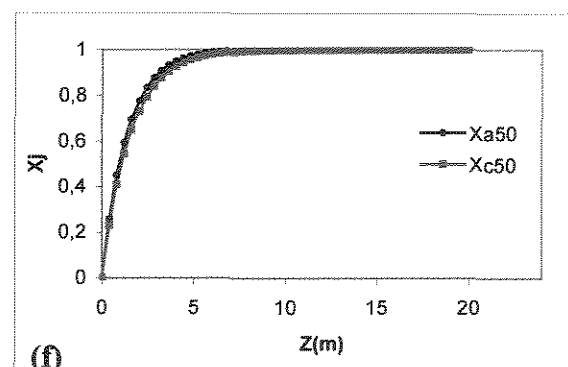
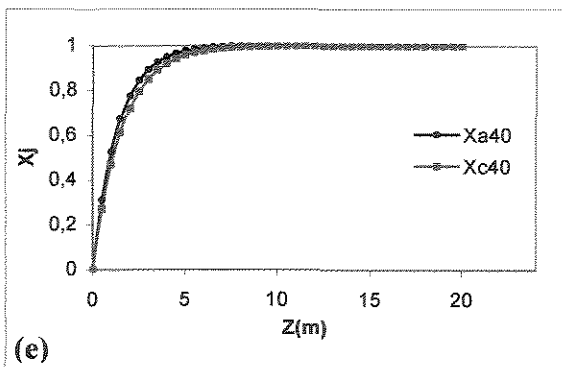
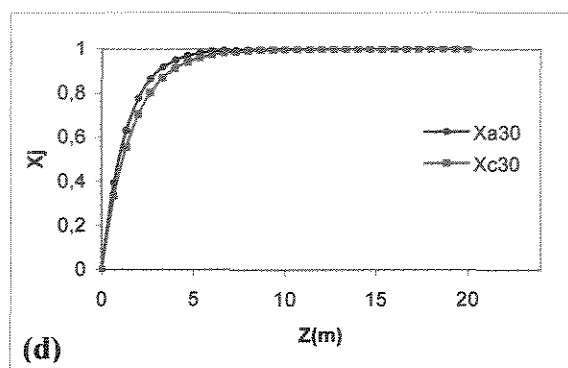
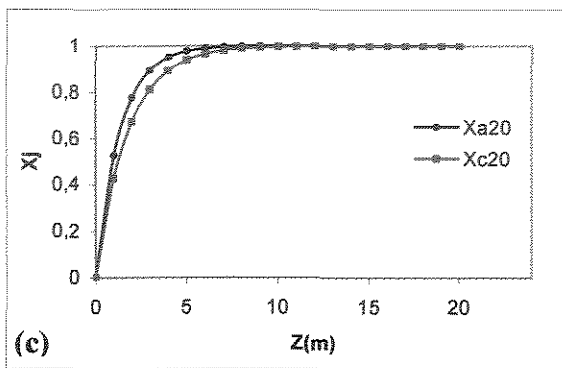
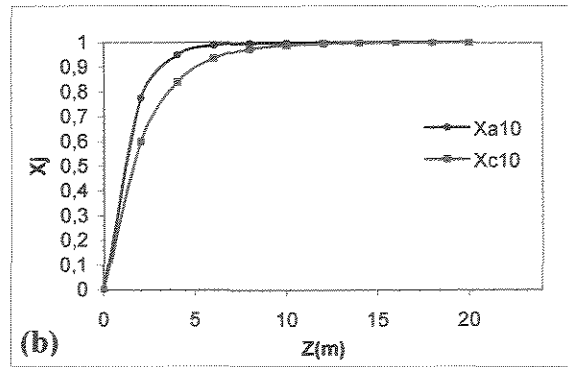
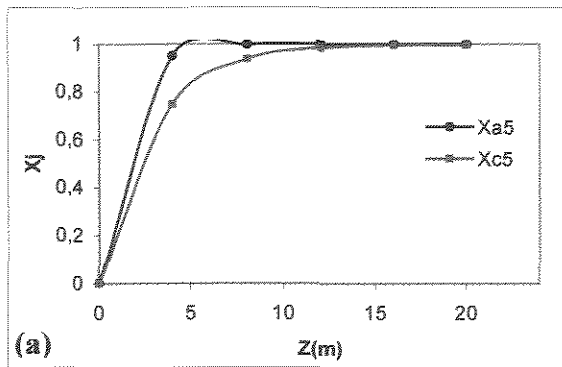
8.3 COMPUTATIONAL VALIDATION

The comparative results in isothermal condition of analytic conversion (X_{aN}) and computational conversion (X_{cN}) from coarse grid ($N=5$) toward $N=200$ finites volumes versus length of tubular reactor (Z) are exhibited in Figure 8.3. All figures have same properties, and approximations, they vary only in number of finites volumes. The data used are given in Table 3.1.

The Figure 8.3 (a) shows the comparative results of isothermal analytic conversion (X_{a5}) with isothermal computational conversion (X_{c5}) with $N=5$ finites volumes. The average relative error is around 5,90% between analytic and numerical results.

The Figure 8.3 (b) presents the comparative results of isothermal analytic conversion (X_{a10}) with isothermal computational conversion (X_{c10}) with $N=10$ finites volumes. The average relative error between analytic and numerical results is around 4,38%.

The Figure 8.3 (c) contains the comparative results of isothermal analytic conversion (X_{a20}) with isothermal computational conversion (X_{c20}) with $N=20$ finites volumes. The average relative error (2,85%) between analytic and numerical results is a quite good performance for the solution procedure.



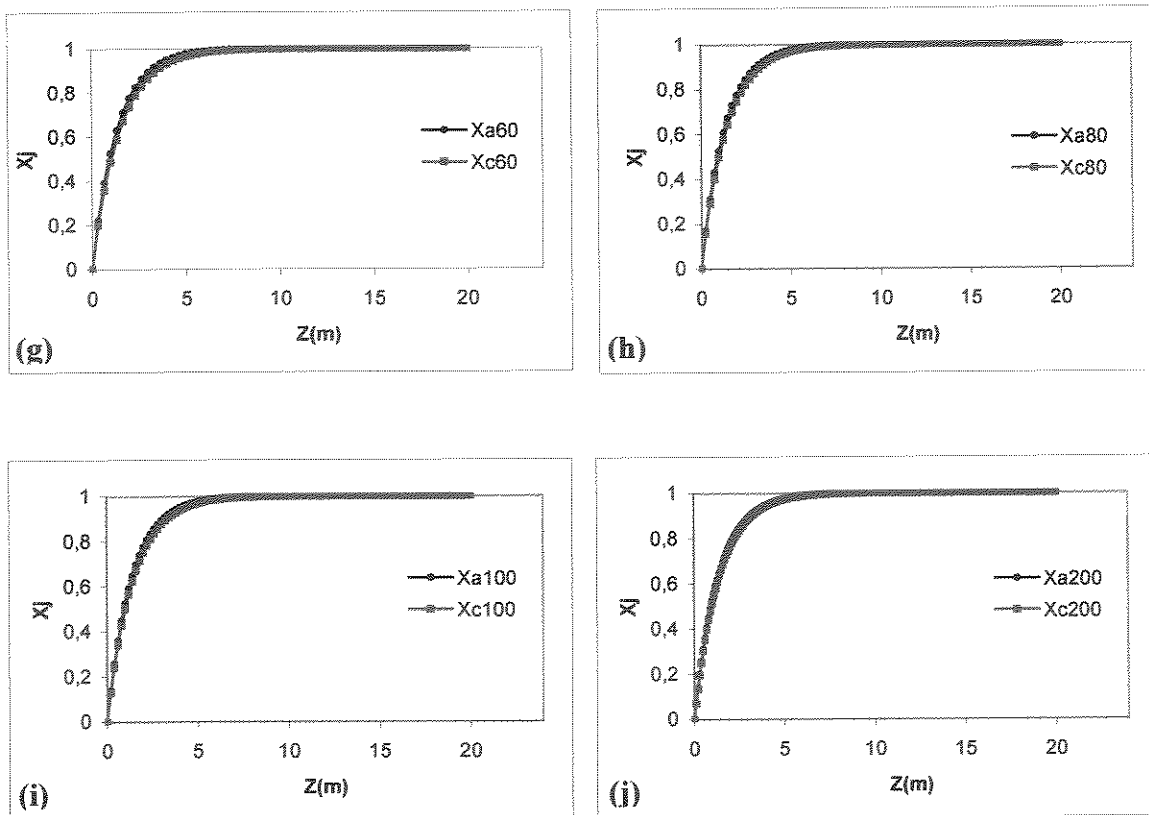


Figure 8.3 Computational or numerical validation of the number of finite volume with analytic results.

Figures 8.3 (d), (e) and (f) depict the comparison between the predictions by analytical and numerical solution, for different finite volume numbers. Both presented the same qualitative and quantitative behavior and thus is an important feature to be considered in the numerical solution procedure validation. The comparative results with $N=50$ finites and the average relative error of 1,40% between analytic and numerical results is used to exhibit the simulation results in the present thesis as shown in Figure 8.3 (f).

The Figure 8.3 (g)-(j) have same performance that the Figures 8.3 (a)-f), then the average relative errors are showed in the Table 8.1.

Table 8.1 Average relative error with different finite volumes

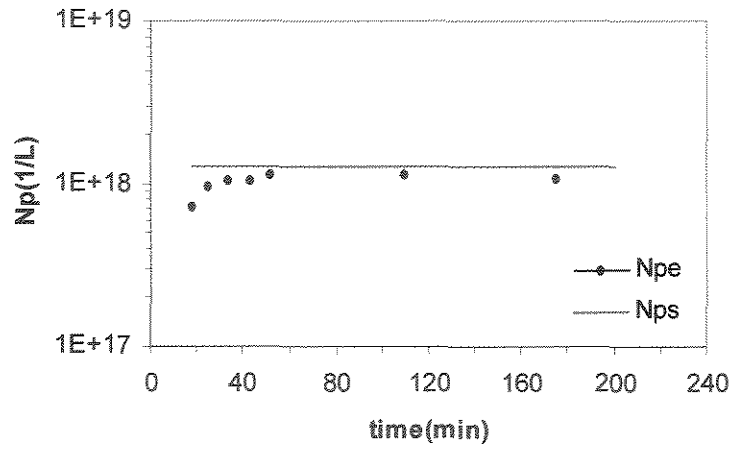
Number of Finite volume(N)	Average relative error (%)
5	5,90
10	4,38
20	2,85
30	2,12
40	1,68
50	1,40
60	1,19
80	0,92
100	0,75
200	0,39

The table 8.1 exhibits the average relative errors in relation to finites volumes number. As expected it shows the diminution of the average relative errors when the finite volumes number increase. The average relative error for N=200 finites volumes is 0,39%. For number of finite volumes longer than 200 finite volumes, then relative error will decrease slowly so that a numerical minimal realization has been obtained . In fact, values lower than 2% are already acceptable. In this sense a finite number of 50 was choose in all simulation to keep a trade off between accuracy and computer burden.

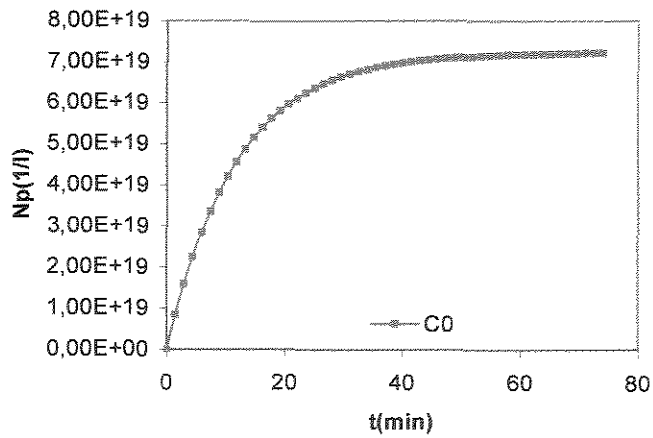
8.4 VALIDATION OF THE PARTICLES NUMBER

The comparative results in isothermal condition the polystyrene particles number (N_p) without baffles inside batch and tubular reactor, respectively versus time (t) are presented in Figure 8.4. The simulations conditions were applied with difference in mathematical model, properties, recipe, constant reaction temperature, numerical method, and type of reactor.

The Figure 8.4 (a) expounds the experimental (N_{pe}) and simulation (N_{ps}) of the total number of particles. The experimental and simulation conditions are feed temperature of 50°C, potassium persulfate (KPS) 0,011 mol/l, sodium dodecyl sulfate (SDS) 0,05 mol/l, no adiabatic process (de la Rosa et al., 1996). The results are obtained with calorimetric technique, since emulsion polymerization proceeds with a heat evolution, the measured heat release from the reaction can be



(a)



(b)

Figure 8.4 Number of particle validation at isothermic condition.

translated into rate of polymerization. Capillary hydrodynamic fractionation (CHDF) was used to determine particle number. It should be noted that initiator concentration did not have a very drastic effect on particle nucleation. De la Rosa et al. (1996) indicated that the experiment results is in a close range within experimental measurement error. Considering the difficulty associated with particle number measurement determination, the model prediction should be considered satisfactory. The particle number of the model prediction is approximately at $1,28 \times 10^{18}$ 1/L as shown in Figure 8.4 (a).

The Figure 8.4 (b) presents the simulation results for the particle number in isothermal condition without baffles inside the tubular reactor. The simulations conditions for one-dimensional mathematical model with the micellar and homogeneous nucleation of particles (Section 4.4.1 and 4.4.2), constant reaction temperature 60°C , the recipe given in Table 3.1 and the properties given in Chapter 3. The number of particle varies between $0-7,22 \times 10^{19}$ 1/L as shown in Figure 8.4 (b).

The comparison of the two Figures 8.4 (a) and (b) show the same qualitative behavior and a reasonable agreement in the quantitative values.

RESUMO DO CAPÍTULO IX

MENDOZA MARÍN, F.L. *Modelagem, simulação e análise de desempenho de reatores tubulares de polimerização com deflectores angulares internos*, 241p. Tese (Doutorado em Engenharia Química – Área de Processos Químicos) – Faculdade de Engenharia Química, Universidade Estadual de Campinas - UNICAMP, 2004.

O Capítulo IX apresenta o análise de sensibilidade do comportamento do reator tubular, sem e com chicanas, em condições isotérmicas e não isotérmicas e em outras condições diferentes que as condições do Capítulo VII, como a temperatura de alimentação e diâmetro do reator. O Capítulo IX é importante porque permite incrementar um maior numero de resultados de simulação para analisar o comportamento do reator na forma mais global e geral sem e com chicanas em condições isotérmicas e não isotérmicas. Os objetivos do Capítulo IX são: analisar o comportamento do reator a outra temperatura de alimentação de 90°C; analisar o comportamento do reator com diâmetro de 0,5 m, ambos sem e com chicanas em condições isotérmicas e não isotérmicas; analisar o comportamento do numero de chicanas em condições isotérmicas e não isotérmicas.

Conclusão do Capítulo IX: No Capítulo IX foram analisados a sensibilidade do comportamento do reator proposto, em condições diferentes aqueles aplicados no Capítulo VII; também foram mostrados análises do comportamento do reator com chicanas em condições isotérmicas e não isotérmicas. O comportamento do reator tubular com diferentes temperaturas de alimentação e diâmetro do reator foram diferentes; em geral pode-se concluir que com temperatura de alimentação de 90°C foram melhores que 60°C e em relação ao diâmetro, o reator com 1 m apresentou melhor desempenho do que o de 0,5 m, para conversão de monômero. A presença das chicanas no reator tubular segundo os resultados do Capítulo VII e IX permite concluir que o sistema com chicanas apresentou melhor desempenho com relação ao numero de partículas, a distribuição do peso molecular, o tamanho das partículas e a distribuição da viscosidade do poliestireno.

CHAPTER IX

PERFORMANCE ANALYSIS OF PROPOSED REACTOR

In this chapter is analyzed the performance sensibility of the tubular reactor without and with baffles under different conditions than those used in Chapter VII, such as feed temperature and reactor diameter, furthermore to analyze the baffles presence inside tubular reactor. This Chapter is important because it increases more number of simulations results that allow to analyze the reactor behavior in form global.

The objective is to observe the impact of the baffles inside the reactor for both isothermal and no isothermal conditions another feed temperature at 90°C and another reactor diameter at 0,5 m.

9.1 FEED TEMPERATURE

The feed temperature effect in the emulsion polymerization process of styrene will be only simulated for monomer conversion, axial velocity, and particles number. Other variables and properties will not be evaluated.

9.1.1 Conversion of monomer

The comparative results of monomer conversion of styrene in isothermal (C) and no isothermal (V) condition between feed temperature at 60°C and 90°C, respectively versus length of tubular reactor (Z) are exhibited in Figure 9.1. The conversions with constant or variable temperature were obtained without and with baffles inside the tubular reactor. The temperature varies inside the reactor in exothermic and adiabatic of emulsion polymerization of styrene.

The Figure 9.1 (a) presents the comparative results in isothermal condition at 60°C (C0-60) and 90°C (C0-90) without baffles into tubular reactor. Both curves have same performance. The monomer conversion at 90°C is larger than monomer conversion at 60°C.

The Figure 9.1 (b) exposes the comparative results in isothermal condition at 60°C (C6-60) and 90°C (C6-90) with Nb=6 baffles within tubular reactor. Both curves have same behavior. The monomer conversion to 90°C is greater than monomer conversion to 60°C.

The Figure 9.1 (c) expounds the comparative results in isothermal condition at 60°C (C18-60) and 90°C (C18-90) with Nb=18 baffles in tubular reactor. Both curves have same behavior. The monomer conversion to 90°C is greater than monomer conversion to 60°C.

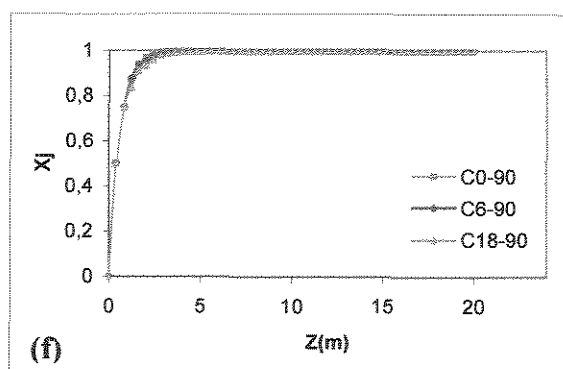
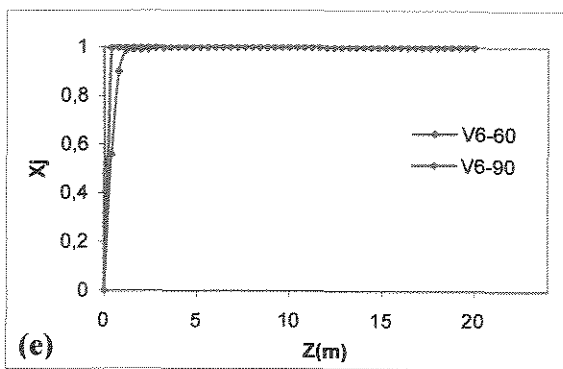
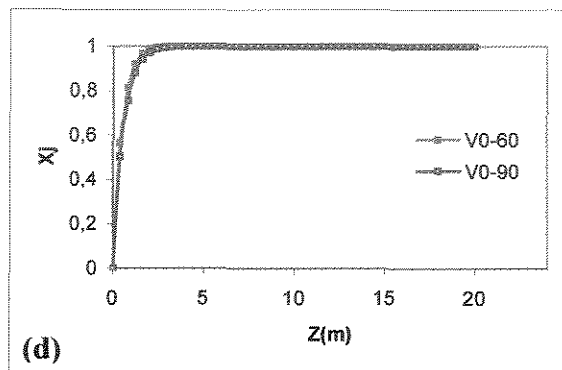
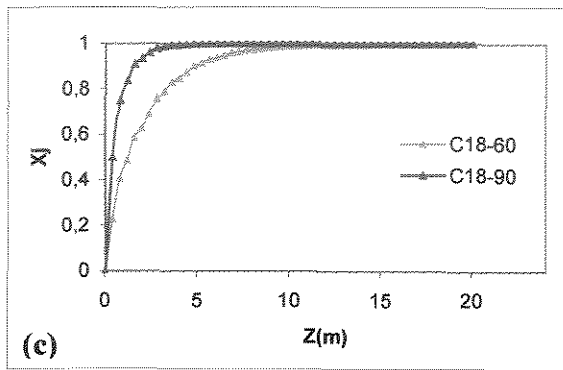
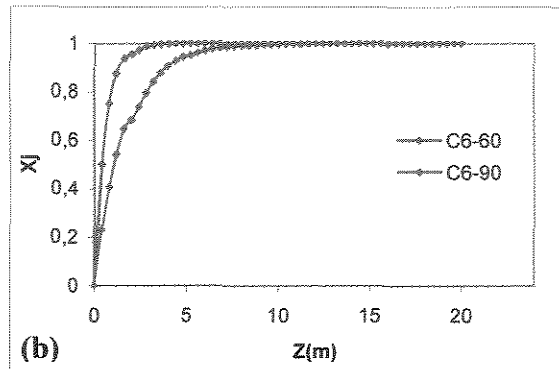
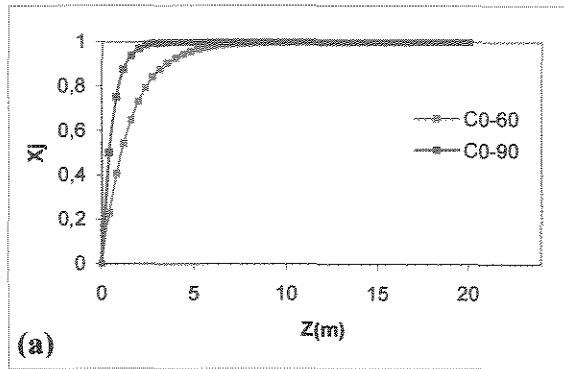
The Figure 9.1 (d) shows the comparative results in no isothermal condition with feed constant temperature at 60°C (V0-60) and 90°C (V0-90) without baffles in the tubular reactor. The wide of separation between the two curves is very small. The no isothermal condition to 60°C is slightly higher than the conversion to 90°C.

The Figure 9.1 (e) presents the comparative results in no isothermal condition (V) with feed constant temperature at 60°C (V6-60) and 90°C (V6-90) with Nb=6 baffles. For the no isothermal condition of 90°C the conversion is higher when compared to 60°C, as expected.

The Figure 9.1 (f) presents the comparative results in isothermal condition (C) with feed constant temperature at 90°C without baffles (C0-90) and with Nb=6, 18 baffles (C6-90, C18-90) into tubular reactor. The three curves have same behavior. The curve C0-90 has slight high monomer conversion than the curves C6-90 and C18-90. When increase the baffles number, the monomer conversion decreases slightly.

The Figure 9.1 (g) exhibits the comparative results in no isothermal condition (V) with feed constant temperature of 90°C without baffles (V0-90) and with Nb=6 baffles (V6-90) into tubular reactor. The curves V0-90 and V6-90 have same behavior. The curve V6-90 has high monomer conversion than the curve V0-90.

The Figure 9.1 (h) shows all comparative results in isothermal condition (C) with Nb=0, 6 and 18 baffles and no isothermal condition (V) with Nb=0 and 6 baffles with feed constant temperature at 90°C within tubular reactor. In no isothermal condition the curves V0-90 and V6-90 have higher conversion than the three curves in isothermal condition.



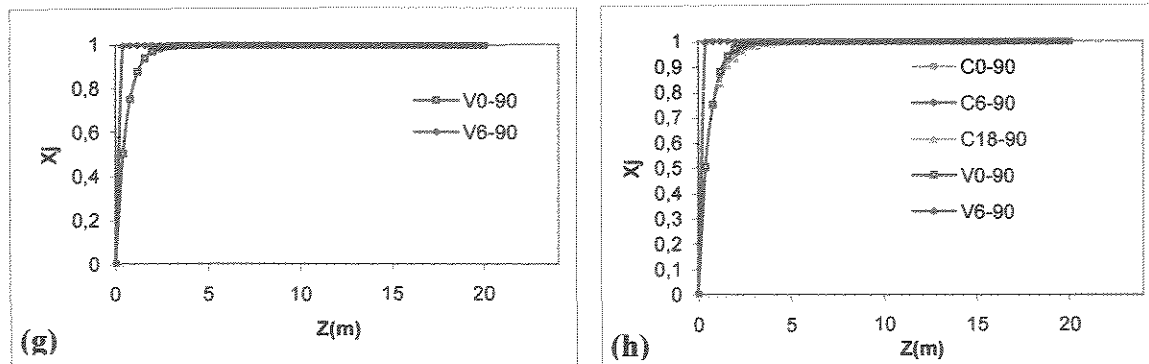


Figure 9.1 Conversion of monomer in feed temperature of 60 and 90°C without ($N_b=0$) and with ($N_b=6, 18$) baffles inside tubular reactor.

In isothermal condition the conversion in feed temperature at 90°C without $N_b=0$ or with $N_b=6, 18$ baffles are higher than the conversion in feed temperature at 60°C. In no isothermal condition the conversion in feed temperature at 90°C without $N_b=0$ or with $N_b=6$ baffles are higher than the conversion in feed temperature at 60°C. In general the conversion obtained in feed temperature at 90°C is higher than conversion obtained in feed temperature at 60°C. In isothermal condition with feed temperature 90°C, when increase the baffles number, the conversion reduces. The feed temperature and baffles number could have influence in the process of emulsion polymerization.

9.1.2 Axial velocity

The comparative results of axial velocity in isothermal (C) and no isothermal (V) condition at feed temperature 60°C and 90°C, respectively versus length of tubular reactor (Z) are depicted in Figure 9.2. The axial velocities were obtained without and with baffles inside tubular reactor. The temperature varies inside tubular reactor in exothermic and adiabatic process of emulsion polymerization reactor of styrene.

The Figure 9.2 (a) exposes the comparative results of axial velocity in isothermal (C) and no isothermal (V) condition at feed temperature 90°C without baffles into tubular reactor. The axial velocity in variable temperature is greater than constant temperature.

The Figure 9.2 (b) exhibits the comparative results of axial velocity in isothermal condition (C) at feed temperature 60°C (C0-60) and 90°C (C0-90) without baffles into tubular. Both curves are straight line. The C0-90 is the greatest than the curve C0-60.

The Figure 9.2 (c) expounds the comparative results of axial velocity in isothermal condition at feed temperature 60°C (C6-60) and 90°C (C6-90) with Nb=6 baffles in tubular reactor. Both curves have same path.

The Figure 9.2 (d) presents the comparative results of axial velocity in isothermal condition at feed temperature 60°C (C18-60) and 90°C (C18-90) with Nb=18 baffles into tubular reactor. Both curves have same path.

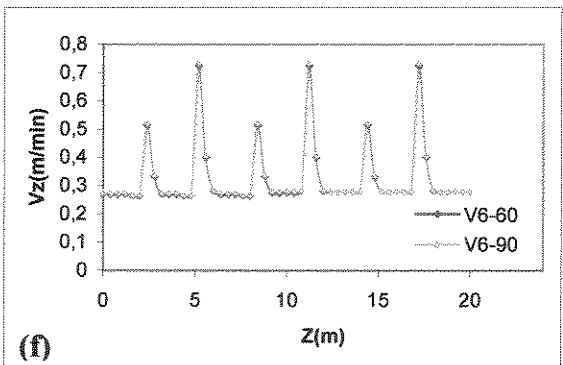
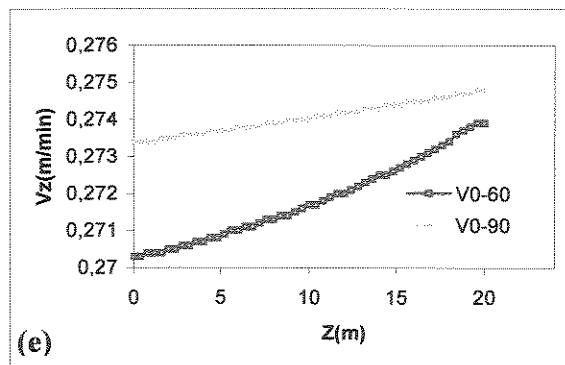
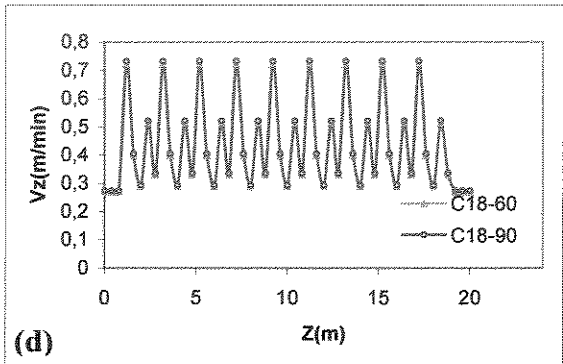
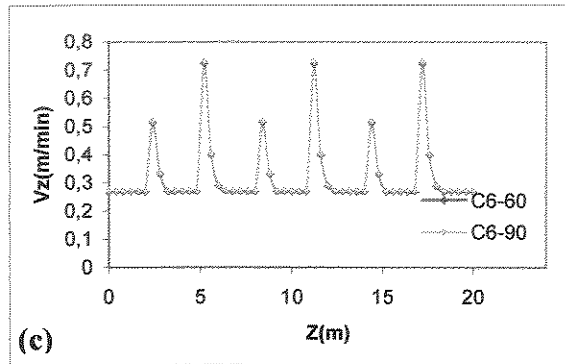
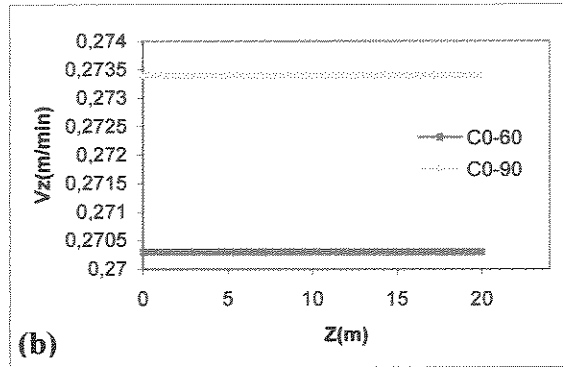
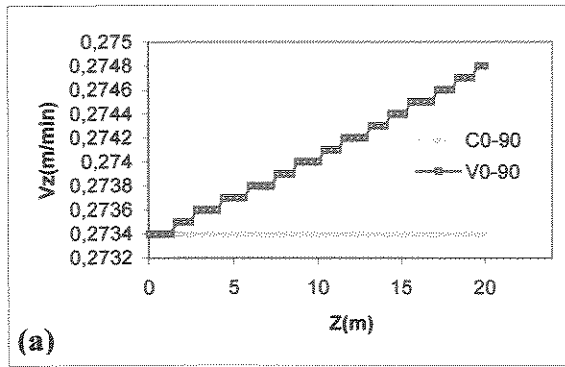
The Figure 9.2 (e) contains the comparative results of axial velocity in no isothermal condition at feed temperature 60°C (V0-60) and 90°C (V0-90) without baffles into tubular reactor. Both curves increase its velocities within tubular reactor, the curve V0-90 is greater than the curve V0-60.

The Figure 9.2 (f) expounds the comparative results of axial velocity in no isothermal condition at feed temperature 60°C (V6-60) and 90°C (V6-90) with Nb=6 baffles in tubular reactor. Both curves have same trajectories.

The Figure 9.2 (g) presents the comparative results in isothermal condition (C) with feed constant temperature 90°C without baffles (C0-90) and with Nb=6, 18 baffles (C6-90, C18-90) into tubular reactor. The curves C6-90 and C18-90 have same path, but the curve C0-90 is straight line.

The Figure 9.2 (h) exhibits the comparative results of axial velocity in no isothermal condition (V) with feed constant temperature at 90°C without baffles (V0-90) and with Nb=6 baffles (V6-90) into tubular reactor. The curve V0-90 appears as straight line, but its real path is in Figure 9.2 (e).

The Figure 9.2 (i) shows the all comparative results of axial velocity in isothermal (C) and no isothermal (V) condition with feed constant temperature at 90°C without and with baffles within tubular reactor. In isothermal (C) and no isothermal (V) condition with baffles posses same paths in according to the baffles number inside tubular reactor. The curves C0-90 and V0-90 appear as straight line, but its real paths are in Figure 9.2 (a).



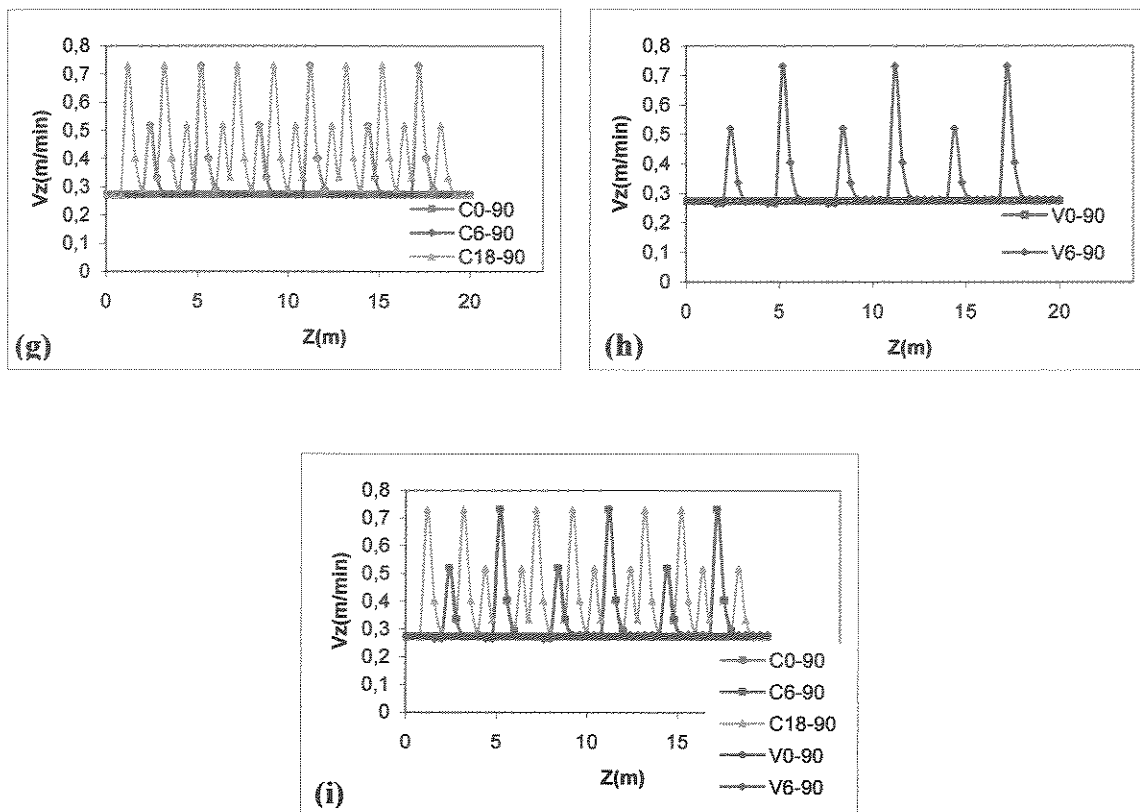


Figure 9.2 Axial velocity in feed temperature of 60 and 90°C without ($N_b=0$) and with ($N_b=6, 18$) baffles inside tubular reactor.

Then the axial velocity at feed temperature 90°C is higher than the axial velocity at feed temperature 60°C in constant or variable reaction temperature into tubular reactor, it are shown in Figures 9.2 (a), (b) and (e). In general the feed temperature at 90°C increases the axial velocity in comparison at feed temperature 60°C without or with baffles into tubular reactor. The trajectories without baffles are same, too the trajectories between baffles in reactor, then the baffles show the location and baffles number inside tubular reactor.

9.1.3 Number of particles

The comparative results of particles number (N_p) of styrene in isothermal (C) and no isothermal (V) condition between feed temperature at 60°C and 90°C, respectively versus length of tubular reactor (Z) are presented in Figure 9.3. The particles number with

constant or variable temperature were obtained without and with baffles inside tubular reactor. The temperature varies inside tubular reactor in exothermic and adiabatic process of emulsion polymerization of styrene.

The Figure 9.3 (a) presents the comparative results in isothermal condition of 60°C (C0-60) and 90°C (C0-90) without baffles into tubular reactor. Both curves have same performance, but the particle number to 90°C is the greatest than particle number to 60°C.

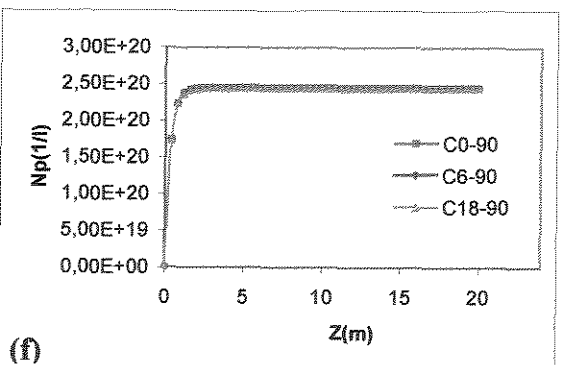
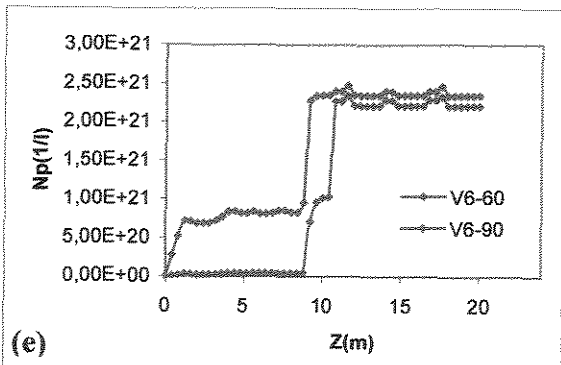
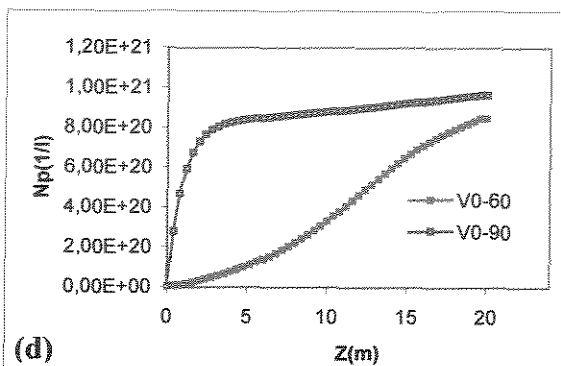
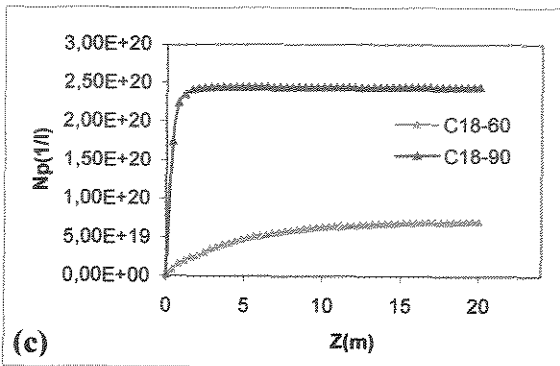
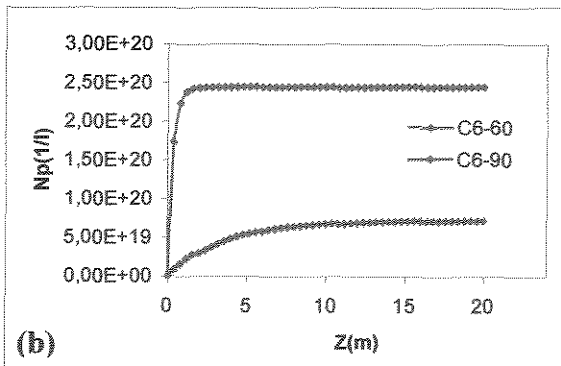
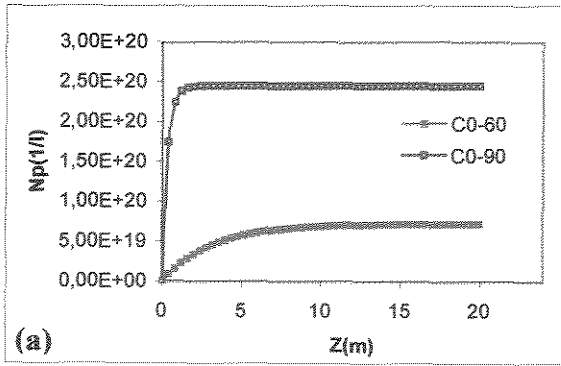
The Figure 9.3 (b) expounds the comparative results of isothermal condition of 60°C (C6-60) and 90°C (C6-90) with Nb=6 baffles within tubular reactor. Both curves have same behavior, but the particle number to 90°C is the greatest than particle number to 60°C.

The Figure 9.3 (c) shows the comparative results of isothermal condition at 60°C (C18-60) and 90°C (C18-90) with Nb=18 baffles in tubular reactor. Both curves have same behavior, but the particles number to 90°C is the greatest than particle number to 60°C.

The Figure 9.3 (d) exhibits the comparative results in no isothermal condition with feed constant temperature at 60°C (V0-60) and 90°C (V0-90) without baffles in tubular reactor. Both curves have different performance. The curve V0-60 describes a different trajectory that the curve V0-90. In no isothermal condition to 90°C the particles number is the highest than in no isothermal condition to 60°C.

The Figure 9.3 (e) contains the comparative results in no isothermal condition with feed constant temperature at 60°C (V6-60) and 90°C (V6-90) with Nb=6 baffles into tubular reactor. The separation wide between the two curves is very irregular. The curve V0-60 describes analogy trajectory that the curve V0-90. The path of two curves are very strange. The particles number in no isothermal condition to 90°C is higher than the particles number to 60°C.

The Figure 9.3 (f) presents the comparative results in isothermal condition (C) with feed constant temperature at 90°C without baffles (C0-90) and with Nb=6, 18 baffles (C6-90, C18-90) into tubular reactor. The three curves have same behavior. The curve C0-90 has slight high particle number than the curves C6-90 and C18-90. When increase the baffles number, the particles number decreases slightly.



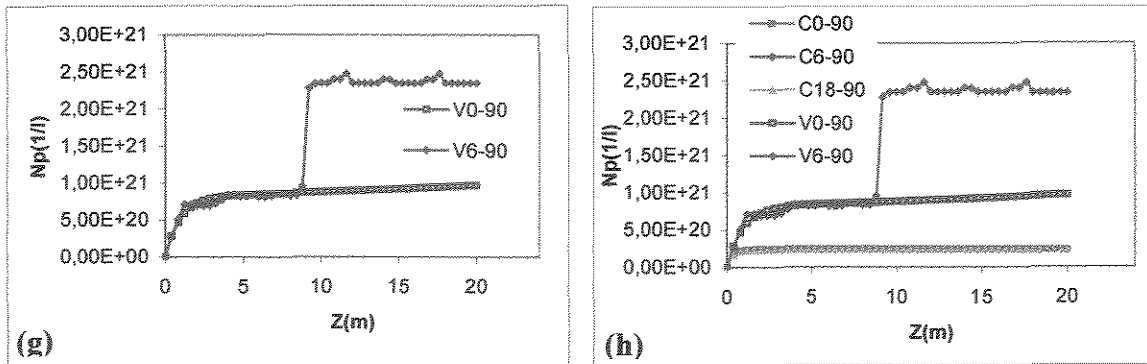


Figure 9.3 Number of particles in feed temperature of 60 and 90°C without ($Nb=0$) and with ($Nb=6, 18$) baffles inside tubular reactor.

The Figure 9.3 (g) exhibits the comparative results in no isothermal condition (V) with feed constant temperature at 90°C without baffles (V0-90) and with $Nb=6$ baffles (V6-90) into tubular reactor. The two curves have different performance. The curve V6-90 has higher particle number than the curves V0-90.

The Figure 9.3 (h) shows the all comparative results in isothermal (C) and no isothermal (V) condition with feed constant temperature at 90°C with $Nb=0, 6$ and 18 baffles within tubular reactor. The curves V0-90 and V6-90 have higher particle number than the three curves in isothermal condition.

In isothermal condition the particles number in feed temperature at 90°C without $Nb=0$ or with $Nb=6, 18$ baffles are higher than the particles number in feed temperature at 60°C. In no isothermal condition the particles number in feed temperature at 90°C without $Nb=0$ or with $Nb=6$ baffles are higher than the particles number in feed temperature at 60°C. In general the particles number obtained in feed temperature of 90°C is higher than particles number obtained in feed temperature at 60°C. In isothermal condition at feed temperature 90°C (Figure 9.3 (g)) when increase the baffles number in reactor diminishes the particles number slightly, but in no isothermal condition, the performance is different. Therefore the feed temperature and baffles number inside tubular reactor have influence in the emulsion polymerization process of styrene.

9.2 REACTOR DIAMETER

The reactor diameter effect in the emulsion polymerization process of styrene will be simulated for monomer conversion, internal transversal area of tubular reactor, axial velocity inside tubular reactor, and particles number. Other variables and properties will not be evaluated.

9.2.1 Conversion of monomer

The comparative results of the monomer conversion (X_j) in isothermal (C) and no isothermal (V) condition of the reactor diameter at $D_r=0,5$ m and $D_r=1$ m, respectively versus length of tubular reactor (Z) are presented in Figure 9.4. The conversions with constant or variable temperature were obtained without and with baffles inside tubular reactor. The temperature varies inside tubular reactor in exothermic and adiabatic of emulsion polymerization of styrene.

The Figure 9.4 (a) contains the comparative results in isothermal condition of the reactor diameter at $D_r=0,5$ m (C0-d.5) and $D_r=1$ m (C0-d1) without baffles into tubular reactor. Both curves have same performance. The monomer conversion to $D_r=1$ m is larger than monomer conversion to $D_r=0,5$ m.

The Figure 9.4 (b) exposes the comparative results in isothermal condition of the reactor diameter at $D_r=0,5$ m (C6-d.5) and $D_r=1$ m (C6-d1) with $N_b=6$ baffles within tubular reactor. Both curves have same behavior. The monomer conversion to $D_r=1$ m is greater than monomer conversion to $D_r=0,5$ m.

The Figure 9.4 (c) expounds the comparative results in isothermal condition of the reactor diameter at $D_r=0,5$ m (C18-d.5) and $D_r=1$ m (C18-d1) with $N_b=18$ baffles in tubular reactor. Both curves have same behavior. The monomer conversion to $D_r=1$ m is greater than monomer conversion to $D_r=0,5$ m.

The Figure 9.4 (d) shows the comparative results in no isothermal condition of the reactor diameter at $D_r=0,5$ m (V0-d.5) and $D_r=1$ m (V0-d1) without baffles in tubular reactor. The monomer conversion to $D_r=1$ m is higher than the conversion to $D_r=0,5$ m.

The Figure 9.4 (e) presents the comparative results in no isothermal condition of the reactor diameter at $D_r=0,5$ m (V6-d.5) and $D_r=1$ m (V6-d1) with $N_b=6$ baffles into tubular reactor. The no isothermal condition to $D_r=1$ m is higher than the conversion to $D_r=0,5$ m.

The curve V6-d.5 between the points (1,2 m, 83,26%) – (3,6 m, 98%) show a decrease in the conversion or its path presents strange behavior. This situation would be by the effect of the diameter reduction, variable temperature and baffles number into tubular reactor.

The Figure 9.4 (f) presents the comparative results in isothermal condition (C) and of the reactor diameter at $Dr=0,5$ m without baffles (C0-d.5) and with $Nb=6, 18$ baffles (C6-d.5, C18-d.5) into tubular reactor. The three curves have same behavior. The curve C0-d.5 has higher monomer conversion than the curves C6-d.5 and C18-d.5. When increase the baffles number, the monomer conversion decreases slightly.

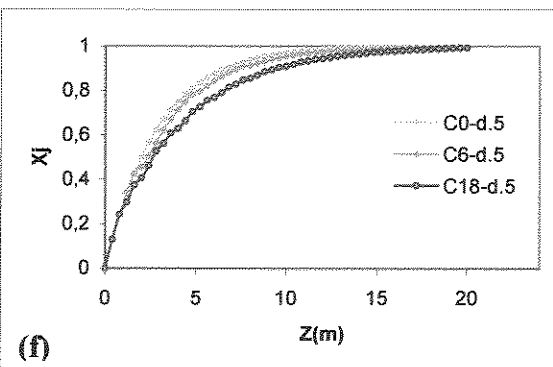
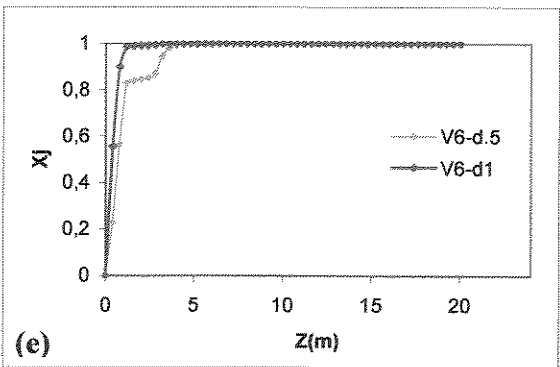
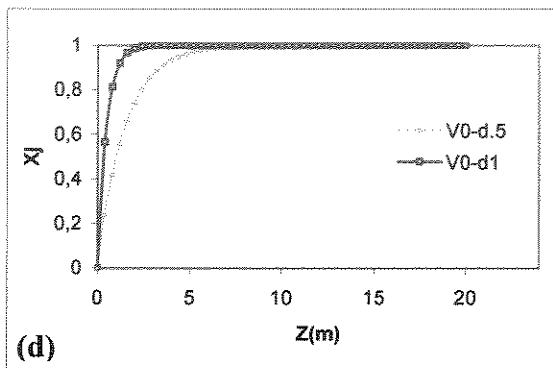
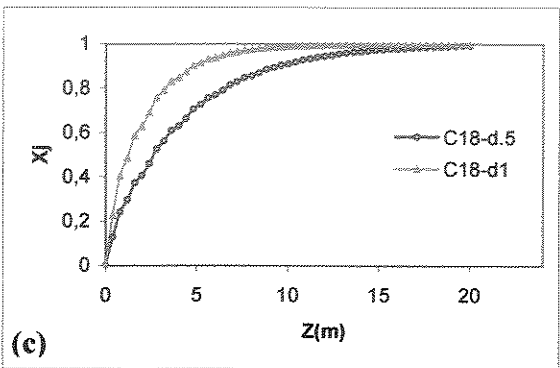
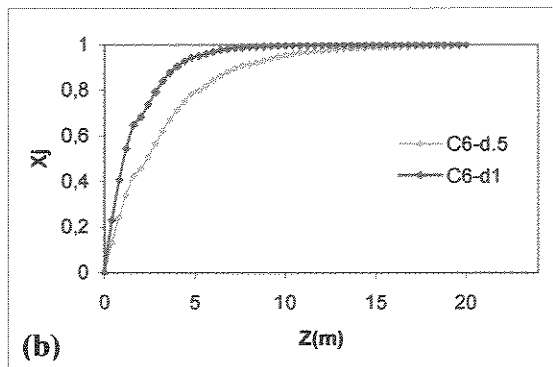
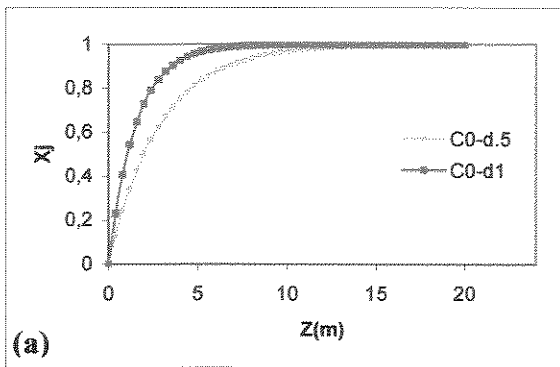
The Figure 9.4 (g) exhibits the comparative results in isothermal condition (C) and of the reactor diameter at $Dr=1$ m without baffles (C0-d1) and with $Nb=6, 18$ baffles (C6-d1, C18-d1) into tubular reactor. The three curves have same behavior. The curve C0-d1 has higher monomer conversion than the curves C6-d1 and C18-d1. When increase the baffles number, the monomer conversion decreases.

The Figure 9.4 (h) presents the comparative results in no isothermal condition (V) and of the reactor diameter at $Dr=0,5$ m without baffles (V0-d.5) and with $Nb=6$ baffles (V6-d.5) into tubular reactor. The curve V6-d.5 has higher monomer conversion than the curves V0-d.5.

The Figure 9.4 (i) exhibits the comparative results in no isothermal condition (V) and of the reactor diameter at $Dr=1$ m without baffles (V0-d1) and with $Nb=6$ baffles (V6-d1) into tubular reactor. The curve V0-d1 and V6-d1 have same behavior. The curve V6-d1 has higher monomer conversion than the curves V0-d1.

The Figure 9.4 (j) shows the all comparative results in isothermal (C) and no isothermal (V) condition of the reactor diameter at $Dr=0,5$ m without and with baffles within tubular reactor. In no isothermal condition the curves V0-d.5 and V6-d.5 have higher conversion than the three curves in isothermal condition.

The Figure 9.4 (k) contains the all comparative results in isothermal (C) and no isothermal (V) condition of the reactor diameter at $Dr=1$ m without and with baffles within tubular reactor. In no isothermal condition the curves V0-d1 and V6-d1 have higher conversion than the three curves in isothermal condition.



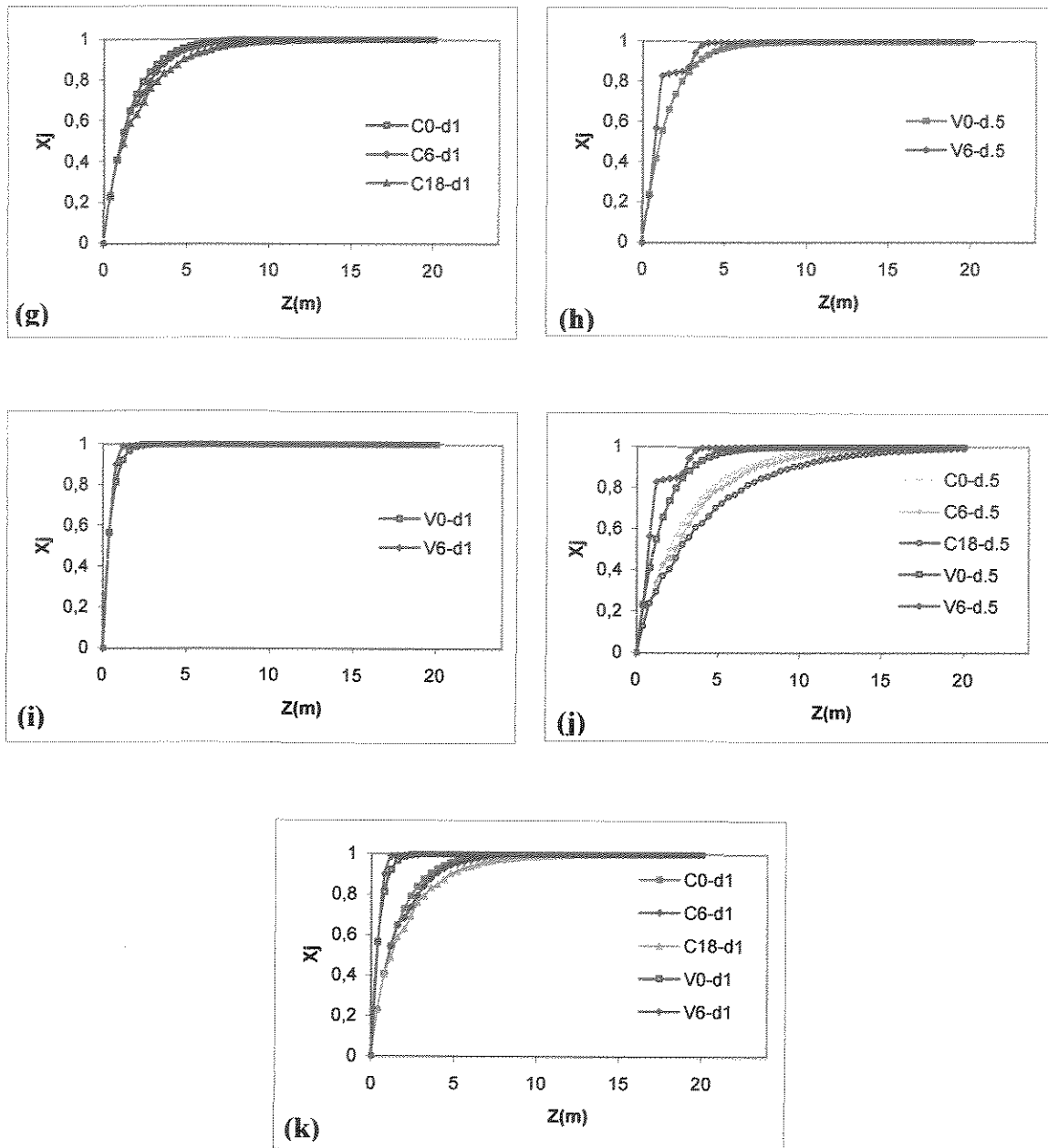


Figure 9.4 Conversion of monomer with diameter of tubular reactor of 0,5 and 1 m without ($N_b=0$) and with ($N_b=6, 18$) baffles.

In isothermal condition the conversion at reactor diameter $D_r=1$ m without $N_b=0$ or with $N_b=6$, 18 baffles are higher than the conversion with reactor diameter $D_r=0,5$ m. In no isothermal condition the conversion with $D_r=1$ m without $N_b=0$ or with $N_b=6$ baffles are higher than the conversion at $D_r=0,5$ m. In general the conversion obtained to $D_r=1$ m is higher than conversion obtained to $D_r=0,5$ m. In isothermal condition when increases the baffles number in reactor, the conversion decrease as shown in Figures 9.4 (f) and (g). In general with variable reaction temperature inside tubular reactor at $D_r=0,5$ m or $D_r=1$ m, the conversions are higher than constant reaction temperature. Therefore the reactor diameter and baffles number inside tubular reactor have influence in the emulsion polymerization process of styrene.

9.2.2 Internal transversal area

The comparative results of internal transversal area (A_z) in isothermal (C) and no isothermal (V) condition between reactor diameter at $D_r=0,5$ m and $D_r=1$ m, respectively versus length of tubular reactor (Z) are shown in Figure 9.5. The transversal areas were obtained without and with baffles inside tubular reactor. The temperature varies inside tubular reactor in exothermic and adiabatic of emulsion polymerization process of styrene.

The Figure 9.5 (a) has the comparative results of transversal area at diameter of $D_r=0,5$ m ($N_b0-d.5$) and $D_r=1$ m (N_b0-d1) without baffles into tubular reactor. Both curves have same behavior. The transversal area to $D_r=1$ m is greater than transversal area to $D_r=0,5$ m.

The Figure 9.5 (b) exposes the comparative results of transversal area at $D_r=0,5$ m ($N_b6-d.5$) and $D_r=1$ m (N_b6-d1) with $N_b=6$ baffles within tubular reactor. Both curves have same behavior. The transversal area to $D_r=1$ m is greater than transversal area to $D_r=0,5$ m.

The Figure 9.5 (c) expounds the comparative results of transversal area at $D_r=0,5$ m ($N_b18-d.5$) and $D_r=1$ m (N_b18-d1) with $N_b=18$ baffles in tubular reactor. Both curves have same behavior. The transversal area to $D_r=1$ m is greater than transversal area to $D_r=0,5$ m.

The Figure 9.5 (d) shows all results of the comparative distribution of transversal area with reactor diameter at $D_r=0,5$ m with $N_b=0$, 6, and 18 baffles in tubular reactor, $N_b0-d.5$, $N_b6-d.5$, and $N_b18-d.5$, respectively. They have same behavior, except the curve $N_b0-d.5$ is straight line path.

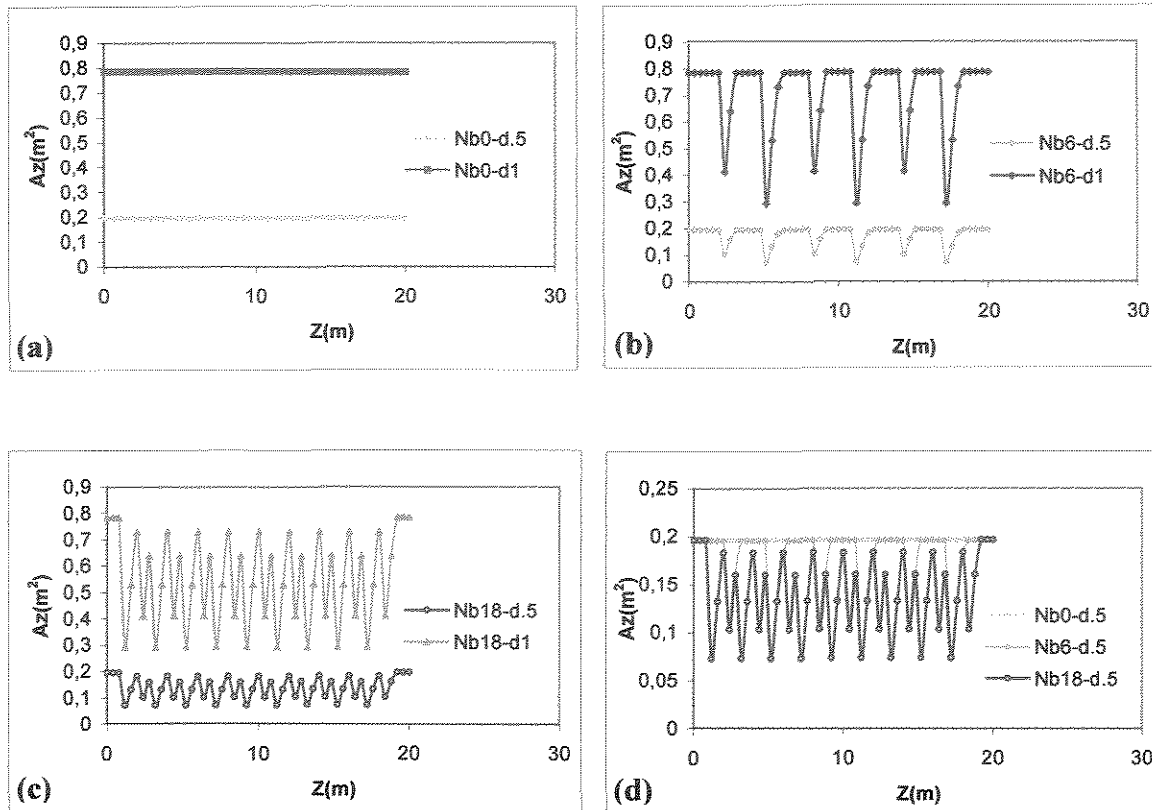


Figure 9.5 Internal transversal area with diameter of tubular reactor of 0,5 and 1 m without ($Nb=0$) and with ($Nb=6, 18$) baffles.

Then the transversal area with reactor diameter to $Dr=1$ m is greater than the transversal area with reactor diameter to $Dr=0,5$ m. The trajectory of the curves with $Nb=0, 6, \text{ or } 18$ baffles prove the location and baffles number inside tubular reactor.

9.2.3 Axial velocity

The comparative results of axial velocity (V_z) in isothermal (C) and no isothermal (V) condition at reactor diameter $Dr=0,5$ m and $Dr=1$ m, respectively versus length of tubular reactor (Z) are shown in Figure 9.6. The axial velocities were obtained without and with baffles inside tubular reactor. The temperature varies inside tubular reactor in exothermic and adiabatic of emulsion polymerization process of styrene.

The Figure 9.6 (a)-(b) expose the comparative results of axial velocity in isothermal (C) and no isothermal (V) condition with diameter at $Dr=0,5$ m (C0-d.5) and (V0-d.5) and $Dr=1$ m (C0-d1) and (V0-d1), respectively without baffles into tubular reactor. Both figures

have same behavior, but the curve C0-d.5 has different path than the curve C0-d1. The axial velocity in variable temperature to $Dr=0,5$ m or $Dr=1$ m is greater than axial velocity to $Dr=0,5$ m or $Dr=1$ m.

The Figure 9.6 (c) exhibits the comparative results of axial velocity in isothermal condition at $Dr=0,5$ m (C0-d.5) and $Dr=1$ m (C0-d1) without baffles within tubular reactor. Both curves have same behavior. The axial velocity to $Dr=0,5$ m is greater than axial velocity to $Dr=1$ m.

The Figure 9.6 (d) expounds the comparative results of axial velocity in isothermal condition at $Dr=0,5$ m (C6-d.5) and $Dr=1$ m (C6-d1) with $Nb=6$ baffles in tubular reactor. Both curves have same behavior. The axial velocity to $Dr=0,5$ m is greater than axial velocity to $Dr=1$ m.

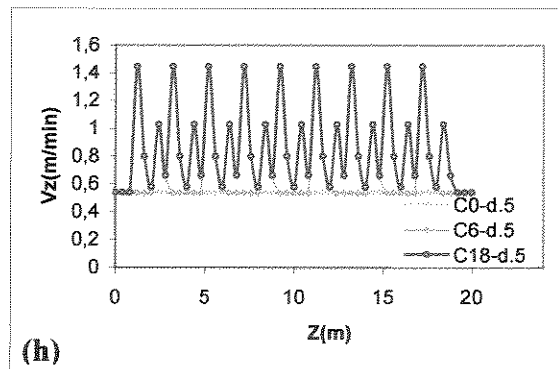
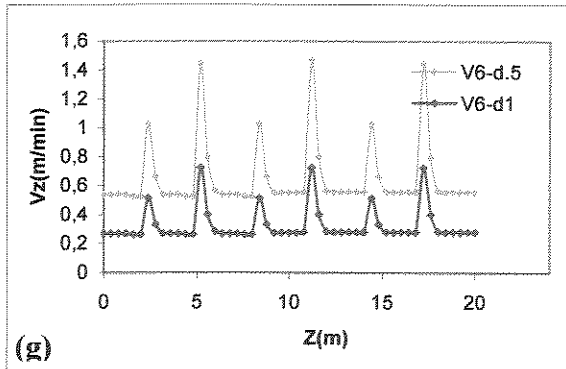
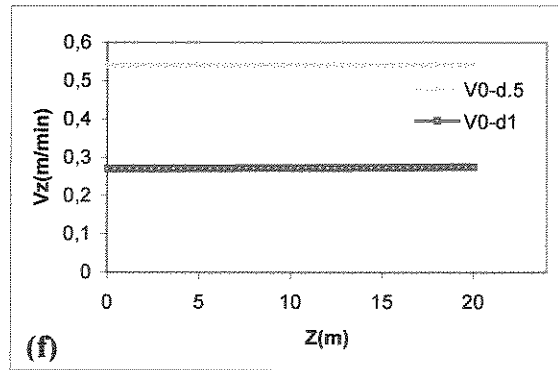
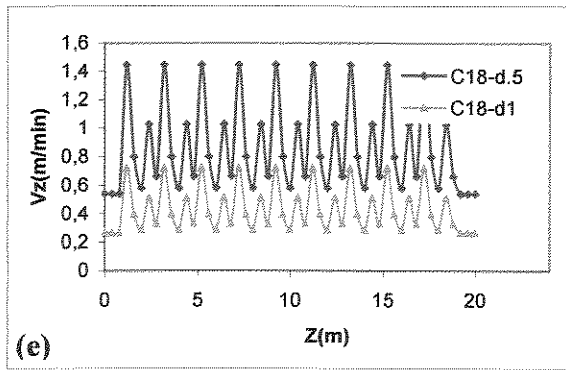
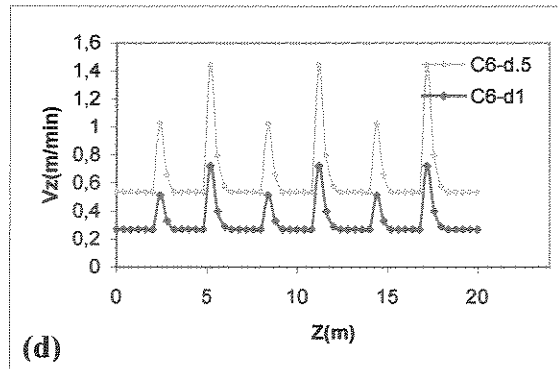
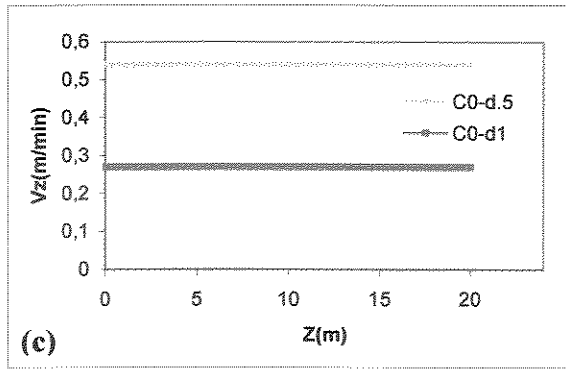
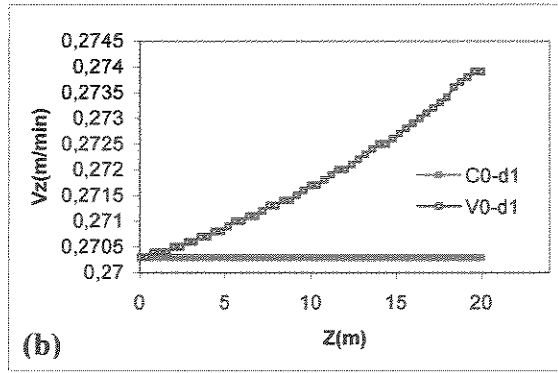
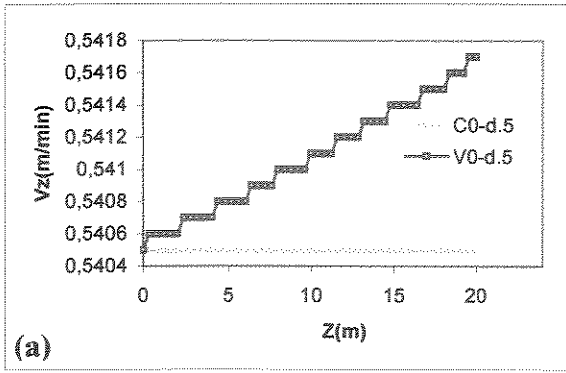
The Figure 9.6 (e) presents the comparative results of axial velocity in isothermal condition at $Dr=0,5$ m (C18-d.5) and $Dr=1$ m (C18-d1) with $Nb=18$ baffles into tubular reactor. The axial velocity to $Dr=0,5$ m is greater than axial velocity to $Dr=1$ m.

The Figure 9.6 (f) contains the comparative results of axial velocity in no isothermal condition at $Dr=0,5$ m (V0-d.5) and $Dr=1$ m (V0-d1) without baffles into tubular reactor. Both curves have same behavior and they are straight line. The axial velocity to $Dr=0,5$ m is greater than axial velocity to $Dr=1$ m.

The Figure 9.6 (g) expounds the comparative results of axial velocity in no isothermal condition at $Dr=0,5$ m (V6-d.5) and $Dr=1$ m (V6-d1) with $Nb=6$ baffles in tubular reactor. Both curves have same behavior. The axial velocity at $Dr=0,5$ m is greater than axial velocity at $Dr=1$ m.

The Figure 9.6 (h) exhibits the comparative results of axial velocity (V_z) in isothermal condition (C) at $Dr=0,5$ m without baffles (C0-d.5) and with $Nb=6, 18$ baffles (C6-d.5, C18-d.5) into tubular reactor. The curves C6-d.5 and C18-d.5 have same path, but the curve C0-d.5 is straight line.

The Figure 9.6 (i) exhibits the comparative results of axial velocity (V_z) in isothermal condition (C) at $Dr=1$ m without baffles (C0-d1) and with $Nb=6, 18$ baffles (C6-d1, C18-d1) into tubular reactor. The curves C6-d1 and C18-d1 have same trajectory, and the curve C0-d1 appears as straight line.



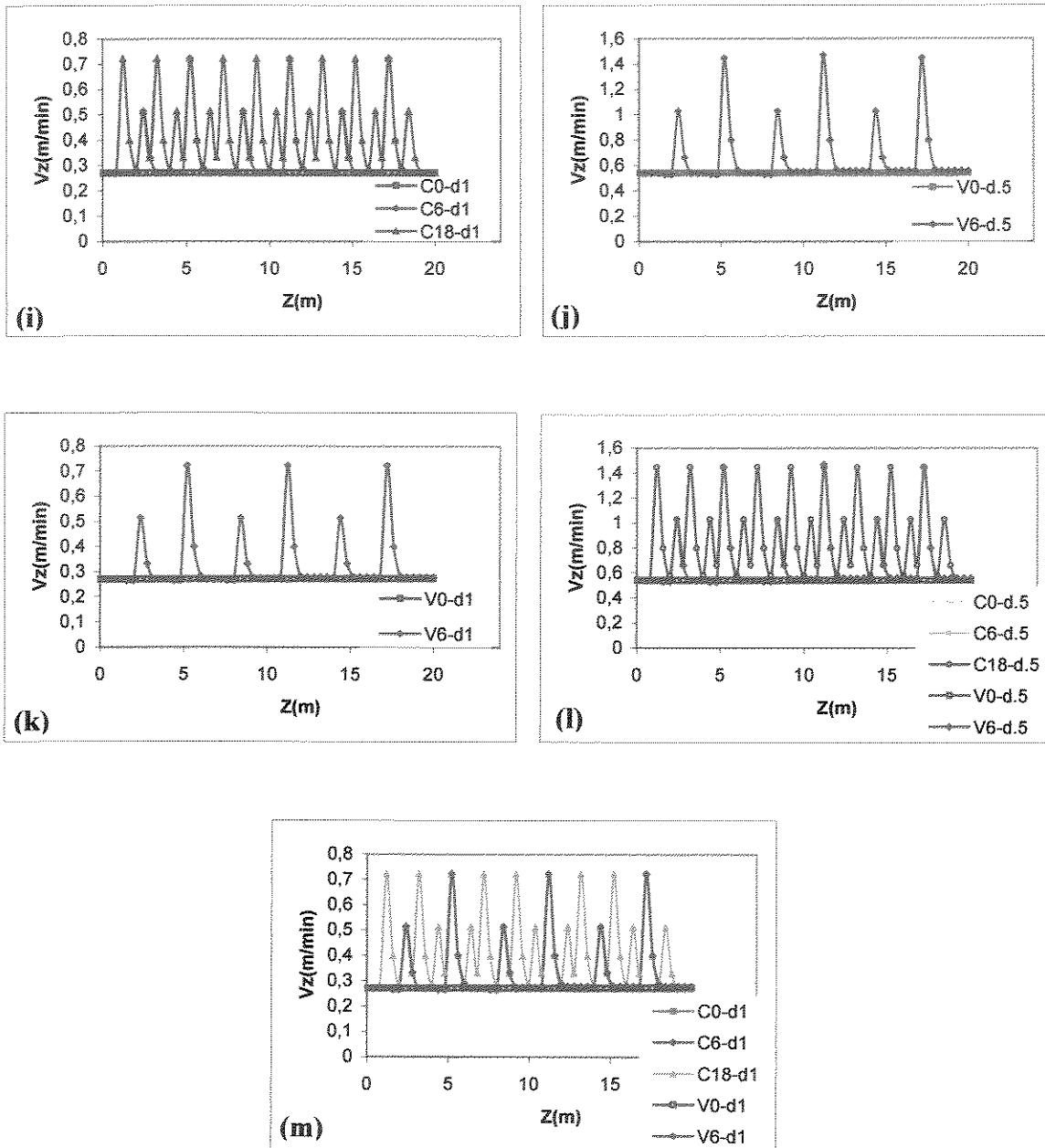


Figure 9.6 Axial velocity with diameter of tubular reactor of 0,5 and 1 m without ($Nb=0$) and with ($Nb=6, 18$) baffles.

The Figure 9.6 (j) presents the comparative results of axial velocity (V_z) in no isothermal condition (V) at $Dr=0,5$ m without baffles (V0-d.5) and with $Nb=6$ baffles (V6-d.5) into tubular reactor. The curve V0-d.5 appears as straight line, but its real curve is in Figure 9.6 (a).

The Figure 9.6 (k) shows the comparative results of axial velocity (V_z) in no isothermal condition (V) at $Dr=1$ m without baffles (V0-d1) and with $Nb=6$ baffles (V6-d1) into tubular reactor. The curve V0-d1 appears as straight line, but its real curve is in Figure 9.6 (b).

The Figure 9.6 (l) shows all comparative results of axial velocity (V_z) in isothermal (C) and no isothermal (V) condition at $Dr=0,5$ m without and with baffles within tubular reactor. The curves C0-d.5 and V0-d.5 appear as straight line, but in the case of the curve V0-d.5 its real paths is in Figure 9.2 (a).

The Figure 9.6 (m) expounds all comparative results of axial velocity (V_z) in isothermal (C) and no isothermal (V) condition at $Dr=1$ m without and with baffles within tubular reactor. The curves C0-d1 and V0-d1 appear as straight line, but in the case of the curve V0-d1 its real paths is in Figure 9.2 (b).

Then the axial velocity with reactor diameter at $Dr=0,5$ m is greater than the axial velocity with reactor diameter at $Dr=1$ m. The trajectories of the curves in constant or variable reaction temperature into reactor with baffles describe same path. The trajectories of the curves in no isothermal condition without baffles suffer the temperature effect, such as Figures 9.6 (a) and (b). Therefore the trajectories of the curves in isothermal or no isothermal condition with baffles show the location and baffles number inside tubular reactor.

9.2.4 Number of particles

The comparative results of the particles number (N_p) in isothermal (C) and no isothermal (V) condition at reactor diameter $Dr=0,5$ m and $Dr=1$ m, respectively versus length of tubular reactor (Z) are shown in Figure 9.7. The particles number were obtained without and with baffles inside tubular reactor. The temperature varies inside tubular reactor in exothermic and adiabatic of emulsion polymerization process of styrene.

The Figure 9.7 (a) presents the comparative results of the particles number in isothermal condition with reactor diameter at $Dr=0,5$ m (C0-d.5) and $Dr=1$ m (C0-d1) without baffles into tubular reactor. Both figures have same behavior. The particles number to $Dr=1$ m is greater than particles number to $Dr=0,5$ m.

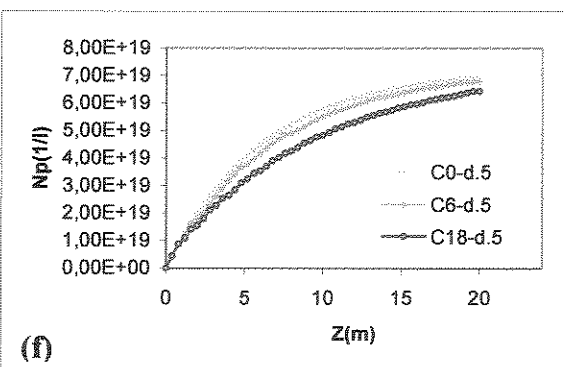
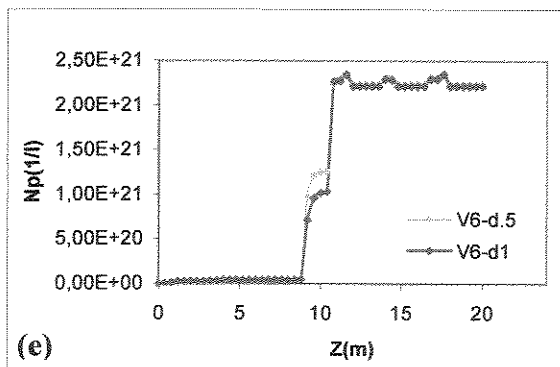
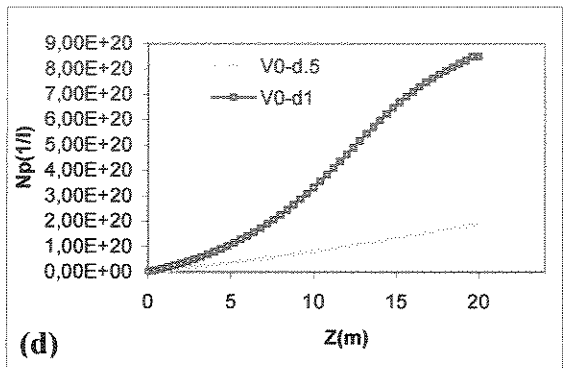
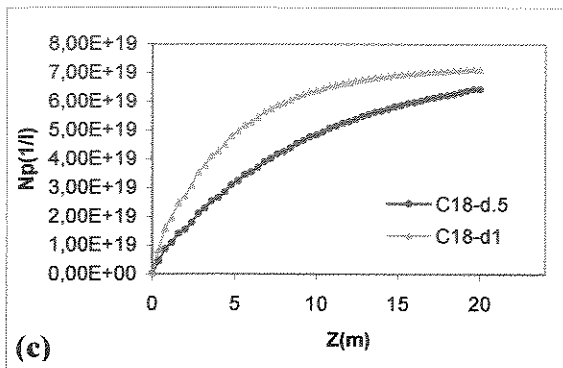
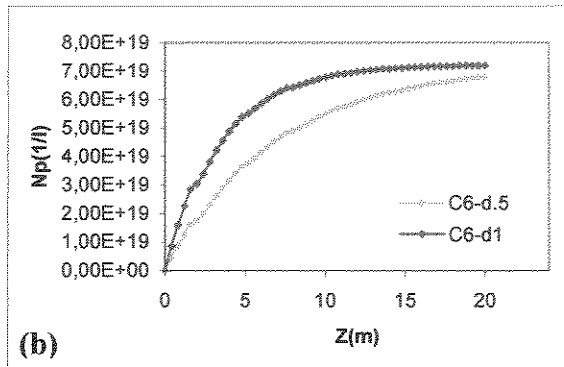
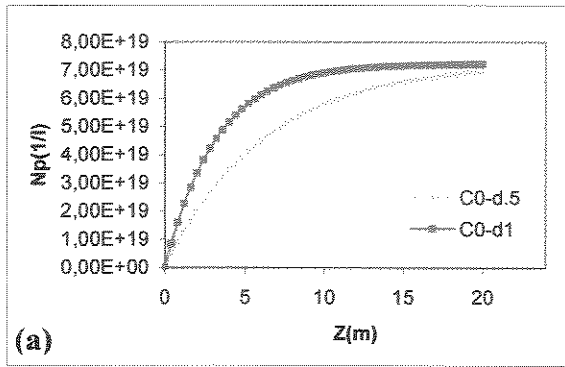
The Figure 9.7 (b) exhibits the comparative results of the particles number in isothermal condition at $Dr=0,5$ m (C6-d.5) and $Dr=1$ m (C6-d1) with $Nb=6$ baffles within tubular reactor. Both curves have same behavior. The particles number at $Dr=1$ m is greater than particles number at $Dr=0,5$ m.

The Figure 9.7 (c) expounds the comparative results of the particles number in isothermal condition at $Dr=0,5$ m (C18-d.5) and $Dr=1$ m (C18-d1) with $Nb=18$ baffles in tubular reactor. Both curves have same behavior. The particles number to $Dr=1$ m is greater than axial velocity to $Dr=0,5$ m.

The Figure 9.7 (d) presents the comparative results of the particles number in no isothermal condition at $Dr=0,5$ m (V0-d.5) and $Dr=1$ m (V0-d1) without baffles into tubular reactor. The particles number to $Dr=1$ m is greater than particles number to $Dr=0,5$ m. The curve V0-d.5 has different path that the curve V0-d1. The curve V0-d.5 is straight line, but the curve V0-d1 is not straight line.

The Figure 9.7 (e) contains the comparative results of the particles number in no isothermal condition at $Dr=0,5$ m (V6-d.5) and $Dr=1$ m (V6-d1) with $Nb=6$ baffles into tubular reactor. In general, both curves have same behavior, but the curve V6-d.5 has slight difference. The particles number to $Dr=0,5$ m is slightly higher than particles number to $Dr=1$ m.

The Figure 9.7 (f) presents the comparative results of the particles number in isothermal condition (C) at $Dr=0,5$ m without baffles (C0-d.5) and with $Nb=6, 18$ baffles (C6-d.5, C18-d.5) into tubular reactor. The three curves have same behavior. The curve C0-d.5 has higher particle number than the curves C6-d.5 and C18-d.5. When increase the baffles number, the particle number decreases.



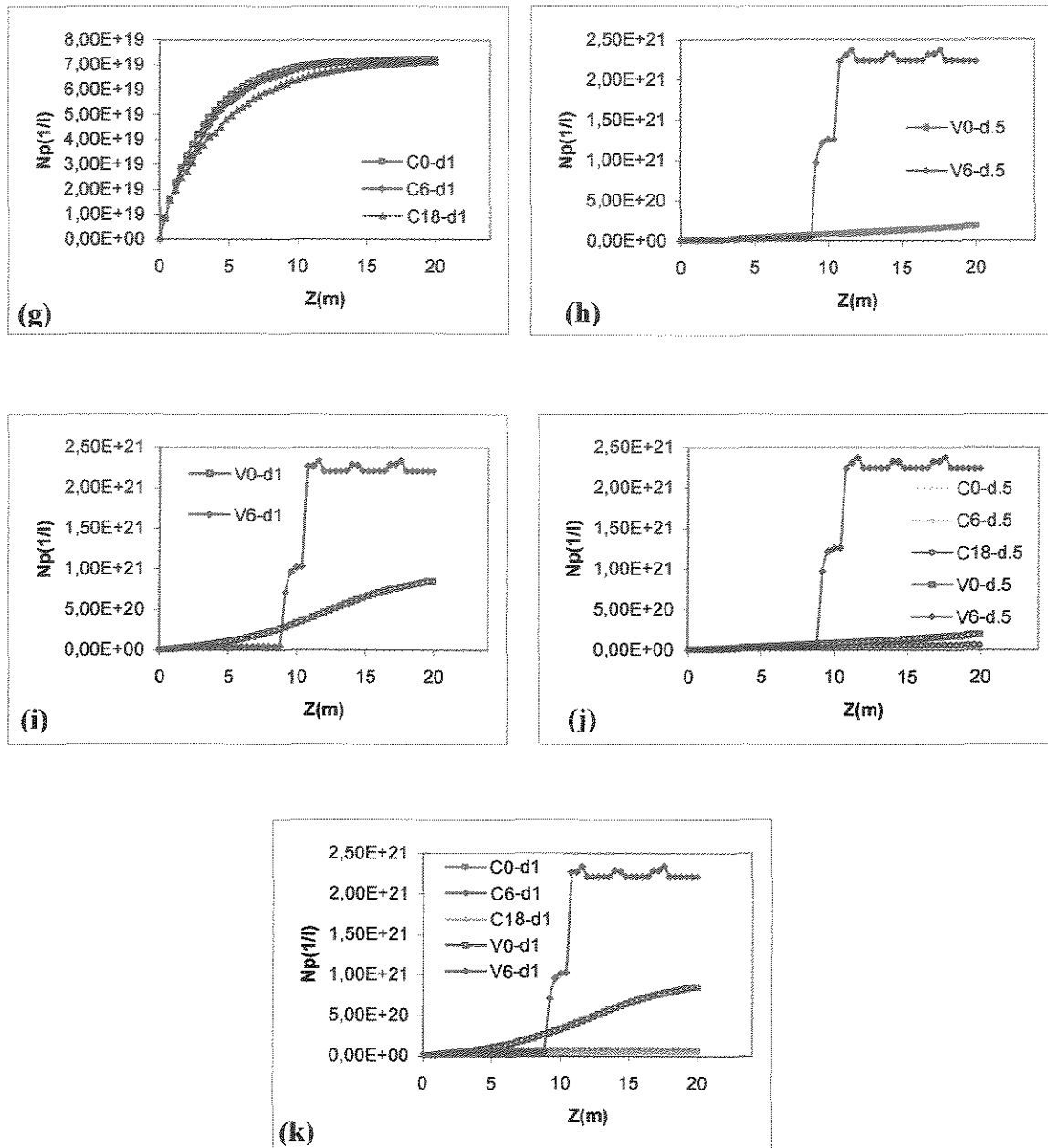


Figure 9.7 Number of particles with diameter of tubular reactor of 0,5 and 1 m without ($Nb=0$) and with ($Nb=6, 18$) baffles.

The Figure 9.7 (g) exhibits the comparative results of the particles number in isothermal condition (C) at $Dr=1$ m without baffles (C0-d1) and with $Nb=6, 18$ baffles (C6-d1, C18-d1) into tubular reactor. The three curves have same behavior. The curve C0-d1 has higher particle number than the curves C6-d1 and C18-d1. When increase the baffles number, the particle number decreases.

The Figure 9.7 (h) presents the comparative results of the particles number in no isothermal condition (V) at $Dr=0,5$ m without baffles (V0-d.5) and with $Nb=6$ baffles (V6-d.5) into tubular reactor. The two curves have different behaviors. The curve V6-d.5 has higher particle number than the curves V0-d.5.

The Figure 9.7 (i) exhibits the comparative results of the particles number in no isothermal condition (V) at $Dr=1$ m without baffles (V0-d1) and with $Nb=6$ baffles (V6-d1) into tubular reactor. The curve V6-d1 has higher particles number than the curves V0-d1.

The Figure 9.7 (j) shows all comparative results of the particles number in isothermal (C) and no isothermal (V) condition at $Dr=0,5$ m without and with baffles within tubular reactor. In no isothermal condition the curves V0-d.5 and V6-d.5 have higher particles number than the three curves in isothermal condition.

The Figure 9.7 (k) contains all comparative results of the particles number in isothermal (C) and no isothermal (V) condition at $Dr=1$ m without and with baffles within tubular reactor. In no isothermal condition the curves V0-d1 and V6-d1 have higher particles number than the three curves in isothermal condition.

Then the particles number with reactor diameter to $Dr=1$ m is greater than the particles number with reactor diameter to $Dr=0,5$ m. In isothermal condition at $Dr=0,5$ m or $Dr=1$ m when increase the baffles number into reactor, the particles number decrease, Figures 9.7 (f), (g), respectively. In no isothermal condition at $Dr=0,5$ m or $Dr=1$ m when increase the baffles number inside tubular reactor, the curves V6-d.5 or V6-d1 have different results that isothermal condition as shown in Figures 9.7 (h) and (i), respectively. The trajectory of the curves in isothermal or no isothermal condition in general would have different source effects, such as, variable temperature, reactor diameter, location and baffles number inside tubular reactor as shown in Figures 9.7 (j) and (k), respectively.

9.3 NUMBER OF BAFFLES INSIDE TUBULAR REACTOR

The baffles number effect within tubular reactor will be analyzed, this analysis will be made by means of monomer conversion, internal transversal area, axial velocity, temperature distribution, polymer concentration, radicals concentration, initiator concentration, particles number, molecular weight distribution, polymer particles size, density of polymer and monomer, head loss and pressure drop. The analysis take in it count the feed temperature (T_f), constant or variable reaction temperature ($T_r=C$ or V), diameter of the reactor (D_r), and baffles number (N_b).

9.3.1 Conversion of Monomer

9.3.1.1 Simulation to $T_f=60^\circ\text{C}$, $T_r=C$ and V , $D_r=1$ m, $N_b=6$ and 18

The variation of the baffles number in isothermal and no isothermal condition are presented in Figures 7.6 (d), (e) and (f). When the baffles number increase in reactor, the monomer conversion almost no change as shown in Figure 7.6 (d). Now in the Figure 7.6 (f) the monomer conversion with variable reaction temperature is higher than constant reaction temperature.

9.3.1.2 Simulation to $T_f=90^\circ\text{C}$, $T_r=C$ and V , $D_r=1$ m, $N_b=6$ and 18

The variation of the baffles number in isothermal and no isothermal condition are shown in Figures 9.1 (g) and (h). When the baffles number increase in reactor, the monomer conversion is almost the same as shown in Figure 9.1 (f). Then the Figure 9.1 (h) presents similar conversions in constant reaction temperature when increase the baffles number in reactor, but in variable reaction temperature there is a increment in conversion when increases the baffles number.

9.3.1.3 Simulation to $T_f=60^\circ\text{C}$, $T_r=C$ and V , $D_r=0,5$ m, $N_b=6$ and 18

The variation of baffles number in isothermal and no isothermal condition are depicted in Figures 9.4 (f), (h) and (j). When the baffles number increase in reactor, the monomer conversion diminishes as shown in Figure 9.4 (f). While the Figure 9.4 (h) shows different performance, the increment of the baffles number exhibits opposite results. Now in the Figure 9.4 (j) the monomer conversion with variable reaction temperature is higher than constant reaction temperature.

9.3.2 Internal Transversal Area

9.3.2.1 Simulation to $T_f=60$ or 90°C , $T_r=C$ or V , $D_r=1$ m, $N_b=6$ and 18

The variation of the baffles number in reactor is shown in Figure 7.7 (d). When the baffles number increases in reactor, the paths present more points as geometric effects when the baffles number diminishes within reactor. Then when increases the baffles number inside reactor, the geometric effects could affect in the process of emulsion polymerization.

9.3.2.2 Simulation to $T_f=60$ or 90°C , $T_r=C$ or V , $D_r=0,5$ m, $N_b=6$ and 18

The variation of the baffles number in reactor is shown in Figure 9.5 (d). When the baffles number increase present more points as geometric effects when the baffles number diminishes within reactor. Then when increases the baffles number inside reactor, the geometric effects could affect in the process of emulsion polymerization.

The Figure 7.7 (d) and Figure 9.5 (d) show same performance, but the internal transversal varies between $0,2934-0,785$ m² and $0,0733-0,1963$ m², respectively.

9.3.3 Axial Velocity

9.3.3.1 Simulation to $T_f=60^\circ\text{C}$, $T_r=C$ and V , $D_r=1$ m, $N_b=6$ and 18

The variation of the baffles number in reactor are shown in Figures 7.8 (d), (e) and (f). When the baffles number increase in axial coordinate, the distribution of the velocity in axial direction has uniform tendency as baffles number exist into reactor, they can be observed in the Figures 7.8 (d), (e) and (f).

9.3.3.2 Simulation to $T_f=90^\circ\text{C}$, $T_r=C$ and V , $D_r=1$ m, $N_b=6$ and 18

The variation of the baffles number inside tubular reactor are exhibited in Figures 9.2 (g), (h) and (i). In all previously cited figures the distribution of the velocity is according to the baffles number inside tubular reactor.

9.3.3.3 Simulation to $T_f=60^\circ\text{C}$, $T_r=C$ and V , $D_r=0,5$ m, $N_b=6$ and 18

The variation of the baffles number into tubular reactor are presented in Figures 9.6 (h), (j) and (l). These figures confirm the results of the Figures 7.8 (d), (e), (f) and Figures 9.2 (g), (h), (i). Where the baffles number inside tubular reactor determine the distribution

of the axial velocity. The trajectory of the velocities are according to the baffles number within reactor.

9.3.4 Axial Temperature Distribution

The comparative results of the variation of the baffles number inside tubular reactor is shown in Figure 7.9 (c). The simulation conditions were the feed temperature, 60°C, diameter of the reactor, 1 m, and without or with baffles. The curve V6 shows augment of temperature in axial direction. Then when increase the baffles number in reactor, the axial temperature exhibits the tendency to the augment.

9.3.5 Concentration of Polymer

The variation of the baffles number in isothermal and no isothermal condition are presented in Figures 7.10 (d), (e), (f). The some simulation conditions were the feed temperature, 60°C, reactor diameter, 1 m, and baffles number of 6 and 18. In Figure 7.10 (d) when the baffles number increase in reactor, the concentration of polystyrene diminishes. Now in the Figure 7.10 (f) the concentration of polystyrene with variable reaction temperature is higher than constant reaction temperature.

9.3.6 Concentration of Radicals

The variation of the baffles number in isothermal and no isothermal condition are shown in Figures 7.11 (d), (e), (f). The simulation conditions were the feed temperature, 60°C, diameter of the reactor, 1 m, and baffles number of 6 and 18. In the Figure 7.11 (d) when the baffles number increase in reactor, the concentration of radicals slightly diminishes. Now in the Figure 7.11 (f) the concentration of radicals with variable reaction temperature is higher than constant reaction temperature.

9.3.7 Concentration of Initiator

The variation of the baffles number in isothermal and no isothermal condition are stated in Figures 7.12 (d), (e), (f). The simulation conditions were the feed temperature, 60°C, diameter of the reactor, 1 m, and baffles number of 6 and 18. In the Figure 7.12 (d) when the baffles number increase in reactor, the concentration of initiator diminishes slightly its consumption. The concentration of initiator in curve V6 is consumed faster than in curve V0. Now in the Figure 7.12 (f) the concentration of initiator with variable

temperature (V6) decrease almost all its concentration that in constant temperature decrease a little (C6, C18).

9.3.8 Number of Particles

9.3.8.1 Simulation to $T_f=60^\circ\text{C}$, $T_r=C$ and V , $D_r=1$ m, $N_b=6$ and 18

The variation of the baffles number in isothermal and no isothermal condition are exposed in Figures 7.13 (d), (e), (f). In the Figure 7.13 (d) when the baffles number increase in reactor, the particles number diminish. While the Figure 7.13 (e) shows different performance, the increment of the baffles number exhibits opposite results. Now in the Figure 7.13 (f) the particles number with variable temperature is higher than constant temperature.

9.3.8.2 Simulation to $T_f=90^\circ\text{C}$, $T_r=C$ and V , $D_r=1$ m, $N_b=6$ and 18

The variation of the baffles number in isothermal and no isothermal condition are shown in Figures 9.3 (f), (g), (h). When the baffles number increase in reactor, the particles number slightly diminishes as shown in Figure 9.3 (f). As long as the Figure 9.3 (g) exhibits opposite results when baffles number increase. Then the Figure 9.3 (h) presents a tendency of reduction of the particles number in constant reaction temperature and augment in variable reaction temperature when increase the baffles number in reactor.

9.3.8.3 Simulation to $T_f=60^\circ\text{C}$, $T_r=C$ and V , $D_r=0,5$ m, $N_b=6$ and 18

The variation of baffles number in isothermal and no isothermal condition are presented in Figures 9.7 (g), (i), (k). When the baffles number increase in reactor, the particles number somewhat diminish as shown in Figure 9.7 (g). While the Figure 9.7 (i) shows different performance, the increment of the baffles number exhibits opposite results. Now in the Figure 9.7 (j) the particles number with variable reaction temperature is higher than constant reaction temperature.

9.3.9 Molecular Weight Distribution

The variation of the baffles number in isothermal and no isothermal condition are shown in Figures 7.15 and 7.16. The simulation conditions were the feed temperature, 60°C , diameter of the reactor, 1 m, and baffles number of 6 and 18. These figures have average molecular weight, polydispersity, mole fraction and weight fraction. The

comparison of the Figures 7.15 (a)-7.16 (a), 7.15 (c)-7.16 (b), 7.15 (e)-7.16 (c), and 7.15 (g)-7.16 (d) present same performance, however the variation of the results can be different a little. With reference to the comparison of the Figures 7.14 (b)-7.15 (b), 7.14 (d)-7.15 (d), 7.14 (f)-7.15 (f), and 7.14 (h)-7.15 (h) show different performance. Moreover the average molecular weight and polydispersity are pretty different, the polydispersity is almost uniform when increase the baffles number in variable temperature.

9.3.10 Size of Polymer Particles

The variation of the baffles number in isothermal and no isothermal condition are exhibited in Figures 7.17 (f), (g), (h). The simulation conditions were the feed temperature, 60°C, diameter of the reactor, 1 m, and baffles number of 6 and 18. In the Figure 7.17 (f) when the baffles number increase in reactor, the particle number slightly diminishes its size. While the Figure 7.17 (g) shows different performance, the increment of the baffles number exhibits opposite results. Now in the Figure 7.17 (h) the size of polymer particle with variable reaction temperature are less high than constant reaction temperature.

9.3.11 Viscosity Distribution

The variation of the baffles number in isothermal and no isothermal condition are shown in Figures 7.18 (b)-(c), (d)-(e). The simulation conditions were the feed temperature, 60°C, diameter of the reactor, 1 m, and baffles number of 6 and 18. In the Figures 7.18 (b)-(c) when the baffles number increase in reactor, the viscosity distribution show same distribution. While in the Figures 7.18 (d)-(e) expose different behavior, these figures show that when increase the baffles number the viscosity is constant and diminish.

9.3.12 Density of Polymer And Monomer

The comparative results of the variation of the baffles number inside tubular reactor are shown in Figures 7.19 (c), (d). The simulation conditions were the feed temperature, 60°C, diameter of the reactor, 1 m, and baffles number of 6 and 18. When the baffles number increase the wide of the curves of polymer and monomer present some diminution in the Figures 7.19 (c) and (d), respectively.

9.3.13 Head loss

The variation of the baffles number in isothermal and no isothermal condition are shown in Figures 7.20 (d), (e), (f). The simulation conditions were the feed temperature, 60°C, diameter of the reactor, 1 m, and baffles number of 6 and 18. In the Figure 7.20 (d) when the baffles number increase in reactor, the head loss increase its values according to the baffles number, before situation is equal in the Figure 7.20 (e). Now in the Figure 7.20 (f) the head loss with variable temperature is slightly less than the constant temperature, therefore the head loss receives the effects of the baffles number and temperature.

9.3.14 Pressure Drop

The variation of the baffles number in isothermal and no isothermal condition are exhibited in Figures 7.21 (d), (e), (f). The simulation conditions were the feed temperature, 60°C, diameter of the reactor, 1 m, and baffles number of 6 and 18. In the Figure 7.21 (d) when the baffles number increase in reactor, the pressure drop increase its values according to the baffles number, before situation is equal in the Figure 7.21 (e). Now in the Figure 7.21 (f) the pressure drop with variable temperature is slightly lower than constant temperature. Therefore the pressure drop receives the effects of the baffles number and temperature.

RESUMO DO CAPÍTULO X

MENDOZA MARÍN, F.L. *Modelagem, simulação e análise de desempenho de reatores tubulares de polimerização com deflectores angulares internos*, 241p. Tese (Doutorado em Engenharia Química – Área de Processos Químicos) – Faculdade de Engenharia Química, Universidade Estadual de Campinas - UNICAMP, 2004.

O Capítulo X representa a discussão dos resultados da presente tese em forma comparativa sem e com chicanas dentro do reator tubular em condições isotérmicas e não isotérmicas. O Capítulo X é importante porque permite examinar e obter algumas explicações e conclusões sobre o tema investigado como o comportamento das simulações para um melhor e seguro escalonamento a outras condições operacionais. Os objetivos do Capítulo X são: examinar os resultados de simulação sem e com chicanas dentro do reator tubular e em condições isotérmicas e não isotérmicas.

Conclusão do Capítulo X: No Capítulo X foram apresentados as análises globais de todos os resultados de simulação segundo os diferentes condições aplicados na presente tese. A análise apresenta-se em três situações: reator tubular sem chicanas, reator tubular com chicanas e o reator tubular em condições isotérmicas e não isotérmicas. Em cada caso foram discutidos os resultados mais significativos e essenciais que permitiram diferenciar o comportamento do reator em diferentes condições como temperatura de reação constante e variável, reator tubular sem e com chicanas, temperatura de alimentação, diâmetro do reator, receita, processo adiabático, reação exotérmica, calor de reação constante e velocidade completamente desenvolvido; também obter conclusões sobre modelagem, o método numérico aplicado, os algoritmos dos programas em Fortran e a presença das chicanas. O Capítulo X ressalta o comportamento do reator tubular em relação as características essenciais do fenômeno investigado.

obtained for constant temperature (C0). According to the Figures 9.1 (a) and (d) the conversion with feed temperature at 90°C is larger than the conversion with feed temperature at 60°C in constant or variable reaction temperature as expected. Moreover in the Figure 9.1 (h) the monomer conversion with variable reaction temperature (V0-90) is slightly larger than that for constant reaction temperature (C0-90). In agreement with the Figures 9.4 (a) and (d) the monomer conversion at reactor diameter of $Dr=1$ m is larger than the conversion at reactor diameter of $Dr=0,5$ m, for both in isothermal and no isothermal condition, respectively. As can be seen in Figure 9.4 (j) the monomer conversion with variable reaction temperature (V0-d.5) is larger than the monomer conversion for constant reaction temperature (C0-d.5). Then the monomer conversion with variable reaction temperature is larger than the monomer conversion at constant reaction temperature for the feed temperature as well as for the reactor diameter that were used in this work.

The simulation results of *internal transversal area* (A_z) in different conditions versus along the reactor length (Z) are exhibited in Figures 7.7 and 9.5. In the Figure 7.7 (a) the internal transversal area is constant. According to the Figure 9.5 (a) it is possible to observe that the internal transversal area is constant for reactor diameter at $Dr=0,5$ m (Nb0-d.5) or $Dr=1$ m (Nb0-d1). The internal transversal area has effect in the emulsion polymerization process of styrene.

The simulation results of the *axial velocity* (V_z) in different conditions along the reactor length (Z) are exposed in Figures 7.8, 9.2 and 9.6. In the Figure 7.8 (a) the axial velocity (C0) is constant when the reaction temperature is constant, this condition was used as developed flow for the tubular reactor without baffles. In the same Figure 7.8 (a) it can be seen that the axial velocity (V0) increases for variable reaction temperature. The Figure 9.2 (a) gives same behavior that the Figure 7.8 (a), but with feed temperature at 90°C. It can be noted in Figure 9.2 (b) that the axial velocity (C0-90) with feed temperature to 90°C is larger than the axial velocity (C0-60) with feed temperature at 60°C. As can be seen in Figure 9.2 (e), the axial velocity increases with feed temperature at 60°C or 90°C. Now the Figure 9.6 (a) presents the same behavior than the Figures 9.2 (a) and 7.8 (a), but with reactor diameter at $Dr=0,5$ m. In Figure 9.6 (c) is shown the same behavior than the Figure 9.2 (b), but with reactor diameter of $Dr=0,5$ and $Dr=1$ m. Other Figure 9.6 (f) presents constant axial velocities along the axis z . Therefore the axial velocity with variable reaction

temperature is higher than the axial velocity for constant reaction temperature. The axial velocity suffer the geometric and temperature effects too.

The predictions results of the *axial temperature distribution* (T) in different conditions along the reactor length (Z) are depicted in Figure 7.9. The axial temperature (V0) is variable along the axis z as may be seen from Figure 7.9. The axial temperature varies in exothermic and adiabatic process and density of polymer and monomer is allowed to change. With reference to the Figure 7.9 (c) the axial temperature was compared for others results, where axial temperature without baffles (V0) is higher than isothermal condition (C). Then according to the exothermic reaction and adiabatic process and variable density of polymer and monomer, The axial temperature distribution varies inside the tubular reactor according to the exothermic reaction and adiabatic process.

The simulation results of the *concentration of polystyrene* (CPs) in different conditions along the reactor length (Z) are expounded in Figure 7.10. The concentration of polystyrene in variable reaction temperature (V0) is higher than the concentration of polystyrene for constant reaction temperature (C0) as shown in Figure 7.10 (a). The concentration of polystyrene in constant or variable reaction temperature is exhibited as a base to compare to others results as shown in Figures 7.10 (d), (e) and (f). And these results are due to the temperature effect.

The simulation results of the *radical concentrations* (CRw) in different conditions along the reactor length (Z) are exposed in Figure 7.11. The concentration of radicals in variable reaction temperature (V0) is the higher than the concentration of radicals in constant reaction temperature (C0) as shown in Figure 7.11 (a). Therefore the concentration of radicals in variable reaction temperature is larger than in constant reaction temperature, this result is due to the temperature effect.

The simulation results of the *concentration of initiator* (CI) in different conditions along the reactor length (Z) are presented in Figure 7.12. The concentration of initiator in variable reaction temperature (V0) is consumed quicker than the concentration of initiator in constant reaction temperature (C0) as shown in Figure 7.12 (a). Therefore the concentration of initiator in variable reaction temperature is larger than in constant reaction temperature, this result could be by the temperature effect.

The simulation results of the *particles number* (N_p) in different conditions along the reactor length (Z) are shown in Figures 7.13, 9.3 and 9.7. According to the Figure 7.13 (a) can be observed that the particles number for variable reaction temperature (V0) is higher than to constant reaction temperature (C0). Moreover in the Figures 7.13 (d), (e) and (f) the particles number in constant or variable reaction temperature is shown as a base to compare whit others results. In Figures 9.3 (a) and (d) it is clear that the particles number with feed temperature to 90°C is higher than the conversion with feed temperature to 60°C in constant or variable reaction temperature. Another Figures 9.3 (f), (g) and (h) contain the particles number as a base to compare with other results. While in the Figure 9.3 (i) the particles number with variable reaction temperature (V0-90) is the higher than to constant reaction temperature (C0-90) beneath feed temperature to 90°C. As far as the diameter reactor is concerned the Figures 9.7 (a) and (d) the particles number at reactor diameter $D_r=1$ m is higher than the conversion at reactor diameter $D_r=0,5$ m, both in isothermal and no isothermal condition, respectively. With reference to the Figures 9.7 (f), (g), (h), (i), (j) and (k) the particles number in isothermal and no isothermal condition are plotted as base of comparison. Looking at Figure 9.7 (j), it can be observed that the number of particle with variable reaction temperature (V0-d.5) is higher than the particles number in constant reaction temperature (C0-d.5). Then the particles number with variable reaction temperature is higher than the particles number in constant reaction temperature at feed temperature or reactor diameter simulated.

The simulation results of the *molecular weight distribution* in different conditions of average molecular weight and polydispersity versus monomer conversion (X_j), mole (X_{pi}) and weight (W_{pi}) fraction versus chain size of the polymer (i) are shown in Figure 7.14. With references to the Figures 7.14 (a) and (b) indicate that the number average molecular (M_nC0) and the weight average molecular (M_wC0) in isothermal condition are different to the number average molecular (M_nV0) and the weight average molecular (M_wV0) for the no isothermal condition. On the other hand it can be observed that the polydispersity has same behavior, but the point upon the curves are different as shown in Figures 7.14 (c) and (d). The geometric chain length distribution normalized or mole fraction in no isothermic condition has better chain distribution than mole fraction for isothermic condition as shown in Figures 7.14 (e) and (f). Concerning to the Figures 7.14 (g) and (h) the molecular weight distribution normalized or weight fraction in no isothermic

condition presents closer chain distribution than the weight fraction in isothermic condition. Therefore the molecular weight distribution improves with variable reaction temperature for the tubular reactor. Also the polydispersity in variable reaction temperature is more uniform for high conversions of monomer which are obtained for non isothermal conditions.

The simulation results of the *polymer particles size* for different conditions along the reactor length (Z) are shown in Figure 7.17. The unswollen polymer particles size in variable reaction temperature (V0) are smaller than the unswollen polymer particles size for constant reaction temperature (C0) as shown in Figure 7.17 (c). In relation to the can be observed that The polymer particles size in isothermal and no isothermal condition were plotted (Figures 7.17 (f), (g) and (h)) as a base to compare with others results as baffled tubular reactor. Therefore the polymer particles size diminishes when the reactor was submitted to variable reaction temperature. Then the variable reaction temperature inside the tubular reactor has effect in the size of polymer particles with opposite results to the concentration of monomer, axial velocity, axial temperature, concentration of polymer, concentration of radicals, and molecular weight distribution.

The simulation results of *viscosity distribution* in different conditions versus monomer conversion (X_j) are exposed in Figure 7.18. The viscosity distribution in variable reaction temperature (V0) decreases when compared to constant reaction temperature (C0) as shown in the Figures 7.18 (d) and (a), respectively. The viscosity is maintained almost constant from the inlet to 3 m long of the tubular reactor in variable reaction temperature as shown in Figure 7.18 (b), but the viscosity distribution for constant reaction temperature increases from inlet up to reactor exit, as shown in Figure 7.18 (a). Therefore the viscosity for variable reaction temperature is less than the viscosity for constant reaction temperature and the variable reaction temperature has effect at the viscosity distribution.

The simulation results of the *density of polymer and monomer* in different conditions versus axial temperature (T) are shown in Figure 7.19. Both the density of polystyrene (PV0) and monomer styrene (MV0) decrease from feed until reactor outlet in adiabatic process. This reduction is uniform along side tubular reactor as shown in Figure 7.19 (b). Therefore, the density of polymer and monomer decrease with variable reaction temperature.

The simulation results of the *head loss* (H_f) for different conditions along the reactor length (Z) are presented in Figure 7.20. The head loss in variable reaction temperature (V0) is the higher than the head loss in constant reaction temperature (C0) as shown in Figure 7.20 (a). The head loss at constant or variable reaction temperature is exhibited as a base to compare with others results as shown in Figures 7.20 (d), (e) and (f).

The simulation results of the *pressure drop* (ΔPr) in different conditions along the reactor length (Z) are shown in Figure 7.21. The pressure drop for variable reaction temperature (V0) is higher than the pressure drop for constant reaction temperature (C0) as shown in Figure 7.21 (a). Therefore the pressure drop in variable reaction temperature is larger than in constant reaction temperature, this result could be by the axial velocity and axial temperature effect.

10.2 TUBULAR REACTOR WITH BAFFLES

The simulation results of the *monomer conversion* (X_j) in different conditions along the reactor length (Z) are displayed in Figures 7.6, 9.1 and 9.4. For isothermic condition when the baffles number increase in reactor, the monomer conversion diminishes as shown in Figure 7.6 (d). While the Figure 7.6 (e) shows different performance in no isothermic condition, the increment of the baffles number exhibits opposite results. Looking at the Figure 7.6 (f) the monomer conversion with variable reaction temperature is higher than for constant reaction temperature. According to the Figure 9.1 (f) when the baffles number increase in isothermic condition, the monomer conversion slightly diminishes. As long as the Figure 9.1 (g) exhibits opposite results when baffles number increase in no isothermic condition. Concerning to the Figure 9.1 (h) it can be seen a tendency of the conversion decrease for constant reaction temperature when increase the baffles number in the reactor. In isothermic condition and reactor diameter of $D_r=0,5$ m when the baffles number increase, the monomer conversion diminishes as shown in Figure 9.4 (f). On the other hand the Figure 9.4 (h) shows different performance for no isothermic condition and reactor diameter at $D_r=0,5$ m. Whilst in the Figure 9.4 (j) the monomer conversion with variable reaction temperature is higher than constant reaction temperature. Then the monomer conversion for constant reaction temperature diminishes when the baffles number increase.

The predictions results for *internal transversal area* (A_z) in different conditions along the reactor length (Z) are exhibited in Figures 7.7 and 9.5. In agreement with the Figure 7.7 (d) when the baffles number increase in reactor, the paths present more points as geometric effects that when the baffles number diminishes. This same effect can be observed in Figure 9.5 (d) at reactor diameter $D_r=0,5$ m. In fact the internal transversal area is a geometric fact that affects in the emulsion polymerization process.

The simulation results of the *axial velocity* (V_z) in different conditions along the reactor length (Z) are shown in Figures 7.8, 9.2 and 9.6. When the baffles number increase, the distribution of the velocity in axial direction has a tendency to be uniform as depicted in Figures 7.8 (d), (e) and (f). In all previously cited figures the distribution of the velocity is according to the baffles number; these same results are shown in Figures 9.2 (g), (h) and (i) and Figures 9.6 (h), (j) and (l). Therefore the baffles number determine the distribution and trajectory of the axial velocity within tubular reactor. Moreover the axial velocity suffer the effects of the baffles number, reactor geometric (diameter), feed temperature, and axial variable reaction temperature.

The simulation results of the *axial temperature distribution* (T) in different conditions along the reactor length (Z) are revealed in Figure 7.9. When the baffles number increase the curves V_6 increases in quantity in axial direction as shown in Figure 7.9 (b), (c). This behavior is by the augment from fully developed and diminution until fully developed of the axial velocity beneath or over baffles as shown for example in Figure 7.8. The position of internal transversal area inside the tubular reactor has effect in reactant mix as shown in Figure 7.7. The localization of axial velocity and position of transversal area has effect until half reactor in axial temperature distribution, after the increment of the temperature give constant monomer conversion as shown e.g. Figure 7.6 in variable reaction temperature. Then when increase the baffles number, the axial temperature exhibits the tendency to increase due to better mix and heat transfer condition.

The simulation results of the *concentration of polystyrene* (CPs) in different conditions along the reactor length (Z) are shown in Figure 7.10. In isothermic condition when the baffles number increases, the concentration of polystyrene decreases as shown in Figure 7.10 (d). While the Figure 7.10 (e) presents different performance in no isothermic condition, the increment of the baffles number leads to opposite results. The concentration of polystyrene with variable reaction temperature (Figure 7.10 (f)) is higher than constant

reaction temperature. The concentration of polystyrene decreases when the baffles number increase inside reactor in isothermal, but in no isothermal condition show opposite results. Therefore the concentration of polystyrene suffers the effects of the baffles number, and the axial variable reaction temperature.

The simulation results of the *concentration of radicals* (CR_w) in different conditions along the reactor length (Z) are exposed in Figure 7.11. In isothermic condition when the baffles number increase into reactor, the concentration of radicals slightly diminishes as shown in Figure 7.11 (d). According to the Figure 7.11 (e) shows different performance in no isothermic condition, the increment of the baffles number exhibits opposite results, the curve V6 has the highest concentration of radicals from the half of the reactor. In agreement with the Figure 7.11 (f) the concentration of radicals with variable temperature is higher than constant temperature. Then the concentration of radicals diminishes when the baffles number increase in isothermal condition, but the curve V6 increases the radicals. Therefore the concentration of radicals suffers the effects of the baffles number, and the axial variable reaction temperature.

The simulation results of the *concentration of initiator* (CI) in different conditions along the reactor length (Z) are presented in Figure 7.12. In isothermic condition when the baffles number increase in reactor, the concentration of initiator diminishes slightly its consumption as shown in Figure 7.12 (d). But the Figure 7.12 (e) shows different performance, the increment of the baffles number exhibits opposite results, the curve V6 is consumed very quick. With regard to the Figure 7.12 (f) the concentration of initiator with variable temperature (V6) decrease almost all that the constant temperature decrease a little (C6, C18). Then the concentration of initiator is consumed less when the baffles number increase in isothermal condition, but the curve V6 is consumed very quick. Therefore the concentration of initiator suffers the effects of the baffles number, and the axial variable reaction temperature.

The predictions results of the *particles number* (N_p) in different conditions along the reactor length (Z) are shown in Figures 7.13, 9.3 and 9.7. In isothermic condition when the baffles number increase in reactor, the particles number diminish as shown in Figure 7.13 (d). According to the Figure 7.13 (e) shows different performance, the increment of the baffles number exhibits opposite results. As for the Figure 7.13 (f) the particles number with variable temperature (V6) is higher than constant temperature (C6, C18). In isothermic

condition at feed temperature 90°C when the baffles number increase in reactor, the particles number slightly diminishes as shown in Figure 9.3 (f). As long as the Figure 9.3 (g) exhibits opposite results when baffles number increase in no isothermic condition at feed temperature 90°C . Now the Figure 9.3 (h) presents a tendency of reduction of the particles number in constant temperature, but in variable temperature shows opposite results when increase the baffles number. On the other hand in isothermic condition at reactor diameter $D_r=0,5$ m when the baffles number increase in reactor, the particles number somewhat diminish as shown in Figure 9.7 (f). While the Figure 9.7 (h) shows different performance in no isothermic condition at reactor diameter $D_r=0,5$ m, the increment of the baffles number exhibits opposite results. According to the Figure 9.7 (l) the particles number with variable reaction temperature is higher than constant reaction temperature. Then the particles number in variable reaction temperature (V6-d.5) is higher than the particles number in constant reaction temperature (C6-d.5, C18-d.5). Therefore the particles number suffers the effects of the baffles number, reactor geometric (diameter), the feed temperature, and the axial variable reaction temperature.

The predictions results of the *molecular weight distribution* in different conditions of average molecular weight and polydispersity versus monomer conversion (X_j), and mole (X_{pi}) and weight (W_{pi}) fraction versus chain size of the polymer (i) are shown in Figures 7.15 and 7.16. The comparison of the Figures 7.15 (a)-7.16 (a), 7.15 (c)-7.16 (b), 7.15 (e)-7.16 (c), and 7.15 (g)-7.16 (d) present same performance, however the variation of the results can be different a little. With reference to the comparison of the Figures 7.14 (b)-7.15 (b), 7.14 (d)-7.15 (d), 7.14 (f)-7.15 (f), and 7.14 (h)-7.15 (h) show different performance. Moreover the average molecular weight and polydispersity are pretty different, the polydispersity is almost uniform when increase the baffles number in variable reaction temperature. Then the number and weight molecular improve its distribution, the polydispersity is more uniform, the mole and weight fraction improve its distribution when the baffles number increase inside the tubular reactor. Therefore the molecular weight distribution suffers the effects of the baffles number, and the axial variable reaction temperature.

The simulation results of the *polymer particles size* in different conditions along the reactor length (Z) are shown in Figure 7.17. In isothermic condition when the baffles number increase in reactor, the particle number slightly diminishes its size as shown in

Figure 7.17 (f). Now the Figure 7.17 (g) shows different performance in no isothermic condition, the increment of the baffles number exhibits opposite results. But in the Figure 7.17 (h) the size of polymer particle with variable reaction temperature are less high than the polymer particles size in constant reaction temperature. Then the polymer particle size diminishes when the baffles number increase into reactor. Therefore the polymer particle size suffers the effects of the baffles number, and the axial variable reaction temperature.

The simulation results of *viscosity distribution* in different conditions versus monomer conversion (X_j) are exposed in Figure 7.18. In isothermic condition when the baffles number increase in reactor, the viscosity distribution show same distribution as shown in Figures 7.18 (b)-(c). While in the Figures 7.18 (d)-(e) expose different behavior in no isothermic condition, these figures show that when increase the baffles number the viscosity is constant and diminish. Then the viscosity in variable reaction temperature decrease when the baffles number increase inside the tubular reactor. Therefore the viscosity distribution suffers the effects of the baffles number, and axial variable reaction temperature.

The simulation results of the *density of polymer and monomer* in different conditions versus axial temperature (T) are expounded in Figure 7.19. When the baffles number increase the wide of the curves of polymer and monomer present some diminution in the Figures 7.19 (c) and (d), respectively, because the density of monomer increase its slightly values. Then the distribution of points over the trajectories of the density of polymer and monomer can be observed that are different when the baffles number increase into reactor. Therefore the density of polymer and monomer suffer the effects of the baffles number, and axial variable reaction temperature.

The simulation results of the *head loss* (H_f) in different conditions along the reactor length (Z) are presented in Figure 7.20. In isothermic condition when the baffles number increase in reactor, the head loss increase its values according to the baffles number as shown in Figure 7.20 (d), before situation is equal in the Figure 7.20 (e). But in the Figure 7.20 (f) the head loss with variable temperature is slightly less than the constant temperature. Then head loss varies according to the location and baffles number inside the tubular reactor. Therefore the head loss receives the effects of the baffles number, internal angle baffle, baffle length, baffle separation, baffle location and axial variable temperature.

The simulation results of the *pressure drop* (ΔPr) in different conditions along the reactor length (Z) are shown in Figure 7.21. In isothermic condition when the baffles number increase in reactor, the frictional pressure drop increase its values according to the baffles number as shown in Figure 7.21 (d), before situation is equal in the Figure 7.21 (e). Now in the Figure 7.21 (f) the frictional pressure drop with variable temperature is slightly less than constant temperature. Then the frictional pressure drop varies according to the location and baffles number within tubular reactor. Therefore the pressure drop receives the effect of the baffles number, internal angle baffle, baffle length, baffle separation, baffle location and axial variable temperature.

10.3 ISOTHERMAL AND NO ISOTHERMAL TUBULAR REACTOR

The results in isothermal and no isothermal condition without and with baffles inside the tubular reactor with different performance and the causes such as the constant reaction temperature, variable reaction temperature, tubular reactor without baffles, tubular reactor with baffles, feed temperature, tubular reactor diameter, recipe, adiabatic process, reaction heat, exothermic reaction and fully developed velocity at reactor inlet are shown in Figures 7.6-7.8, 7.13, 9.1-9.7. They influence in the reactor performance and the emulsion polymerization process of styrene. But the recipe, adiabatic process, reaction heat, exothermic reaction and fully developed velocity at reactor inlet are maintained constants in the present thesis.

The Figure 7.6 (f) shows that the conversions of monomer in no isothermic condition are higher than the conversion in isothermic condition without and/or with baffles inside the tubular reactor for conditions of exothermic, adiabatic, variable density and others approximations. One can extend the before results when is simulated at feed temperature 90°C as shown in Figure 9.1, and at reactor diameter 0,5 m as shown in Figure 9.4.

The Figure 7.13 (f) show that the particles number in no isothermic condition are larger than the particles number in isothermic condition without and/or with baffles inside the tubular reactor for conditions of exothermic, adiabatic, variable density, and others approximations. One can extend the before results when is simulated at feed temperature 90°C as shown in Figure 9.3, and at reactor diameter 0,5 m as shown in Figure 9.7.

In reference to the internal transversal area as shown in Figures 7.7 and 9.5 and axial velocity as shown in Figures 7.8, 9.2 and 9.6 vary according to the position and baffles number inside the tubular reactor. In isothermic and no isothermic condition will be supposed that the internal transversal area will not suffer any dilation without or with baffles inside the tubular reactor. The axial velocities in no isothermic condition are higher than the axial velocity in isothermic condition without and/or with baffles inside the tubular reactor.

The Table 10.1 shows a results resume of the constant reaction temperature (CRT) and the variable reaction temperature (VRT) of emulsion polymerization process of styrene without and with baffles inside polymerization tubular reactor. The conversion and particles number in variable reaction temperature show different performance that in constant reaction temperature with baffles. On the other hand reactor without baffles are validated with analytical (our results), experimental (literature) and simulation (literature) results as described in Chapter VIII, they are concordant.

Table 10.1 The conversion and particles number in constant and variable reaction temperature.

EFFECT		CRT		VRT	
		Nb=0	Nb=6, 18	Nb=0	Nb=6
Xj	Tf=60°C, Dr=1 m	Similar the Fig. 7.6 (a, d, f) to Fig. 8.1 (c, d), Fig.8.2 (a).	Diminish Fig. 7.6 (b, c, d, f).	Similar the Fig. 7.6 (a, e, f) to Fig. 8.1 (c, d), Fig.8.2 (a).	Augment V6 Fig. 7.6 (b, e, f).
	Tf=90°C, Dr=1 m	Similar the Fig. 9.1 (a, g, i) to our results Fig. 7.6: Tf=60°C, Dr=1 m.	Diminish Fig. 9.1 (b, c, g, i).	Similar the Fig. 9.1 (d, h, i) to our results Fig. 7.6: Tf=60°C, Dr=1 m.	Augment V6 Fig. 9.1 (e, g, h).
	Tf=60°C, Dr=0,5 m	Similar the Fig. 9.4 (a, g, k) to our results Fig. 7.6: Tf=60°C, Dr=1 m.	Diminish Fig. 9.4 (b, c, g, k).	Similar the Fig. 9.4 (d, e, k) to our results Fig. 7.6: Tf=60°C, Dr=1 m.	Augment V6 Fig. 9.4 (e, h, j).
Np	Tf=60°C, Dr=1 m	Similar the Fig. 7.13 (a, d, f) to Fig. 8.4 (a).	Diminish Fig. 7.13 (b, c, d, f).	Similar the Fig. 7.13 (a, e, f) to Fig. 8.4 (a).	Augment V6 Fig. 7.13 (b, e, f).
	Tf=90°C, Dr=1 m	Similar the Fig. 9.3 (a, g, i) to our results Fig. 7.13: Tf=60°C, Dr=1 m.	Diminish Fig. 9.3 (b, c, g, i).	Similar the Fig. 9.3 (d, h, i) to our results Fig. 7.13: Tf=60°C, Dr=1 m.	Augment V6 Fig. 9.3 (e, g, h).
	Tf=60°C, Dr=0,5 m	Similar the Fig. 9.7 (a, g, k) to our results Fig. 7.13: Tf=60°C, Dr=1 m.	Diminish Fig. 9.7 (b, c, g, k).	Similar the Fig. 9.7 (d, e, k) to our results Fig. 7.13: Tf=60°C, Dr=1 m.	Augment V6 Fig. 9.7 (e, h, j).

In reference to the others results such as the axial temperature, concentration of polymer, concentration of radicals, concentration of initiator, head loss, and pressure drop at feed temperature 90°C and reactor diameter $D_r=0,5$ m could have same performance that the monomer conversion (X_j) and particles number (N_p) present in Table 10.1. In particular molecular weight distribution, size of polymer particle, viscosity distribution, and variable density of polymer and monomer could have different performance as described in Sections 7.10, 7.11, 7.12, and 7.14.1, respectively. Regarding molecular weight distribution in variable reaction temperature is better its distribution that in constant reaction temperature as shown in Figures 7.14, 7.15 and 7.16. As for size of polymer particle in variable or constant reaction temperature diminishes its size until uniform distribution as shown in Figure 7.17. As to viscosity distribution in variable reaction temperature diminishes its viscosity as shown in Figure 7.18. According to density of polymer and monomer in variable reaction temperature diminishes both densities as shown in Figure 7.19.

CONCLUSIONS

The results found in the thesis reveal the following:

The mathematical models that describe all the obtained results appear to be suitable for the research objectives. The simulations showed good concordance with analytical and experimental results of the literature in isothermic and no isothermic condition, without baffles. For the case with baffles the data were available.

The finite volume method have been applied successful. It allowed to reproduce the analytical and experimental results. It showed to be a robust method with conservativeness, boundedness, and transportiveness of the fluid flow of emulsion polymerization process of styrene at isothermic and no isothermic condition, without and with baffles inside tubular reactor.

The numerical method algorithm was developed based on the cause-effect and antecedent-consequence procedure, and as mentioned it worked well for all the considered situation.

The model equation were based on mass, momentum and energy conservation principles, coupled with the rate of emulsion polymerization for the styrene. They were developed for the reactor tubular without and with baffles. The propose design showed to be more suitable to achieve better product characterization number of particles, molecular weight distribution, size of polymer particles, and viscosity distribution at isothermic condition. The same may be said for the reactor under non isothermic conditions when compared with the isothermal ones.

SUGGESTIONS

In order to continue this research, a just point could be to work out on the approximations considered in this thesis, in such way to allow more complete process description. Among them could be mentioned to increase the model dimensionality (since only one dimensional approach was adopted), take into account the dynamics and do not assume fully developed laminar flow.

An interesting analysis to be made is that related to the impact of the baffles geometry, baffle inclination and size as well as the baffles arrangements. Also the reactor behavior is important to have a general idea of this alternative design. Some possible arrangements are proposed in Figures I (a), (b) and (c).

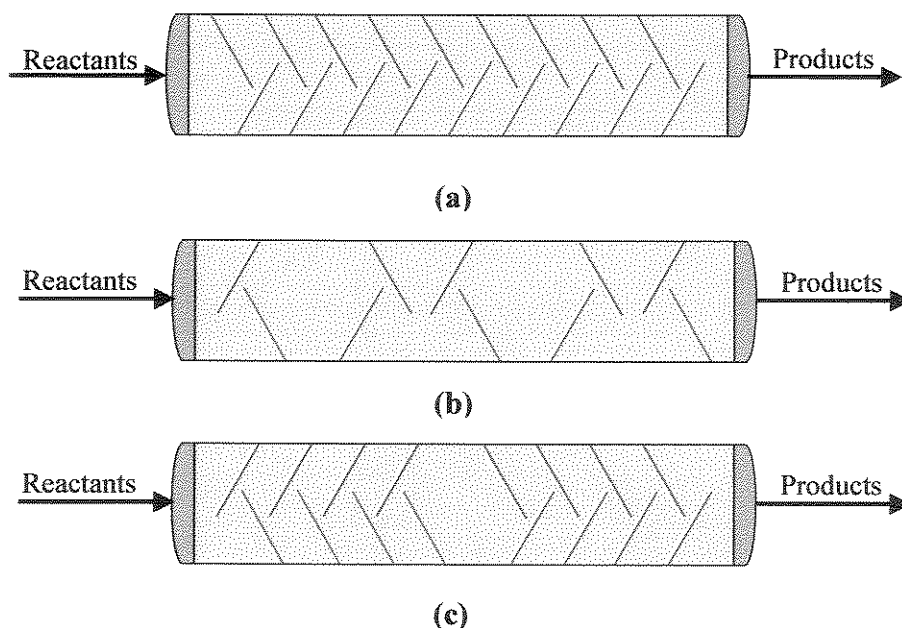


Figure I Angle baffles arrangement inside tubular reactor with mix arrangement (symmetric and asymmetric).

BIBLIOGRAPHY

AGARWAL, S.S. AND KLEINSTREUR, C. Analysis of styrene polymerization in a continuous flow tubular reactor. *Chemical Engineering Science*, vol.41, 12, 3101-3110, 1986.

ALAMDARI, F., EDWARDS, S.C., AND HAMMOND, S.P., Microclimate Performance of an open atrium office building: The Institution of Mechanical Engineers, London, p.81, 1991.

ANDERSON, J.D.Jr., *Fundamentals of Aerodynamics*, 2nd Edition McGraw-Hill, New York, 1991.

APOSTOL, T.M.; *Calculus Vol. I*; 2nd Ed.; John Wiley & Sons; N.Y., USA.; 1967.

ASTARITA, G. *Mass Transfer with Chemical Reaction*, Elsevier, Amsterdam, 1967.

ASUA, J.M., De La Cal, J.C., Entry and Exit rate coefficients in emulsion polymerization of styrene. *J. Appl Polym. Sci.*, 42, 1869-77, 1991.

AZEVEDO, S.F., ROMERO-OGAWA, M.A., WARDLE, A.P., Modeling of Tubular Fixed Bed Catalytic Reactors; A Brief Review, *Chemical Engineering Research and Design*, 68(A6), 483-502, 1990.

BAI, X.S., AND FUCHS, L., Numerical Model for Turbulent Diffusion flames with applications. In "Computational Fluid Dynamics" (C. Hirsch, J. Periaux and W. Kordulla, eds.). Elsevier, Amsterdam, vol.1, p=169, 1992.

BARRET, K.E.J. *Dispersion polymerization in organic media*. New York: Wiley, 1975.

BASSET, D. AND HAMIELEC, A. E.; *Emulsion Polymer and Emulsion Polymerization*; ACS Symp. Series No.165, The American Chemical Society, Washington, D.C., 1981.

BATAILE, P., VAN, B.T. and PHAM, Q.B.; *Emulsion Polymerization of Styrene. I. Review of Experimental Data and Digital Simulation*; *Journal of Polymer Science: Polymer Chemistry Edition*, Vol.20, 795-810 (1982).

BATAILE, P. and GONZALEZ, A.; *Emulsion Polymerization of Styrene. III. Effect of Ti(III) and Cl(1) on the Polymerization of Styrene Initiated by Potassium Persulfate*; *Journal of Polymer Science: Polymer Chemistry Edition*, Vol.22, 1409-1417 (1984).

BATAILE, F., BATAILE, P., FORTIN, R. *Emulsion Polymerization of Styrene. IV. Effect of Co(II), Ni(II) and Pb(II) on the Polymerization of Styrene Initiated by Potassium Persulfate*; *Journal of Polymer Science: Polymer Chemistry Edition*, Vol.26, 1471-7 (1988).

- BILLMEYER, F.W., Polymers, KIRK OTHMER Encyclopedia of Chemical Technology, Ed. 3ra., Vol.18, 745-755, 1982.
- BIRD, R.B., STEWART, W.E. AND LIGHTFOOT, E.N. Transport Phenomena; John Wiley-Sons, Inc.; New York; 1960.
- BLACKLEY, D.C., SEBASTIAN SARD. Influence of surfactant type and purity upon emulsion copolymerization of styrene and acrylic acid. Br. Polym. J. 19, 25-30, 1987.
- BLACKLEY, D.C. Emulsion Polymerization; Applied science; London, 1975.
- BLACKLEY, D.C., SEBASTIAN SARD. Effects of inorganic electrolytes upon emulsion polymerization reactions I. Effects upon kinetics of styrene emulsion. Br. Polym. J. 19, 313-26, 1989.
- BOCKHORN, H., Mathematical Modeling, ULLMANN'S Encyclopedia of Industrial Chemistry, Vol.B1, 2, 1992.
- BOJARINOW, A.I. AND KAFAROW, W.W. Optimierungsmethoden in der chemischen Technologie, Verlag Chemie, Weinheim, 1972.
- BOYCE, W.E. AND DI PRIMA, R.C.; Equações Diferenciais Elementares e Problemas de Valores de Contorno; 6th Ed.; Livros Técnicos e Científicos Editora, S.A.; 1997.
- BRANDRUP, J. AND IMMERGUT, E.H.; Polymer Handbook; 2th Ed.; Jonh Wiley & Sons; N.Y., USA.; 1st ed., 1966, 2nd ed., 1975, 3rd ed., 1989.
- BUCKLEY, P.S. Techniques of Process Control; Robert E. Krieger Publishing Comapny, Huntington, 1979.
- BURKHOLDER, L. A Companion to the Philosophy of Science: Computing. Blackwell Publishers Ltd; Oxford, Great Britain, 2001.
- CARBERRY, J.J., Chemical and Catalytic Reaction Engineering, McGraw-Hill, Inc., 1976.
- CANEGALLO, S., STORTI, G., MORBIDELLI, M., CARRA, S. Densimetry for on-line conversion monitoring in emulsion homo- and copolymerization. J. Appl. Polym Sci. , 47, 961-79, 1993.
- CAMPBELL, J.D., MAsC Thesis. Department of Chemical Engineering, McMaster University, 1985.
- CARNAVOS, T.C.; Cooling Air in Turbulent Flow with Internally Finned Tubes; Heat Transfer Engineering; vol.1, 2, 41-46 (1979).
- CARRAHER, Ch.E. Polymer Chemistry. Ed.4th, Marcel Dekker, Inc., N.Y., 1996.
- CEREDA, R.L.D. AND MALDONADO, J.C.; Introdução ao FORTRAN 77 para Microcomputadores; McGraw – Hill, S.P., Brasil; 1987.

CHEN, C.C. and NAUMAN, E.B.; Verification of a Complex, Variable Viscosity Model for a Tubular Polymerization Reactor; *Chemical Engineering Science*, Vol. 44, 1, 179-188 (1989).

CHEN, B.H., DAÍ, Q.L. e LU, D.W., Development and modeling a loop fluidized bed reactor with baffle for propylene ammoxidation, *Ch. Eng. Sc.*, Vol.51, 2983-2988, 1996.

CHERN, C.S., Diffusion-Controlled semibatch Emulsion Polymerization of Styrene; *Journal of Applied Polymer science*, Vol.56, 221-230 (1995).

COLENBRANDER, G.W., CFD research for the petrochemical industry. *Appl. Sci. Res.* 48, 211, 1991.

CORMICK, J.M. AND SALVADORI, M.G.; Métodos Numéricos em FORTRAN; Editora da Universidade de São Paulo, Brasil; 1971.

COULSON, J.M., RICHARDSON, J.F., BACHKURST, J.R. e HARKER, J.H., *Chemical Engineering*, Vol.6., Butterworth Heinemann, 2ed, 1997.

DAMKÖHLER, G. Einfluss von Diffusion, Strömung und Wärmetransport auf die Ausbeute bei chemischtechnischen Reaktionen, VDI Verlag, Leverkusen 1957.

DANCKWERTS, P.V., *Gas-Liquid Reactions*, McGraw Hill, London, 1970.

DAVIS, M.E.; *Numerical Methods and Modeling for Chemical Engineers*; John Wiley-Sons, Inc.; New York; 1984.

De la ROSA, L.V., SUDOL, E.D., EL-AASSER, M.S., KLEIN, A. Details of the emulsion polymerization of styrene using a reaction calorimeter. *J.Polym Sci. Chem. Part.A Polymer Chemistry*, 34, 461-73, 1996.

De SAINT VENANT, B., Note a Joindre un Mémoire sur la Dynamique des Fluides, *Comptes Rendus*, 17, 1240, 1843.

DICKINSON R.G. PhD Thesis. Department of Chemical Engineering, University of Waterloo, 1976.

DOMINGUES, A., Modelagem e Simulação de Processo de Oxidação do Etanol a Acetaldeído, Tese de Mestrado, FEQ/UNICAMP, Campinas, 1992.

DOTSON, N.A., GALVÁN, R., LAURENCE, R.L. AND TIRREL, M.; *Polymerization Process Modeling*; John Wiley-Sons, Inc.; New York; 1996.

DOUGHERTY, E.P.; The SCOPE Dynamic Model for Emulsion Polymerization I. Theory; *J. Appl. Polym. Sc.*; vol.32, 3051-3078 (1986).

ELLIS, T.M.R., PHILIPS, I.R. AND LAHEY, T.M.; *FORTRAN 90 Programming*; Addison – Wesley Published Ltd.; England; 1996.

ELIAS, H. G. *An Introduction to Plastics*. VCH Weinheim, N.Y., 1993.

- ELIAS, H. G. An Introduction to Polymer Science. VCH Weinheim, N.Y., 1997.
- FARINAS, M.I., GARON, A. e LOUIS, K.S., Study of heat transfer in a horizontal cylinder with fins, *Ver. Gen. Therm*, 36, 398-410, 1997.
- FARKAS, A., Catalysis and Catalysts, ULLMANN'S Encyclopedia of Industrial Chemistry, Vol.A5, 358-362, 1992.
- FELDON, M., MccANN, R.F. AND LAUNDRIE, R.W.; Continuous Emulsion Polymerization in a Tubular Reactor; *India Rubber World* ; 128, 1, 51, 1953.
- FERNANDEZ, F.A.N.; LONA BATISTA, L.M.F., Fluidized bed Reactor and Physical-Chemical Properties Modeling for Polyethylene Production. *Comp.Chem. Eng.*, 23,S803-S806, 1999.
- FIKENTSCHER, H.; *Angew. Chem.* 51, 433, 1938.
- FIKENTSCHER, H., GERRENS,H. AND SCHULLER, H.; *Angew. Chem.* 72, 856, 1960.
- FIKENTSCHER, H.; *Kunststoffe*, 53, 734, 1963.
- FINCH, J.A. e DOBBY, G.S., Column flotation, Pergamon Press, Oxford, 33, 1990.
- FITCH, R.M. AND TSAI, C.H.; Particle Formation in Polymer Colloids. III. Prediction of the number of particles by homogeneous nucleation theory. In: Fitch, R.M., Editor. *Polymer Colloids*. New York: Plenum Press, 73, 1971a.
- FITCH, R.M. AND TSAI, C.H; Homogeneous nucleation of polymer colloids. IV. The role of soluble oligomeric radicals. In: Fitch, R.M., Editor. *Polymer Colloids*. New York: Plenum Press, 103, 1971b.
- FITCH, R.M. Latex particle nucleation and growth. In: Basset, D.R., Hamielec, A.E., editors. *Emulsion polymers and emulsion polymerization*. Washington, D.C. : American Chemical Society, 1-29, 1981.
- FITCH, R.M.; *Polymer Colloids: A Comprehensive Introduction*; Academic Press, Inc.; 1997.
- FOGLER, H. S., *Element of Chemical Reaction Engineering*, Prentice-Hall, Inc., Englewood Cliffs, New Jersey, 1986.
- FORNEY, L.J. e NAFIA, N., Eddy contac model: CFD simulations of liquid reactions in nearly homogeneous turbulence, *Ch.Eng.Sc.*, 55,6049-6058, 2000.
- FOX, R.W. AND McDONALD, A.T. *Introdução á Mecânica dos Fluidos*. Ed.4ta, Edt. John Willey & Sons, R.J., 1992.
- FRANK-KAMENETZKI, D.A. *Diffusion and Heat Transfer in Chemical Kinetics*, 2nd ed., Plenum, New York, 1969.

- FRANKS, R.G.E; Modeling and Simulation in Chemical Engineering; John Willey & Sons, Inc.; USA; 1972.
- FROMENT, G.F. AND BISCHOFF, K.B.; Chemical Reactor Analysis and Design; Second Edition; John Willey-Sons; 1990.
- GAO, J. AND PENLIDIS, A. ; Mathematical Modeling and Computer Simulator/database for Emulsion Polymerizations; Prog. Polym. Sci. ;27, 403-535 (2002).
- GARDON J.L.; Emulsion Polymerization.I. Recalculation and extension of the Smith-Ewart theory. J. Polym. Sci. Chem. 6, 623-41, 1968a.
- GARDON J.L.; Emulsion Polymerization.II. Review of experimental data in the context of the revised Smith-Ewart theory. J. Polym. Sci. Chem. 6, 643-64, 1968b.
- GARDON J.L.; Emulsion Polymerization.III. Theoretical prediction of the effects of slow termination rate within latex particles. J. Polym. Sci. Chem. 6, 665-86, 1968c.
- GARDON J.L.; Emulsion Polymerization.IV. Concentration of monomers in latex particles. J. Polym. Sci. Chem. 6, 2859-79, 1968d.
- GERRENS, H.; Z. Elektrochem. 60, 400, 1956.
- GERRENS, H.; Ber. Bunsenges. Phys. Chem. 67, 741, 1963.
- GERRENS, HEINZ; On Semicontinuous Emulsion Polymerization; (Sty and MA) J. Polymer Sci. Part C, No.27. pp. 77-93 (1969).
- GERRENS, HEINZ; Chem. Ing. Tech. 52, 477, 1980; Chemical Engineering, 4, 1, 1981.
- GERRENS, HEINZ; Chem. Tech., 380, June, 1982; 434, July, 1982.
- GHOSH, M. and FORSYTH, T.H.; Continuous Emulsion Polymerization of Styrene in a Tubular Reactor; ACS Symp. Ser., 24, 367-378 (1976).
- GIANNETTI, E. Nucleation mechanisms and particle size distributions of polymer colloids. AIChE J. 39, 1210-27, 1993.
- GILBERT, R.G.; Emulsion Polymerization, A Mechanistic Approach; Academic Press; London; 1995.
- GONZALES, P.R.A.; M.S. Thesis, Chem. Eng. Dept., Lehigh Univ., Bethlehem, Pennsylvania, 1974.
- GOULD, L.A. Chemical Process Control; Theory and Applications, Addison-Wesley Publishing Company, Reading, 1969.
- GRADSHTEYN, I.S. AND RYZHIK, I.M.; Table of Integrals, Series, and Products; 4th Ed.; Academic Press, Inc., N.Y., 1965.

GRIFFIN, M.E., DIWAKER, R., ANDERSON, J.D., AND JONES, E., Computational Fluid Dynamics applied to flows in an internal combustion engine. AIAA 16th Aerospace Sciences Meet., paper 78-57, January, 1978.

HAMIELEC, A.E., and TOBITA, H., Polimerization Processes, ULLMANN'S Enciclopedia of Industrial Chemistry, Vol.A21, 305-428, 1992.

HAMIER, J. e SALIM, E.D., Toward steady state direct solid sample analysis by inductively coupled plasma atomic spectrometry: qualitative evaluation of Na intraplasmic powdered sample digester, Spectrochimica acta part B 53, 1303-1315, 1998.

HANDBOOK of Chemistry and Physics, David R. Lide, Edition 78th; CRC PRESS, INC, 1997-1998.

HANS-GEORG, E. An Introduction to Polymer Science. VCH, Germany, 1997.

HANSEN, F.K. and UGELSTAD, J.; Particle Nucleation in Emulsion Polymerization: I. A Theory for Homogeneous Nucleation; Journal of Polymer Sci.: Polymer Chemistry Edition; vol.16, 1953-1979 (1978).

HANSEN, F.K. and UGELSTAD, J.; Particle formation Mechanism. In: Piirma I, editor. Emulsion Polymerization. New York: Academic Press, 51-92, 1982.

HARADA, M., NOMURA, M., KOJIMA, H., EGUCHI, W. and NAGATA, S.; Rate of Emulsion Polymerization of Styrene; Journal of Polymer Science, Vol.16, 811-833 (1972).

HARKINS, W. D. A general Theory of the Mechanism of Emulsion Polymerization; Journal Chem. Phys., Vol.13; 381, 1945.

HARKINS, W. D. A general Theory of the Mechanism of Emulsion Polymerization; Journal Chem. Phys., Vol.14, 47, 1946.

HARKINS, W. D. A general Theory of the Mechanism of Emulsion Polymerization; Journal Am. Chem. Soc., Vol.69; 1428, 1947.

HARKINS, W. D. ; Journal Polym. Sci.; 5, 217, 1950.

HARKNESS, M.R. A computer simulation of the bulk polymerization of polystyrene in a tubular reactor. M.S. Thesis, Rensselaer Polytechnic Institute, Troy, New York, 1982.

HARRIS, C.K., ROEKAERTS, D., AND ROSENDAL, F.J.I., Computational Fluid Dynamics for chemical reaction engineering, Chem Eng. Sci. 51, 1569, 1995.

HAWKETT, B.S., NAPPER, D.H., GILBERT, R.G. Radicals capture efficiencies in emulsion polymerization. J. Polym Sci Chem., 19, 3173-9, 1981.

HEMPEL, C.G.; Philosophy of Natural Science; Englewood Cliffs, NJ: Prentice-Hall, 1966.

HENKEL, K.D., BUNA, A.G. and SCHKOPAU, Reactor Types and Their Industrial Applications (Reactor of Polimerization), ULLMANN'S Encyclopedia of Industrial Chemistry, Vol.B4, 87-120 (1992).

HESSENBRUCH, A.; History of Science: Calculating Devices, Computing; Fitzray Dearborn Publishers, London, Chicago, 2000.

HLAVACEK, V., PUSZYNSKY, J.A., VILJOEN, H.J. and GATICA, J.E., Model Reactors and Their Design Equations, ULLMANN'S Encyclopedia of Chemical Chemistry, Vol.B4, 121-165 (1992).

HOLLAND, Ch.D. AND ANTHONY, R.G. Fundamentals of Chemical Reaction Engineering; Prentice Hall; New Jersey, USA; 1989.

HUI, A.W. AND HAMIELEC, A.E. J. Appl. Polym. Sci., 16, 749-769, 1972.

HUI, A.W., HAMIELEC, A.E., KIRCHNER, K. AND RIEDERLE, K. Angew. Makromol. Chem 111, 1-16, 1983.

ISSA, R.I. AND KEMPF, M.H.W.; Simulation of Slug flow in horizontal and nearly horizontal pipes with the two-fluid model; International Journal of Multiphase Flow, 29, 69-95; 2003.

JAMES, Jr., H.L., PIIRMA, I. Molecular weight development in styrene and methyl methacrylate emulsion polymerization. Polym. Prepr. 16, 198-204, 1975.

JAMES, D.H. AND CASTOR, W.M. Styrene, ULLMANN'S Encyclopedia of Industrial Chemistry, Vol.A 25, 1994.

JOHANSEN, S.T., AND KOLBEINSEN, L., "Applications of Computational Fluid Dynamics in Optimization and Design of Metallurgical Processes", SINTEF Materials Technology, N-7034 Trondheim- NTH, Norway, 1996.

KAFAROW, W.W. Kybernetische Methoden in der Chemie und chemischen Technologie, Verlag Chemie, Weinheim, 1971.

KHANNA, R. and SEINFELD, J.H., Mathematical Modeling of Packed Bed Reactors: Numerical Solutions and Control Model Development, Advances in Chemical Engineering, Academic Press Inc., 16, 227-235, 1987.

KIPARISSIDES, C. Polymerization Reactor Modeling: A Review of Recent Developments and Future Directions. Chemical Eng. Science, Vol.51, No.10, 1996.

KLAUS, G. Worterbuch der Kybernetik, Fischer Verlag, Frankfurt, 1969.

KOLHAPURE, N.H. e FOX, R.O., CFD analysis of micromixing effects on polimerization in tubular low-density polyethylene reactors, Ch.Eng.Sc., 54, 3233-3242, 1999.

KRUIS, F.E. e FALK, L., Mixing and Reaction in a tubular jet reactor: A comparison of experiments with model based on a prescribed PDF, Ch. Eng. Cs. Vol.51, 10, 24392448, 1996.

- KUIPERS, J.A.M. AND SWAAIJ, P.M.VAN; Computational Fluid Dynamics Applied to Chemical Reaction Engineering; Advances Chemical Engineering Vol.24, 1998.
- KUMAR, A. AND GUPTA, S.K.; Fundamentals of Polymer Science and Engineering; Tata McGraw – Hill Publishing Co. Ltd., New Delhi, India; 1978.
- KUOCHEN, T. e FOX, R.O., Modeling the scalar dissipation rate for turbulent series-parallel reaction, Ch.Eng.Sc. Vol.51.,10, 1929-1938, 1996.
- LANTHIER, R. ; U.S. Patent 3,551,396 (to Gulf Oil Canada, Ltd.) December, 29, 1970.
- LAZZARINI, A., Science Requirement for the LIGO beam tube baffles. Laser Interferometer Gravitational Wave Observatory -LIGO-, California Institute of Technology LIGO Project. [Http://www.ligo.caltech.edu/](http://www.ligo.caltech.edu/) ; 1996.
- LEITHOLD, L.; O Cálculo com Geometria Analítica, Vol. I, II; 3rd Ed.; Harbra Ltda.; 1994.
- LENK, R.S.; Polymer Rheology; Applied Science Publishers Ltd; London; 1978.
- LEVESNPIEL, O., Engenharia de Reações Químicas, Volume 1 – Cinética Química Aplicada, Editora Edgard Blucher Ltda, 1983a.
- LEVESNPIEL, O., Engenharia de Reações Químicas, Volume 1 – Cálculo de Reatores, Editora Edgard Blucher Ltda, 1983b.
- LICHTI, G., HAWKETT, B.S., GILBERT, R.G. and NAPPER, D.H.; Styrene Emulsion Polymerization: Particle-Size Distributions; Journal of Polymer Science: Polymer Chemistry Edition, Vol.19, 925-938 (1981).
- LUYBEN, W.L.; Process Modeling, Simulation, and Control for Chemical Engineers; McGraw – Hill International Book Company; S.P. Brasil; 1990.
- LYNN, S. and HUFF, J.E.; Polymerization in a Tubular Reactor; AIChE Journal; vol.17, 2, 475-481 (1971).
- MACIEL FILHO, R., Oxidação Catalítica de Etanol a Acetaldeído sobre Catalisador de Óxido de Ferro-Molibdênio, Tese de Mestrado, FEQ/UNICAMP, Campinas, 1985.
- MACIEL FILHO, R., Modeling and Control of Multitubular Reactors, Ph.D., Thesis, University of Leeds, Leeds, 1989.
- MACIEL FILHO, R., and DOMINGUES, A., Multitubular Reactor for Obtención of Acetaldehyde by Oxidation of Ethyl Alcohol, Chemical Engineering Science, Turin, Itália, 1992.
- MAKOWSKY, J.A.; The impact of Model theory on Theoretical Computer Science. Logic, Methodology and Philosophy of science IX. D. Prawitz, B. Skyrms and D. Westerstahl editors. Elsevier Science B.V., 1994.

- MALISKA, C.I.R.; *Transferência de Calor e Mecânica dos Fluidos Computacional, Fundamentos e Coordenadas Generalizadas*; Livros Técnicos e Científicos Editora S.A.; Rio de Janeiro; 1995.
- MAMPAEY, F., AND XU, Z.A., An Experimental and simulation study of mould filling combined with heat transfer. In "Computational Fluid Dynamics'92". Elsevier, Amsterdam, vol.1, 421, 1992.
- MATHEWS, J.H.; *Numericals Methods for mathematics, Science and Engineering*; Prentice Hall Englewood Cliffs, New Jersey, USA; 1992.
- MATSUNAGA, K., MIJATA, H., AOKI, K., AND ZHU, M., Finite-difference simulation of 3D vortical flows past road vehicles. *Vehicle Hydrodynamics*, SAE Special Publication 908, 65, 1992.
- MARCIA, A.G.R. AND VERA LUCIA da R.L.; *Calculo Numérico, Aspectos Teóricos e Computacionais*; Segunda Ed.; Makron Books; S.P., Brasil; 1998.
- MAUL, J. AND HÜLS, A.G. *Polystyrene and Styrene Copolymers*; ULLMANN'S Encyclopedia of Industrial Chemistry, Vol.A 21, 1992.
- MAVROS, P., DANIILIDOU, A e PAPTASIOTSOU, F., Internal circulation and mixing in flotation columns, *Chem. Eng. Res. Des.*, 73^A, 733-738, 1995.
- MAYER, M.J.J., van den BOOMEN, A.M., PAQUET, D.A., MEULDIJK, J. and THOENES, D.; The Polymerization Rate of Freshly Nucleated Particles during Emulsion Polymerization with Micellar Nucleation; *Journal of Polymer Science: Part A: Polymer Chemistry*, Vol.34, 1747-1751 (1996).
- MAYO, W.E.; *Theory and Problems of Programming with Fortran 90*; Schaum's Outline Series, The McGraw-Hill Companies; New York; 1996.
- McGREAVY, C. and NAIM, H., Reduced Dynamic Model of Fixed Bed Reactor, *The Canadian Journal of Chemical Engineering*, 55, June, 326-332, 1977.
- McGREAVY, C., On-Line Control System for Chemical Reaction Process, *Computers Chem. Eng.*, 7, 4, 529-566, 1983.
- McGREAVY, C. and MACIEL FILHO, R., Influence of Flow Distribution on Heat Transfer in Multitubular Catalytic Reactors, 3rd Latin American Conf. Heat and Mass Tr., Mexico, 1988.
- McGREAVY, C. and MACIEL FILHO, R., Dynamic and Control of Chemical Reactors, presented at IFAC Dynamic and Control Chemical Reactors, Maastricht, The Netherlands, 1989.
- McGREAVY, C.; *Polymer Reaction Engineering*; Blackie Academic & Professional; New York; 1994.

- MILLER, C.M., CLAY, P.A., GILBERT, R.G., EL-AASSER, M.S. Na experimental investigation on the evolution of the molecular weight distribution in styrene emulsion polymerizaion. *J. Polym. Sci. Chem.* 35(6), 989-1006, 1997.
- MIN,K.W. AND RAY,W.H.; On the mathematical modeling of emulsion polymerization reactors; *J. Macromol. SCI- Chem.*, C11(2), 177-255(1974).
- MIRZA, S. AND SOLIMAN, H.M. The influence of internalfins on mixed convection inside horizontal tubes, *Int. Commun. Heat Mass Transfer*, 12, 191-200, 1985.
- MORBIDELLI, M., STORTI, G., CARRA, S. Role of micellar equilibria on modeling of batch emulsion polymerization reactors. *J. Appl. Polym. Sci.* 28, 901-19, 1975.
- MORGAN, J.S. AND SCHONFELDER, J.L. Fortran 90 Course Notes; The University of Liverpool; 1997.
- MORTON, M., SALATIELLO, P.P., LANDFIELD, H. Absolute propagation rates in emulsion polymerization. III. Styrene and Isoprene. *J. Polym. Sci*, VIII, 279-87, 1952.
- MOURA, J.C., Oxidação de Etanol a Acetaldeído sobre Catalisador de Cobre Oxidado, Tese de Doutorado, FEQ/UNICAMP, Campinas, 1984.
- MOYS, M.H., ENGELBRECHT, J. e TERCLANCHE, N., The design of baffles to reduce axial mixing in flotation columns, in *Column'91*, (eds) G.E. Agar, B.J. Huls e D.B. Hyma, CIM, Sudbury, Ontario, 1, 275-288 , 1991.
- NAPPER, D.H. AND ALEXANDER, A .E. Polymerization of vinyl acetate in aqueous media. Part. II. The kinetic behavior in the presnce of low concentration of added soaps. *J. Polym. Sci.* 61, 127, 1962.
- NAUMAN, E.B.; *Chemical Reactor Design*; John Wiley & Sons; New York; 1987.
- NAVIER,M., Mémoire sur les Lois du Mouvement des Fluides. *Men. De l'Acad. De Sci.* 6, 389, 1827.
- NOMURA, M., KOJIMA, H., HARADA, M., EGUCHI, W., NAGATA,S. Continuous flow operation i n emulsion p olymerization o s styrene. *J. Appl. Polym. Sci.*, 15, 675-91, 1971.
- NORRISH, R.G.W. AND BROOKMAN, E.F. *Proc. Roy. Soc. (London)*, A171, 147, 1939.
- ODIAN, G.; *Principles of Polymerization*; 3th Ed.; John Wiley & Sons, Inc.; N.Y.; 1991.
- PAQUET, D.A. AND RAY, W.H.; Tubular Reactors for Emulsion Polymerization: I Experimental Investigation; Reactor, kinetics and catalysis; *AIChE journal*, vol.40 No.1, january 1994a.
- PAQUET, D.A. AND RAY, W.H.; Tubular Reactors for Emulsion Polymerization: II Model Comparison with Experiments; *AIChE journal*, vol.40 No.1, january 1994b.

PATANKAR, S.V., IVANOVIC, M. and SPARROW, E.M.; Analysis of Turbulent Flow and Heat Transfer in Internally Finned Tubes and Annuli; Journal of Heat Transfer; vol.101, 29-37 (1979).

PATANKAR, S.V.; Numerical Heat Transfer and Fluid Flow; Hemisphere Publishing Corporation; New York, 1980.

PENBOSS, I. A., NAPPER, D.H., GILBERT, R.G. Styrene emulsion polymerization. J. Chem. Soc. Faraday Trans. 79, 1257-71, 1983.

PENDILIS, A., MACGREGOR, J.F. AND HAMIELEC, A.E; Mathematical Modeling of Emulsion Polymerization Reactors; Computer Application in The Polymer Laboratory, American Chemical Society, 1986.

PERRY, R.H. AND GREEN, D.W.; Perry's Chemical Engineering Handbook; 7th Ed.; McGraw – Hill, USA; 1997.

PIIRMA, I., KAMATH, V.R., MORTON, M. The kinetics of styrene emulsion polymerization. Polym. Prepr, 16, 187-91, 1975.

PIIRMA, I.; Emulsion Polymerization; Academic Press, Inc.; N.Y.; 1982.

POEHLEIN, G.W., OTTEWILL, R.H. AND GOODWIN, J.W.; Science and Technology of Polymer Colloids, Vols I and II of NATO-ASI Series, Series E: Applied Sciences, N0.67, Martinus Nijhoff Publishers, The Hague, The Netherlands, 1983.

POISSON, S.D., Mémoire sur les Equations Générales de l'Equilibre et du Mouvement des Corps Solides Elastiques et des Fluides. J. de L'Ecole Polytechn., 13, 139, 1831.

PRAKASH, C. AND PATANKAR, S.V. Combined Free and forced convection in vertical tubes with radial internal fins, ASME J.Heat Transfer 103, 566-572, 1981.

PRIEST, W.J. Particle growth in the aqueous polymerization of vinyl acetate. J. Phys. Chem. 56, 1077-83, 1952.

RAY, W. HARMON; On the mathematical modeling of polymerization reactors; J. MACROMOL. Sci.- Revs. Macromol. Chem., C8(1), pp. 1-56, (1972).

RAY, W. HARMON; Current Problems in Polymerizations Reaction Engineering. ACS Symp. Ser. 226, 101, 1983.

RAWLINGS, J.B. AND RAY, W.H.; The modeling of batch and continuous emulsion polymerization reactors. Part I: Model formulation and sensitivity to parameters; Polymer Engineering and science, Mid-march, Vol.28. No.5, 1988a.

RAWLINGS, J.B. AND RAY, W.H.; The modeling of batch and continuous emulsion polymerization reactors. Part II: Comparison with experimental data from continuous stirred tank reactors; Polymer Engineering and science, mid-march, Vol.28. No.5, 1988b.

REICHERT, K.H. AND MORITZ, H.U.; Polymer Reaction Engineering, Comprehensive Polymer Science, vol3, Pergamon Press, New York, p.327, 1989.

REILLY, M.J.; Computer Programs for Chemical Engineering Education; Sterling Swift publishing company, Texas, U.S., 1972.

ROLLINS, A.L., PATTERSON, W.I., HUNEAULT, R. and BATAILE, P.; The Effect of Flow Regime on the Continuous Emulsion Polymerization of Styrene in a Tubular Reactor; The Canadian Journal of Chemical Engineering, Vol.55, 565-571 (1977).

ROLLINS, A.L., PATTERSON, W.I., ARCHAMBAULT, J. AND BATAILE, B.; Polymerization Reactors and Processes; J.N. Henderson and T.C. Bouton, eds; pp-113-136; ACS Symp. Ser. , 104, Washigton, D.C.; 1979.

RUDIN, A., The elements of Polymer Science and Engineering, na introductory text for engineers and chemist. Ed.1th, EDT. Academic Press Inc., N.Y., 1982.

RUSTUM, I.M. AND SOLIMAN, H.M.; Numerical Analysis of Laminar mixed convection in Horizontal Internally finned tubes; Int. J. Heat Mass Transfer; Vol.33, No.7; 1485, 1990.

SAID, Z.F.M. Molecular weight distributions in the thermally initiated emulsion polymerization of styrene. Makromol. Chem. , 192, 405-14, 1991.

SALAZAR, A., GUGLIOTTA, L.M., VEJA, J.R., MEIRA, G.R. Molecular weight control in a starved emulsion polymerization os styrene. Ind. Engng. Chem. Res. 37, 3582-91, 1998.

SCHLICHTING, H., "Boundary Layer Theory". McGraw-Hill, New York, 1975.

SCHMIDT, A.D. AND RAY, W.H. Chem. Eng. Sci., 36, 1401, 1981.

SCHOLTENS, C. A.; Process Development for Continuous Emulsion Copolymerization; CIP-DATA Library Technische Universiteit Eindhoven, Ter Verkrijging van de graad van Doctor, 2002.

SCHULZ, G.V. AND HARBORTH, G. Makromol. Chem., 1. 106, 1947.

SEBASTIAN, D.H. AND BIESENBERGER, J. A.; Polymerization Engineering, Wiley, New York, 1983.

SEPPALA, J.V. AND REICHERT, K.H.; "Trends in Polymer Reaction Engineering," Kem-Kem 17, 346, 1990.

SHAH, Y.T., Design Parameters For Mechanically Agitated Reactors(Polimerization Reactors), AIChE, Vol.17, 141-161, 1991.

SHAW, C.T., "Predicting Vehicle Aerodynamics Using Computational Fluid Dynamics –A User's Perspective", Research in Automotive Aerodynamics, SAE Special Publication 747, p=119, Feb. 1988.

SIROLA, J.J., Industrial Applications of Chemical Process Synthesis, AIChE, Vol.23, 1-62, 1996.

SIMON, E. Justus Liebigs Ann. Chem. 31, 265, 1839.

SMITH, WENDELL V. Journal of Chemical Physics, Vol.70, 3695, 1948.

SMITH, WENDELL V. AND EWART, ROSWELL H. Kinetics of Emulsion Polymerization. Journal of Chemical Physics, Vol.16, No.6, 592, 1948.

SMITH, WENDELL V. Journal Am. Chem. Soc., Vol.71; 4077, 1949.

SONG, Z. and POEHLEIN, G.W.; Particle Formation in Emulsion Polymerization: Particle Number at Steady State; J. Macromol. Sci. –Chem., A25(12), 1587-1632 (1988a).

SONG, Z. and POEHLEIN, G.W.; Particle Formation in Emulsion Polymerization: Transient Particle Concentration; J. Macromol. Sci. –Chem., A25(12), 403-443 (1988b).

SONG, Z. and POEHLEIN, G.W.; Particle Formation in Emulsifier-Free Aqueous-Phase Polymerization of Styrene; Journal of Colloid and Interface Science 128, 2, 501-10 (1989a).

SONG, Z. and POEHLEIN, G.W.; Particle Formation in Emulsifier-Free Aqueous-Phase Polymerization: Stage 1; Journal of Colloid and Interface Science 128, 2, 486-500 (1989b).

SONG, Z. and POEHLEIN, G.W.; Kinetic of Emulsifier-Free Emulsion Polymerization of Styrene; Journal of Polymer Science: Part A: Polymer Chemistry, 28, 2359-92 (1990).

SPIEGEL, M.R.; Advanced Calculus: Theory and Problems; McGraw – Hill Book Company; N.Y.; 1963.

STEELE, D.H. MRI Project No.6450, Midwest Research Institute, Kansas City, Mo., 1992.

STEIJSIGER, C., LANKHORST, C.M., AND ROMAN, Y.R., Influence of Gas phase Reaction of the Deposition rate of silicon carbide from the precursor methyltrichlorosilane and hydrogen. In "Numerical Method in Engineering'92". Elsevier, Amsterdam, p.857, 1992.

STOKES, G.G., On the Theories of internal friction of fluids in motion. Trans. Camb. Phil. Soc., 8, 287, 1845.

STREVEL, D.P., TOLEDO, E.C.V. e MACIEL FILHO, R., Estratégias de Redução para Modelos Dinâmicos Envolvendo Processos Químicos e Bioquímicos em Reatores de Leito Fixo ENEMP – Congresso Brasileiro de Sistemas Particulados, São Carlos, SP, 1997.

STREVEL, D.P., TOLEDO, E.C.V. e MACIEL FILHO, R., Modelos Dinâmicos reduzidos para Reatores Multifásicos: Químicos e Bioquímicos XIII Congresso Chileno de Engenharia Química, ELAIQ'98 – II Encuentro Latino-Americano de Engenharia Química, Chile, pag. 699-707, 1998.

STREVEL, D.P., TOLEDO, E.C.V. e MACIEL FILHO, R., Analysis of Different Reduction Techniques in Kinetic Dynamic Models for Bichemical and Catalytic Chemical Processes on Fixed Bed Reactors, The Forth Talian Conference on Chemical and Process Engineering – IcheaP-4, Florence, Italy, 1999.

SUDOL, E.D., EL-AASSER, M.S. and VANDERHOFF, J.W.; Kinetics and Successive Seeding of Monodisperse Polystyrene Latexes: II. Azo Initiators with and without Inhibitors; *Journal of Polymer Science:Part A: Polymer Chemistry*, Vol.24, 3515-3527 (1986).

SUDOL, E.D., EL-AASSER, M.S. and VANDERHOFF, J.W.; Kinetics and Successive Seeding of Monodisperse Polystyrene Latexes: I. Initiation via Potassium Persulfate; *Journal of Polymer Science:Part A: Polymer Chemistry*, Vol.24, 3499-3513 (1986).

TARMY, B.L., Reactor Technology, KIRK OTHMER Encyclopedia of Chemical Technology, Ed. 3ra, Vol.19, 879-914, 1982.

TOLEDO, E.C.V. e MACIEL FILHO, R., Reduced Reliable Models for Fixed Bed Catalytic Reactors: Control Applications, ECCE-1 – The First European Congress on Chemical Engineering, pg. 93-96, Vol.1, Florence, Italy, May 4-7, 1997a.

TOLEDO, E.C.V. e MACIEL FILHO, R., Dynamic and Advanced Control of a Fixed Bed Catalytic Reactors, ENPROMER'97 - 1º Congresso de Engenharia de Processos do Mercosul, pg. 69-70, Bahia Blanca, Argentina, 1 al 4 Setiembre, 1997b.

TOLEDO, E.C.V. e MACIEL FILHO, R., Desenvolvimento de Modelos Internos e Avaliação de Controladores Avançados em Reatores de Leito Fixo, XVII CILAMCE – Congreso Íbero Latino-Americano de Métodos Computacionais em Engenharia, Brasília, DF, Outubro, 1997c.

TOLEDO, E.C.V. e MACIEL FILHO, R., Avaliação de Controladores Avançados na Política Operacional de Reatores Catalíticos de Leito Fixo, XII COBEQ – Congresso Brasileiro de Engenharia Química, Porto Alegre, RS, Setembro, 1998a.

TOLEDO, E.C.V. e MACIEL FILHO, R., Modelos Dinâmicos e a Avaliação de Diferentes Controladores Avançados em Reatores Catalíticos de Leito Fixo, XVIII Interamerican Congress of Chemical Engineering, San Juan, Puerto Rico, December 6 to 10, 1998 b.

TOLEDO, E.C.V., Modelagem, Simulação e Controle de Reatores Catalíticos de Leito Fixo, Tese de Doutorado, FEQ/UNICAMP, Campinas, 1999.

TOLEDO, E.C.V. e MACIEL FILHO, R., Modelling, Simulation and Control of na Autorefrigerated Polymerization Reactor; Laboratorio de Otimização, Projeto e Controle Avanzado(LOPCA), Departamento de Processos Químicos, Universidade de Campinas(UNICAMP), 2000a.

TOLEDO, E.C.V., MARTINI, R.F. and MACIEL FILHO, R., Development of high Performance Operation Strategies for Polymerization Reactor; *Computer and Chemical Engineering*; 24, 481-486, 2000b.

TRAMBOUZE, P., Computational Fluid Dynamics applied to chemical reaction engineering. *Ver. Inst. Francais du Petrole* 48(6), 595, 1993.

TROMMSDORFF, E., KOEHLE, H. AND LAGALLY, P. *Makromol. Chem.*, 1, 169, 1948.

- TUCKER III, C.L.; Fundamentals of Computer Modeling for Polymer Processing; Hanser Publishers, Munich Vienna New York, 1989.
- VAN HERK, A.M., AND GERMAN, A.L; Modeling of emulsion co- and terpolymerizations: wil it be ever possible?. *Macromol Theor Simul* 7, 557-65, 1998.
- VAN KREVELEN, D.W. *Chem Eng Sci* 8, 5, 1958.
- VAN KREVELEN, D.W.; Properties of Polymers; Elsevier Science Publishers B.V.; N.Y.; 1990.
- VERSTEEG, H.K. AND MALALASEKERA, W.; An Introduction to Computational Fluid Dynamics, The Finite Volume Method; 2nd Ed.; Addison Wesley Longman Limited; 1998.
- WEICHENG, F.; Computer Modeling of Combustion Processes with 80 figures and the program of GM80. International Academic Publishers, Pergamon Press. 1991.
- WENDT, J.F.; Computational Fluid Dynamics; Springer-Verlag; USA; 1992.
- WESTERTERP, K.R. and WIJNGAARDEN, R.J.; Principles of Chemical Reaction Engineering; ULLMANN'S Encyclopedia of Industrial Chemistry, Vol.B4, 5-83 (1992).
- WRAGG, A.A. e LEONTARITIS, A.A., Loca mass transfer and current distribution in baffled and unbaffled paeallel plate electrochemical reactors, *Ch. Eng Jo urnal*, 66, 1-10, 1997.
- YOUNG, R. J. Introduction to Polymer. Chapman and Hall, Great Britain, 1989.